

*Midwest State's Regional Pooled Fund Research Program
Fiscal Year 1995-1996 (Year 6)
NDOR Research Project Number SPR-3(017)*

TWO APPROACH GUARDRAIL TRANSITIONS FOR CONCRETE SAFETY SHAPE BARRIERS

Submitted by

Ronald K. Faller, Ph.D., P.E.
Research Associate Engineer

John D. Reid, Ph.D.
Associate Professor

John R. Rohde, Ph.D., P.E.
Associate Professor

Dean L. Sicking, Ph.D., P.E.
Associate Professor and MwRSF Director

Eric A. Keller, E.I.T.
Computer Design Technician II

MIDWEST ROADSIDE SAFETY FACILITY

Civil Engineering Department
University of Nebraska-Lincoln
1901 "Y" Street, Building "C"
Lincoln, Nebraska 68588-0601
(402) 472-6864

Submitted to

MIDWEST STATE'S REGIONAL POOLED FUND PROGRAM

Nebraska Department of Roads
1500 Nebraska Highway 2
Lincoln, Nebraska 68502

MwRSF Research Report No. TRP-03-69-98

Technical Report Documentation Page

1. Report No. SPR-3(017)	2.	3. Recipient's Accession No.	
4. Title and Subtitle Two Approach Guardrail Transitions for Concrete Safety Shape Barriers		5. Report Date May 15, 1998	
		6.	
7. Author(s) Faller, R.K., Reid, J.D., Rohde, J.R., Sicking, D.L., and Keller, E.A.		8. Performing Organization Report No. TRP-03-69-98	
9. Performing Organization Name and Address Midwest Roadside Safety Facility (MwRSF) University of Nebraska-Lincoln 1901 Y St., Bldg. C Lincoln, NE 68588-0601		10. Project/Task/Work Unit No.	
		11. Contract © or Grant (G) No. SPR-3(017)	
12. Sponsoring Organization Name and Address Midwest States Regional Pooled Fund Program Nebraska Department of Roads 1500 Nebraska Highway 2 Lincoln, Nebraska 68502		13. Type of Report and Period Covered Final Report 1996-1998	
		14. Sponsoring Agency Code	
15. Supplementary Notes Prepared in cooperation with U.S. Department of Transportation, Federal Highway Administration			
16. Abstract (Limit: 200 words) Two approach guardrail transitions for use with concrete safety shape barriers were developed and crash tested. For this study, the transition systems were attached to the New Jersey safety shape concrete barrier; however, it is believed that these transition systems could be easily adapted to the F-shape barrier with no need for further crash testing. Both transition designs were constructed with two nested thrie beam rails measuring 2.66-mm thick. The first transition design was supported by nine W150x13.5 steel posts measuring 1,981-mm long, while the second transition design was supported by nine 152-mm x 203-mm wood posts measuring 2,134-mm long. For both systems, post spacings consisted of one at 292 mm, five at 476 mm, and three at 952 mm. A triangular-shape concrete curb was constructed below the thrie beam rail on each approach guardrail transition system. The two transition systems successfully met the Test Level 3 requirements specified in NCHRP Report 350: <i>Recommended Procedures for the Safety Performance Evaluation of Highway Features</i> .			
17. Document Analysis/Descriptors Highway Safety, Guardrail Longitudinal Barrier, Approach Guardrail Transition		18. Availability Statement No restrictions. Document available from: National Technical Information Services, Springfield, Virginia 22161	
19. Security Class (this report) Unclassified	20. Security Class (this page) Unclassified	21. No. of Pages 156	22. Price

DISCLAIMER STATEMENT

The contents of this report reflect the views of the authors who are responsible for the facts and the accuracy of the data presented herein. The contents do not necessarily reflect the official views or policies of the State Highway Departments participating in the Midwest State's Regional Pooled Fund Research Program nor the Federal Highway Administration. This report does not constitute a standard, specification, or regulation.

ACKNOWLEDGMENTS

The authors wish to acknowledge several sources that made a contribution to this project: (1) the Midwest States Regional Pooled Fund Program funded by the Iowa Department of Transportation, Kansas Department of Transportation, Minnesota Department of Transportation, Missouri Highway and Transportation Department, Nebraska Department of Roads, South Dakota Department of Transportation, and Wisconsin Department of Transportation for sponsoring this project; (2) MwRSF personnel for constructing the barriers and conducting the crash tests; (3) Center for Infrastructure Research, Engineering Research Center, and the University of Nebraska-Lincoln for matching support, and (4) Daniel Mushett of Buffalo Specialty Products - Timber Division for donating wood posts and blockouts.

A special thanks is also given to the following individuals who made a contribution to the completion of this research project.

Midwest Roadside Safety Facility

B.G. Pfeifer, Ph.D., P.E., Research Associate Engineer
J.C. Holloway, Research Associate Engineer
K.L. Krenk, Field Operations Manager
M.L. Hanau, Laboratory Mechanic I
Undergraduate and Graduate Assistants

Iowa Department of Transportation

David Little, P.E., Design Methods Engineer

Kansas Department of Transportation

Ron Seitz, P.E., Road Design Squad Leader

Minnesota Department of Transportation

Ron Cassellius, Research Program Coordinator

Missouri Department of Transportation

Vince Imhoff, P.E., Senior Research and Development Engineer

Nebraska Department of Roads

Leona Kolbet, Research Coordinator
Ken Sieckmeyer, Transportation Planning Manager

Ohio Department of Transportation

Larry Shannon, P.E., Standards and Geometrics Engineer
Monique Evans, P.E., Standards Engineer

South Dakota Department of Transportation

David Huff, P.E., Research Engineer

Wisconsin Department of Transportation

Rory Rhinesmith, P.E., Chief Roadway Development Engineer
Fred Wisner, Standards Development Engineer

Federal Highway Administration

Jack Latterell, P.E., Iowa Division Office
Milo Cress, P.E., Nebraska Division Office
John Ballantyne, P.E., Region VII

Dunlap Photography

James Dunlap, President and Owner

TABLE OF CONTENTS

	Page
TECHNICAL REPORT DOCUMENTATION PAGE	i
DISCLAIMER STATEMENT	ii
ACKNOWLEDGMENTS	iii
TABLE OF CONTENTS	v
List of Figures	viii
List of Tables	xi
1 INTRODUCTION	1
2 LITERATURE REVIEW	2
3 TEST REQUIREMENTS AND EVALUATION CRITERIA	4
3.1 Test Requirements	4
3.2 Evaluation Criteria	4
4 SAFETY SHAPE BARRIER	6
4.1 Background	6
4.2 New Jersey Safety Shape	6
4.3 End Section Design	6
5 APPROACH GUARDRAIL TRANSITION - STEEL POSTS (DESIGN NO. 1)	10
6 TEST CONDITIONS	20
6.1 Test Facility	20
6.2 Vehicle Tow and Guidance System	20
6.3 Test Vehicles	20
6.4 Data Acquisition Systems	32
6.4.1 Accelerometers	32
6.4.2 Rate Transducer	33
6.4.3 High-Speed Photography	33
6.4.4 Pressure Tape Switches	39
6.4.5 Approach Guardrail Transition Instrumentation	39
<u>Strain Gauges</u>	39
<u>String Potentiometers</u>	42
7 COMPUTER SIMULATION (DESIGN NO. 1)	44

8 CRASH TEST NO. 1 (DESIGN NO. 1 - STEEL POSTS)	45
8.1 Test ITNJ-1	45
8.2 Test Description	45
8.3 Barrier Damage	46
8.4 Vehicle Damage	46
8.5 Occupant Risk Values	46
8.6 Discussion	47
9 DISCUSSION AND MODIFICATIONS (DESIGN NO. 2)	57
10 CRASH TEST NO. 2 (DESIGN NO. 2 - STEEL POSTS)	60
10.1 Test ITNJ-2	60
10.2 Test Description	60
10.3 Barrier Damage	61
10.4 Vehicle Damage	61
10.5 Occupant Risk Values	61
10.6 Discussion	62
10.7 Barrier Instrumentation Results	62
11 SUMMARY AND CONCLUSIONS - STEEL POST SYSTEM	75
12 APPROACH GUARDRAIL TRANSITION - WOOD POSTS (DESIGN NO. 3)	77
13 CRASH TEST NO. 3 (DESIGN NO. 3 - WOOD POSTS)	83
13.1 Test ITNJ-3	83
13.2 Test Description	83
13.3 Barrier Damage	84
13.4 Vehicle Damage	84
13.5 Occupant Risk Values	84
13.6 Discussion	85
13.7 Barrier Instrumentation Results	85
14 DISCUSSION AND MODIFICATIONS (DESIGN NO. 4)	98
15 CRASH TEST NO. 4 (DESIGN NO. 4 - WOOD POSTS)	102
15.1 Test ITNJ-4	102
15.2 Test Description	102
15.3 Barrier Damage	103
15.4 Vehicle Damage	103
15.5 Occupant Risk Values	103
15.6 Discussion	104
16 SUMMARY AND CONCLUSIONS - WOOD POST SYSTEM	114

17 REFERENCES 116

18 APPENDICES 118

- APPENDIX A - SUMMARY OF STATES' EXISTING TRANSITION DESIGNS .. 119
- APPENDIX B - TYPICAL BARRIER VII INPUT FILE 122
- APPENDIX C - ACCELEROMETER DATA ANALYSIS 125
- APPENDIX D - ACCELEROMETER DATA ANALYSIS 132
- APPENDIX E - RATE TRANSDUCER DATA ANALYSIS 139
- APPENDIX F - ACCELEROMETER DATA ANALYSIS 141
- APPENDIX G - RATE TRANSDUCER DATA ANALYSIS 148
- APPENDIX H - ACCELEROMETER DATA ANALYSIS 150

List of Figures

	Page
1. Design Details for New Jersey Concrete Safety Shape End Section, Design No. 1	8
2. Reinforcement Details, Design No. 1	9
3. Installation Layout and Design Details, Design No. 1	12
4. Design Details, Design No. 1	13
5. Approach Guardrail Transition, Design No. 1	14
6. Approach Guardrail Transition, Design No. 1	15
7. Approach Guardrail Transition, Design No. 1	16
8. New Jersey Connector Plate, Design No. 1	17
9. New Jersey Connector Plate Fabrication Details, Design No. 1	18
10. New Jersey Connector Plate Steel Components, Design No. 1	19
11. Test Vehicles, Test ITNJ-1 and ITNJ-2	22
12. Vehicle Dimensions, Test ITNJ-1	23
13. Vehicle Dimensions, Test ITNJ-2	24
14. Test Vehicles, Test ITNJ-3 and ITNJ-4	25
15. Vehicle Dimensions, Test ITNJ-3	26
16. Vehicle Dimensions, Test ITNJ-4	27
17. Vehicle Target Locations, Test ITNJ-1	28
18. Vehicle Target Locations, Test ITNJ-2	29
19. Vehicle Target Locations, Test ITNJ-3	30
20. Vehicle Target Locations, Test ITNJ-4	31
21. Location of High-Speed Cameras, Test ITNJ-1	34
22. Location of High-Speed Cameras, Test ITNJ-2	36
23. Location of High-Speed Cameras, Test ITNJ-3	37
24. Location of High-Speed Cameras, Test ITNJ-4	38
25. Strain Gauge and String Potentiometer Locations, Test ITNJ-2	40
26. Strain Gauge Locations, Test ITNJ-3	41
27. Summary of Test Results and Sequential Photographs, Test ITNJ-1 (Design No. 1)	48
28. Additional Sequential Photographs, Test ITNJ-1 (Design No. 1)	49
29. Impact Location, Test ITNJ-1 (Design No. 1)	50
30. Barrier Damage, Test ITNJ-1 (Design No. 1)	51
31. Cracking in Concrete End Section, Test ITNJ-1 (Design No. 1)	52
32. Final Post Positions, Test ITNJ-1 (Design No. 1)	53
33. Final Post Positions, Test ITNJ-1 (Design No. 1)	54
34. Vehicle Damage, Test ITNJ-1 (Design No. 1)	55
35. Occupant Compartment Deformation, Test ITNJ-1 (Design No. 1)	56
36. Barrier and Post Modifications, Design No. 2	59
37. Summary of Test Results and Sequential Photographs, Test ITNJ-2 (Design No. 2)	63
38. Additional Sequential Photographs, Test ITNJ-2 (Design No. 2)	64
39. Documentary Photographs, Test ITNJ-2 (Design No. 2)	65
40. Documentary Photographs, Test ITNJ-2 (Design No. 2)	66

41. Impact Location, Test ITNJ-2 (Design No. 2)	67
42. Barrier Damage, Test ITNJ-2 (Design No. 2)	68
43. Barrier Damage, Test ITNJ-2 (Design No. 2)	69
44. Final Post Positions, Test ITNJ-2 (Design No. 2)	70
45. Final Post Positions, Test ITNJ-2 (Design No. 2)	71
46. Vehicle Damage, Test ITNJ-2 (Design No. 2)	72
47. Occupant Compartment Deformation, Test ITNJ-2 (Design No. 2)	73
48. Installation Layout and Design Details, Design No. 3	80
49. Design Details, Design No. 3	81
50. Approach Guardrail Transition, Design No. 3	82
51. Summary of Test Results and Sequential Photographs, Test ITNJ-3 (Design No. 3)	86
52. Additional Sequential Photographs, Test ITNJ-3 (Design No. 3)	87
53. Documentary Photographs, Test ITNJ-3 (Design No. 3)	88
54. Documentary Photographs, Test ITNJ-3 (Design No. 3)	89
55. Impact Location, Test ITNJ-3 (Design No. 3)	90
56. Barrier Damage, Test ITNJ-3 (Design No. 3)	91
57. Barrier Damage, Test ITNJ-3 (Design No. 3)	92
58. Final Post Positions, Test ITNJ-3 (Design No. 3)	93
59. Final Post Positions, Test ITNJ-3 (Design No. 3)	94
60. Vehicle Damage, Test ITNJ-3 (Design No. 3)	95
61. Occupant Compartment Deformation, Test ITNJ-3 (Design No. 3)	96
62. Barrier and Post Modifications, Design No. 4	100
63. Approach Guardrail Transition, Design No. 4	101
64. Summary of Test Results and Sequential Photographs, Test ITNJ-4 (Design No. 4)	105
65. Additional Sequential Photographs, Test ITNJ-4 (Design No. 4)	106
66. Documentary Photographs, Test ITNJ-4 (Design No. 4)	107
67. Documentary Photographs, Test ITNJ-4 (Design No. 4)	108
68. Impact Location, Test ITNJ-4 (Design No. 4)	109
69. Barrier Damage, Test ITNJ-4 (Design No. 4)	110
70. Barrier Damage, Test ITNJ-4 (Design No. 4)	111
71. Vehicle Damage, Test ITNJ-4 (Design No. 4)	112
72. Occupant Compartment Deformation, Test ITNJ-4 (Design No. 4)	113
C-1. Graph of Longitudinal Deceleration, Test ITNJ-1	126
C-2. Graph of Longitudinal Occupant Impact Velocity, Test ITNJ-1	127
C-3. Graph of Longitudinal Occupant Displacement, Test ITNJ-1	128
C-4. Graph of Lateral Deceleration, Test ITNJ-1	129
C-5. Graph of Lateral Occupant Impact Velocity, Test ITNJ-1	130
C-6. Graph of Lateral Occupant Displacement, Test ITNJ-1	131
D-1. Graph of Longitudinal Deceleration, Test ITNJ-2	133
D-2. Graph of Longitudinal Occupant Impact Velocity, Test ITNJ-2	134
D-3. Graph of Longitudinal Occupant Displacement, Test ITNJ-2	135
D-4. Graph of Lateral Deceleration, Test ITNJ-2	136
D-5. Graph of Lateral Occupant Impact Velocity, Test ITNJ-2	137

D-6. Graph of Lateral Occupant Displacement, Test ITNJ-2	138
E-1. Graph of Roll, Pitch, and Yaw Angular Displacements, Test ITNJ-2	140
F-1. Graph of Longitudinal Deceleration, Test ITNJ-3	142
F-2. Graph of Longitudinal Occupant Impact Velocity, Test ITNJ-3	143
F-3. Graph of Longitudinal Occupant Displacement, Test ITNJ-3	144
F-4. Graph of Lateral Deceleration, Test ITNJ-3	145
F-5. Graph of Lateral Occupant Impact Velocity, Test ITNJ-3	146
F-6. Graph of Lateral Occupant Displacement, Test ITNJ-3	147
G-1. Graph of Roll, Pitch, and Yaw Angular Displacements, Test ITNJ-3	149
H-1. Graph of Longitudinal Deceleration, Test ITNJ-4	151
H-2. Graph of Longitudinal Occupant Impact Velocity, Test ITNJ-4	152
H-3. Graph of Longitudinal Occupant Displacement, Test ITNJ-4	153
H-4. Graph of Lateral Deceleration, Test ITNJ-4	154
H-5. Graph of Lateral Occupant Impact Velocity, Test ITNJ-4	155
H-6. Graph of Lateral Occupant Displacement, Test ITNJ-4	156

List of Tables

	Page
1. NCHRP Report 350 Evaluation Criteria for 2000P Pickup Truck Crash Test (1)	5
2. Strain Gauge Results, Test ITNJ-2 (Design No. 2)	74
3. Summary of Safety Performance Evaluation Results - Steel Post System	76
4. Strain Gauge Results, Test ITNJ-3 (Design No. 3)	97
5. Summary of Safety Performance Evaluation Results - Wood Post System	115

1 INTRODUCTION

In 1996, the State Highway Departments of Iowa, Kansas, Minnesota, Missouri, Nebraska, South Dakota, and Wisconsin requested that the Midwest Roadside Safety Facility (MwRSF) develop two approach guardrail transitions to meet the Test Level 3 (TL-3) criteria provided in NCHRP Report 350 *Recommended Procedures for the Safety Performance Evaluation of Highway Features* (1). The primary design guidelines stated that both transition designs should be compatible with concrete safety shape barriers. One transition design was to be constructed with W150x13.5 steel posts, and the second transition design was to be configured using 152-mm x 203-mm wood posts.

Design considerations for both transition designs included safety, economy, structural integrity, constructability, and maintenance. The tasks to be performed included reviewing the existing transition designs for the member states of the Pooled Fund Program, selecting a specific barrier shape, redesigning and/or modifying the selected barrier's end section (i.e., steel reinforcement and geometry), analyzing and designing two approach guardrail transitions using steel posts and wood posts, and crash testing the new designs. The final designs and full-scale vehicle crash testing, which successfully met all NCHRP Report 350 requirements, are described in this report.

Finally, a less-conservative design philosophy was used for both transition designs. This methodology was selected since there was significant potential for these transition designs to be implemented widely by the State Highway Departments. Therefore, a low-cost approach was believed to be warranted since it would result in a significant cost savings on both a state and national level.

2 LITERATURE REVIEW

Since the inception of the NCHRP Report 350 guidelines only three research studies, all in 1994, have been performed to develop, test, and evaluate thrie beam approach guardrail transitions attached to concrete safety shape parapets according to the TL-3 criteria.

Researchers at the MwRSF, in cooperation with the Midwest States Regional Pooled Fund Program, successfully developed and tested an approach guardrail transition for use with the single-slope concrete median barrier (2-3). The transition was constructed with 3.43-mm thick thrie beam rails and was supported by nine W150x13.5 steel posts. Post spacings consisted of one at 292 mm, five at 476 mm, and three at 952 mm. Specially designed steel structural tube blockouts were used to connect the thrie beam rail to the steel posts.

An approach guardrail transition for use with the New Jersey safety shape barrier was tested according to TL-3 of NCHRP Report 350 at the Southwest Research Institute (SwRI) (4). During the impact, the pickup truck was contained but after redirection the vehicle rolled onto its side. Thus, the test failed NCHRP Report 350 requirements. The transition was constructed with two 2.66-mm thick nested thrie beam rails and was supported by eight 152 mm x 203 mm timber posts. Post spacings consisted of one at 292 mm, three at 476 mm, and four at 952 mm. In 1993, the MwRSF crash tested a transition which attached to a New Jersey safety shape concrete end section similar to that used by SwRI according to the NCHRP Report 230 safety standards (5). This NCHRP Report 230 crash test was performed unsuccessfully with a 2,041-kg sedan impacting a thrie beam approach guardrail transition, revealing a potential for wheel snagging on the concrete end section (6).

Researchers at the Texas Transportation Institute (TTI) successfully designed and tested an approach guardrail transition for use with a concrete safety shape barrier according to the TL-3 of

NCHRP Report 350 (7). The transition was constructed with a 3.43-mm thick thrie beam rail, two nested 3.43-mm thick W-beam to thrie beam transition sections, and was supported by six 178-mm diameter timber posts. Post spacings consisted of four at 476 mm, one at 952 mm, and one at 1,905 mm. The cylindrical wood posts made this transition unacceptable for the Midwest Regional Pooled Fund States.

A review was also performed on each states' existing thrie beam transition designs attached to concrete safety shapes, rectangular parapets, or any other concrete bridge railing configuration. The review revealed that transition designs differed significantly between states, and that some states had several designs included in their standard plans, as shown in Appendix A.

3 TEST REQUIREMENTS AND EVALUATION CRITERIA

3.1 Test Requirements

Longitudinal barriers, such as approach guardrail transitions, must satisfy the requirements provided in NCHRP Report 350 to be accepted for use on new construction projects or as a replacement for existing transition designs not meeting current safety standards. According to Test Level 3 (TL-3) of NCHRP Report 350, approach guardrail transitions must be subjected to two full-scale vehicle crash tests: (1) a 2,000-kg pickup truck impacting at a speed of 100.0 km/hr and at an angle of 25 degrees; and (2) an 820-kg small car impacting at a speed of 100.0 km/hr and at an angle of 20 degrees. However, three beam barriers struck by small cars have been shown to meet safety performance standards and to be essentially rigid (8-10), with no significant potential for occupant risk problems arising from wheel snagging on the posts or on the concrete parapet's end section. Therefore, the 820-kg small car crash test was deemed unnecessary for this project.

3.2 Evaluation Criteria

Evaluation criteria for full-scale vehicle crash testing are based on three appraisal areas: (1) structural adequacy; (2) occupant risk; and (3) vehicle trajectory after collision. Criteria for structural adequacy are intended to evaluate the ability of the barrier to contain, redirect, or allow controlled vehicle penetration in a predictable manner. Occupant risk evaluates the degree of hazard to occupants in the impacting vehicle. Vehicle trajectory after collision is a measure of the potential for the post-impact trajectory of the vehicle to cause subsequent multi-vehicle accidents, thereby subjecting occupants of other vehicles to undue hazard or to subject the occupants of the impacting vehicle to secondary collisions with other fixed objects. These three evaluation criteria are defined in Table 1. The full-scale vehicle crash tests were conducted and reported in accordance with the

procedures provided in NCHRP Report No. 350.

Table 1. NCHRP Report 350 Evaluation Criteria for 2000P Pickup Truck Crash Test (1).

Structural Adequacy	A. Test article should contain and redirect the vehicle; the vehicle should not penetrate, underride, or override the installation although controlled lateral deflection of the test article is acceptable.
Occupant Risk	D. Detached elements, fragments or other debris from the test article should not penetrate or show potential for penetrating the occupant compartment, or present an undue hazard to other traffic, pedestrians, or personnel in a work zone. Deformations of, or intrusions into, the occupant compartment that could cause serious injuries should not be permitted.
	F. The vehicle should remain upright during and after collision although moderate roll, pitching, and yawing are acceptable.
Vehicle Trajectory	K. After collision it is preferable that the vehicle's trajectory not intrude into adjacent traffic lanes.
	L. The occupant impact velocity in the longitudinal direction should not exceed 12 m/sec and the occupant ridedown acceleration in the longitudinal direction should not exceed 20 G's.
	M. The exit angle from the test article preferably should be less than 60 percent of test impact angle, measured at time of vehicle loss of contact with test device.

4 SAFETY SHAPE BARRIER

4.1 Background

A review of the pooled fund states' transition designs for use with safety shape bridge rails indicated that many different design details are incorporated by the states. Since all of the existing designs would be required to be redesigned and retested to the NCHRP Report 350 standards, there was an opportunity to greatly reduce total development costs and possibly cut construction costs by developing a single, concrete safety shape end section and transition that all member states could adopt.

4.2 New Jersey Safety Shape

It was determined that all seven member states were currently using New Jersey safety shape bridge railings and barriers, and that only one state was also using the F-shape barrier configuration. This fact, coupled with our belief that the new design could be modified for use with the F-shape with only minor modifications to the concrete end section and guardrail attachment hardware, led to our selection of the New Jersey safety shape for this design. Since the F-shape offers a slight improvement in safety performance from the New Jersey safety shape with its slight reduction in vehicle roll angles, vehicular climb heights, and increased vehicle stability (11-12), we believe that its use with the new transition design would not require additional testing.

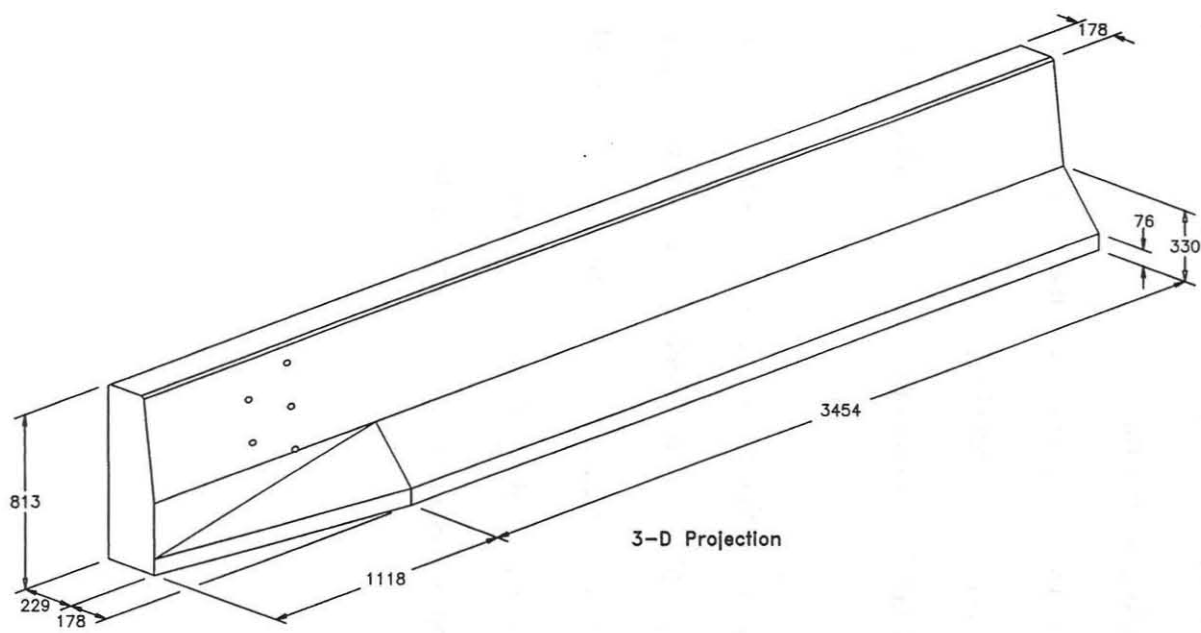
4.3 End Section Design

The initial investigation of the member states' concrete end section designs showed significant differences in geometries, reinforcement, and material specifications. Many of these designs involve warping the safety shape into a vertical wall before the approach railing is attached. Other designs incorporate large flared sections that move the end of the concrete section away from

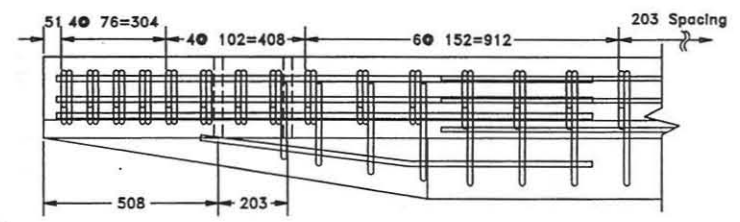
the face of the approach railing. All of these designs require special form work to construct, greatly increasing the cost of these transition designs. One design objective was to develop a standardized concrete end section accommodating the member states' existing standard bridge plans and eliminating the need for special forming, thus substantially reducing construction costs.

For the standardized design shown in Figures 1 and 2, the end sections of the New Jersey safety shape barrier were modified to prevent vehicle snagging and to increase its structural capacity in the critical regions. In order to minimize the potential for wheel snagging on the concrete end section, styrofoam inserts were utilized in standard safety shape barrier forms to produce a simple termination geometry without costly form work. Because of high lateral forces imparted to the concrete end section, the longitudinal and vertical reinforcement at the end was modified to increase the structural capacity. An ultimate strength analysis or *yield line analysis* was used to determine the required steel reinforcement for the last 4,572 mm of concrete barrier (13-14). The size and spacing of the longitudinal and vertical reinforcement in the last 1675 mm of the New Jersey safety shape is shown in Figures 1 and 2.

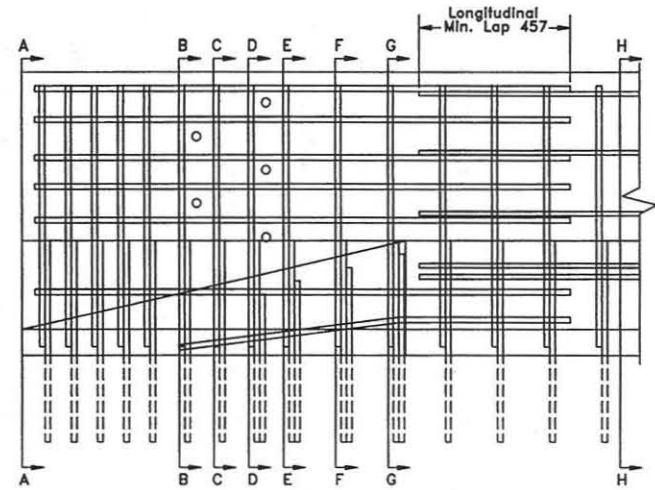
The test fixture was a 4,572-mm long concrete section anchored to an existing concrete foundation measuring approximately 457 to 559-mm thick with no reinforcement. This concrete foundation was used to simulate an actual rigid foundation typically located below the concrete end section. ASTM A615M (Grade 60) steel reinforcement was used throughout the concrete barrier. All concrete (30 percent limestone and 70 percent sand-gravel mix) had minimum 28-day concrete compressive strengths of 41.37 Mpa.



3-D Projection

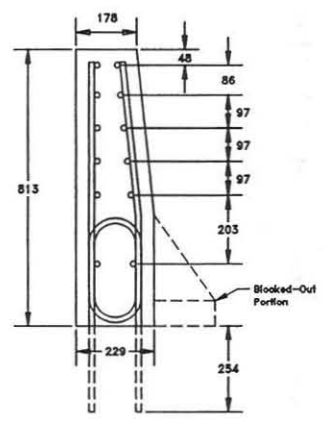


Plan View

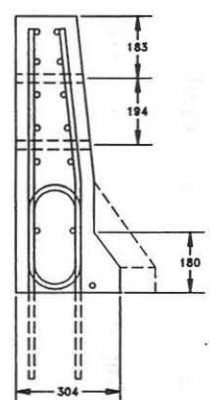


Front Elevation

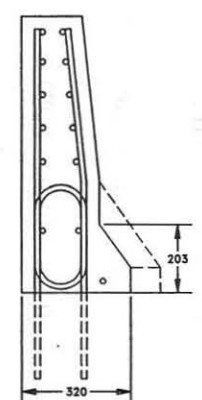
- NOTES:
 (1) 40mm minimum concrete cover
 (2) ASTM A615M reinforcement (Grade 60)



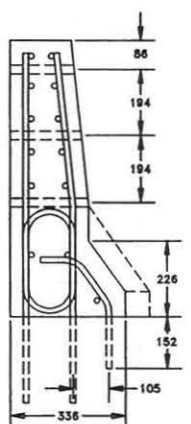
Section A-A



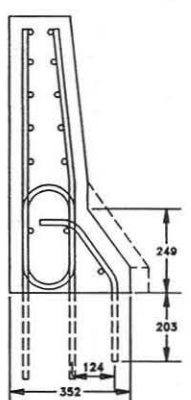
Section B-B



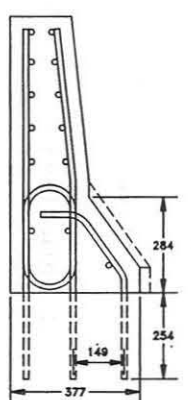
Section C-C



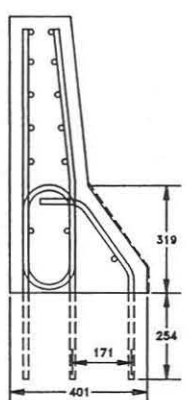
Section D-D



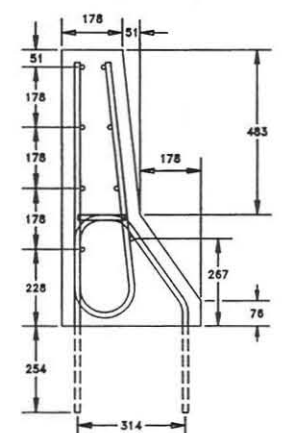
Section E-E



Section F-F



Section G-G



Section H-H

Long. Rebar:	1601	1601, 1602	1601, 1602	1601, 1602	1601, 1602	1601, 1602	1601, 1602	1301
Vert. Rebar:	1603, 1605	1603, 1605	1603, 1605	1603, 1605, 1606	1603, 1605, 1607	1603, 1605, 1608	1603, 1605, 1609	1604, 1610, 1611

Figure 1. Design Details for New Jersey Concrete Safety Shape End Section, Design No. 1

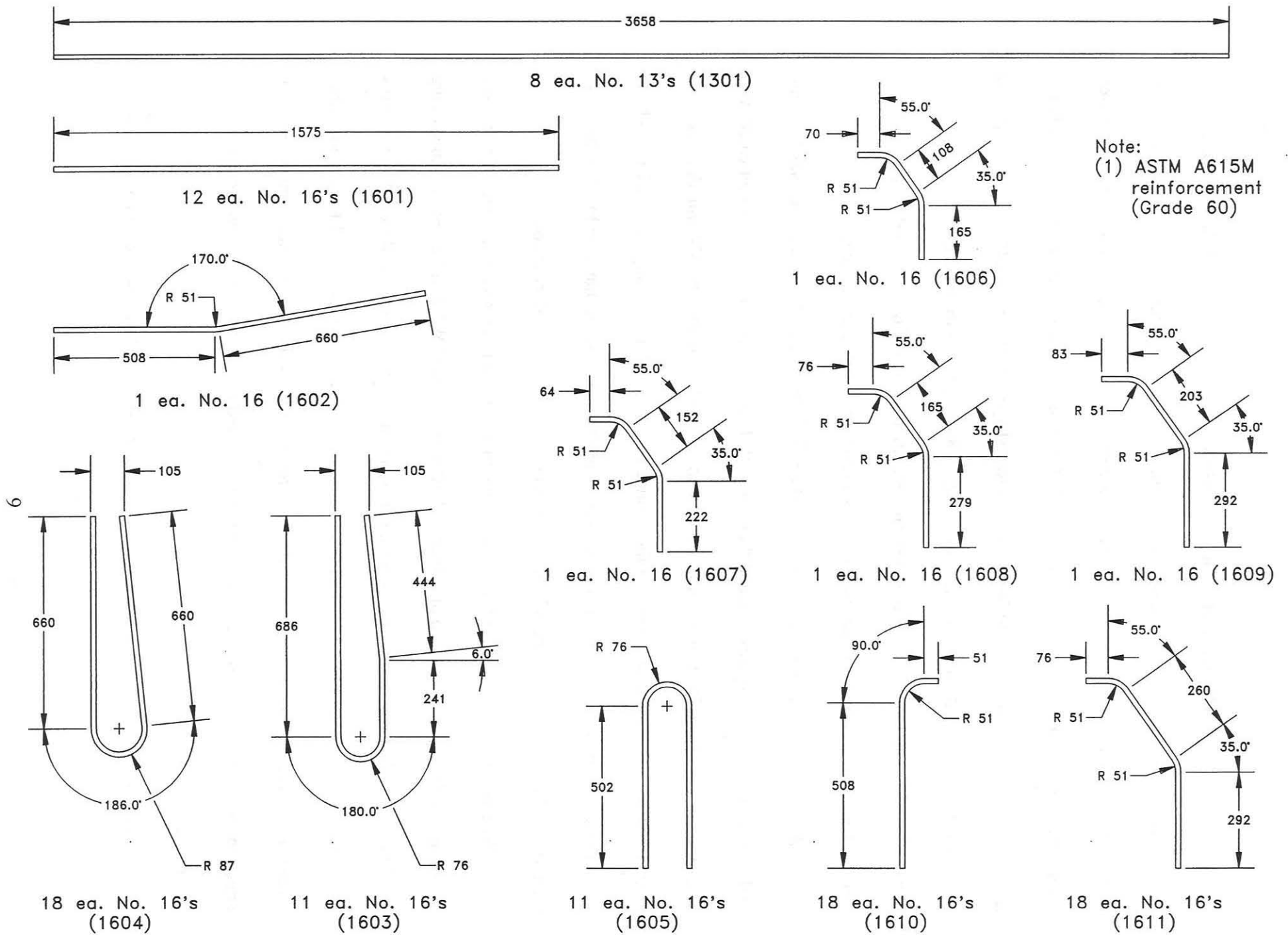


Figure 2. Reinforcement Details, Design No. 1

5 APPROACH GUARDRAIL TRANSITION - STEEL POSTS (DESIGN NO. 1)

The total length of the installation was 25,340 mm. The test installation, as shown in Figures 3 through 10, consisted of seven major structural components: (1) a 4,572-mm long New Jersey safety shape end section; (2) a 4,572-mm long x 102-mm high x 178-mm wide triangular curb; (3) an 813-mm long steel thrie beam to New Jersey safety shape connector plate (NJ connector plate); (4) a thrie beam terminal connector; (5) two nested 3,810-mm long thrie beam rail sections (2.66 mm); (6) a 1905-mm long W-beam to thrie beam transition section (2.66 mm); and (7) a 15240-mm long W-beam rail section (2.66 mm) attached to a simulated anchorage device.

A painted, NJ connector plate connected the thrie beam rail to the New Jersey safety shape end section, as shown in Figures 3, 5, and 8 through 10. The NJ connector plate was fabricated with 6.35-mm thick ASTM A36 steel. External dimensions were 813-mm long by 534-mm deep. A long, sloped section was placed on the end of the connector plate to eliminate any potential for vehicle snagging which may result from a "reverse hit" impact. Five 22-mm diameter by 305-mm long ASTM A325 bolts connected the NJ connector plate to the concrete safety shape.

The system was constructed with seventeen guardrail posts, as shown in Figures 3 through 7. Post nos. 1 through 15 consisted of galvanized, ASTM A36 steel W150x13.5 sections measuring 1829-mm long. Post nos. 16 and 17 were timber posts measuring 140-mm wide x 190-mm deep x 1080-mm long and were placed in steel foundation tubes. The timber posts and foundation tubes were part of an anchorage system used to develop the required tensile capacity of the guardrail. Lap-splice connections between the rail sections were configured to reduce vehicle snagging at the splice during the crash tests.

For post nos. 1 through 7, a structural tube spacer blockout, developed previously at MwRSF

(2-3), was chosen for use with thrie beam guardrail, as shown in Figures 3 and 4. The tube spacer was selected since it eliminates problems associated with the torsional collapse commonly observed to occur with wide-flanged blockouts. At post no. 8, W150x13.5 by 435-mm long spacer blockouts were used. For post nos. 9 through 15, W150x13.5 by 337-mm long spacer blockouts were used with steel W-beam backup plates at all post locations except at rail splices.

The soil embedment depths for post nos. 1 through 7, 8, and 9 through 15 were 1092 mm, 1080 mm, and 1132 mm, respectively, as shown in Figures 3 and 4. The steel posts were placed in a compacted coarse, crushed limestone material that met Grading B of AASHTO M147-65 (1990) as found in NCHRP Report 350. However, the soil-aggregate material was relatively poorly-graded within specification limits, consisting of the maximum amount of larger size aggregates and the minimum amount of medium size aggregates and fines.

Curbs are often used to provide roadway drainage near the ends of a bridge in the transition region. Therefore, a triangular-shape concrete curb, as shown in Figures 3, and 5 through 7, was constructed below the thrie beam rail to determine if the curb would adversely effect the safety performance of the new transition design.

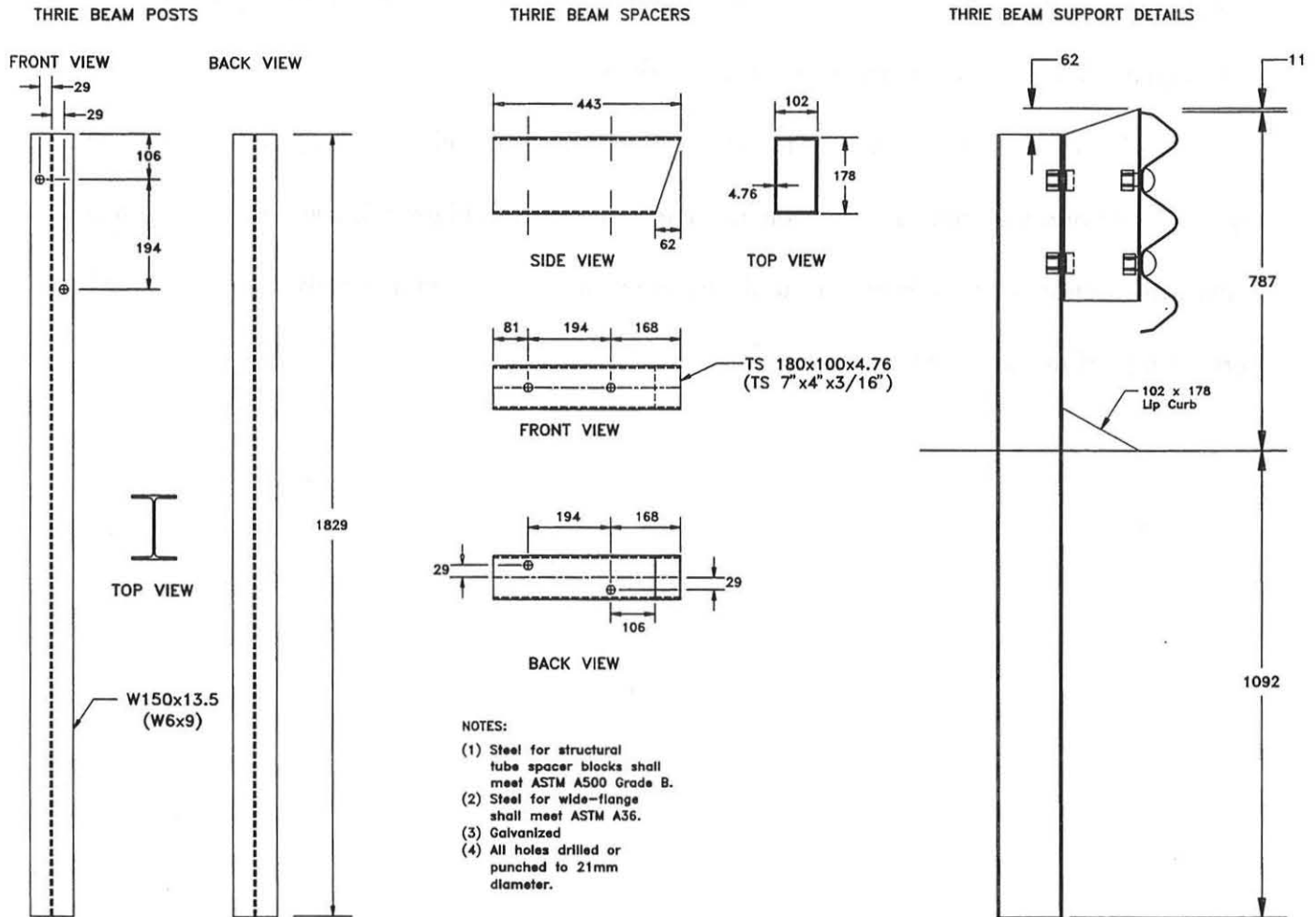
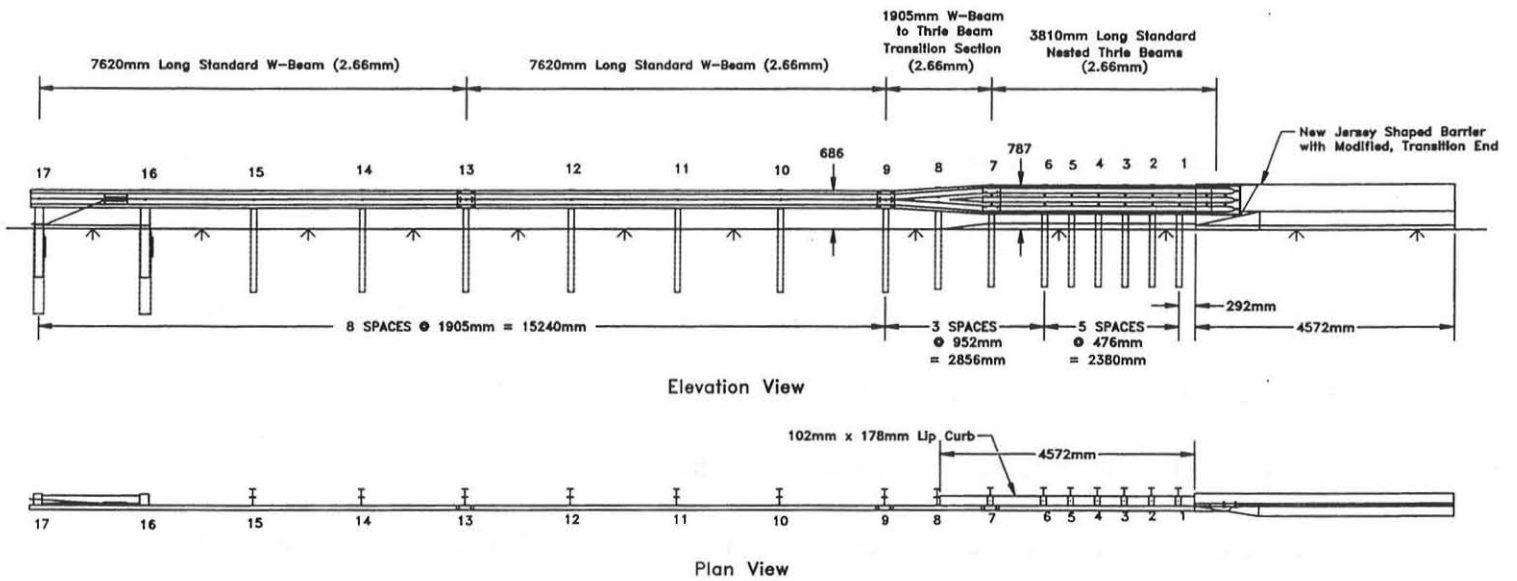
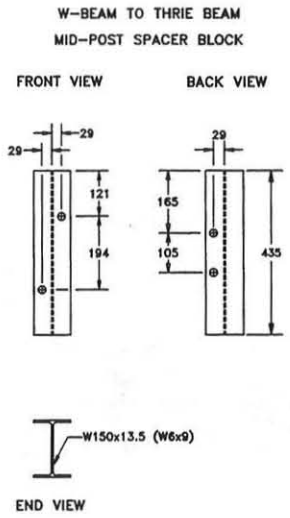
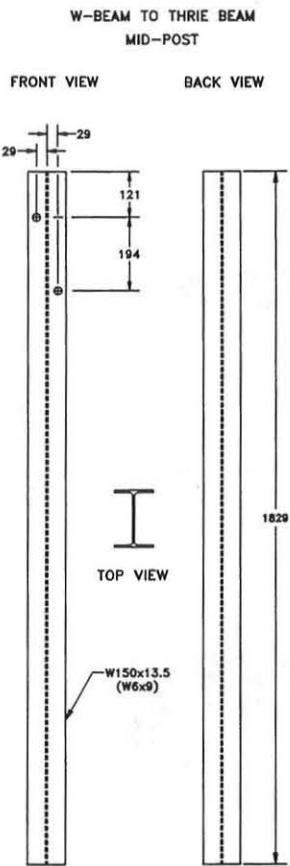
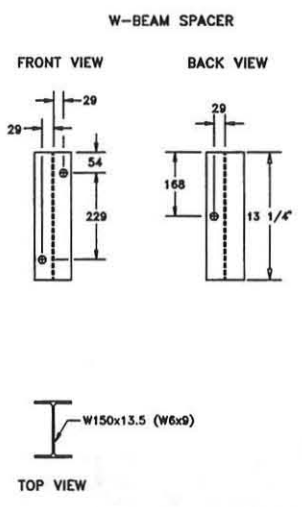
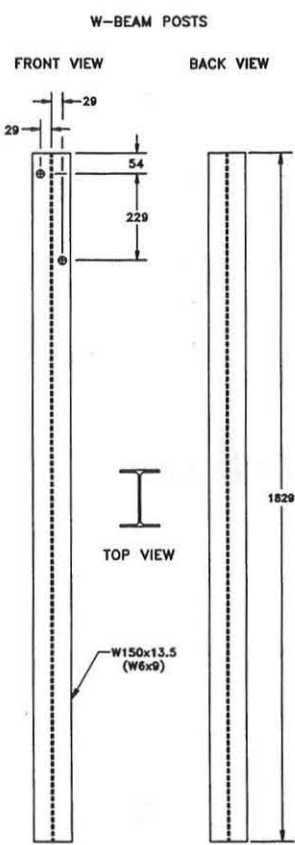
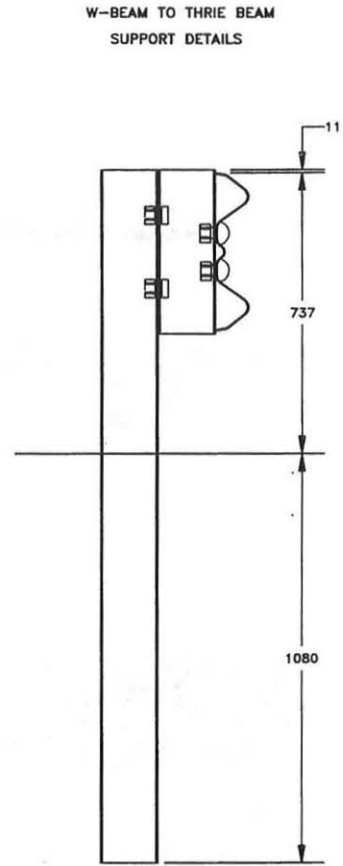


Figure 3. Installation Layout and Design Details, Design No. 1



- Notes:
- (1) Steel for wide-flange posts and spacer blocks shall meet ASTM A36
 - (2) Galvanized
 - (3) All holes punched or drilled to 21mm diameter



- Notes:
- (1) Steel for wide-flange posts and spacer blocks shall meet ASTM A36
 - (2) Galvanized
 - (3) All holes punched or drilled to 13/16" diameter

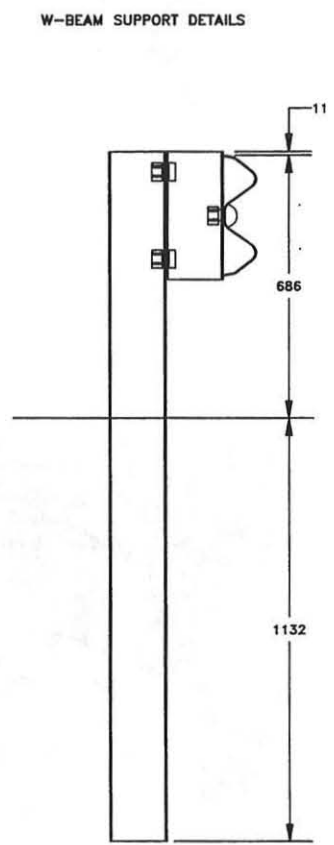


Figure 4. Design Details, Design No. 1

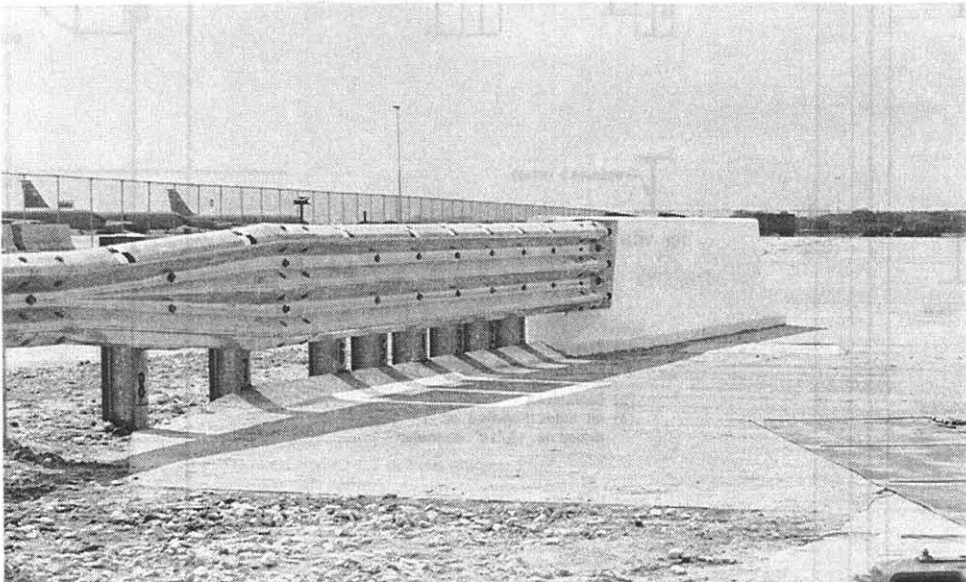
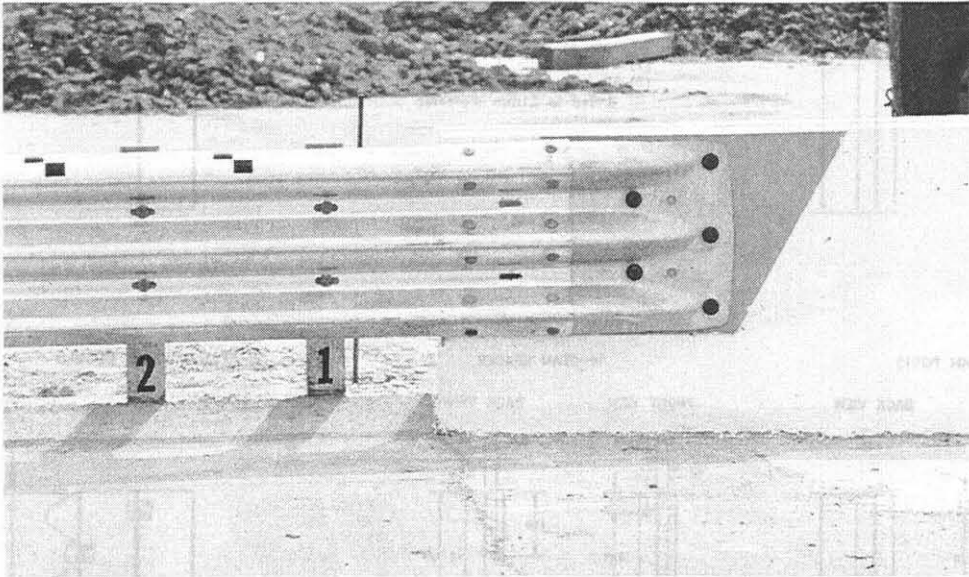
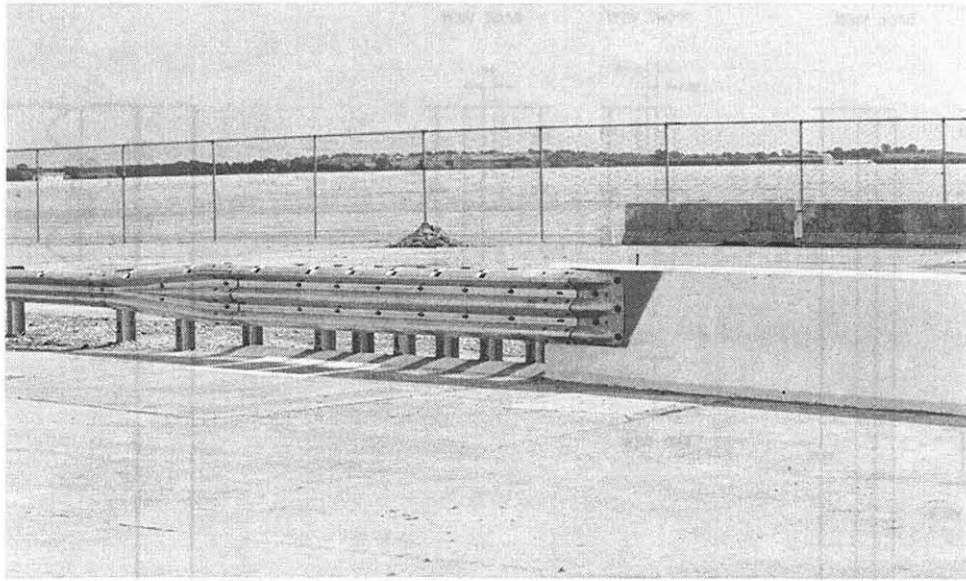


Figure 5. Approach Guardrail Transition, Design No. 1

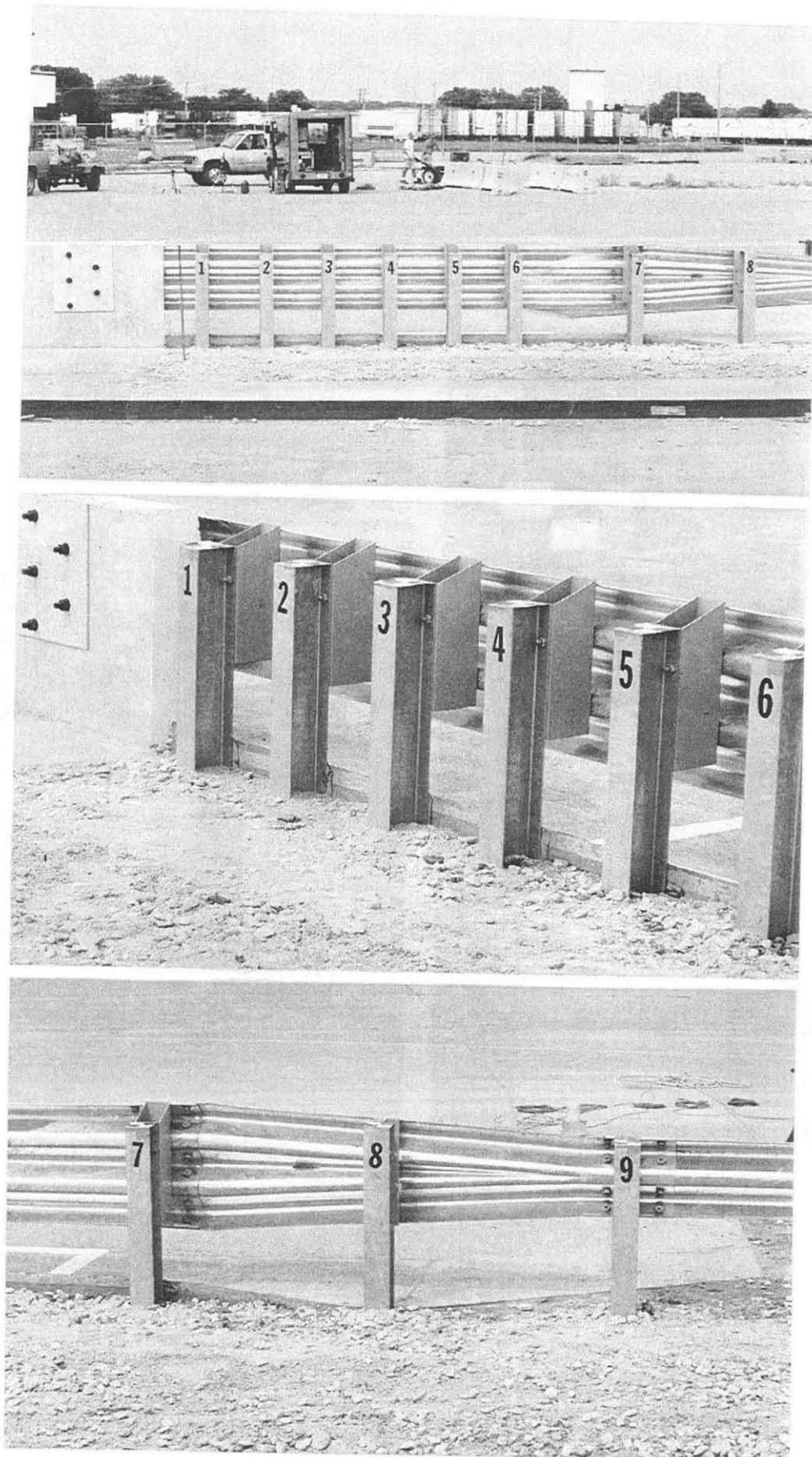


Figure 6. Approach Guardrail Transition, Design No. 1

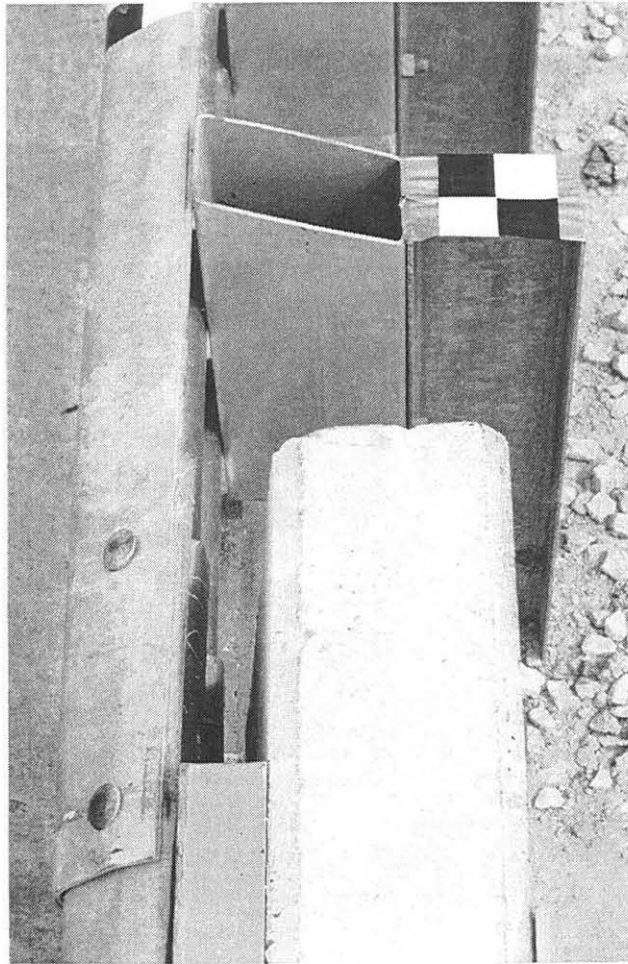
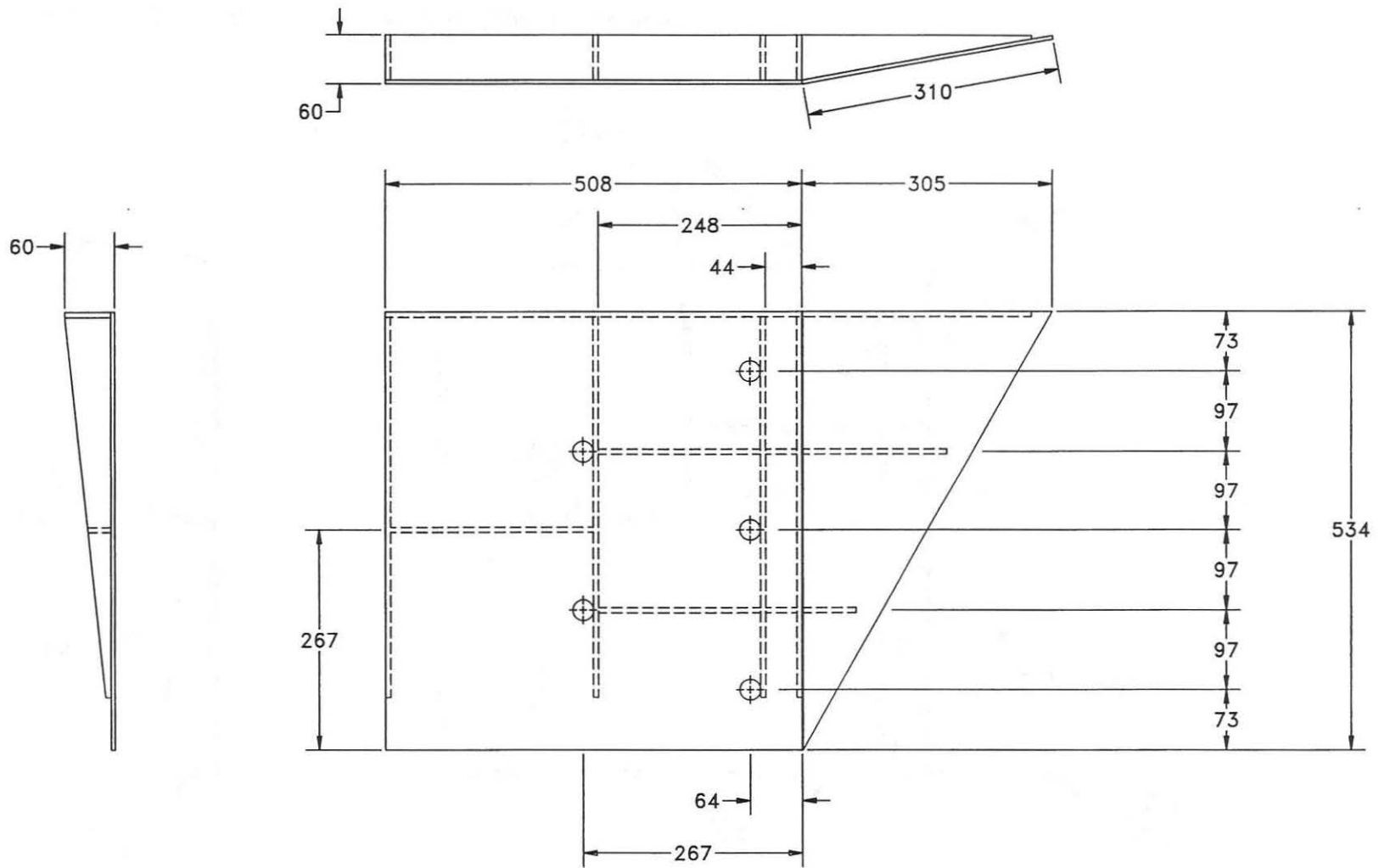


Figure 7. Approach Guardrail Transition, Design No. 1



17

Notes:

1. All steel shall conform to ASTM A36.
2. Flat plate panels are 4.76mm thick.
3. Stiffeners are 6.35mm thick.
4. All hole diameters are 25mm.
5. Weld components with E60 rod.
6. Galvanize or paint.

Welding Instructions:

- (a) Stiffeners located on the outside edges of the cover plates shall be welded as follows: 4.76mm continuous back weld on external sides and 4.76mm fillet weld by 25mm long spaced at 51mm on internal sides.
- (b) Stiffeners located on the inside of the cover plates shall be welded as follows: 4.76mm fillet weld by 25mm long spaced at 51mm.
- (c) Rectangular and triangular cover plates shall be welded together with a 4.76mm continuous back weld on both sides.

Figure 8. New Jersey Connector Plate, Design No. 1

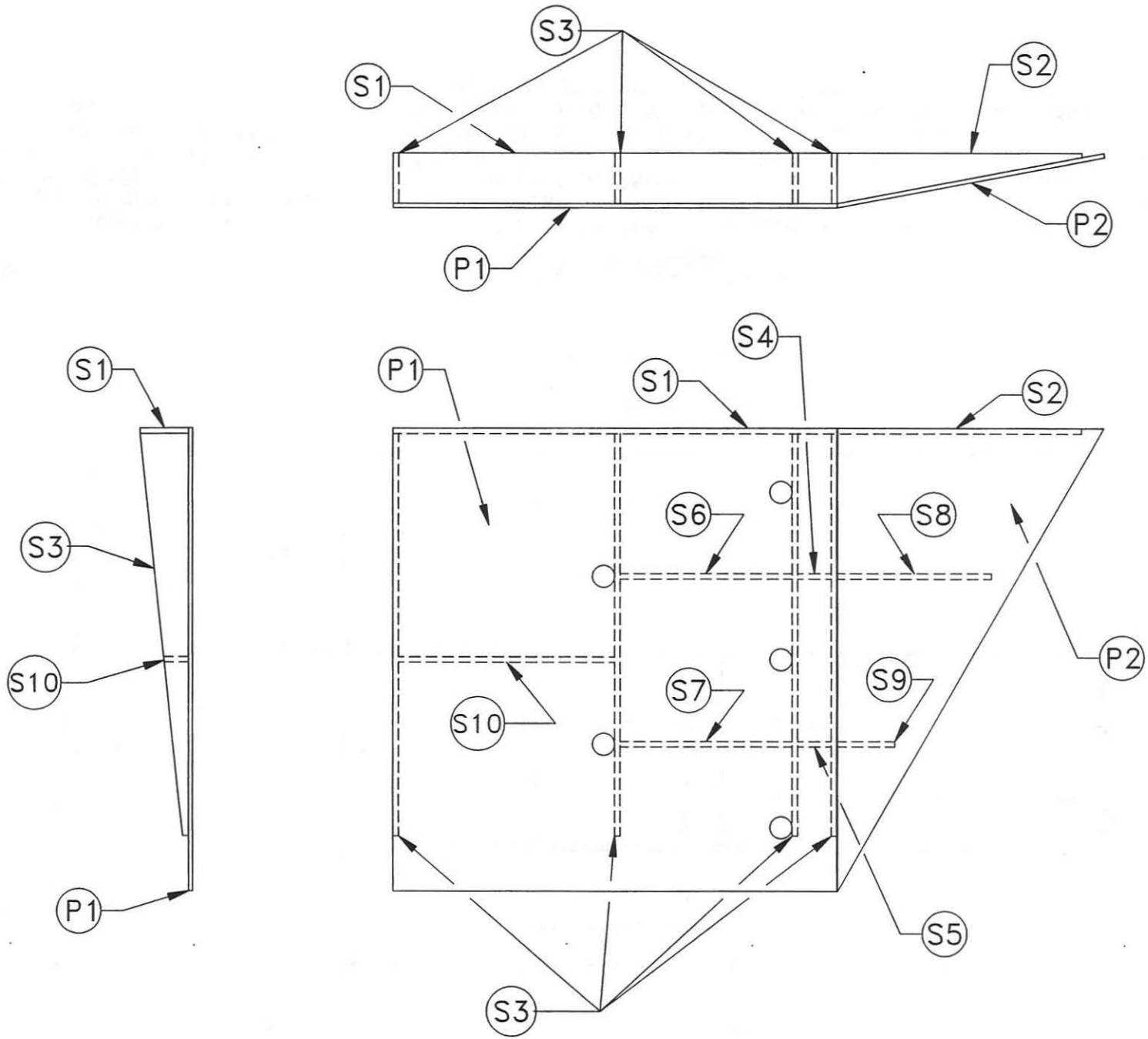
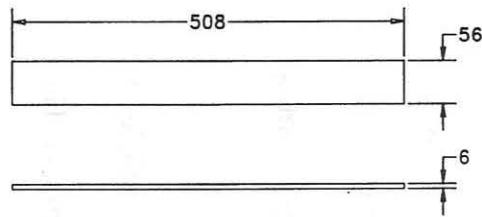
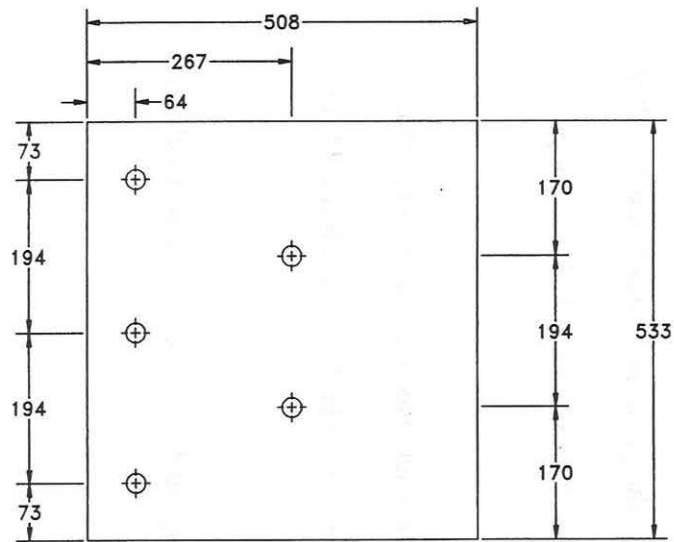
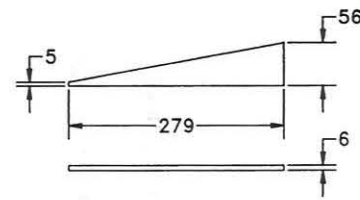


Figure 9. New Jersey Connector Plate Fabrication Details, Design No. 1



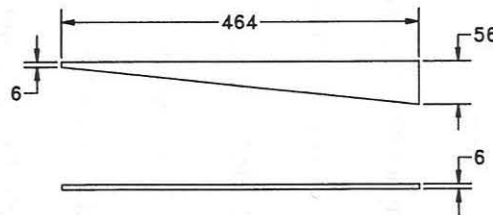
Stiffener #1: 1 each

(S1)



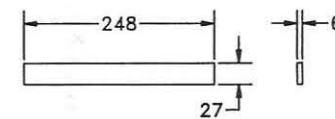
Stiffener #2: 1 each

(S2)



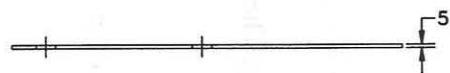
Stiffener #3: 4 each

(S3)



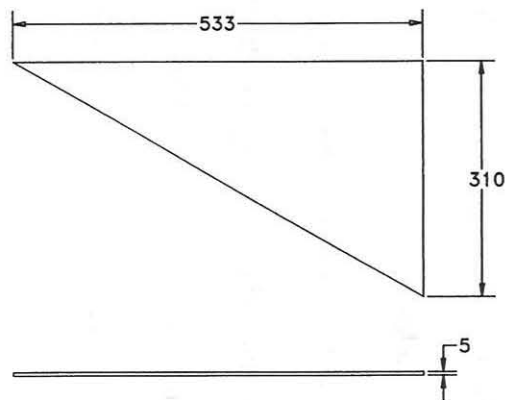
Stiffener #10: 1 each

(S10)



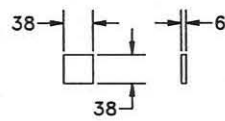
Cover Plate #1

(P1)



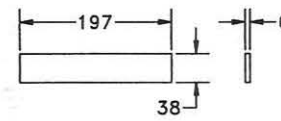
Cover Plate #2

(P2)



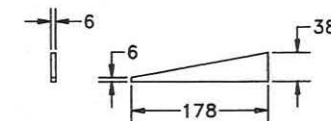
Stiffener #4: 1 each

(S4)



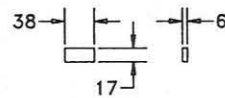
Stiffener #6: 1 each

(S6)



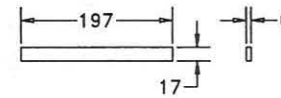
Stiffener #8: 1 each

(S8)



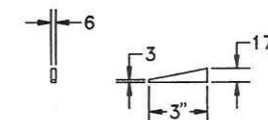
Stiffener #5: 1 each

(S5)



Stiffener #7: 1 each

(S7)



Stiffener #9: 1 each

(S9)

19

Figure 10. New Jersey Connector Plate Steel Components, Design No. 1

6 TEST CONDITIONS

6.1 Test Facility

The testing facility is located at the Lincoln Air-Park on the NW end of the Lincoln Municipal Airport and is approximately 8.0 km NW of the University of Nebraska-Lincoln. The site is protected by an 2.44-m high chain-link security fence.

6.2 Vehicle Tow and Guidance System

A reverse cable tow system with a 1:2 mechanical advantage was used to propel the test vehicles. The distance traveled and the speed of the tow vehicle were one-half that of the test vehicle. The test vehicle was released from the tow cable before impact with the bridge rail. A fifth wheel, built by the Nucleus Corporation, was located on the tow vehicle and used in conjunction with a digital speedometer to increase the accuracy of the test vehicle impact speed.

A vehicle guidance system developed by Hinch (15) was used to steer the test vehicle. A guide-flag, attached to the front-left wheel and the guide cable, was sheared off before impact. The 9.5-mm diameter guide cable was tensioned to approximately 13.3 kN, and supported laterally and vertically every 30.48 m by hinged stanchions. The hinged stanchions stood upright while holding up the guide cable, but as the vehicle was towed down the line, the guide-flag struck and knocked each stanchion to the ground. The vehicle guidance system was approximately 457.2-m long.

6.3 Test Vehicles

For test ITNJ-1, a 1988 Chevrolet C-2500 ¾-ton pickup truck was used as the test vehicle. The test inertial and gross static weights were 1,994 kg. The test vehicle is shown in Figure 11, and vehicle dimensions are shown in Figure 12.

For test ITNJ-2, a 1991 Chevrolet C-2500 ¾-ton pickup truck was used as the test vehicle.

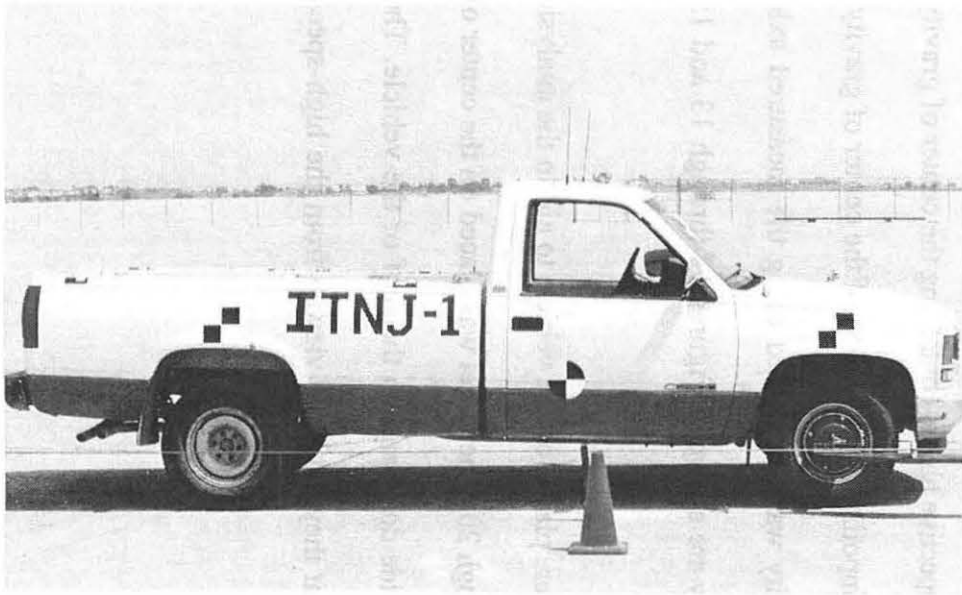
The test inertial and gross static weights were 1,977 kg. The test vehicle is shown in Figure 11, and vehicle dimensions are shown in Figure 13.

For test ITNJ-3, a 1990 Chevrolet C-2500 $\frac{3}{4}$ -ton pickup truck was used as the test vehicle. The test inertial and gross static weights were 1,987 kg. The test vehicle is shown in Figure 14, and vehicle dimensions are shown in Figure 15.

For test ITNJ-4, a 1988 Chevrolet C-2500 $\frac{3}{4}$ -ton pickup truck was used as the test vehicle. The test inertial and gross static weights were 1,999 kg. The test vehicle is shown in Figure 14, and vehicle dimensions are shown in Figure 16.

The Suspension Method (16) was used to determine the vertical component of the center of gravity for the test vehicles. This method is based on the principle that the center of gravity of any freely suspended body is in the vertical plane through the point of suspension. The vehicle was suspended successively in three positions, and the respective planes containing the center of gravity were established. The intersection of these planes pinpointed the location of the center of gravity. The longitudinal component of the center of gravity was determined using the measured axle weights. The location of the final centers of gravity are shown in Figures 12 through 13 and 15 through 16.

Square, black and white-checked targets were placed on the vehicle to aid in the analysis of the high-speed film, as shown in Figures 11 through 20. One target was placed on the center of gravity on the driver's side door, the passenger's side door, and on the roof of the vehicle. The remaining targets were located for reference so that they could be viewed from the high-speed cameras for film analysis.



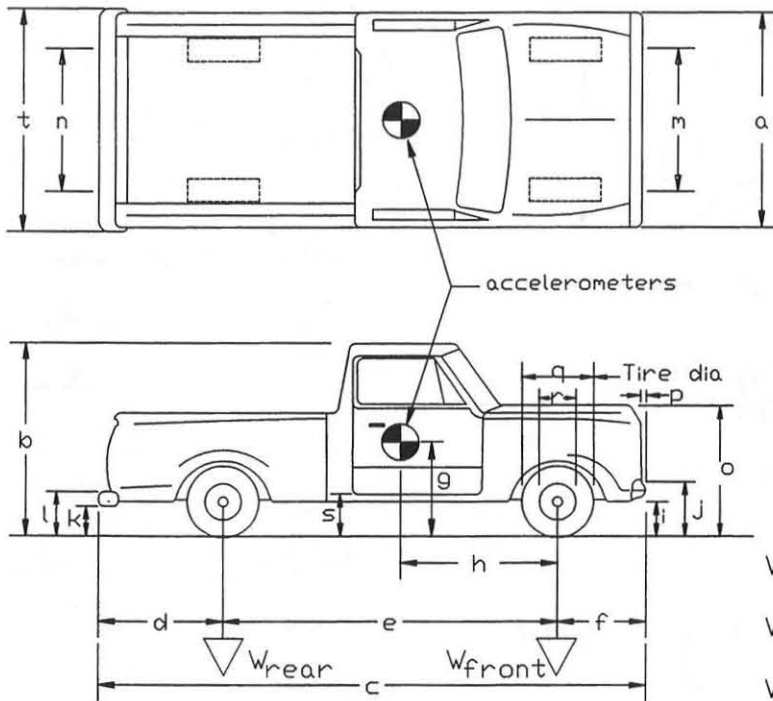
22



Figure 11. Test Vehicles, Test ITNJ-1 and ITNJ-2

Date: 8/21/96 Test Number: ITNJ-1 Model: 2500 Rd/Wh
 Make: Chevrolet Vehicle I.D.#: 1GCFC24K4JE189961
 Tire Size: 225/75 R16 Year: 1988 Odometer: 148051

*(All Measurements Refer to Impacting Side)



Vehicle Geometry - mm

a 1880 b 1784
 c 5525 d 1321
 e 3340 f 876
 g 686 h 1430
 i 387 j 570
 k 546 l 730
 m 1588 n 1613
 o 965 p 76
 q 737 r 445
 s 425 t 1848

Wheel Center Height Front 356
 Wheel Center Height Rear 356
 Wheel Well Clearance (FR) 845
 Wheel Well Clearance (RR) 908

Engine Type 5.7 L

Engine Size V8

Transmission Type:

Automatic or Manual

FWD or RWD or 4WD

Weights	- kg	Curb	Test Inertial	Gross Static
W_{front}	<u>1190</u>	<u>1130</u>	<u>1130</u>	<u>1130</u>
W_{rear}	<u>929</u>	<u>864</u>	<u>864</u>	<u>864</u>
W_{total}	<u>2119</u>	<u>1994</u>	<u>1994</u>	<u>1994</u>

Note any damage prior to test: NONE

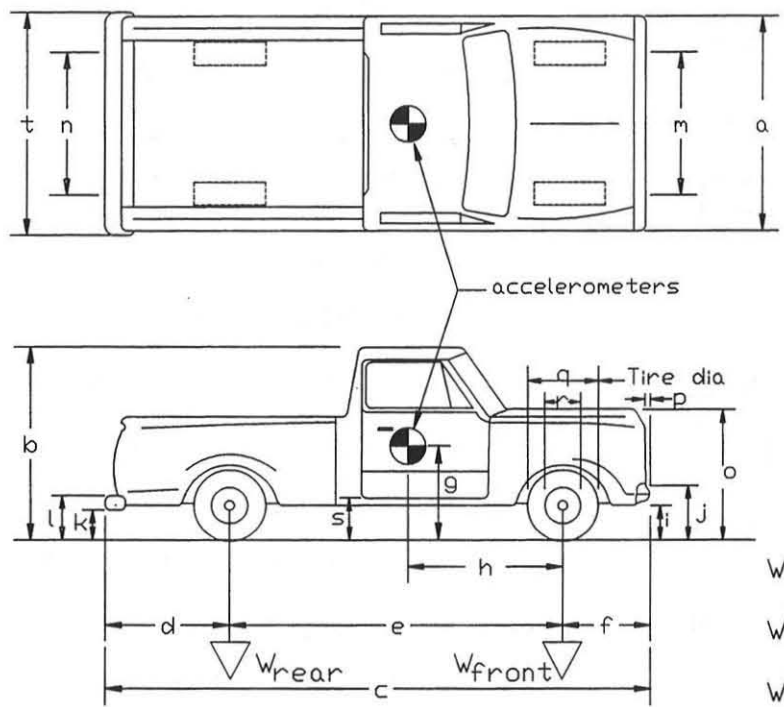
Figure 12. Vehicle Dimensions, Test ITNJ-1

Date: 5-30-97 Test Number: ITNJ-2 Model: 2500
 Make: Chevrolet Vehicle I.D.#: 1GCFE24Z0M2202845
 Tire Size: 245/75 R16 Year: 1991 Odometer: 138299

*(All Measurements Refer to Impacting Side)

Vehicle Geometry - mm

- a 1867 b 1784
- c 5480 d 1238
- e 3340 f 902
- g 728 h 1498
- i 400 j 603
 572 I.S. 730 I.S.
- k 616 nonI.S. l 781 nonI.S.
- m 1588 n 1600
- o 1003 p 83
- q 768 r 438
- s 406 t 1873



- Wheel Center Height Front 368
- Wheel Center Height Rear 368
- Wheel Well Clearance (FR) 832
- Wheel Well Clearance (RR) 864

Weights	Curb	Test Inertial	Gross Static
- kg			
W _{front}	<u>952</u>	<u>1091</u>	<u>1091</u>
W _{rear}	<u>770</u>	<u>886</u>	<u>886</u>
W _{total}	<u>1722</u>	<u>1977</u>	<u>1977</u>

Engine Type V6
 Engine Size 4.3 L
 Transmission Type:
 Automatic or Manual
 FWD or RWD or 4WD

Note any damage prior to test: RR sprung inward, previously used on BEST testing

Figure 13. Vehicle Dimensions, Test ITNJ-2

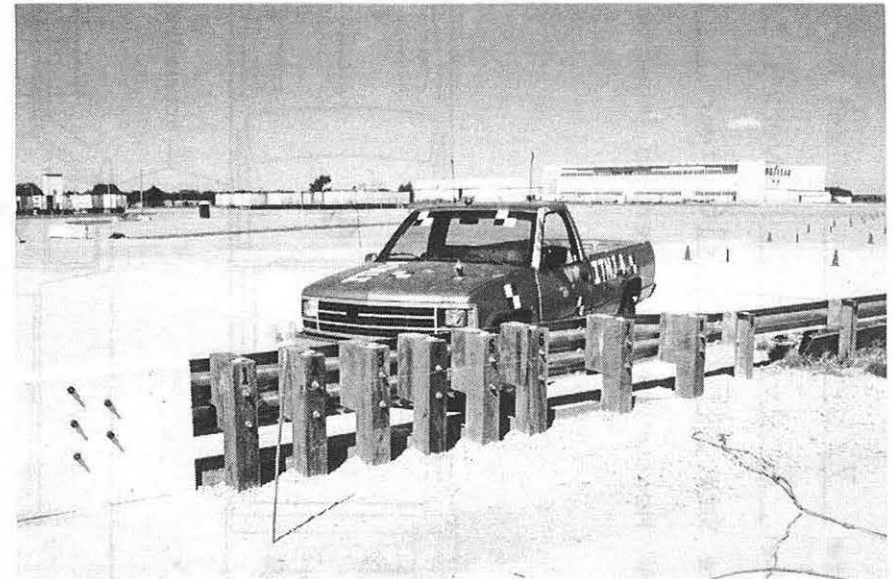


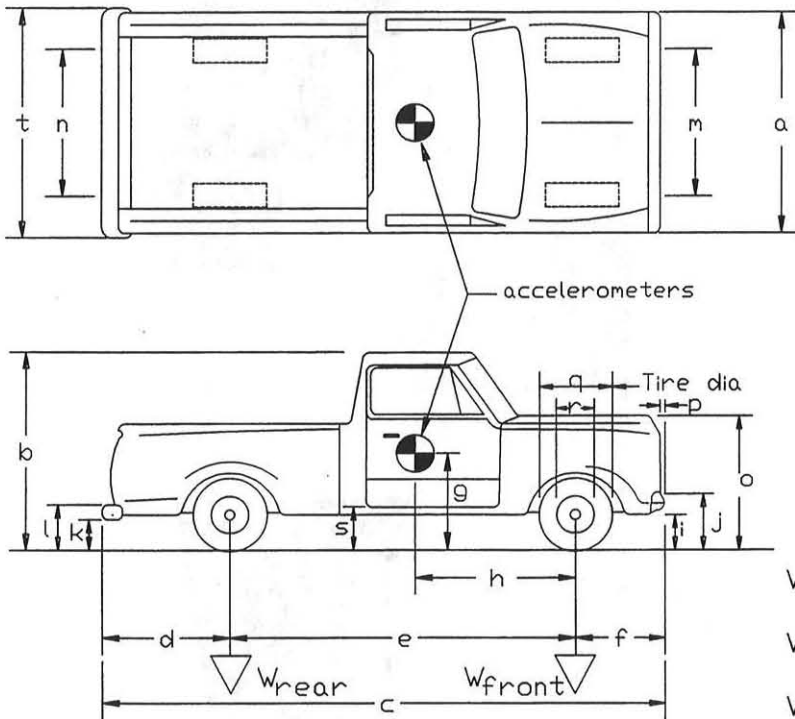
Figure 14. Test Vehicles, Test ITNJ-3 and ITNJ-4

Date: 7/8/97 Test Number: ITNJ-3 Model: 2500

Make: Chevrolet Vehicle I.D.#: 1GCFC24K3LZ255086

Tire Size: 245/75 R16 Year: 1990 Odometer: 132915

*All Measurements Refer to Impacting Side



Vehicle Geometry - mm

a 1880 b 1778
 c 5448 d 1295
 e 3340 f 813
 g 711 h 1454
 i 381 j 597
 k 641/514 l 756
 m 1588 n 1613
 o 1041 p 76
 q 768 r 445
 s 406 t 1867

Wheel Center Height Front 368
 Wheel Center Height Rear 368
 Wheel Well Clearance (FR) 832
 Wheel Well Clearance (RR) 902

Engine Type V-6

Engine Size 3.8 L

Transmission Type:

Automatic or Manual

FWD or RWD or 4WD

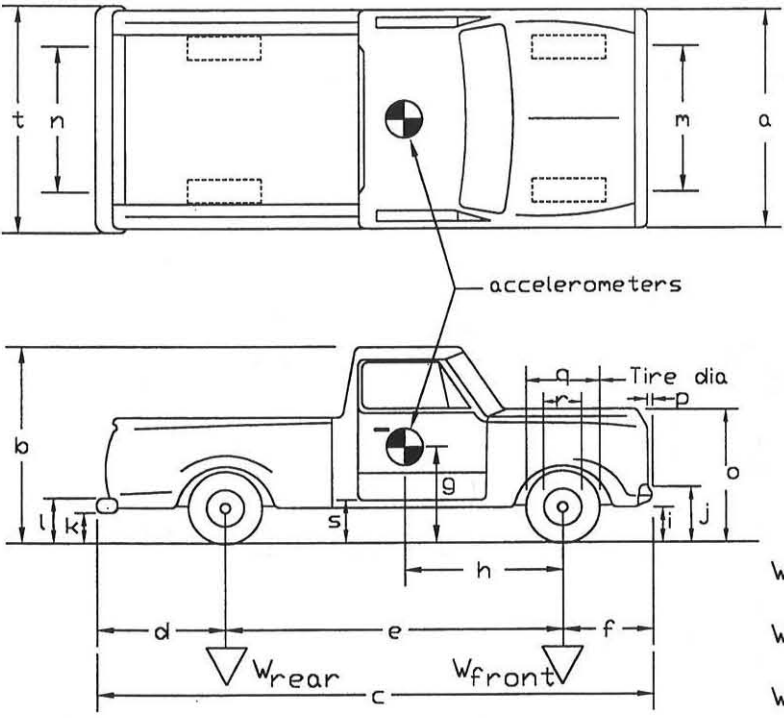
Weights			
- kg	Curb	Test Inertial	Gross Static
W_{front}	<u>1031</u>	<u>1125</u>	<u>1125</u>
W_{rear}	<u>786</u>	<u>866</u>	<u>866</u>
W_{total}	<u>1817</u>	<u>1991</u>	<u>1991</u>

Note any damage prior to test: _____

Figure 15. Vehicle Dimensions, Test ITNJ-3

Date: 9/10/97 Test Number: ITNJ-4 Model: 2500
 Make: Chevrolet Vehicle I.D.#: 1GCFC24K3KZ120317
 Tire Size: 225/75 R16 Year: 1988 Odometer: 232868

*(All Measurements Refer to Impacting Side)



Vehicle Geometry - mm

a	<u>1905</u>	b	<u>1772</u>
c	<u>5486</u>	d	<u>1283</u>
e	<u>3353</u>	f	<u>851</u>
g	<u>713</u>	h	<u>1492</u>
i	<u>381</u>	j	<u>597</u>
k	<u>508</u>	l	<u>705</u>
m	<u>1588</u>	n	<u>1613</u>
o	<u>1016</u>	p	<u>76</u>
q	<u>749</u>	r	<u>432</u>
s	<u>394</u>	t	<u>1829</u>

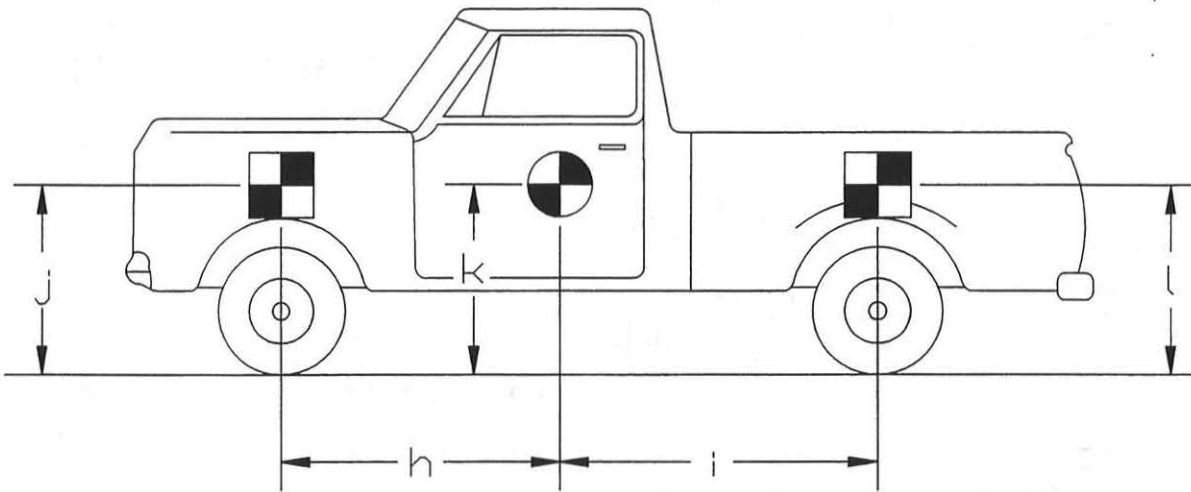
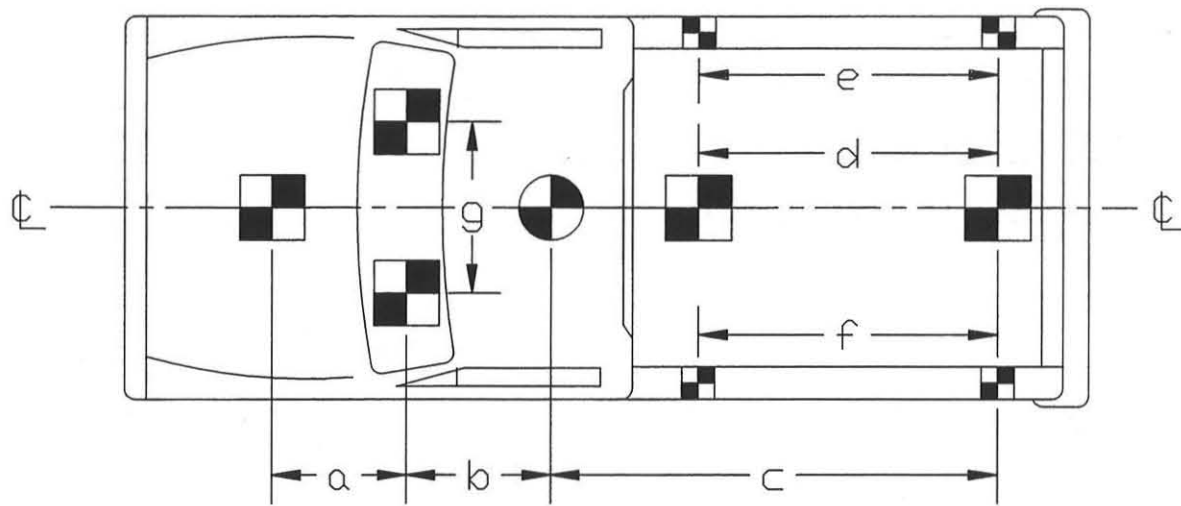
Wheel Center Height Front 343
 Wheel Center Height Rear 870
 Wheel Well Clearance (FR) 356
 Wheel Well Clearance (RR) 819

Engine Type V-8
 Engine Size 350
 Transmission Type:
 Automatic or Manual
 FWD or RWD or 4WD

Weights	Curb	Test Inertial	Gross Static
- kg			
W _{front}	<u>1110</u>	<u>1112</u>	<u>1112</u>
W _{rear}	<u>903</u>	<u>892</u>	<u>892</u>
W _{total}	<u>2013</u>	<u>2004</u>	<u>2004</u>

Note any damage prior to test: _____

Figure 16. Vehicle Dimensions, Test ITNJ-4

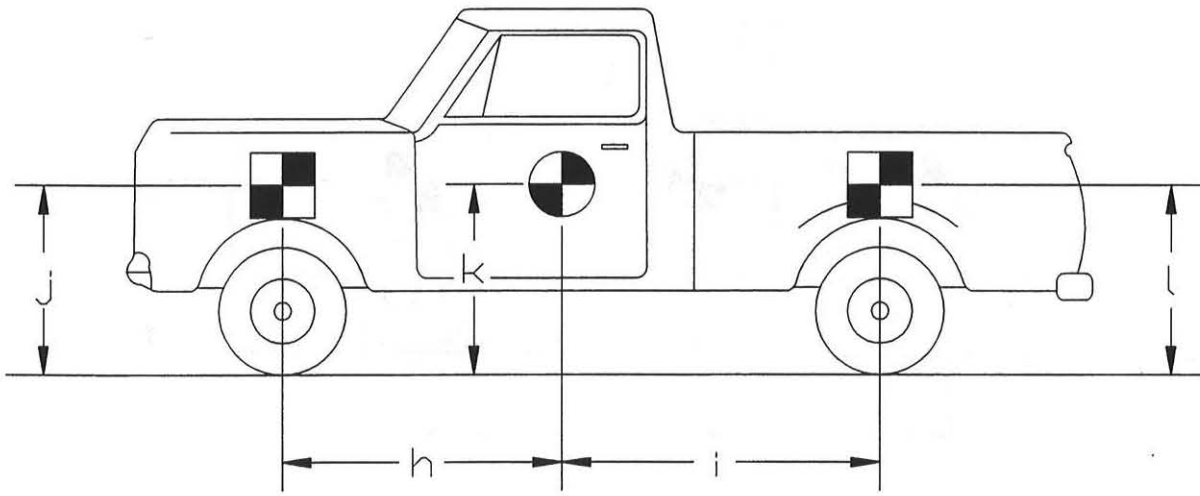
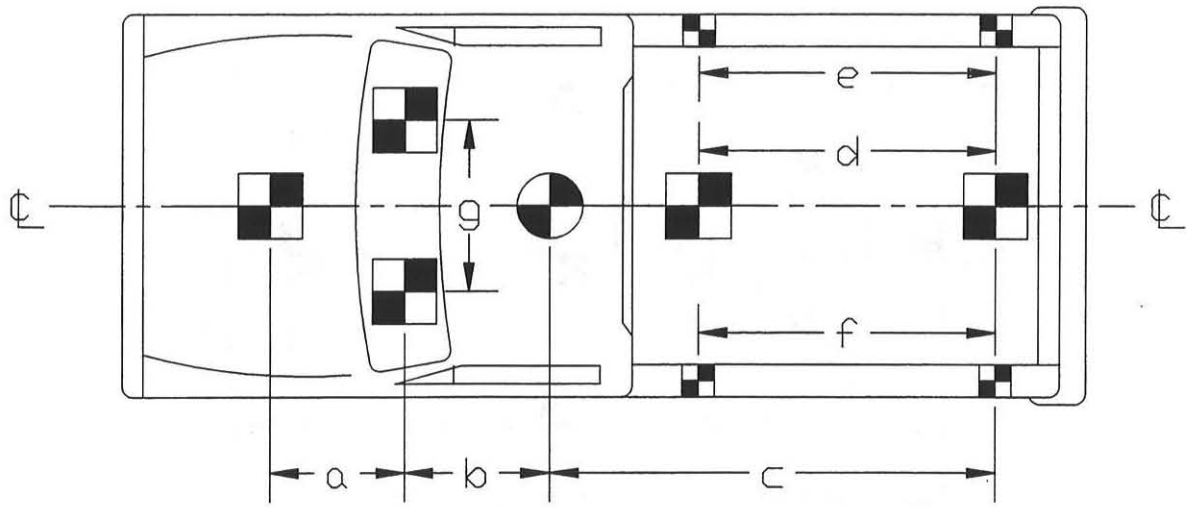


TEST #: ITNJ-1

TARGET GEOMETRY (mm)

a	<u>838</u>	b	<u>610</u>	c	<u>2686</u>	d	<u>1835</u>
e	<u>1835</u>	f	<u>1835</u>	g	<u>946</u>	h	<u>1448</u>
i	<u>1861</u>	j	<u>972</u>	k	<u>711</u>	l	<u>1010</u>

Figure 17. Vehicle Target Locations, Test ITNJ-1

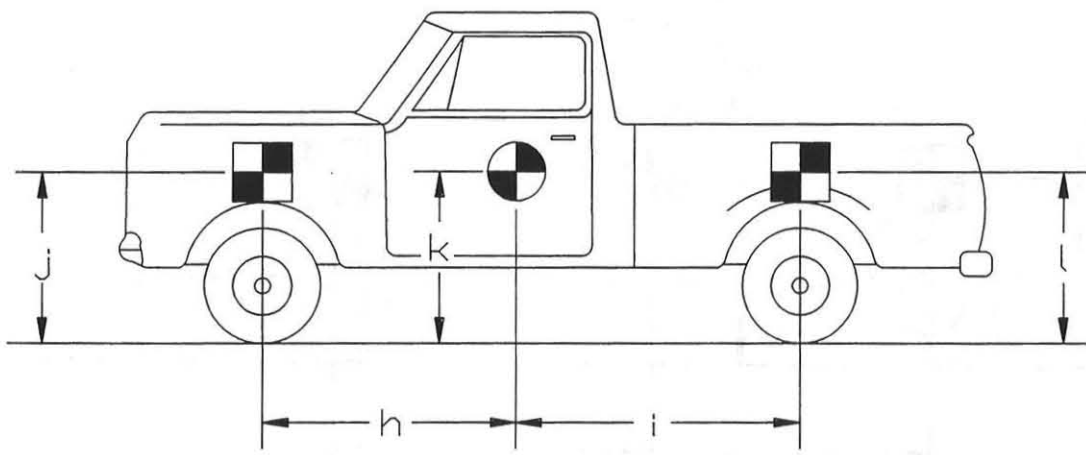
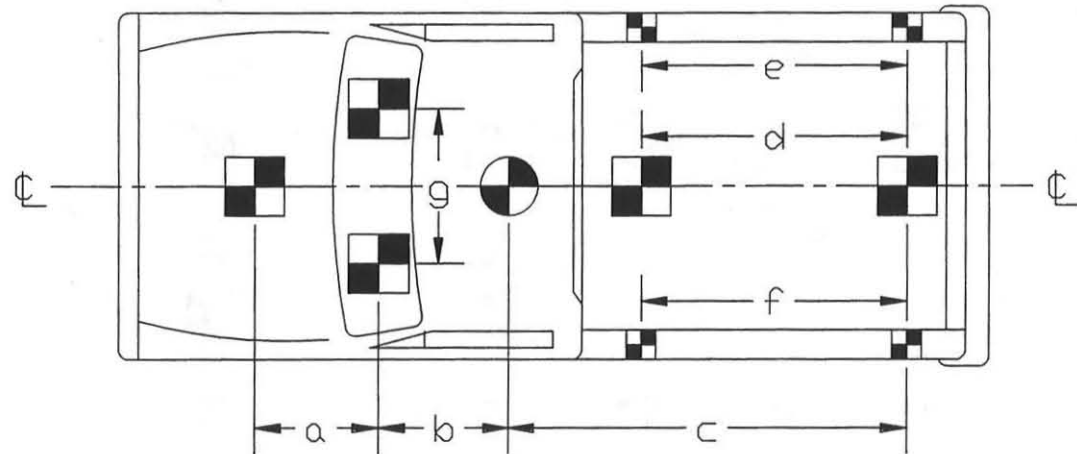


TEST #: ITNJ-2

TARGET GEOMETRY (mm)

a	<u>762</u>	b	<u>781</u>	c	<u>2553</u>	d	<u>1600</u>
e	<u>1746</u>	f	<u>1746</u>	g	<u>940</u>	h	<u>1505</u>
i	<u>1842</u>	j	<u>965</u>	k	<u>724</u>	l	<u>1041</u>

Figure 18. Vehicle Target Locations, Test ITNJ-2

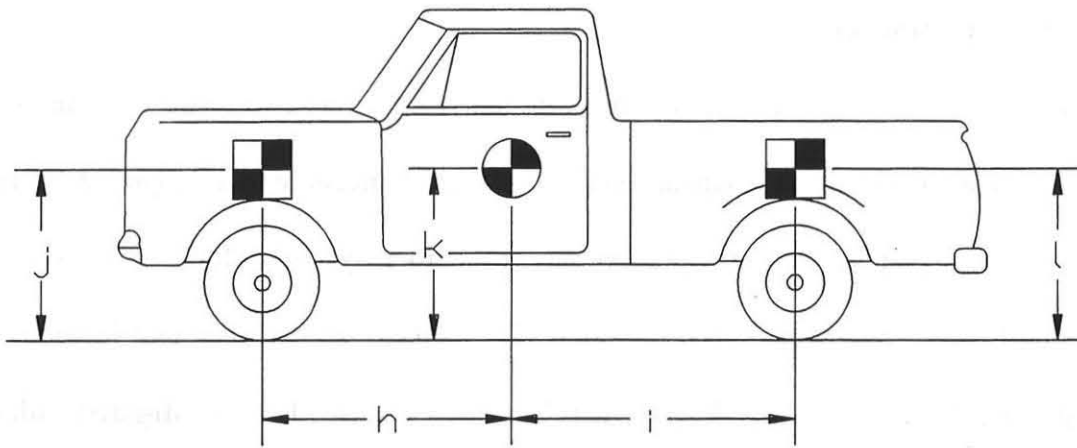
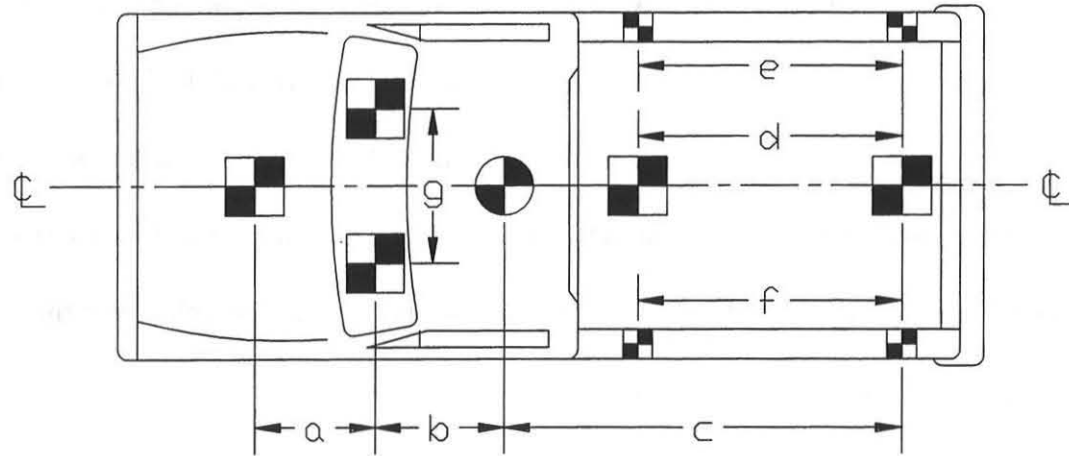


TEST #: ITNJ-3

TARGET GEOMETRY (mm)

a	<u>724</u>	b	<u>730</u>	c	<u>2572</u>	d	<u>1778</u>
e	<u>1740</u>	f	<u>1746</u>	g	<u>940</u>	h	<u>1454</u>
i	<u>1861</u>	j	<u>965</u>	k	<u>711</u>	l	<u>1048</u>

Figure 19. Vehicle Target Locations, Test ITNJ-3



TEST #: ITNJ-4

TARGET GEOMETRY (mm)

a	<u>1181</u>	b	<u>635</u>	c	<u>2591</u>	d	<u>1575</u>
e	<u>1549</u>	f	<u>1549</u>	g	<u>889</u>	h	<u>1492</u>
i	<u>1822</u>	j	<u>953</u>	k	<u>711</u>	l	<u>1016</u>

Figure 20. Vehicle Target Locations, Test ITNJ-4

The front wheels of the test vehicle were aligned for camber, caster, and toe-in values of zero so that the vehicles would track properly along the guide cable. Two 5B flash bulbs were mounted on both the hood and roof of the vehicles to pinpoint the time of impact with the bridge railing on the high-speed film. The flash bulbs were fired by a pressure tape switch mounted on the front face of the bumper. A remote controlled brake system was installed in the test vehicle so the vehicle could be brought safely to a stop after the test.

6.4 Data Acquisition Systems

6.4.1 Accelerometers

One triaxial piezoresistive accelerometer system with a range of ± 200 G's was used to measure the acceleration in the longitudinal, lateral, and vertical directions at a sample rate of 10,000 Hz. The environmental shock and vibration sensor/recorder system, Model EDR-4M6, was developed by Instrumented Sensor Technology (IST) of Okemos, Michigan and includes three differential channels as well as three single-ended channels. The EDR-4 was configured with 6 Mb of RAM memory and a 1,500 Hz lowpass filter. Computer software, "DynaMax 1 (DM-1)" and "DADiSP" were used to digitize, analyze, and plot the accelerometer data.

A backup triaxial piezoresistive accelerometer system with a range of ± 200 G's was also used to measure the acceleration in the longitudinal, lateral, and vertical directions at a sample rate of 3,200 Hz. The environmental shock and vibration sensor/recorder system, Model EDR-3, was developed by Instrumented Sensor Technology (IST) of Okemos, Michigan. The EDR-3 was configured with 256 Kb of RAM memory and a 1,120 Hz lowpass filter. Computer software, "DynaMax 1 (DM-1)" and "DADiSP" were used to digitize, analyze, and plot the accelerometer data.

6.4.2 Rate Transducer

A Humphrey 3-axis rate transducer with a range of 250 deg/sec in each of the three directions (pitch, roll, and yaw) was used to measure the rates of motion of the test vehicle. The rate transducer was rigidly attached to the vehicles near the center of gravity of the test vehicle. Rate transducer signals, excited by a 28 volt DC power source, were received through the three single-ended channels located externally on the EDR-4M6 and stored in the internal memory. The raw data measurements were then downloaded for analysis and plotted. Computer software, "DynaMax 1 (DM-1)" and "DADiSP" were used to digitize, analyze, and plot the rate transducer data.

6.4.3 High-Speed Photography

For test ITNJ-1, four high-speed 16-mm Red Lake Locam cameras, with operating speeds of approximately 500 frames/sec, were used to film the crash test. A Locam with a wide-angle 12.5-mm lens was placed above the test installation to provide a field of view perpendicular to the ground. A Locam with a zoom lens was placed downstream from the impact point and had a field of view parallel to the barrier. A Locam with a zoom lens was placed on the traffic side of the barrier and had a field of view perpendicular to the barrier. A Locam with a 12.5-mm lens was placed upstream and behind the barrier. A schematic of all four camera locations for test ITNJ-1 is shown in Figure 21.

For test ITNJ-2, five high-speed 16-mm cameras, with operating speeds of approximately 500 frames/sec, were used to film the crash test. A Locam with a wide-angle 12.5-mm lens was placed above the test installation to provide a field of view perpendicular to the ground. A Locam with a 76-mm lens was placed downstream from the impact point and had a field of view parallel to the barrier. A Locam with a 17 to 102-mm zoom lens was placed on the traffic side of the barrier and had a field of view perpendicular to the barrier. A Locam was placed upstream and behind the

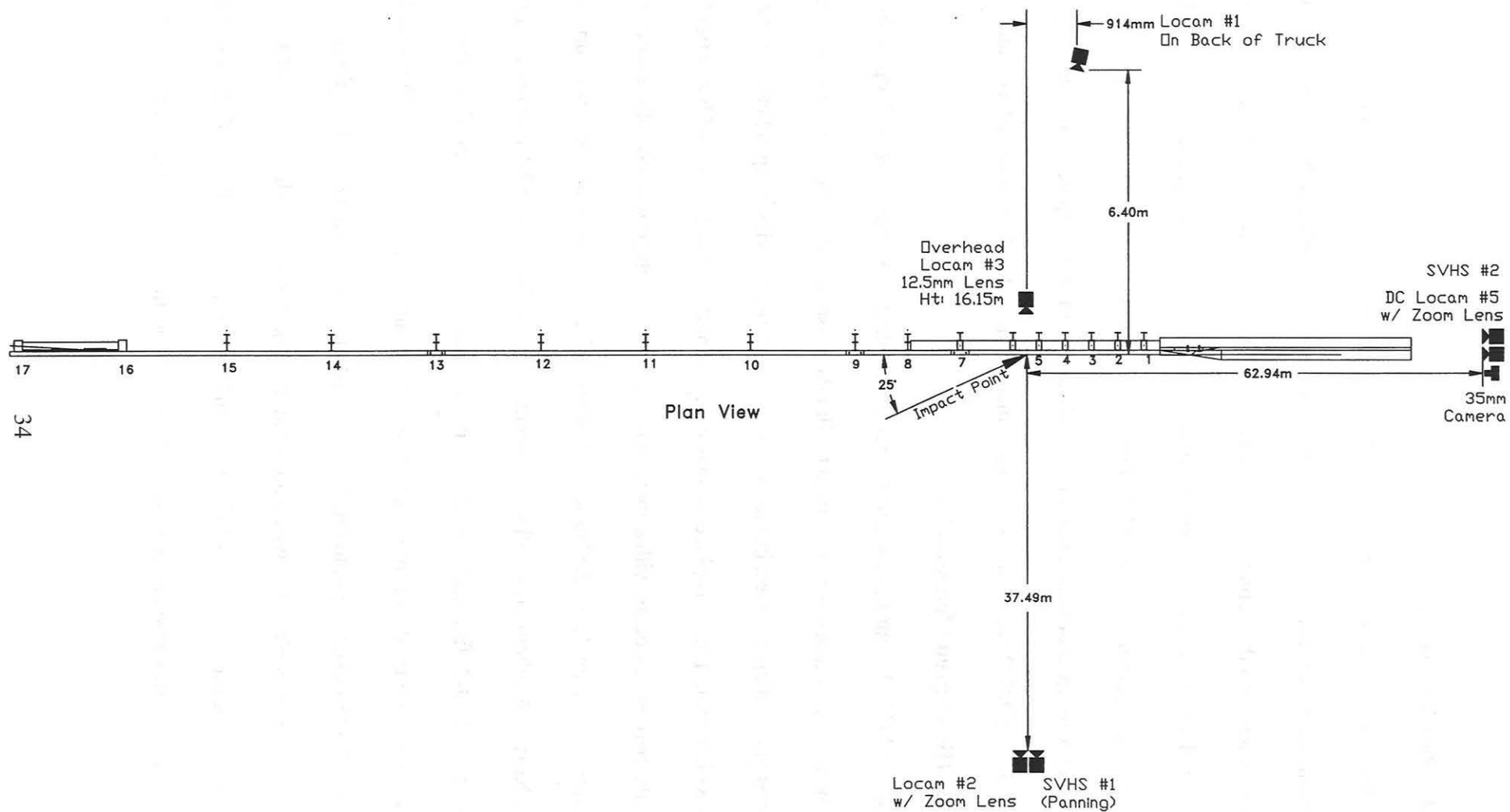


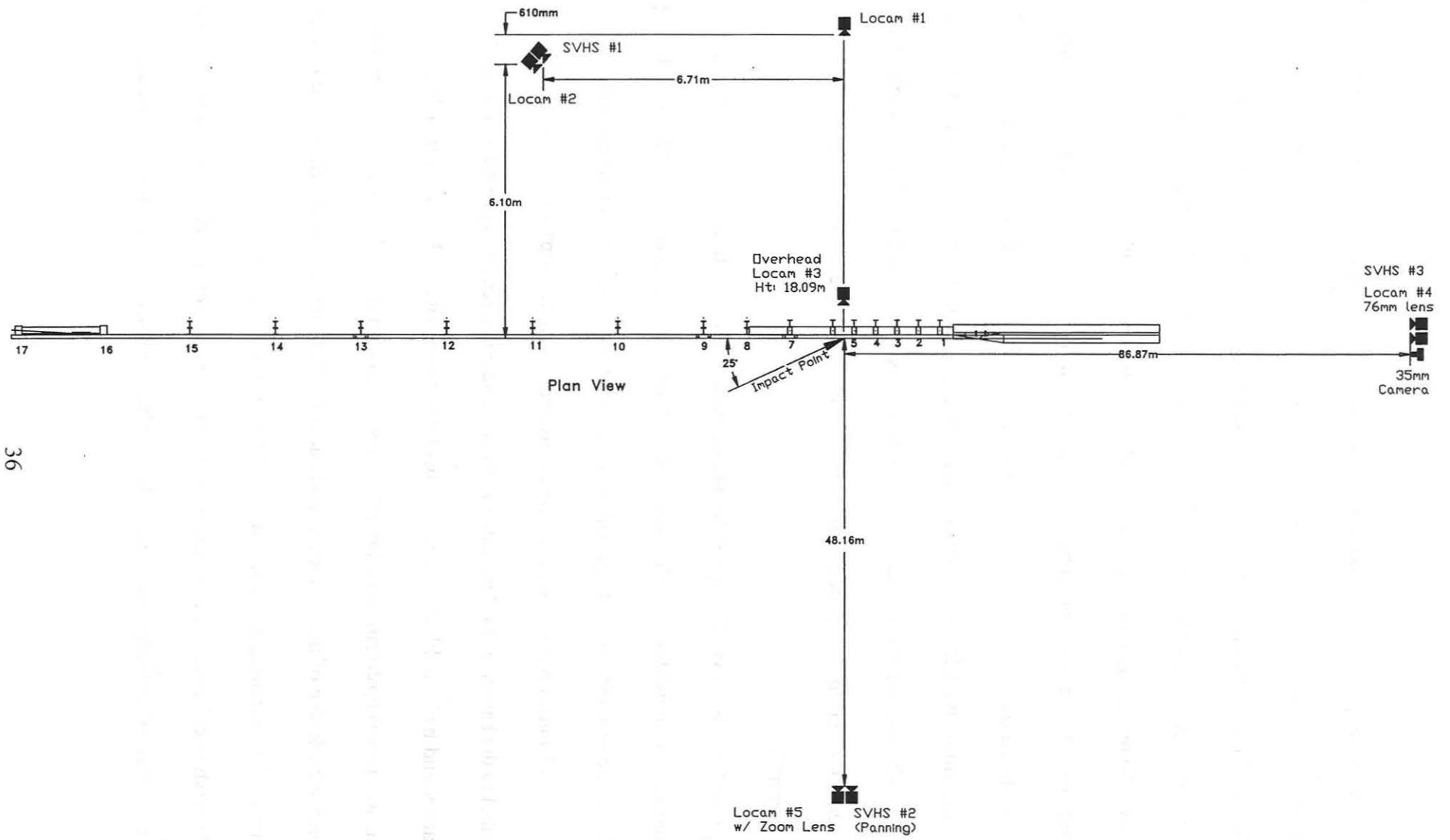
Figure 21. Location of High-Speed Cameras, Test ITNJ-1

barrier. A Locam was placed on the back side of the bridge rail and had a field of view perpendicular to the barrier. A schematic of all five camera locations for test ITNJ-2 is shown in Figure 22.

For test ITNJ-3, five high-speed 16-mm cameras, with operating speeds of approximately 500 frames/sec, were used to film the crash test. A Locam with a wide-angle 12.5-mm lens was placed above the test installation to provide a field of view perpendicular to the ground. A Locam was placed downstream from the impact point and had a field of view parallel to the barrier. A Locam was placed on the traffic side of the barrier and had a field of view perpendicular to the barrier. A Locam with a 12.5 to 75-mm zoom lens was placed upstream and behind the barrier. A Locam with a 12.5 to 75-mm zoom lens was placed on the back side of the bridge rail and had a field of view perpendicular to the barrier. A schematic of all five camera locations for test ITNJ-3 is shown in Figure 23.

For test ITNJ-4, five high-speed 16-mm cameras, with operating speeds of approximately 500 frames/sec, were used to film the crash test. A Locam with a wide-angle 12.5-mm lens was placed above the test installation to provide a field of view perpendicular to the ground. A Locam with a 12.5 to 75-mm zoom lens was placed downstream from the impact point and had a field of view parallel to the barrier. A Locam with a 17 to 102-mm zoom lens was placed on the traffic side of the barrier and had a field of view perpendicular to the barrier. A Locam with a 16 to 64-mm zoom lens was placed upstream and behind the barrier. A Locam with a 16 to 64-mm zoom lens was placed on the back side of the bridge rail and had a field of view perpendicular to the barrier. A schematic of all five camera locations for test ITNJ-4 is shown in Figure 24.

Two white-colored grid, approximately 660-mm square, were painted on the concrete surface on the traffic side of the bridge rail to provide a visible reference system for use in the analysis of



36

Figure 22. Location of High-Speed Cameras, Test ITNJ-2

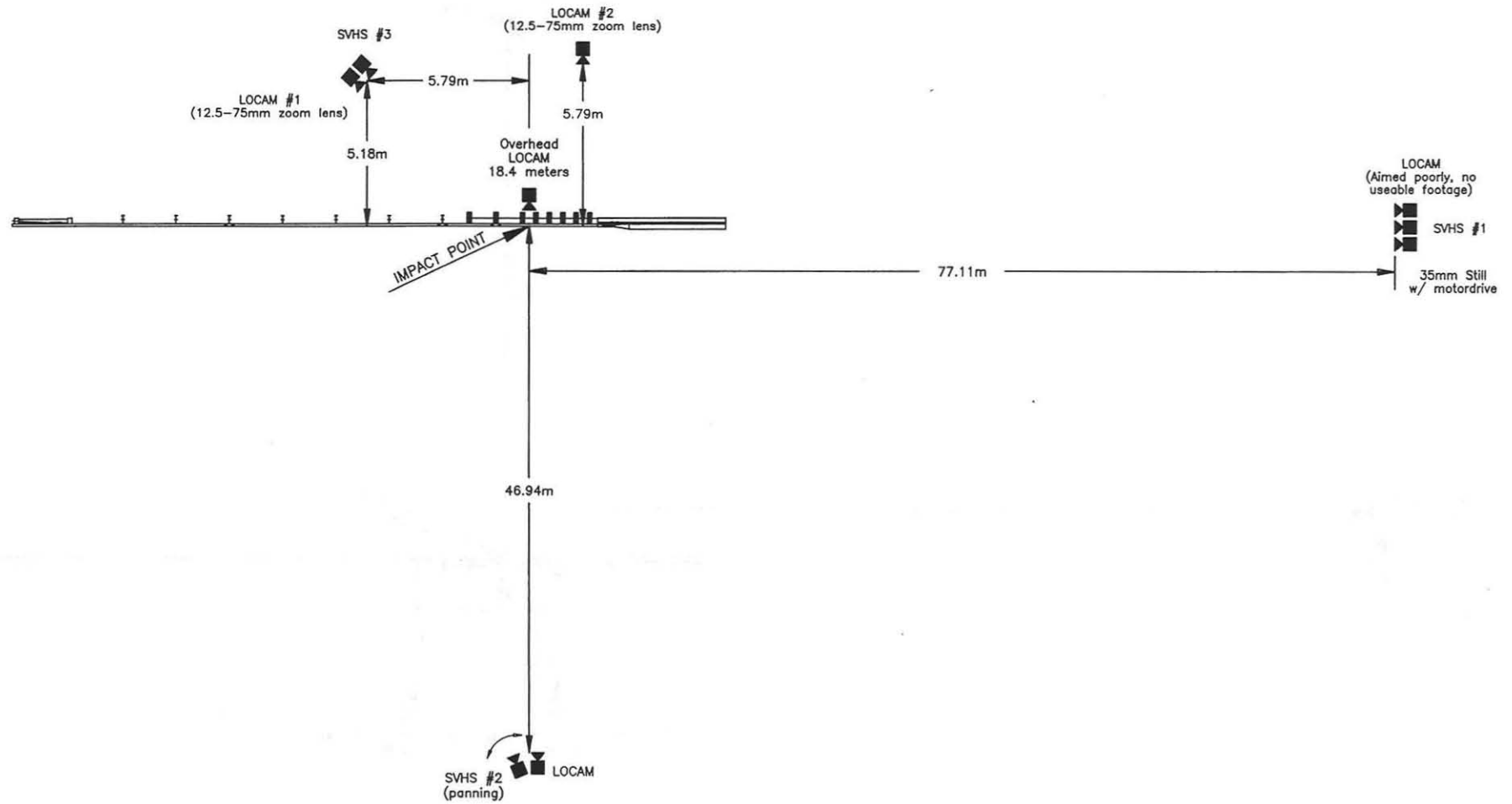


Figure 23. Location of High-Speed Cameras, Test ITNJ-3

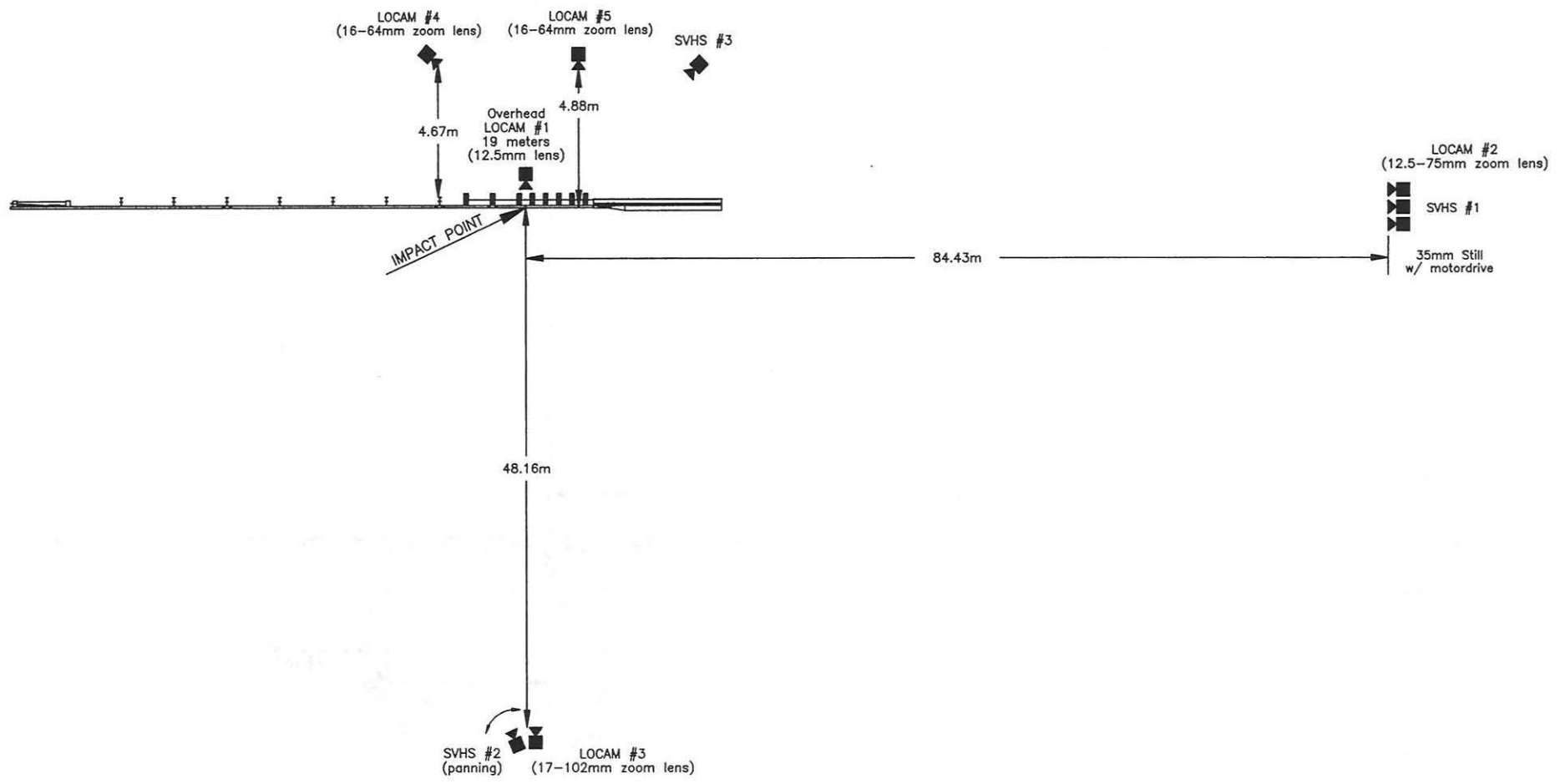


Figure 24. Location of High-Speed Cameras, Test ITNJ-4

the overhead high-speed film. The film was analyzed using the Vanguard Motion Analyzer. Actual camera speed and camera divergence factors were considered in the analysis of the high-speed film.

6.4.4 Pressure Tape Switches

For test ITNJ-1, four pressure-activated tape switches, spaced at 2-m intervals, were used to determine the speed of the vehicle before impact. For tests ITNJ-2 through ITNJ-4, five pressure-activated tape switches, spaced at 2-m intervals, were used to determine the speed of the vehicle before impact. Each tape switch fired a strobe light which sent an electronic timing signal to the data acquisition system as the left front tire of the test vehicle passed over it. Test vehicle speeds were determined from electronic timing mark data recorded on "EGAA" software. Strobe lights and high-speed film analysis are used only as a backup in the event that vehicle speeds cannot be determined from the electronic data.

6.4.5 Approach Guardrail Transition Instrumentation

For tests ITNJ-2 and ITNJ-3, electronic sensors were placed on selected regions and components of the approach guardrail transition (i.e., three beam rail and steel posts). Two types of sensors, strain gauges and string potentiometers, were used for the crash tests and are described below.

Strain Gauges

For test ITNJ-2, sixteen strain gauges were installed on the three beam guardrail and steel posts, consisting of ten gauges located on the back side of the three beam rail and six gauges located on the back side of the steel posts. The strain gauge positions are shown in Figure 25.

For test ITNJ-3, eighteen strain gauges were installed on the back side of the three beam guardrail. The strain gauge positions are shown in Figure 26.

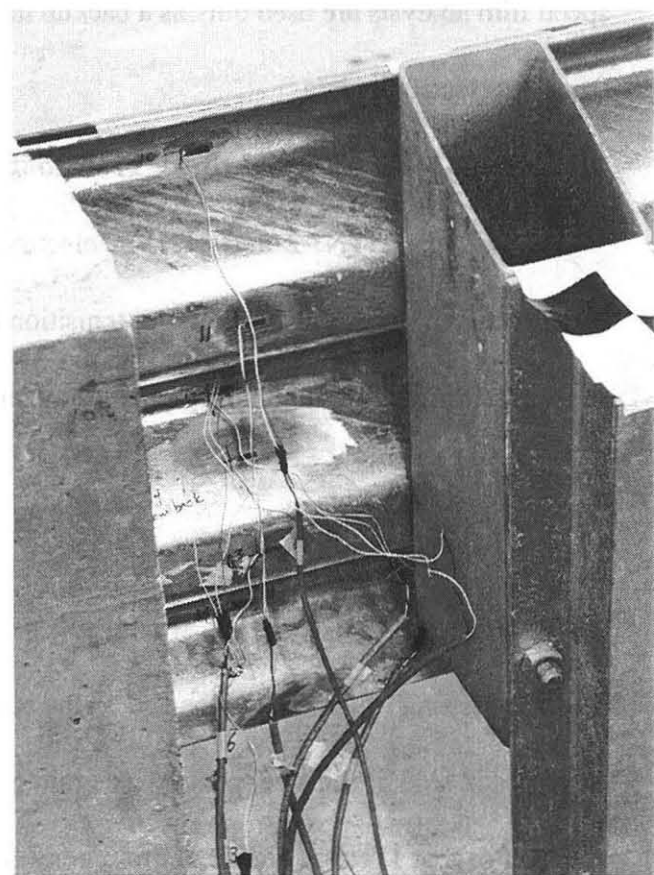
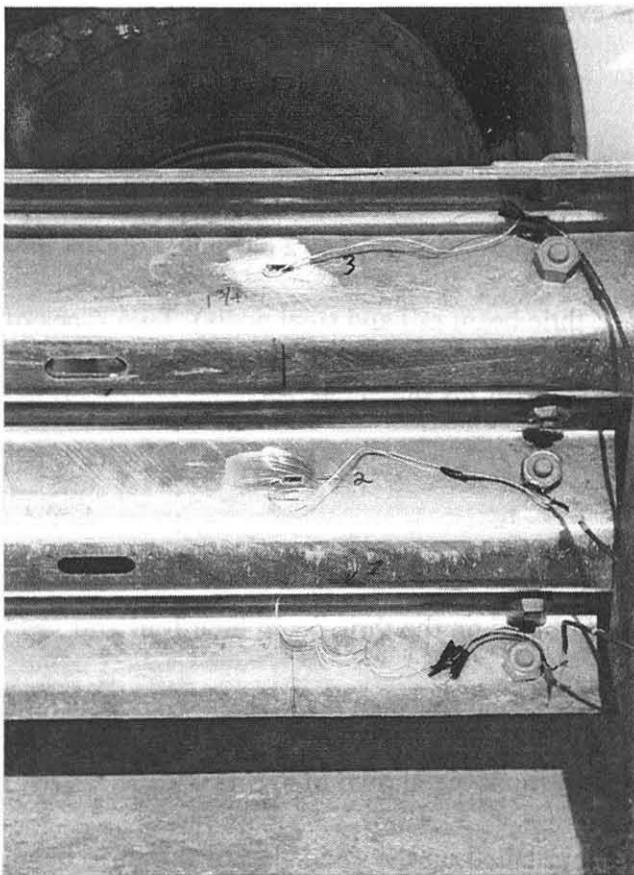
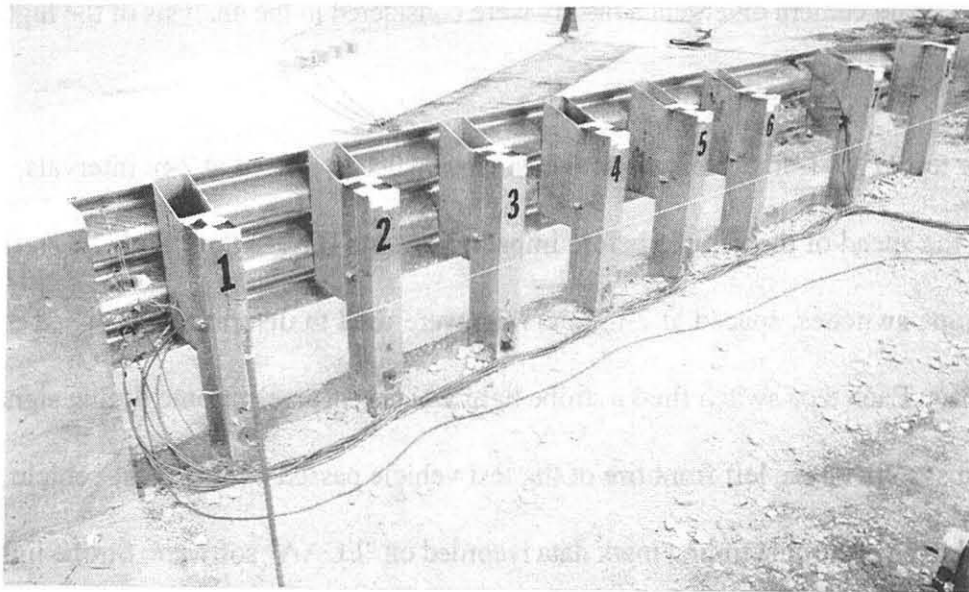


Figure 25. Strain Gauge and String Potentiometer Locations, Test ITNJ-2

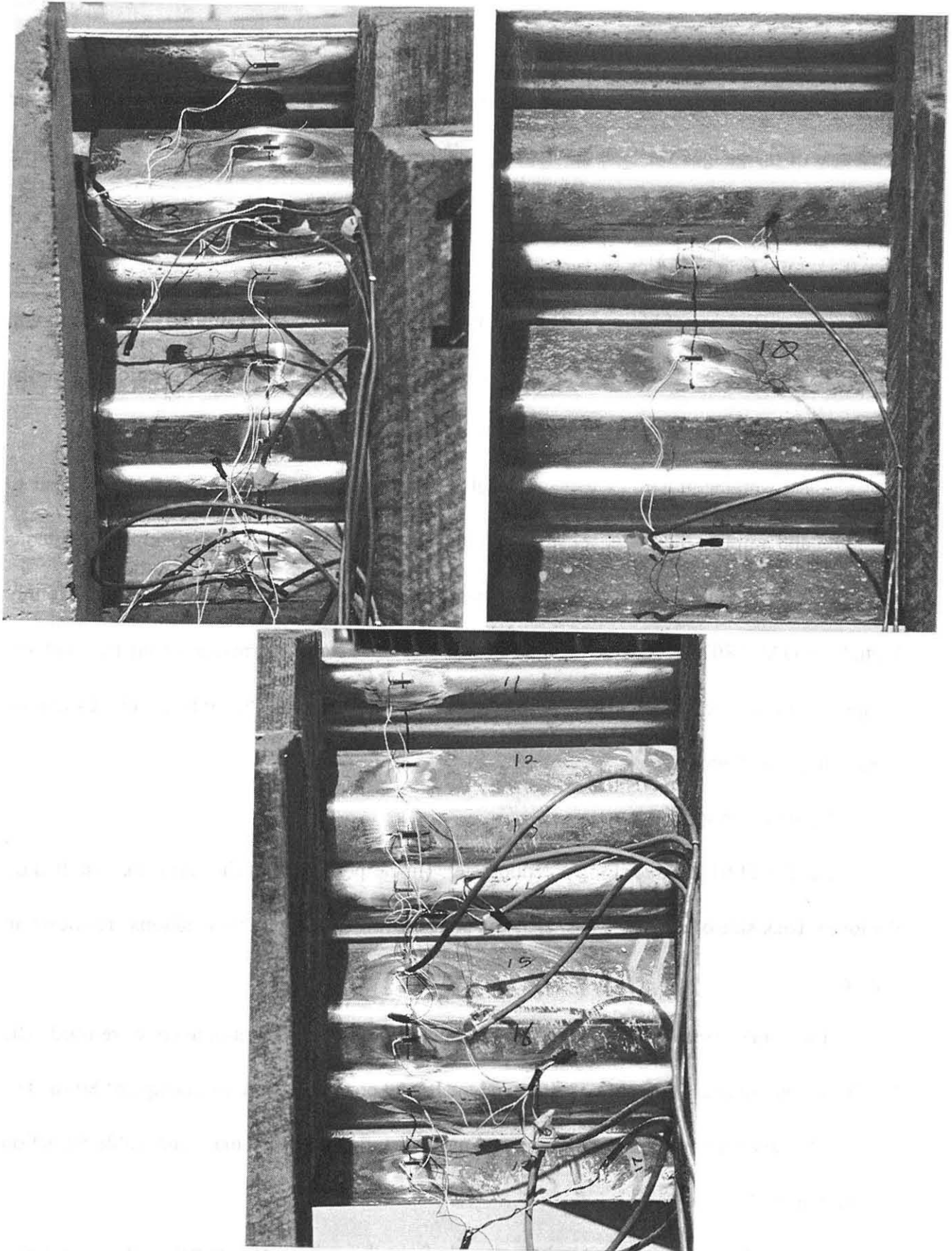


Figure 26. Strain Gauge Locations, Test ITNJ-3

For both tests, weldable strain gauges, type LWK-06-W250B-350, were used. The nominal resistance of the gauges was 350.0 ± 1.4 ohms with a gauge factor equal to 2.02. The operating temperature limits of the gauges was -195 to +260 degrees Celsius. The strain limits of the gauges were 0.5% ($5000 \mu\epsilon$) in tension or compression. The strain gauges were manufactured by the Micro-Measurements Division of Measurements Group, Inc. of Raleigh, North Carolina. The installation procedure required that the metal surface be clean and free from debris and oxidation. Once the surface had been prepared, the gauges were spot welded to the test surface.

A Measurements Group Vishay Model 2310 signal conditioning amplifier was used to condition and amplify the low-level signals to high-level outputs for multichannel, simultaneous dynamic recording on "Test Point" software. After each signal was amplified, it was sent to a Keithly Metrabyte DAS-1802HC data acquisition board, and then stored permanently on the portable computer. The sample rate for all gauges was 5,000 samples per second (5,000 Hz), and the duration of sampling was 5 seconds.

String Potentiometers

For test ITNJ-2, three string potentiometers (linear position transducers) were installed on the lower, back side of steel post nos. 1, 3, and 5. The string potentiometer positions are shown in Figure 26.

Two UniMeasure PA-50 and one UniMeasure PA-80 string potentiometers were used. The PA-50 potentiometers had a range of 50 in. and the PA-80 potentiometers had a range of 80 in. The two PA-50 units were modified for dynamic testing and configured with a maximum cable retraction acceleration of 100 G's.

During the test, the output voltage signals from the string potentiometers were sent to a

Keithly Metrabyte DAS-1802HC data acquisition board, acquired by the "Test Point" software, and then stored permanently on the portable computer. The sample rate for the string potentiometers was 5,000 samples per second (5,000 Hz), and the duration of sampling was 5 seconds.

7 COMPUTER SIMULATION (DESIGN NO. 1)

Computer simulation modeling with BARRIER VII (17) was performed to analyze and predict the dynamic performance of various approach guardrail transition alternatives attached to the New Jersey safety shape concrete end section prior to full-scale vehicle crash testing. The simulations were conducted modeling a 2000-kg pickup truck impacting at a speed of 100.0 km/hr and at an angle of 25 degrees. A typical computer simulation input data file is shown in Appendix B.

Computer simulation was also used to determine the critical impact point (CIP) for the approach guardrail transition. The CIP was based upon the impact condition which produced the greatest potential for wheel-assembly snagging on the lower blunt-end face on the upstream end of the New Jersey concrete safety shape, occurring in combination with the maximum lateral dynamic rail deflection. The researchers believe that wheel snag distances in excess of 51 mm for the steel rim results in an increased potential for snagging and contact on the blunt-end face of the concrete barrier. As previously discussed, the size of the blunt-end face was reduced by incorporating a styrofoam insert in the end of the standard safety shape form.

The results of the computer simulations indicated that the greatest potential for wheel snagging on the upstream end of the concrete end section would occur with an impact between post nos. 5 and 6 or 2,435 mm upstream from the end of the concrete barrier. For the CIP, wheel snag distances for the outer tire and inner steel rim were calculated to be approximately 99 mm and 47 mm, respectively. Additionally, the predicted maximum lateral dynamic rail deflection was 191 mm, as measured to the center height of the rail.

8 CRASH TEST NO. 1 (DESIGN NO. 1 - STEEL POSTS)

8.1 Test ITNJ-1

The 1,994-kg pickup truck impacted the approach guardrail transition (Design No. 1) at a speed of 99.9 km/hr and an angle of 25.0 degrees. A summary of the test results and the sequential photographs are shown in Figure 27. Additional sequential photographs are shown in Figure 28.

8.2 Test Description

Initial impact occurred at the midspan between post nos. 5 and 6 or 2,435-mm upstream from the end of the concrete barrier, as shown in Figure 29. Large lateral dynamic and permanent set barrier deflections occurred, as shown in Figures 27 and 30. This was evidenced by the sharp crease formed in the thrie beam rail at the end of the concrete barrier. During vehicle redirection, the pickup truck's left-front quarter panel extended over the thrie beam, contacting the top corner of the spacer blocks as well as the top edge of the concrete end section. This contact caused moderate tearing of the sheet metal and downward forces applied to the left-front corner of the vehicle. At 0.183 sec after impact, the vehicle became parallel to the barrier with a velocity of 65.2 km/hr. During vehicle tail-slap with the barrier, the rear-end of the vehicle pitched upward moderately, allowing the left-rear corner of the bumper to mount the top of the thrie beam and contact the spacer blocks. At 0.422 sec after impact, the vehicle exited the barrier at an angle of 16.2 degrees and a speed of 64.7 km/hr. Subsequently, the left-front wheel assembly contacted the ground with significant vehicular motions, including counter-clockwise vehicle roll, downward pitching, and clockwise yawing. These angular motions caused the pickup truck to roll over 2½ times. The vehicle's post-impact trajectory is shown in Figure 27. The vehicle came to rest 38.71 m downstream from impact and 15.85 m away from the traffic-side face of the barrier.

8.3 Barrier Damage

Damage to the barrier was moderate, as shown in Figures 30 through 33. Barrier damage consisted mostly of deformed thrie beam, tire marks on the lower upstream face of the concrete end section, and cracking in the concrete end section. Concrete cracking and minor spalling was observed on the upstream end of the concrete end section, as shown in Figure 31. The permanent set of the guardrail and posts is shown in Figures 30 and 32 through 33. The maximum lateral permanent set deflection was approximately 241 mm at post no. 3, as measured in the field. The maximum lateral dynamic deflection was 349 mm at post no. 3, as determined from the high-speed film analysis.

8.4 Vehicle Damage

Exterior and interior vehicle damage was extensive and occurred at several body locations, as shown in Figures 34 and 35. The left-front quarter panel was crushed inward, and the left-side of the front bumper was bent back toward the engine compartment. The engine hood, roof, truck cab, and window glass were severely crushed during the vehicle rollovers. The floorboard of the occupant compartment also sustained significant plastic deformations due to the severe impact with the barrier as well as from vehicle rollover.

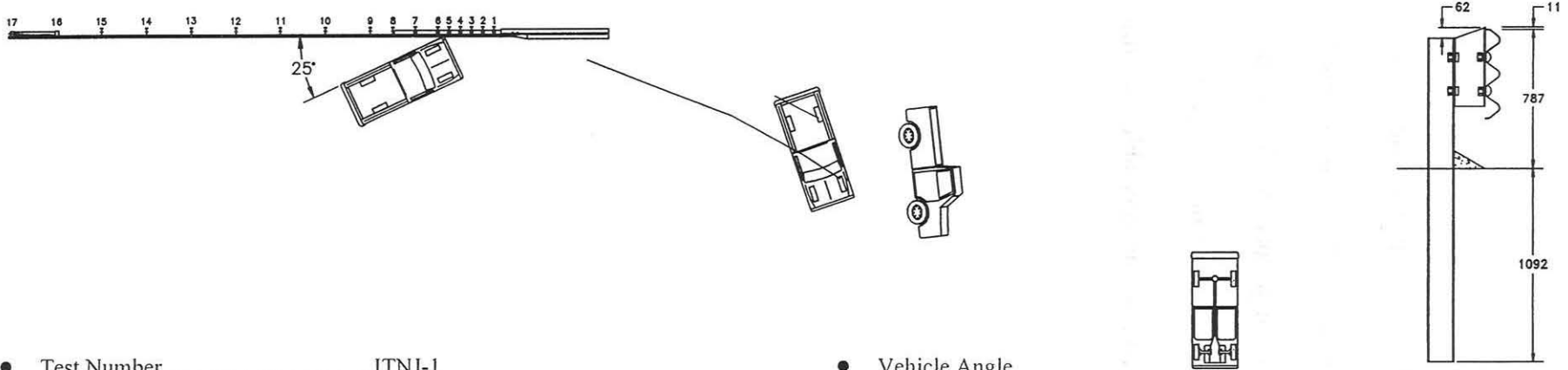
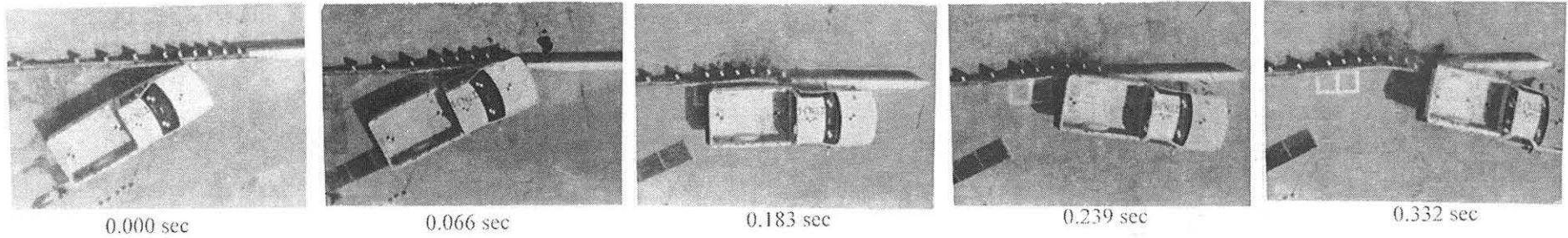
8.5 Occupant Risk Values

The normalized longitudinal and lateral occupant impact velocities were determined to be 10.04 m/sec and 7.75 m/sec, respectively. The maximum 0.010-sec average occupant ridedown decelerations in the longitudinal and lateral directions were 11.90 g's and 15.46 g's, respectively. It is noted that the occupant impact velocities (OIV) and occupant ridedown decelerations (ORD) were within the suggested limits provided in NCHRP Report 350. The results of the occupant risk, determined from accelerometer data, are summarized in Figure 27. Results are shown graphically

in Appendix C.

8.6 Discussion

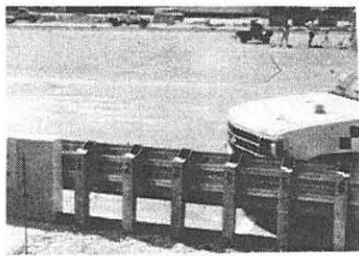
The analysis of the test results for test ITNJ-1 showed that the barrier satisfactorily contained the vehicle but inadequately redirected the vehicle, since the vehicle did not remain upright after collision with the barrier. After collision, the vehicle's trajectory intruded into adjacent traffic lanes. In addition, the vehicle's exit angle was greater than 60 percent of the impact angle. Therefore, test ITNJ-1 conducted on Design No. 1 was determined to be unacceptable according to the NCHRP Report 350 criteria.



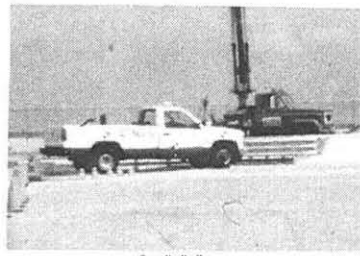
- Test Number ITNJ-1
- Date 8/21/96
- Appurtenance Approach Guardrail Transition to a NJ Safety Shape End Section w/ Curb
- Total Length 25.34 m
- Steel Thrie Beam (Nested)
 - Thickness 2.66 mm
 - Top Mounting Height 787 mm
- Steel Posts
 - Post Nos. 1 - 15 W150x13.5 by 1829-mm long
- Steel Spacer Blocks
 - Post Nos. 1 - 7 TS 180x100x4.76 by 443-mm long
 - Post No. 8 W150x13.5 by 435-mm long
 - Post Nos. 9 - 15 W150x13.5 by 337-mm long
- Soil Type Grading B - AASHTO M 147-65 (1990)
- Vehicle Model 1988 Chevrolet 2500 2WD
 - Curb 2,119 kg
 - Test Inertial 1,994 kg
 - Gross Static 1,994 kg
- Vehicle Speed
 - Impact 99.9 km/hr
 - Exit 64.7 km/hr

- Vehicle Angle
 - Impact 25.0 deg
 - Exit 16.2 deg
- Vehicle Snagging Minor contact on top of spacer blocks and concrete end section
- Vehicle Pocketing Minor
- Vehicle Stability Vehicle rollover
- Occupant Ridedown Deceleration (10 msec avg.)
 - Longitudinal 11.90 < 20 G's
 - Lateral (not required) 15.46
- Occupant Impact Velocity (Normalized)
 - Longitudinal 10.03 < 12 m/s
 - Lateral (not required) 7.75
- Vehicle Damage Extensive
 - TAD¹⁸ NA
 - SAE¹⁹ NA
- Vehicle Stopping Distance 38.71 m downstream
15.85 m on traffic- side face
- Barrier Damage Moderate
- Maximum Deflections
 - Permanent Set 241 mm
 - Dynamic 349 mm

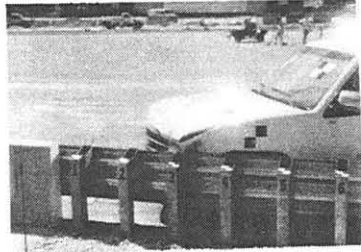
Figure 27. Summary of Test Results and Sequential Photographs, Test ITNJ-1 (Design No. 1)



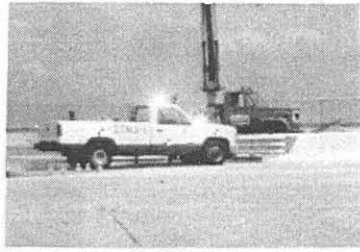
0.000 sec



0.000 sec



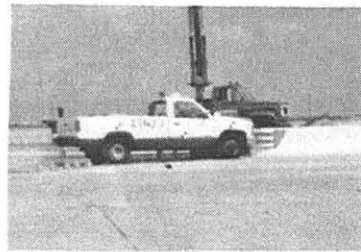
0.031 sec



0.026 sec



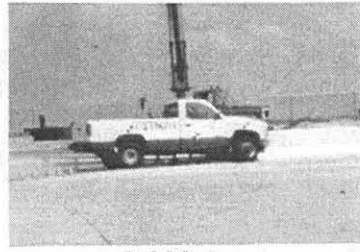
0.064 sec



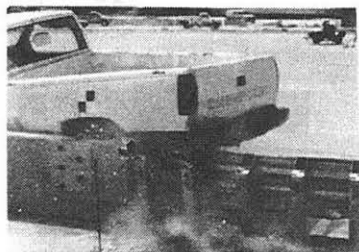
0.059 sec



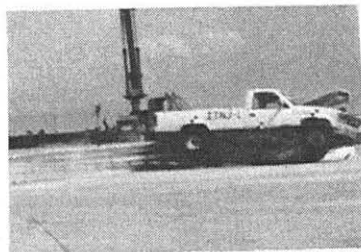
0.114 sec



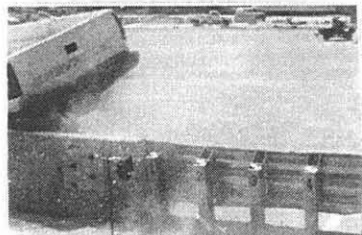
0.099 sec



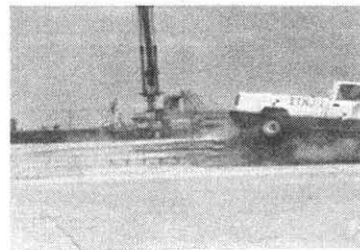
0.266 sec



0.280 sec



0.375 sec



0.380 sec

Figure 28. Additional Sequential Photographs, Test ITNJ-1 (Design No. 1)

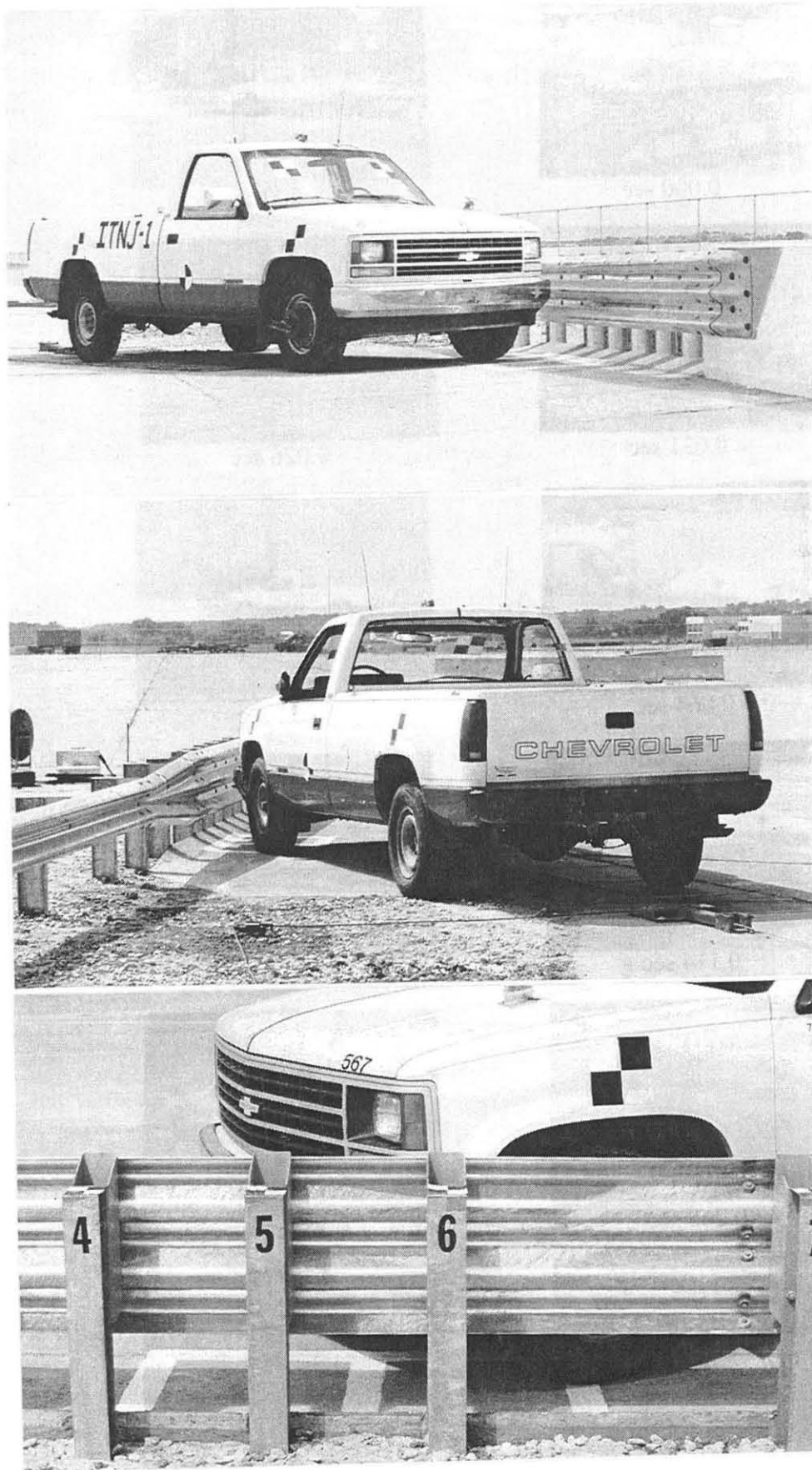


Figure 29. Impact Location, Test ITNJ-1 (Design No. 1)

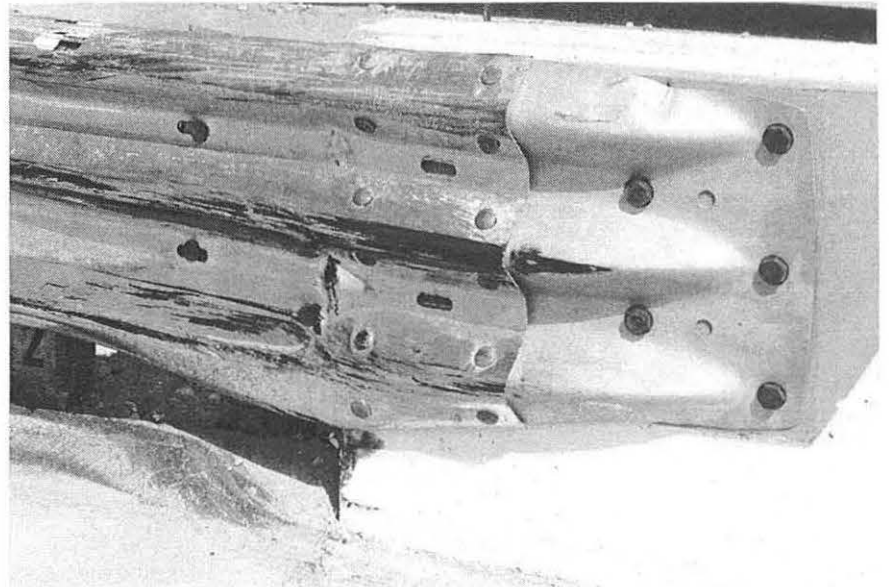
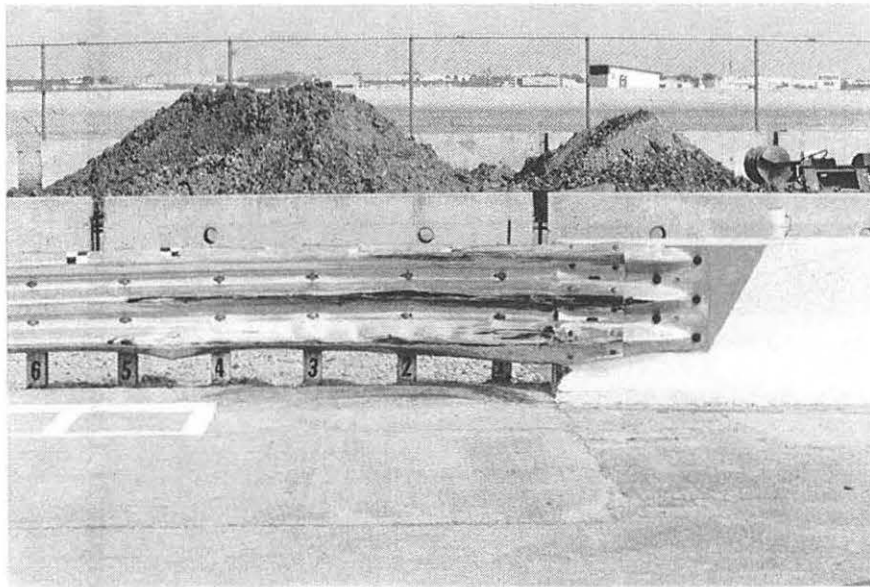
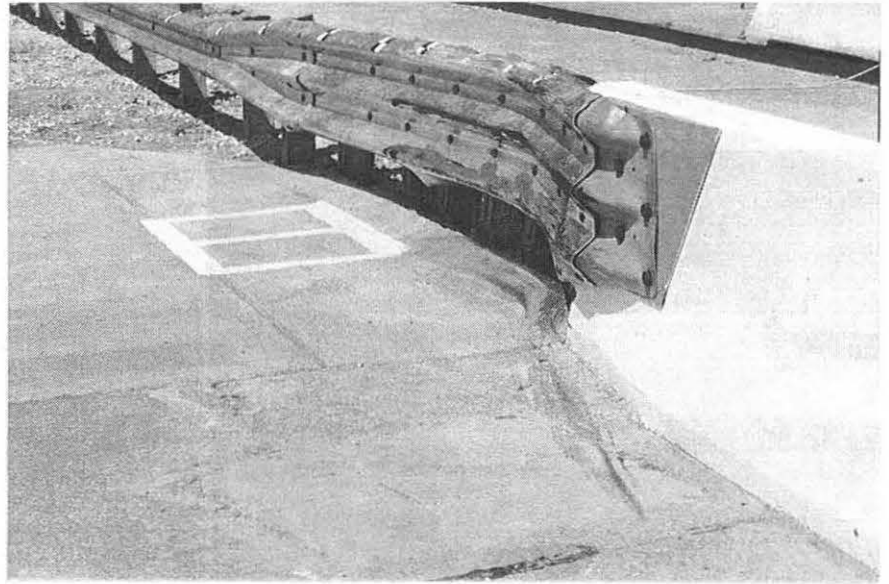


Figure 30. Barrier Damage, Test ITNJ-1 (Design No. 1)

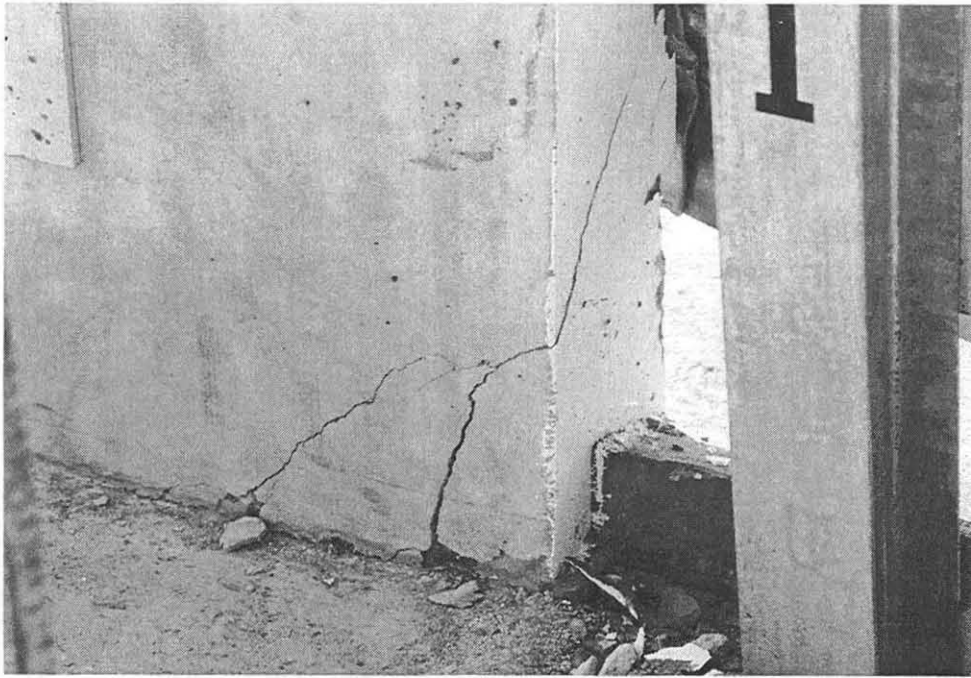


Figure 31. Cracking in Concrete End Section, Test ITNJ-1 (Design No. 1)

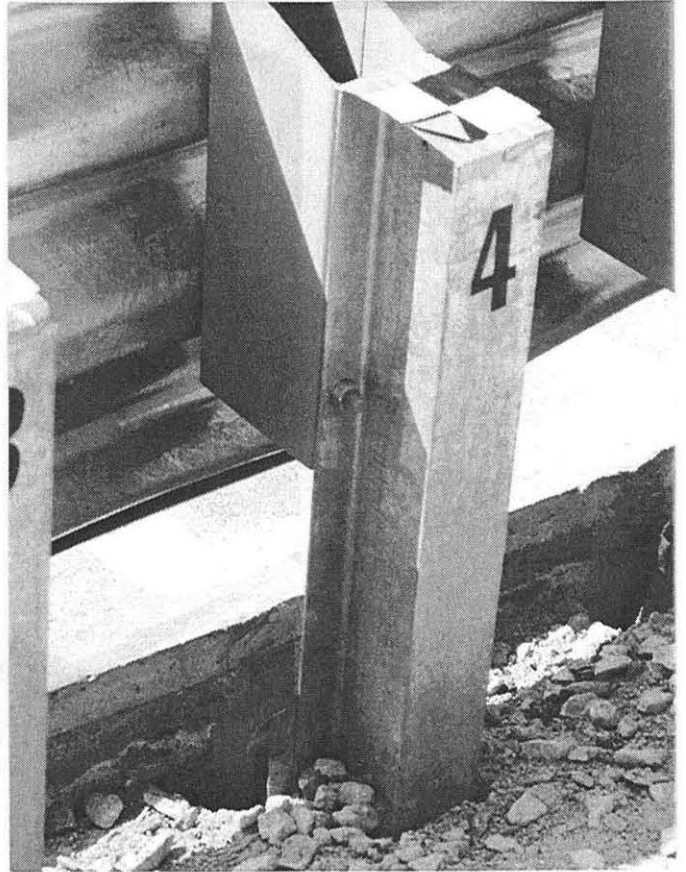
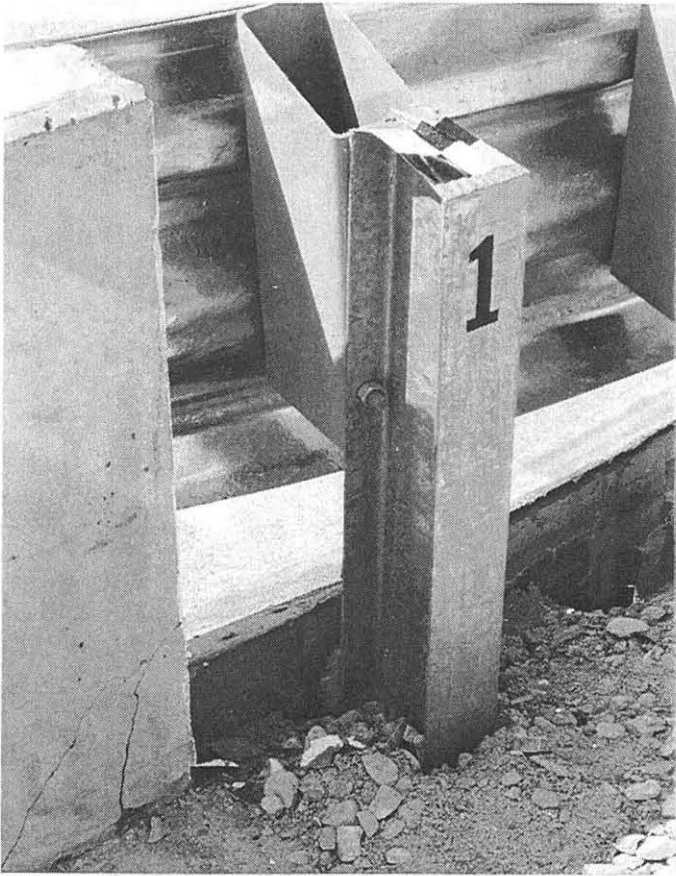


Figure 32. Final Post Positions, Test ITNJ-1 (Design No. 1)

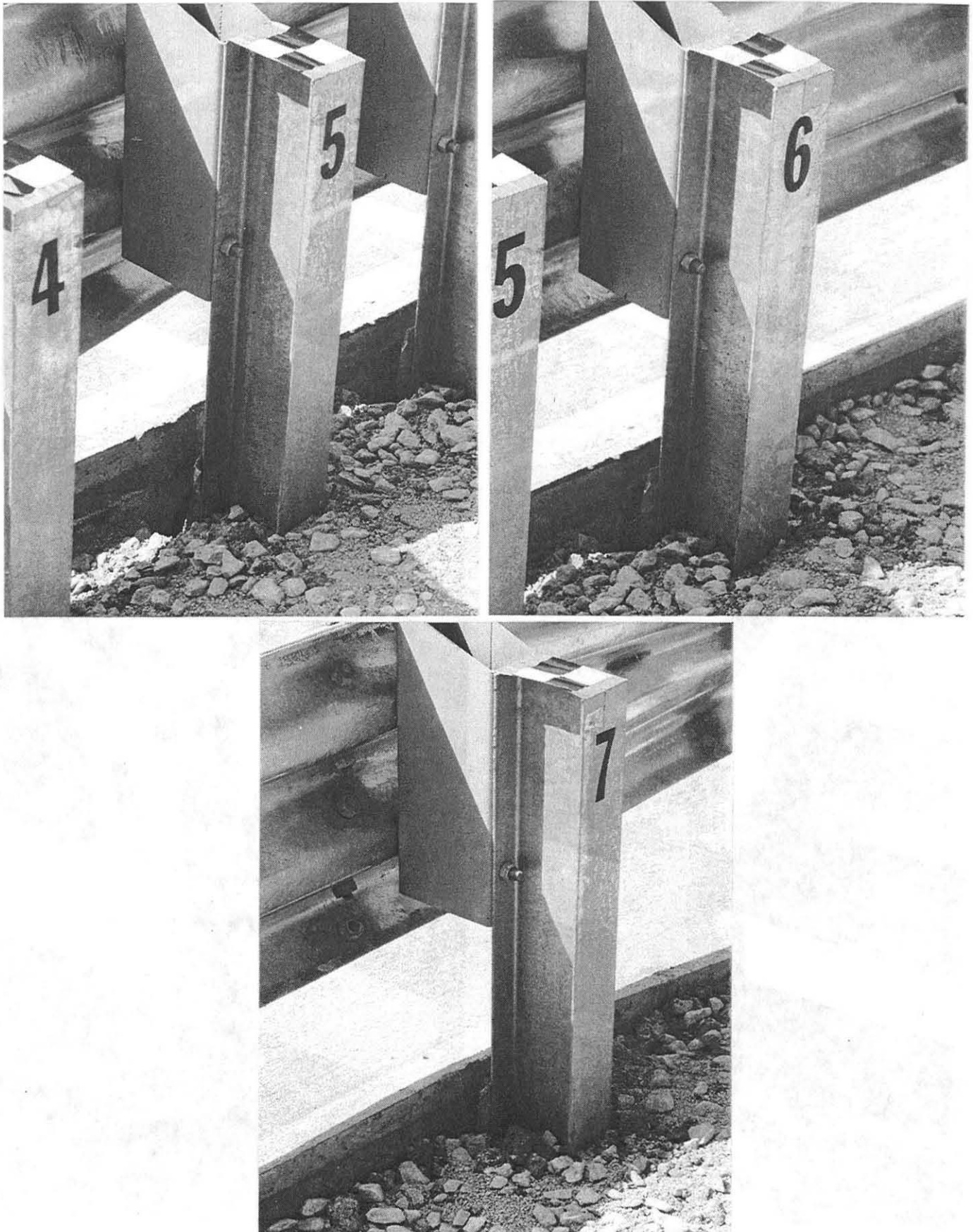


Figure 33. Final Post Positions, Test ITNJ-1 (Design No. 1)



Figure 34. Vehicle Damage, Test ITNJ-1 (Design No. 1)

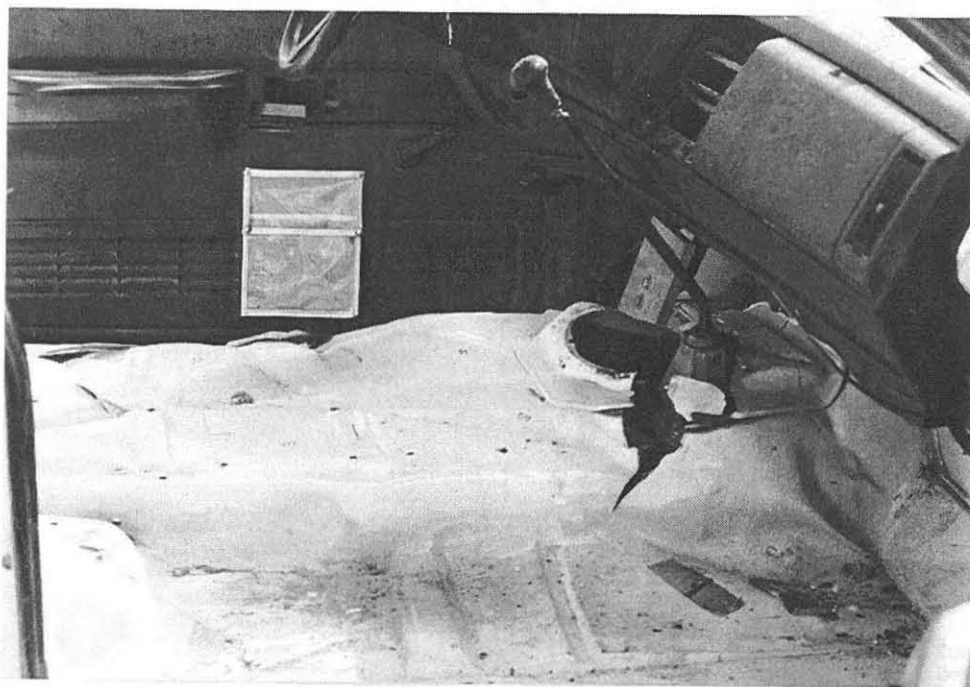


Figure 35. Occupant Compartment Deformation, Test ITNJ-1 (Design No. 1)

9 DISCUSSION AND MODIFICATIONS (DESIGN NO. 2)

Following the unsuccessful crash test of Design No. 1, it was necessary to determine the cause of the poor barrier performance and subsequent vehicle rollover so that design modifications could be made to the system. A careful examination of the damaged barrier system and an analysis of the test results revealed that the dynamic and permanent set barrier deflections were greater than those predicted. It is believed that these excessive barrier deflections occurred due to post-soil forces being significantly lower than expected. These lower post-soil forces may be attributed to the use of a relatively poorly-graded, coarse crushed limestone material meeting NCHRP Report 350 specifications.

As a result of the extensive vehicle penetration into the barrier system, the pickup truck was redirected out of the barrier system at a higher than normal exit angle. Significant roll, pitch, and yaw angular motions were also produced, resulting in vehicle rollover. In addition, the increased vehicle penetration and minor pocketing led to higher than expected impact forces being applied to the concrete end section, resulting in cracking of the safety shape barrier.

After this investigation, we believed that the safety performance of the approach guardrail transition (Design No. 1) could be significantly improved with a reduction in dynamic and permanent set barrier deflections. Several alternatives were investigated for stiffening the approach guardrail system. These alternatives include the following: lengthening the steel posts in the critical region; incorporating a rub-rail below the thrie beam; adding a stiffened beam on the back side of the steel posts and concrete end section; and attaching soil paddles of various sizes to the steel posts.

Following a limited series of dynamic tests with a bogie vehicle impacting posts placed in various NCHRP Report 350 soils and an analytical investigation using BARRIER VII, two major

modifications were made to the approach guardrail transition system. The embedment depth of post nos. 1 through 7 were increased by 152 mm, resulting in a total embedment depth of 1,245 mm. The relatively poorly-graded aggregate material used in Design No. 1 was replaced with a crushed limestone material more consistent with the AASHTO specification. In addition, a 25-mm chamfer was placed on the front vertical edge of the concrete safety shape's upstream end. These modifications, incorporated in Design No. 2, are shown in Figure 36.

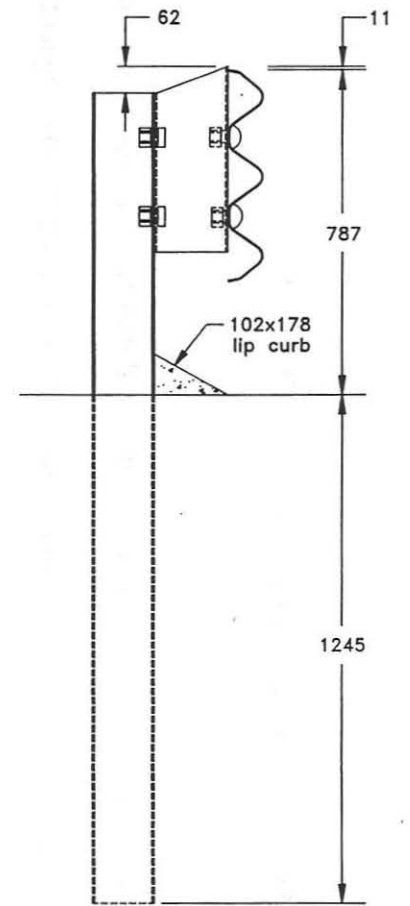
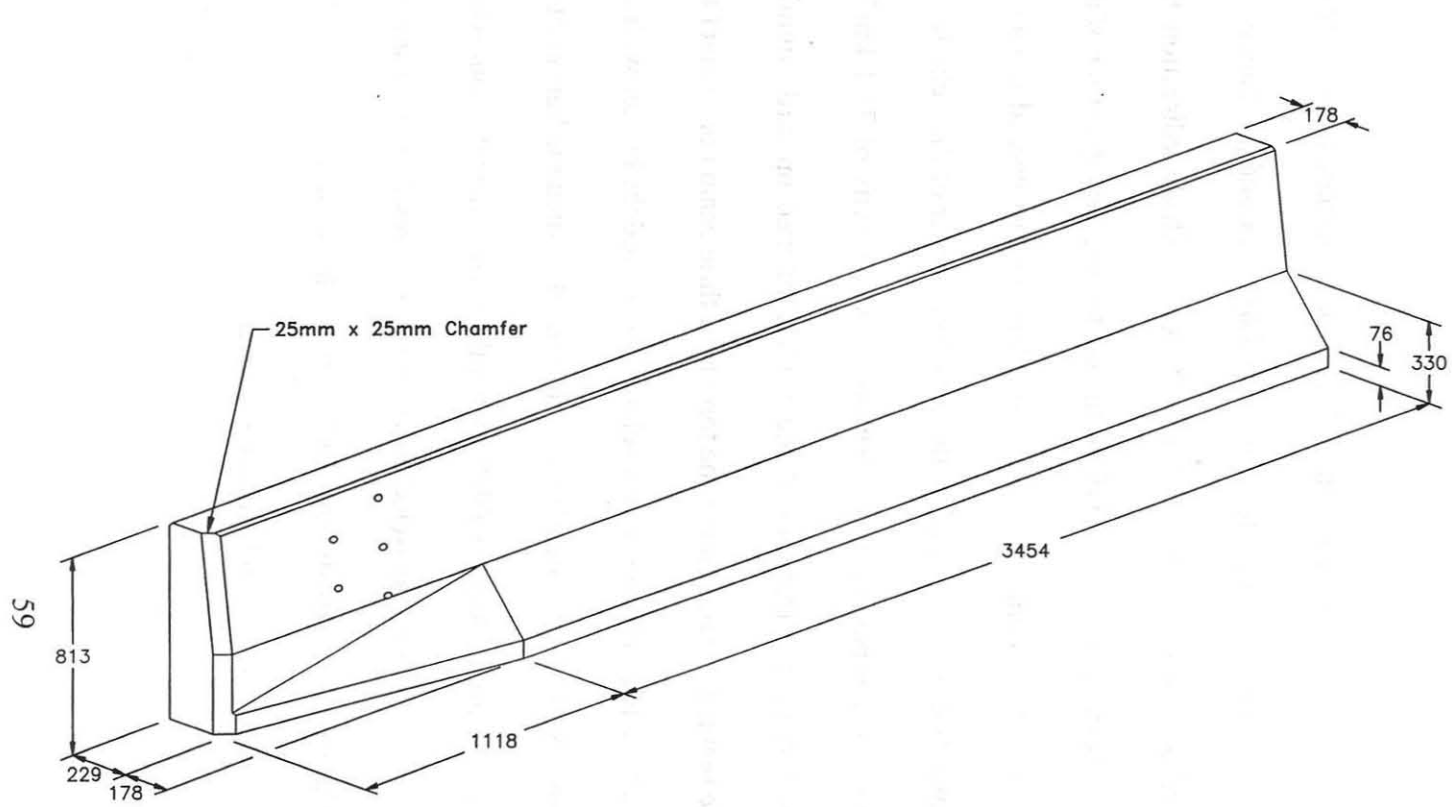


Figure 36. Barrier and Post Modifications, Design No. 2

10 CRASH TEST NO. 2 (DESIGN NO. 2 - STEEL POSTS)

10.1 Test ITNJ-2

The 1,977-kg pickup truck impacted the approach guardrail transition (Design No. 2) at a speed of 101.6 km/hr and an angle of 25.7 degrees. A summary of the test results and the sequential photographs are shown in Figure 37. Additional sequential photographs are shown in Figure 38. Documentary photographs of the crash test are shown in Figures 39 and 40.

10.2 Test Description

Initial impact occurred at the midspan between post nos. 5 and 6 or 2,435-mm upstream from the end of the concrete barrier, as shown in Figure 41. Moderate lateral dynamic and permanent set barrier deflections were encountered, as shown in Figures 37 and 42. During vehicle redirection, the pickup truck's left-front quarter panel extended over the thrie beam, contacting the top corner of the spacer blocks as well as the top edge of the concrete end section. This contact caused moderate tearing of the sheet metal and downward forces applied to the left-front corner of the vehicle. At 0.183 sec after impact, the vehicle became parallel to the barrier with a velocity of 71.1 km/hr. During vehicle tail-slap with the barrier, the rear-end of the vehicle pitched upward slightly; however, the left-rear corner of the bumper did not mount the top of the thrie beam nor contact the spacer blocks. Subsequently, the vehicle began to roll counter-clockwise toward the barrier with the right-side wheels becoming airborne. At 0.329 sec after impact, the vehicle exited the barrier at an angle of 6.9 degrees and a speed of 70.8 km/hr. As the vehicle exited the barrier, the left-front wheel assembly contacted the ground but with minor counter-clockwise vehicle roll, resulting in a smooth and stable vehicle redirection. The vehicle's post-impact trajectory is shown in Figure 37. The vehicle came to rest 76.8 m downstream and 11.2 m behind the barrier.

10.3 Barrier Damage

Damage to the barrier was moderate, as shown in Figures 42 through 45. Barrier damage consisted mostly of deformed thrie beam and tire marks on the lower upstream face of the concrete end section. No cracking was observed in the concrete end section. The permanent set of the guardrail and posts is shown in Figures 42 and 44 through 45. The maximum lateral permanent set deflection was approximately 92 mm at post no. 2 and the midspan between post nos. 2 and 3, as measured in the field. The maximum lateral dynamic deflection was 133 mm at post no. 3, as determined from the high-speed film analysis. It is noted that some dynamic deflection measurements were not available for viewing from the overhead camera due to the vehicle extending over the barrier.

10.4 Vehicle Damage

Vehicle damage was moderate, as shown in Figure 46. The left-front quarter panel was crushed inward, and the left-side of the front bumper was also bent back toward the engine compartment. The left-front wheel assembly was deformed and pushed backward into the firewall. Longitudinal deformations, due to vehicle-rail interlock, were observed along the entire left-side of the vehicle. Maximum occupant compartment deformations to the floorboard and/or firewall in the lateral, longitudinal, and vertical directions were 95 mm, 83 mm, and 83 mm, respectively, as shown in Figure 47.

10.5 Occupant Risk Values

The normalized longitudinal and lateral occupant impact velocities were determined to be 6.94 m/sec and 7.07 m/sec, respectively. The maximum 0.010-sec average occupant ridedown decelerations in the longitudinal and lateral directions were 11.24 g's and 18.43 g's, respectively. It

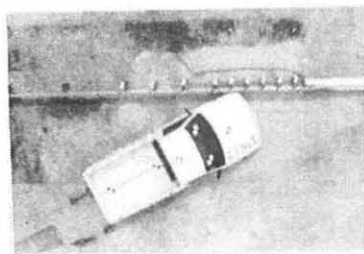
is noted that the occupant impact velocities (OIV) and occupant ridedown decelerations (ORD) were within the suggested limits provided in NCHRP Report 350. The results of the occupant risk, determined from accelerometer data, are summarized in Figure 37. Results are shown graphically in Appendix D. The results from the rate transducer are shown graphically in Appendix E.

10.6 Discussion

The analysis of the test results for test ITNJ-2 showed that the barrier adequately contained and redirected the vehicle with controlled lateral displacement of the barrier. Minor deformations to the occupant compartment were evident but not considered excessive enough to cause serious injuries to the occupants. The vehicle remained upright both during and after the collision. Vehicle roll, pitch, and yaw angular displacements were noted, but they were deemed acceptable because they did not adversely influence occupant safety criteria or cause rollover. After collision, the vehicle's trajectory intruded slightly into adjacent traffic lanes but was determined to be acceptable. In addition, the vehicle's exit angle was less than 60 percent of the impact angle. Therefore, test ITNJ-2 conducted on Design No. 2 was determined to be acceptable according to the NCHRP Report 350 criteria.

10.7 Barrier Instrumentation Results

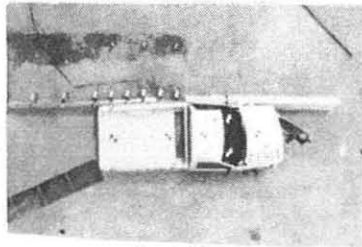
For test ITNJ-2, strain gauges were located on the approach guardrail transition. The results of the strain gauge analysis are provided in Table 2. Although string potentiometers were also used, the results were not provided. Dynamic bogie tests on guardrail posts, instrumented with string potentiometers, later revealed that cable retraction may not occur at the same velocity of the post. This difference resulted in the cable being pushed into a sinusoidal shape, thus making the results invalid.



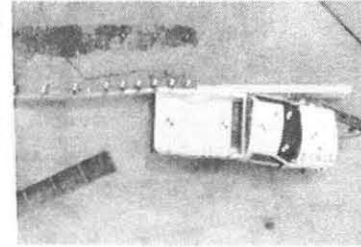
0.000 sec



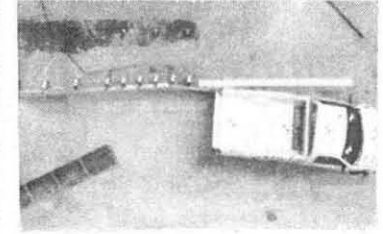
0.066 sec



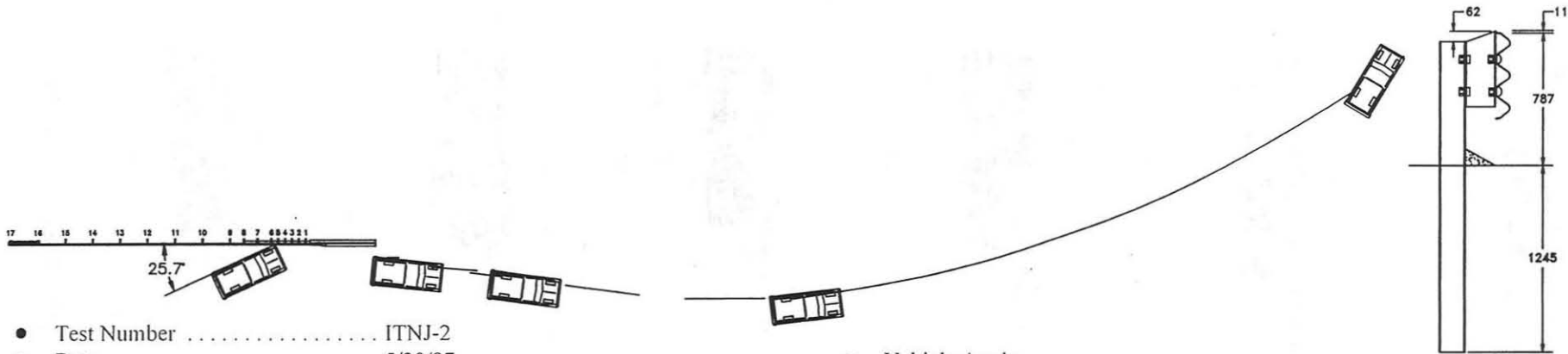
0.176 sec



0.235 sec



0.319 sec

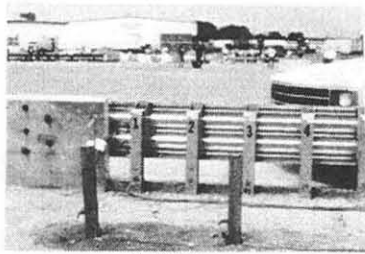


63

- Test Number ITNJ-2
- Date 5/30/97
- Appurtenance Approach Guardrail Transition to a NJ Safety Shape End Section w/ Curb
- Total Length 25.34 m
- Steel Thrie Beam (Nested)
 - Thickness 2.66 mm
 - Top Mounting Height 787 mm
- Steel Posts
 - Post Nos. 1 - 7 W150x13.5 by 1981-mm long
 - Post Nos. 8 - 15 W150x13.5 by 1829-mm long
- Steel Spacer Blocks
 - Post Nos. 1 - 7 TS 180x100x4.76 by 443-mm long
 - Post No. 8 W150x13.5 by 435-mm long
 - Post Nos. 9 - 15 W150x13.5 by 337-mm long
- Soil Type Grading B - AASHTO M 147-65 (1990)
- Vehicle Model 1991 Chevrolet 2500 2WD
 - Curb 1,722 kg
 - Test Inertial 1,977 kg
 - Gross Static 1,977 kg
- Vehicle Speed
 - Impact 101.6 km/hr
 - Exit 70.8 km/hr

- Vehicle Angle
 - Impact 25.7 deg
 - Exit 6.9 deg
- Vehicle Snagging Minor contact on top of spacer blocks and concrete end section
- Vehicle Pocketing None
- Vehicle Stability Satisfactory
- Occupant Ridedown Deceleration (10 msec avg.)
 - Longitudinal 11.24/-17.72 < 20 G's
 - Lateral (not required) 18.43
- Occupant Impact Velocity (Normalized)
 - Longitudinal 6.94 < 12 m/s
 - Lateral (not required) 7.07
- Vehicle Damage Moderate
 - TAD¹⁸ 11-LFQ-5
 - SAE¹⁹ 11LDEW3
- Vehicle Stopping Distance 76.8 m downstream
11.2 m behind
- Barrier Damage Moderate
- Maximum Deflections
 - Permanent Set 92 mm
 - Dynamic 133 mm (visible)

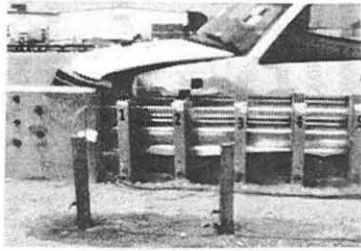
Figure 37. Summary of Test Results and Sequential Photographs, Test ITNJ-2 (Design No. 2)



0.000 sec



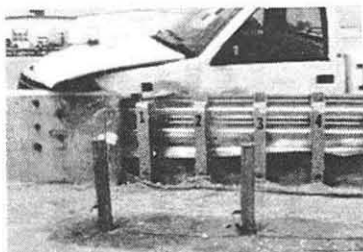
0.000 sec



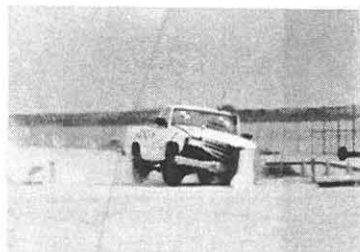
0.076 sec



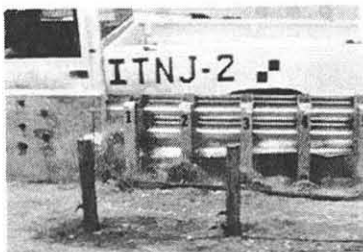
0.086 sec



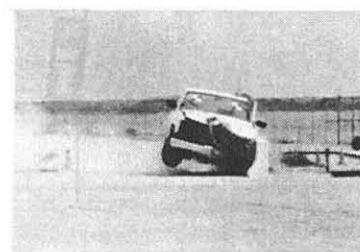
0.098 sec



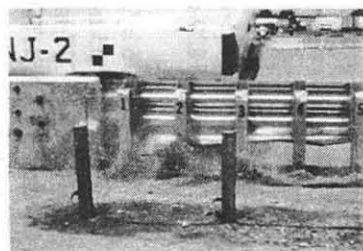
0.120 sec



0.178 sec



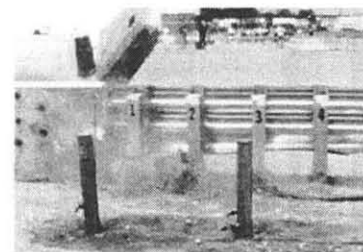
0.176 sec



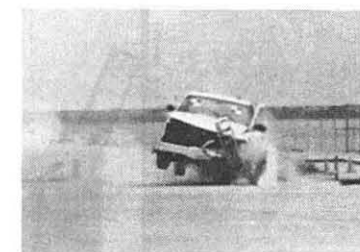
0.238 sec



0.251 sec



0.300 sec



0.329 sec

Figure 38. Additional Sequential Photographs, Test ITNJ-2 (Design No. 2)



Figure 39. Documentary Photographs, Test ITNJ-2 (Design No. 2)

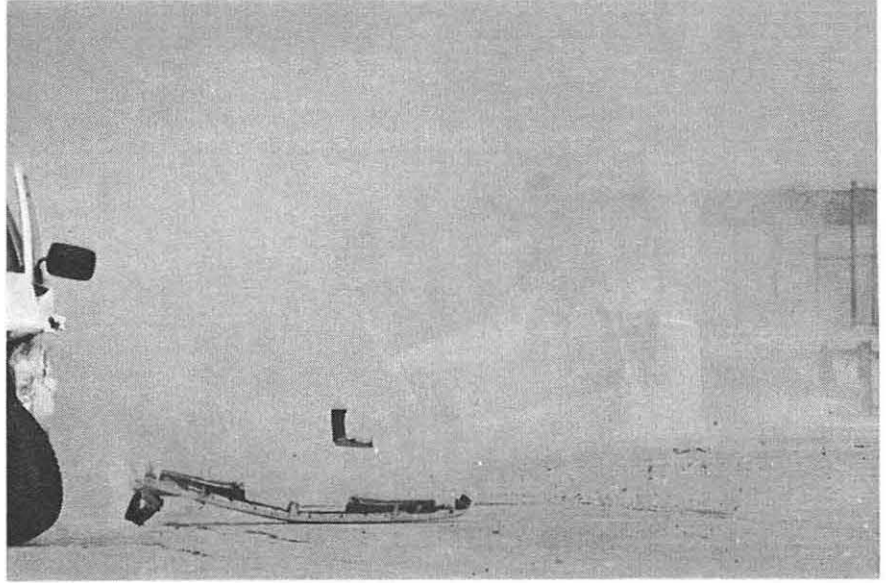
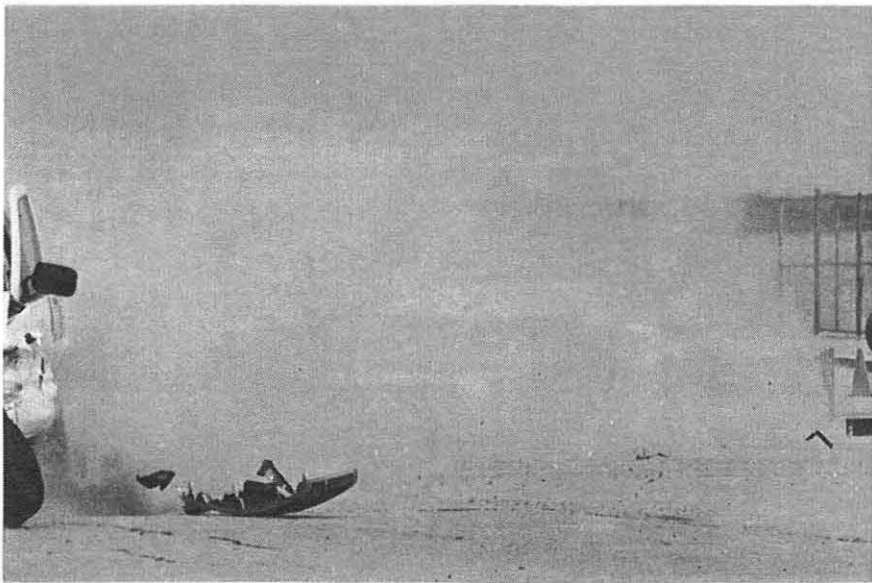
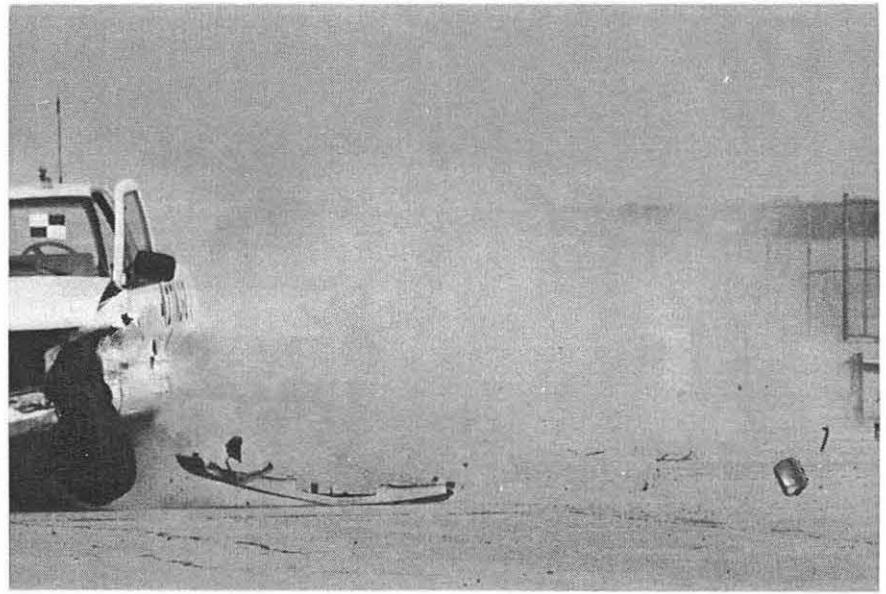


Figure 40. Documentary Photographs, Test ITNJ-2 (Design No. 2)



Figure 41. Impact Location, Test ITNJ-2 (Design No. 2)

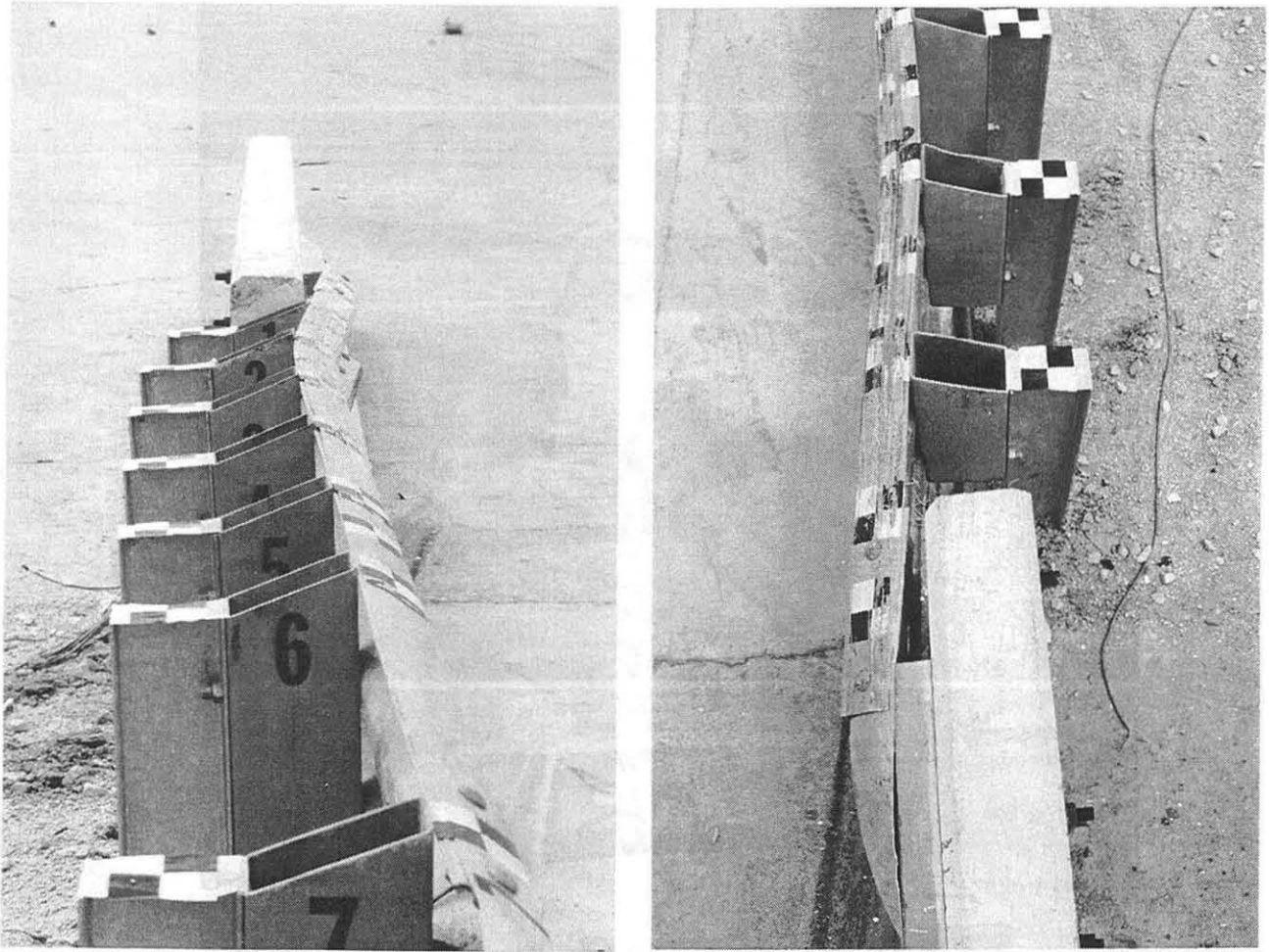


Figure 42. Barrier Damage, Test ITNJ-2 (Design No. 2)

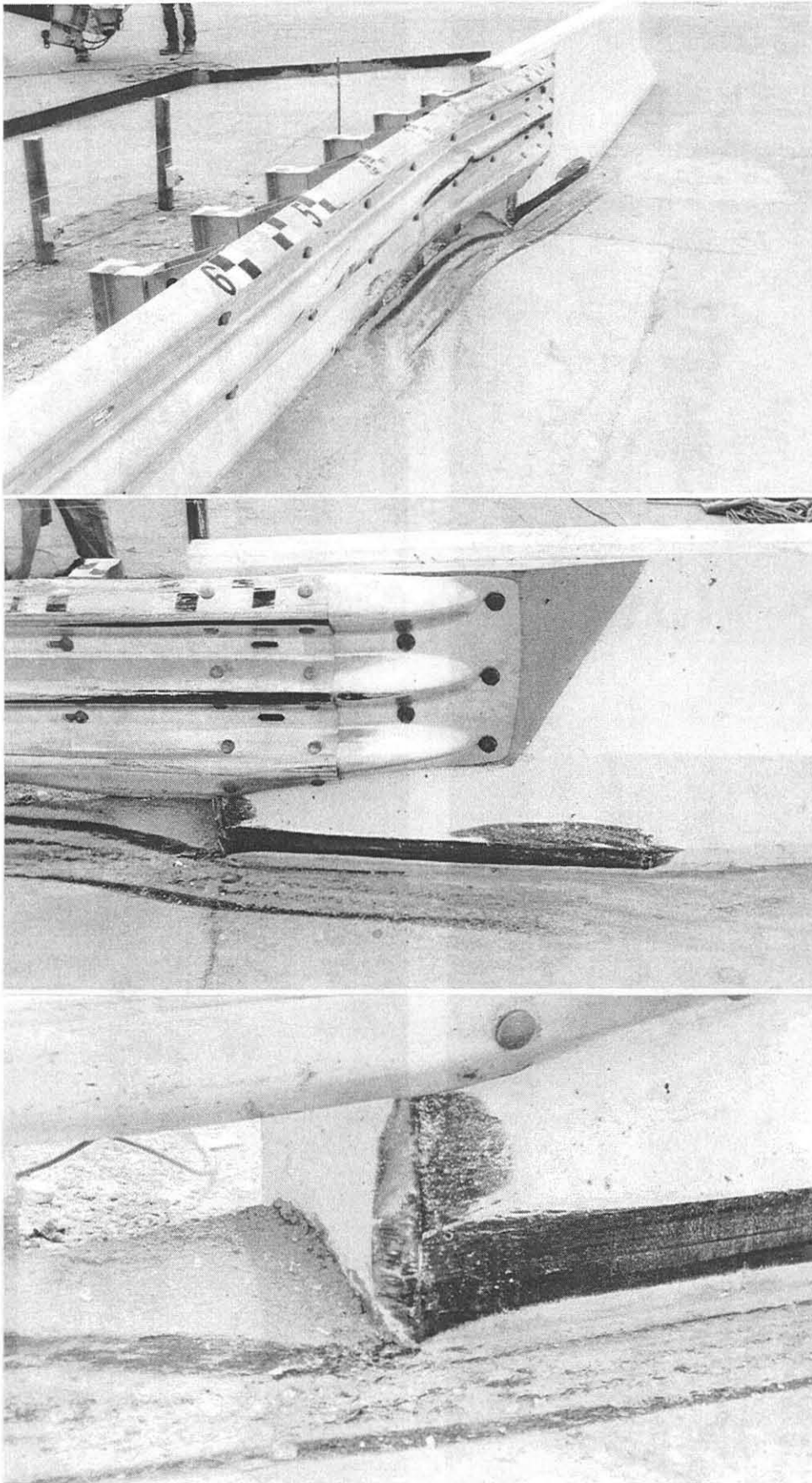


Figure 43. Barrier Damage, Test ITNJ-2 (Design No. 2)

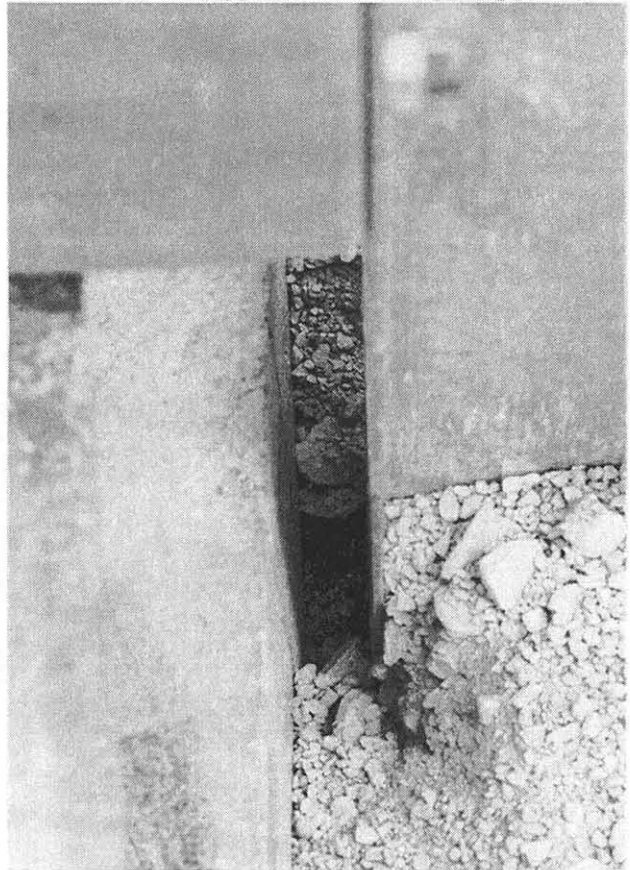
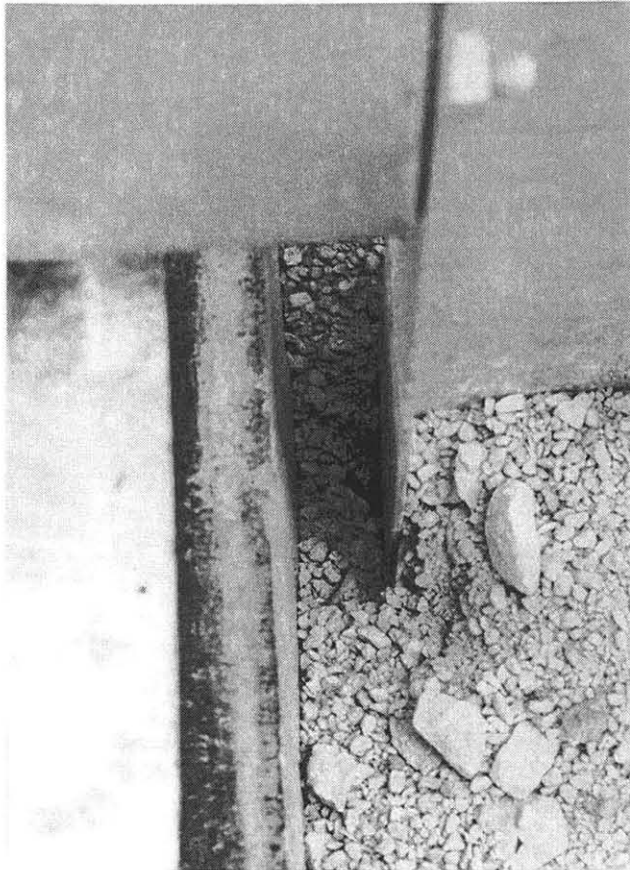
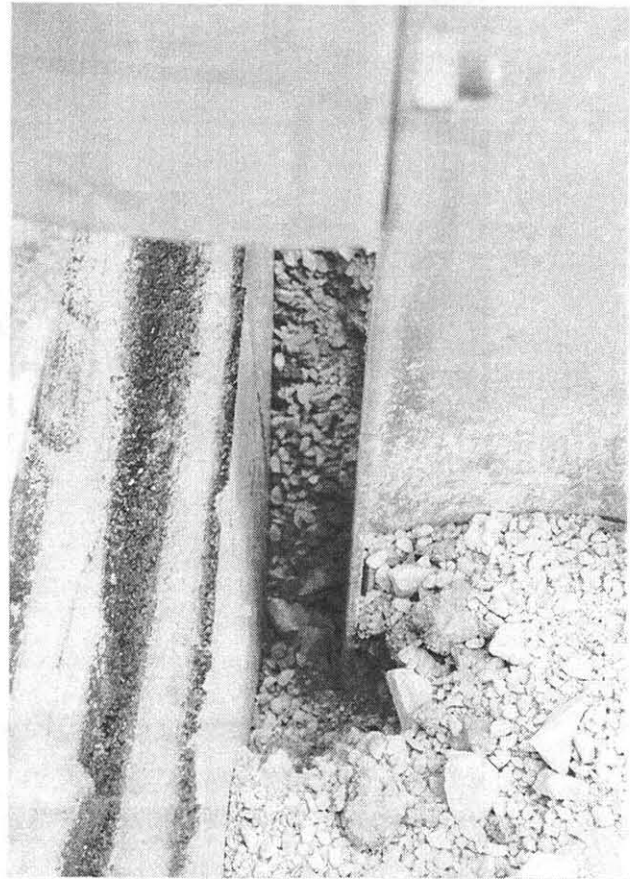
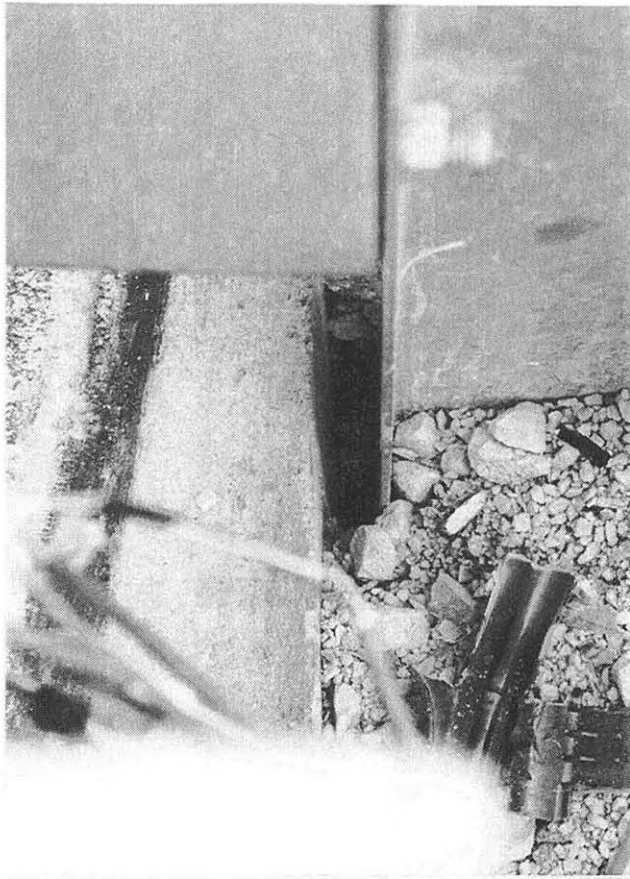


Figure 44. Final Post Positions, Test ITNJ-2 (Design No. 2)



Figure 45. Final Post Positions, Test ITNJ-2 (Design No. 2)



Figure 46. Vehicle Damage, Test ITNJ-2 (Design No. 2)



Figure 47. Occupant Compartment Deformation, Test ITNJ-2 (Design No. 2)

Table 2. Strain Gauge Results, Test ITNJ-2 (Design No. 2)

Hardware Type	Strain Gauge No.	Strain Gauge Location	Maximum μ Strain ¹ (in./in.)	Maximum Stress ² (ksi)	Comments
Thrie Beam	1	Midspan 6/7	283	8.48	Neutral axis below middle peak on back of rail
	2	Midspan 6/7	155	4.65	Neutral axis above middle peak on back of rail
	3	Midspan 6/7	264	7.91	Neutral axis above lower peak on back of rail
Post	4	Post 6	794	23.83	Back-side flange - 23 3/16 in. from top of post
	5	Post 5	835	25.06	Back-side flange - 23 1/8 in. from top of post
	6	Post 4	748	22.44	Back-side flange - 23 1/8 in. from top of post
	7	Post 3	814	24.43	Back-side flange - 23 1/8 in. from top of post
	8	Post 2	687	20.62	Back-side flange - 23 1/8 in. from top of post
	9	Post 1	643	19.29	Back-side flange - 23 3/16 in. from top of post
Thrie Beam	10	Note ³	1463	43.88	Inside of top peak on back of rail
	11	Note ³	1715	NA	Top valley on back of rail
	12	Note ³	1482	44.45	Inside of middle peak on back of rail
	13	Note ³	1139	34.18	Bottom valley on back of rail
	14	Note ³	NA	NA	Inside of bottom peak on back of rail
	15	Note ³	3859	NA	Neutral axis below middle peak on back of rail
	16	Note ³	622	18.66	Neutral axis above middle peak on back of rail

¹ - All strain values are shown as the absolute value only.

² - All elastic stress values are shown as the absolute value only and calculated by multiplying the strain by the modulus of elasticity equal to 30,000 ksi. Minimum yield stress for the post and thrie beam is 36 ksi and 50 ksi, respectively.

³ - Strain gauge location is the midspan between the upstream end of the concrete end section and post no. 1.

NA - Not available.

11 SUMMARY AND CONCLUSIONS - STEEL POST SYSTEM

An approach guardrail transition, consisting of three-beam guardrail, steel posts, structural tube spacer blockouts, and a New Jersey connector plate, was developed and full-scale vehicle crash tested for use with the New Jersey concrete safety shape barrier. Two full-scale vehicle crash tests were performed according to TL-3 of NCHRP Report 350. The first crash test, Test ITNJ-1 (Design No. 1), failed due to vehicle rollover. Lower than expected post-soil forces occurred, thus resulting in excessive barrier deflections. These deflections led to a higher than normal exit angle which occurred simultaneously with significant roll, pitch, and yaw angular motions.

Based on knowledge gained from test ITNJ-1, the approach guardrail transition system was redesigned. The primary changes were to use longer posts and a crushed limestone backfill that more closely met the AASHTO specifications. A second test, Test ITNJ-2 (Design No. 2), was performed on the modified system and was determined to be acceptable according to the safety performance criteria presented in NCHRP Report 350. Thus, an approach guardrail transition for use with the New Jersey concrete safety shape barrier has been successfully developed and meets current safety standards. A summary of the safety performance evaluation for the two tests is provided in Table 3.

It is believed that only minor modifications to the new design will be required to accommodate the F-shape concrete barrier. Additionally, it is believed that no further testing will be required since the F-shape is considered to behave slightly better than the New Jersey shape in crash testing (11-12). Finally, it is believed that this approach guardrail transition system would perform in an acceptable manner when attached to a vertical concrete end section that includes a similar chamfer configuration.

Table 3. Summary of Safety Performance Evaluation Results - Steel Post System

Evaluation Factors	Evaluation Criteria	Test ITNJ-1 (Design No. 1)	Test ITNJ-2 (Design No. 2)
Structural Adequacy	A. Test article should contain and redirect the vehicle; the vehicle should not penetrate, underride, or override the installation although controlled lateral deflection of the test article is acceptable.	U	S
Occupant Risk	D. Detached elements, fragments or other debris from the test article should not penetrate or show potential for penetrating the occupant compartment, or present an undue hazard to other traffic, pedestrians, or personnel in a work zone. Deformations of, or intrusions into, the occupant compartment that could cause serious injuries should not be permitted.	S	S
	F. The vehicle should remain upright during and after collision although moderate roll, pitching and yawing are acceptable.	U	S
Vehicle Trajectory	K. After collision it is preferable that the vehicle's trajectory not intrude into adjacent traffic lanes.	U	M
	L. The occupant impact velocity in the longitudinal direction should not exceed 12 m/sec and the occupant ridedown acceleration in the longitudinal direction should not exceed 20 G's.	S	S
	M. The exit angle from the test article preferably should be less than 60 percent of test impact angle, measured at time of vehicle loss of contact with test devise.	U	S

S - (Satisfactory)
M - (Marginal)
U - (Unsatisfactory)

12 APPROACH GUARDRAIL TRANSITION - WOOD POSTS (DESIGN NO. 3)

Following the successful development of an approach guardrail transition using steel posts and a New Jersey concrete safety shape barrier, a similar research effort was conducted to develop an approach guardrail transition using wood posts. The details of this effort are included in the remaining sections of this research report.

Prior to the selection of the length for post nos. 1 through 8 and the soil-aggregate material for Design No. 3, a limited number of dynamic tests were conducted on steel and wood posts placed in two crushed limestone "soils" both meeting NCHRP 350 specifications. The first soil was the same as used in Design No.2, while the second soil had a reduced amount of material in the middle sieve ranges (3/8 through #10). Both of these soils are classified as well-graded by ASTM requirements. The bogie tests on wood posts were performed to obtain the dynamic response of posts embedded in the two soils (i.e., force vs. deflection) and determine if the posts would fracture during rotation.

The bogie testing of wood posts revealed that posts placed in the second soil required less energy to rotate; however, this difference was largely evidenced in the latter parts of the rotation. During initial post rotation, peak loads were not significantly effected by this slight change in gradation of the two soils. In addition, it was determined that there was only a small probability that the wood posts would fracture during testing of the transition system. Within the range of testing, slight variations in the soil gradation within the specification did not have a significant effect of the performance of these stiff systems. Therefore, the second soil was utilized for Design No. 3, largely because of availability.

Additionally, the results revealed that a 152-mm wide x 203-mm deep x 1829-mm long wood

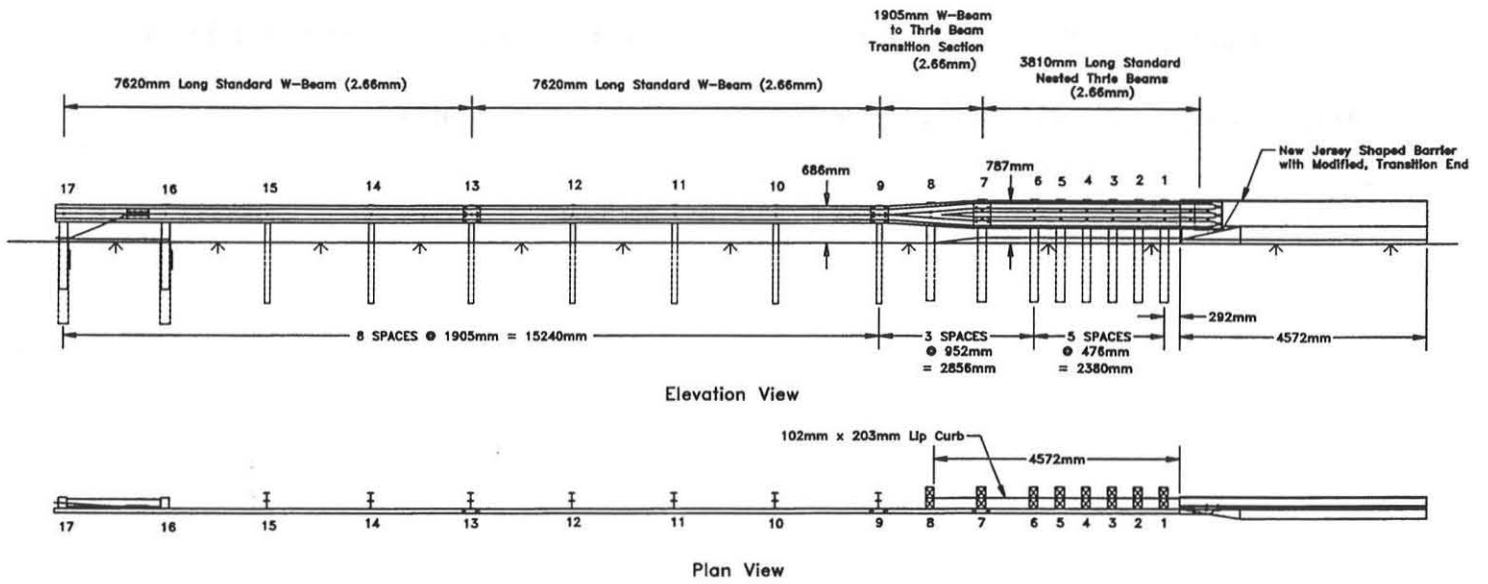
post (1092-mm embedment depth) provided an equivalent load capacity to a 1981-mm long, W150x13.5 steel post (1245-mm embedment). Therefore, 1829-mm long wood posts were chosen for Design No. 3 as the replacement to the 1981-mm long steel posts used previously in Design No. 2. Other modifications of this system from the previous steel systems included the use of wood rather than steel spacer blocks and modifying the geometry of the concrete curb to accommodate the different spacer block depth.

The system was constructed with seventeen guardrail posts, as shown in Figures 48 through 50. Post nos. 1 through 8 consisted of Southern Yellow Pine, Grade No. 1D posts measuring 152-mm wide x 203-mm deep x 1829-mm long. Post nos. 9 through 15 consisted of galvanized, ASTM A36 steel W150x13.5 sections measuring 1829-mm long. Post nos. 16 and 17 were timber posts measuring 140-mm wide x 190-mm deep x 1080-mm long and were placed in steel foundation tubes. The timber posts and foundation tubes were part of an anchorage system used to develop the required tensile capacity of the guardrail. Lap-splice connections between the rail sections were configured to reduce vehicle snagging at the splice during the crash tests.

The soil embedment depths for post nos. 1 through 7, 8, and 9 through 15 were 1092 mm, 1067 mm, and 1127 mm, respectively, as shown in Figures 48 and 49. For post nos. 1 through 7, a wood blockout, measuring 152-mm wide x 203-mm deep x 457-mm long, was used with thrie beam guardrail, as shown in Figures 48 and 49. At post no. 8, a wood blockout, measuring 152-mm wide x 203-mm deep x 457-mm long, was used at the midspan of the W-beam to thrie beam transition section. For post nos. 9 through 15, W150x13.5 by 337-mm long spacer blockouts were used and with steel W-beam backup plates at all post locations except at rail splices.

A triangular-shape concrete curb, measuring 4,572-mm long x 102-mm high x 203-mm wide,

as shown in Figures 48 and 50, was constructed below the thrie beam rail to determine if the curb would adversely effect the safety performance of the new transition design.



Thrie Beam Posts

Thrie Beam Spacers

Thrie Beam Support Details

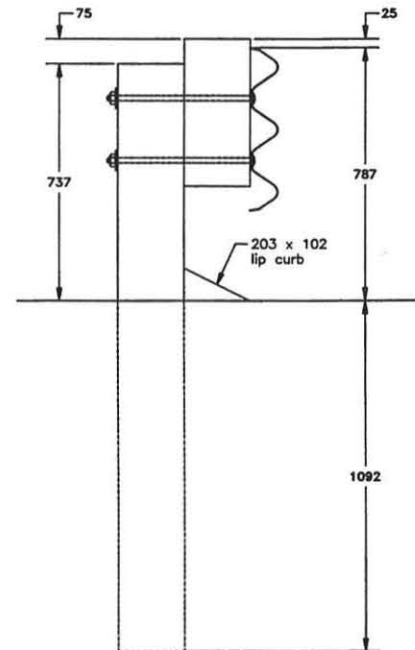
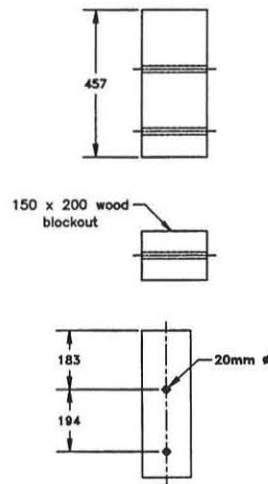
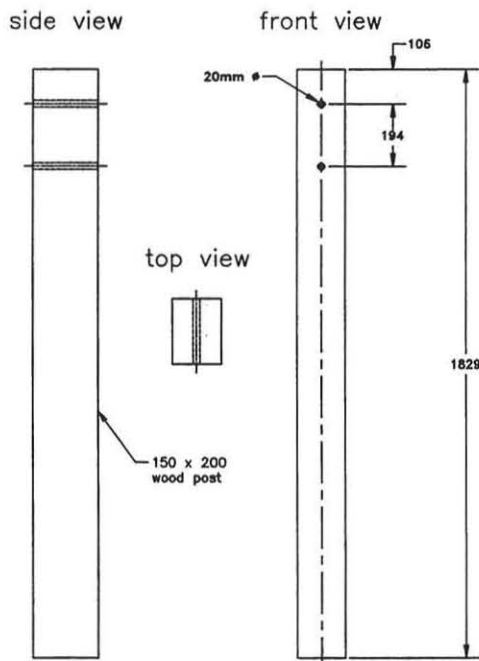
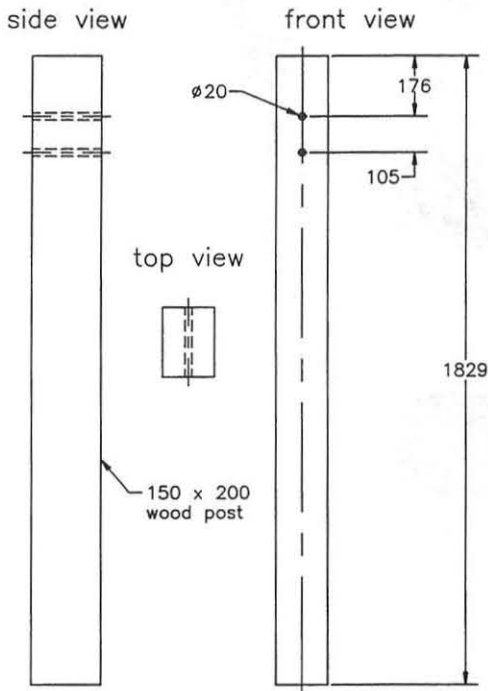
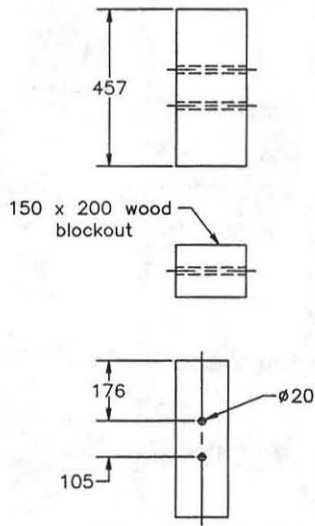


Figure 48. Installation Layout and Design Details, Design No. 3

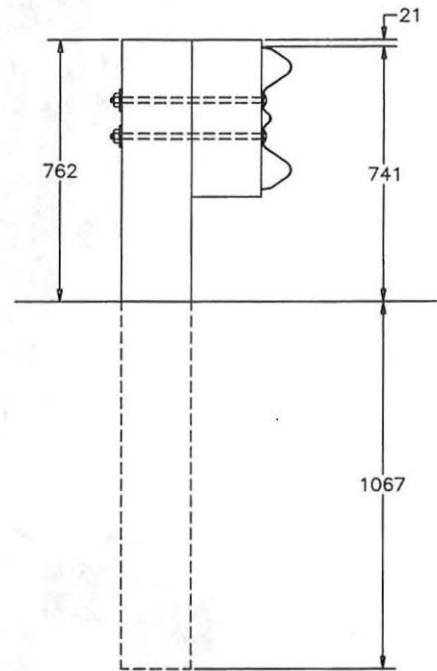
W - Thrie Trans. Post



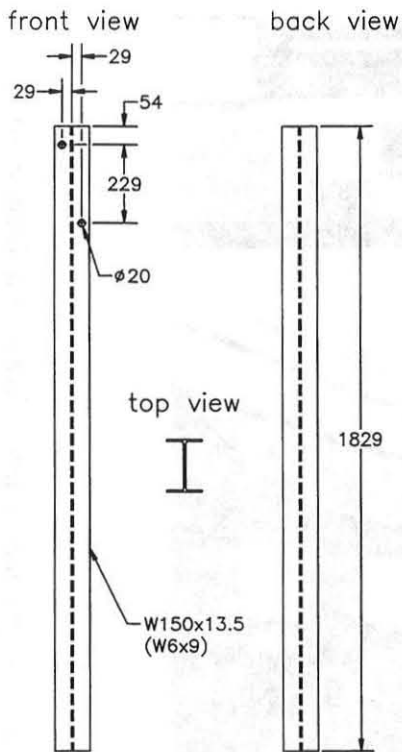
W - Thrie Trans. Spacer



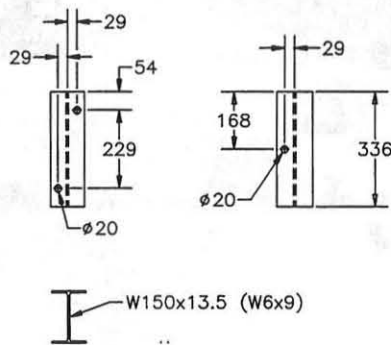
W - Thrie Support Details



W Beam Posts



W Beam Spacers



W Beam Support Details

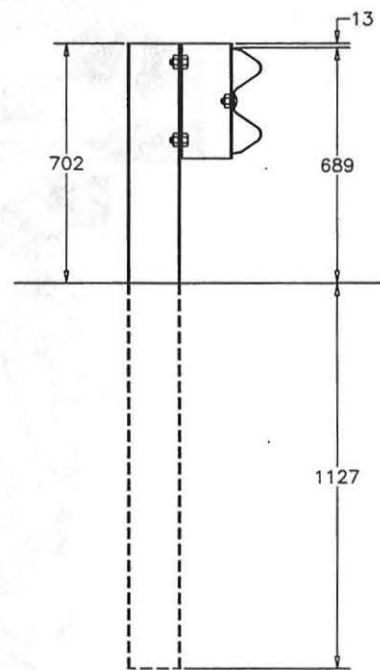


Figure 49. Design Details, Design No. 3

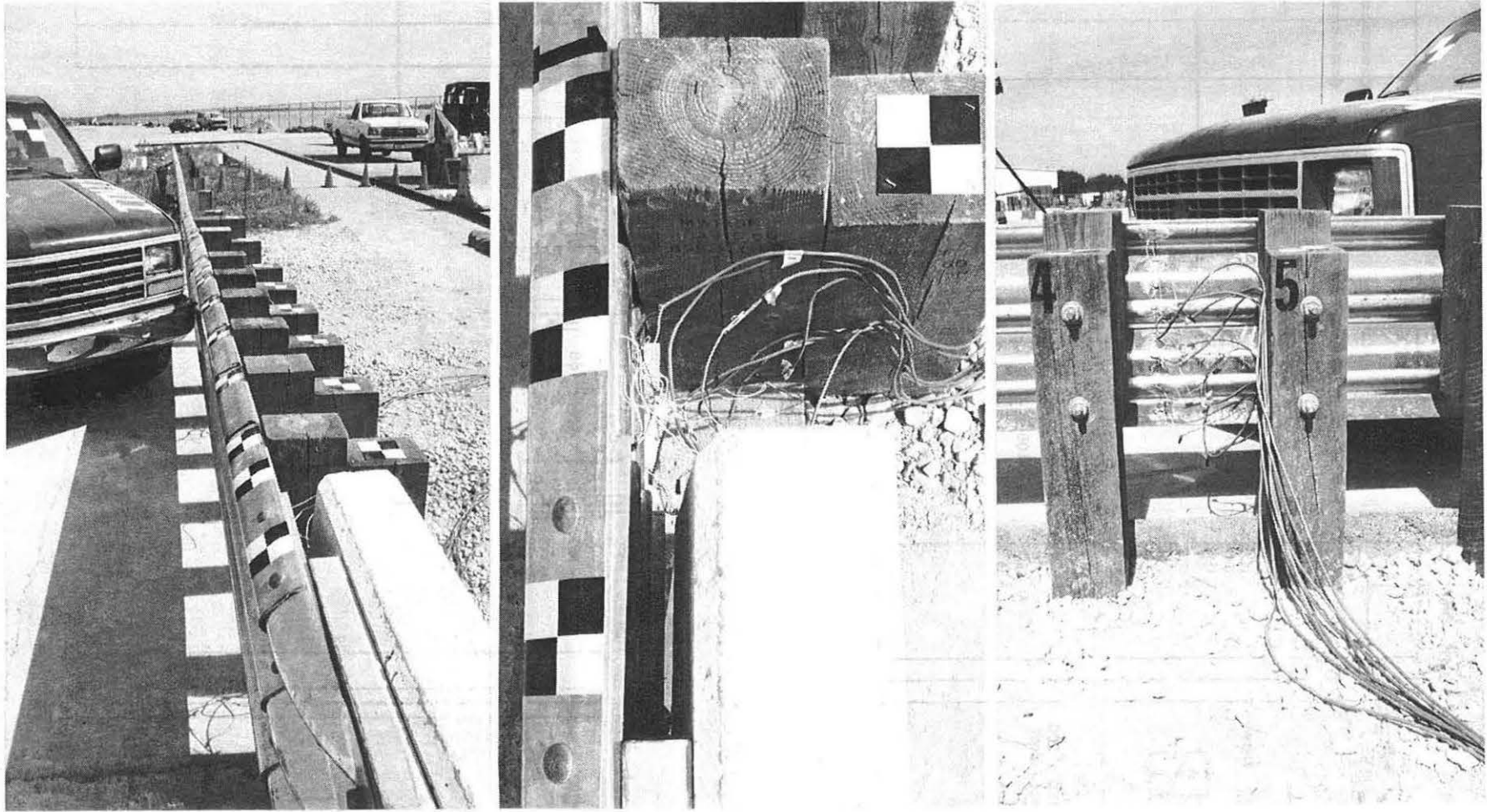


Figure 50. Approach Guardrail Transition, Design No. 3

13 CRASH TEST NO. 3 (DESIGN NO. 3 - WOOD POSTS)

13.1 Test ITNJ-3

The 1,987-kg pickup truck impacted the approach guardrail transition (Design No. 3) at a speed of 102.0 km/hr and an angle of 26.9 degrees. A summary of the test results and the sequential photographs are shown in Figure 51. Additional sequential photographs are shown in Figure 52. Documentary photographs of the crash test are shown in Figures 53 and 54.

13.2 Test Description

Initial impact occurred at the midspan between post nos. 5 and 6 or 2,435-mm upstream from the end of the concrete barrier, as shown in Figure 55. Large lateral dynamic and permanent set barrier deflections occurred, as shown in Figures 51 and 56. This was evidenced by the crease formed in the thrie beam rail near post no. 3. During vehicle redirection, the pickup truck's left-front quarter panel extended over the thrie beam, contacting the top corner of the spacer blocks as well as the top edge of the concrete end section. This contact caused moderate tearing of the sheet metal and downward forces applied to the left-front corner of the vehicle. At 0.208 sec after impact, the vehicle became parallel to the barrier with a velocity of 63.1 km/hr. During vehicle tail-slap with the barrier, the rear-end of the vehicle pitched upward moderately, allowing the left-rear corner of the bumper to mount the top of the thrie beam and contact the several spacer blocks and concrete end section. At 0.401 sec after impact, the vehicle exited the barrier at an angle of 13.1 degrees and a speed of 61.7 km/hr. Subsequently, the left-front wheel assembly contacted the ground with significant vehicular motions, including counter-clockwise vehicle roll, downward pitching, and clockwise yawing. These angular motions caused the pickup truck to roll over 3 times. The vehicle's post-impact trajectory is shown in Figure 51. The vehicle came to rest 44.2 m downstream from

impact and 17.1 m away from the traffic-side face of the barrier.

13.3 Barrier Damage

Damage to the barrier was moderate, as shown in Figures 56 through 59. Barrier damage consisted mostly of deformed thrie beam, tire marks on the lower upstream face of the concrete end section, and cracking in the concrete end section. Concrete cracking and minor spalling was observed on the upstream end of the concrete end section. The permanent set of the guardrail and posts is shown in Figures 51 and 56 through 59. The maximum lateral permanent set deflection was approximately 171 mm at post no. 3, as measured in the field. The maximum lateral dynamic deflection was 264 mm at post no. 3, as determined from the high-speed film analysis.

13.4 Vehicle Damage

Exterior and interior vehicle damage was extensive and occurred to several body locations, as shown in Figures 60 and 61. The left-front quarter panel was crushed inward, and the left-side of the front bumper was also bent back toward the engine compartment. The engine hood, roof, truck cab, and window glass were severely crushed during the vehicle rollovers. The floorboard of the occupant compartment also contained significant plastic deformations due to the severe impact with the barrier as well as from vehicle rollover.

13.5 Occupant Risk Values

The normalized longitudinal and lateral occupant impact velocities were determined to be 8.71 m/sec and 6.71 m/sec, respectively. The maximum 0.010-sec average occupant ridedown decelerations in the longitudinal and lateral directions were 6.27 g's and 15.27 g's, respectively. It is noted that the occupant impact velocities (OIV) and occupant ridedown decelerations (ORD) were within the suggested limits provided in NCHRP Report 350. The results of the occupant risk,

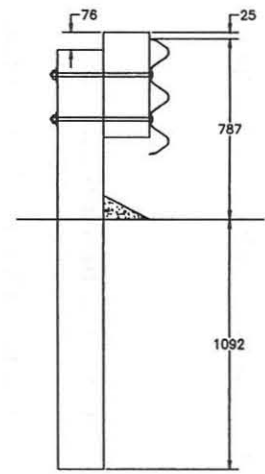
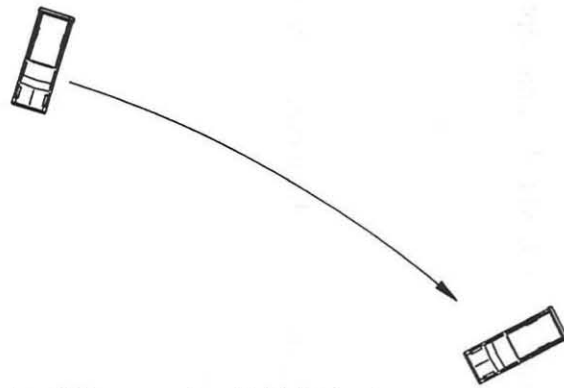
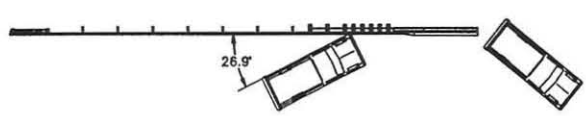
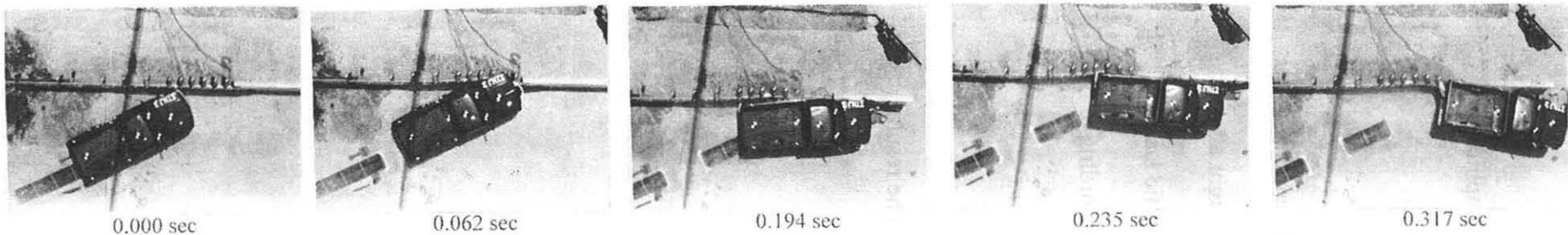
determined from accelerometer data, are summarized in Figure 51. Results are shown graphically in Appendix F. The results from the rate transducer are shown graphically in Appendix G.

13.6 Discussion

The analysis of the test results for test ITNJ-3 showed that the barrier satisfactorily contained the vehicle but inadequately redirected the vehicle, since the vehicle did not remain upright after collision with the barrier. After collision, the vehicle's trajectory intruded into adjacent traffic lanes. Therefore, test ITNJ-3 conducted on Design No. 3 was determined to be unacceptable according to the NCHRP Report 350 criteria.

13.7 Barrier Instrumentation Results

For test ITNJ-3, strain gauges were located on the approach guardrail transition. The results of the strain gauge analysis are provided in Table 4.

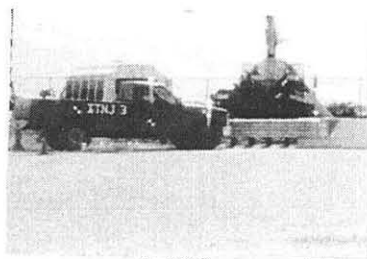


98

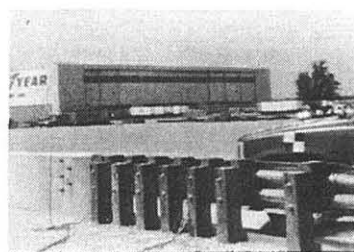
- Test Number ITNJ-3
- Date 7/8/97
- Appurtenance Approach Guardrail Transition to a NJ Safety Shape End Section w/ Curb
- Total Length 25.34 m
- Steel Thrie Beam (Nested)
 - Thickness 2.66 mm
 - Top Mounting Height 787 mm
- Wood Posts
 - Post Nos. 1 - 8 152 mm x 203 mm by 1829-mm long
- Wood Spacer Blocks
 - Post Nos. 1 - 8 152 mm x 203 mm by 457-mm long
- Steel Posts
 - Post Nos. 9 - 15 W150x13.5 by 1829-mm long
- Steel Spacer Blocks
 - Post Nos. 9 - 15 W150x13.5 by 337-mm long
- Soil Type Grading B - AASHTO M 147-65 (1990)
- Vehicle Model 1990 Chevrolet 2500 2WD
 - Curb 1,813 kg
 - Test Inertial 1,987 kg
 - Gross Static 1,987 kg
- Vehicle Speed
 - Impact 102.0 km/hr
 - Exit 61.7 km/hr

- Vehicle Angle
 - Impact 26.9 deg
 - Exit 13.1 deg
- Vehicle Snagging Contact on top of spacer blocks and concrete end section
- Vehicle Pocketing None
- Vehicle Stability Vehicle rollover
- Occupant Ridedown Deceleration (10 msec avg.)
 - Longitudinal 6.27/-7.82 < 20 G's
 - Lateral (not required) 15.27
- Occupant Impact Velocity (Normalized)
 - Longitudinal 8.71 < 12 m/s
 - Lateral (not required) 6.71
- Vehicle Damage Extensive
 - TAD¹⁸ NA
 - SAE¹⁹ NA
- Vehicle Stopping Distance 44.2 m downstream
17.1 m behind
- Barrier Damage Moderate
- Maximum Deflections
 - Permanent Set 171 mm
 - Dynamic 264 mm (visible)

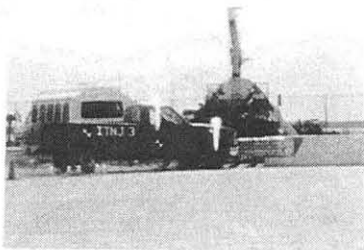
Figure 51. Summary of Test Results and Sequential Photographs, Test ITNJ-3 (Design No. 3)



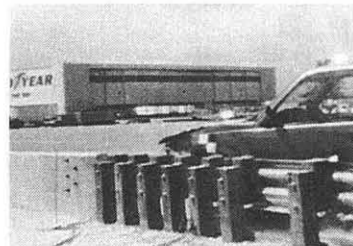
0.000 sec



0.000 sec



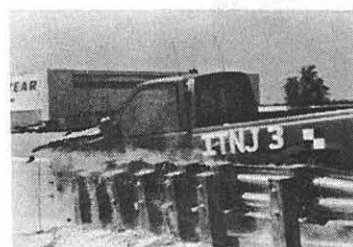
0.034 sec



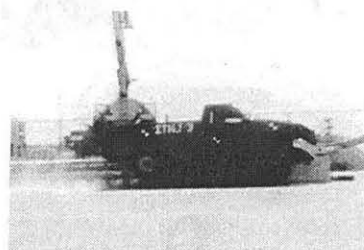
0.038 sec



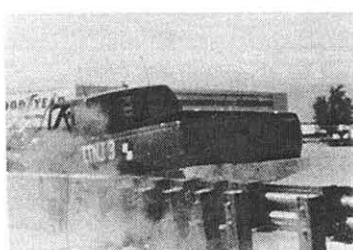
0.110 sec



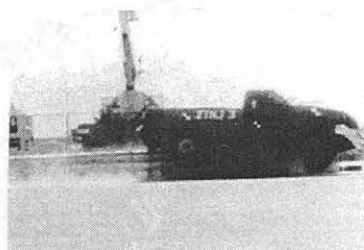
0.101 sec



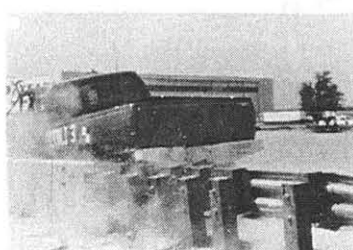
0.236 sec



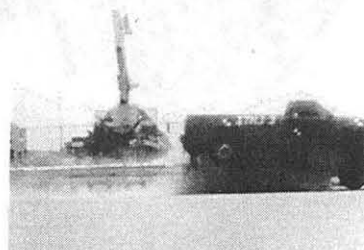
0.236 sec



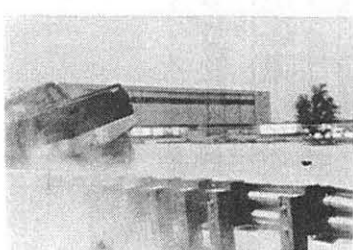
0.276 sec



0.260 sec



0.332 sec



0.403 sec

Figure 52. Additional Sequential Photographs, Test ITNJ-3 (Design No. 3)

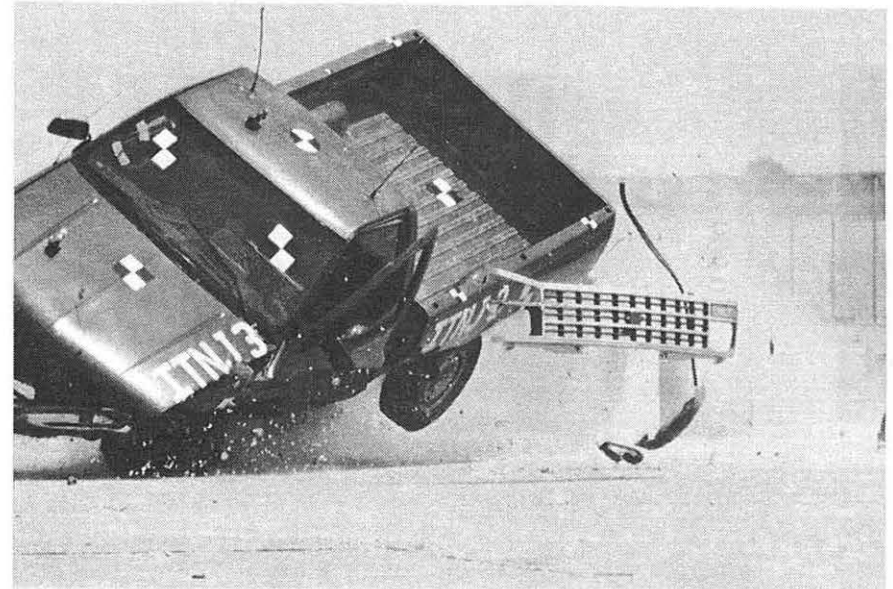
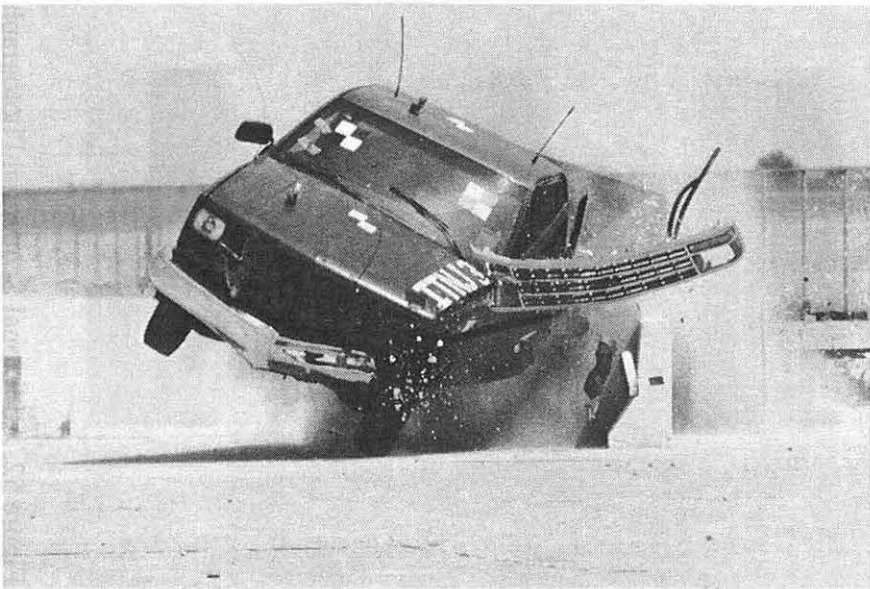
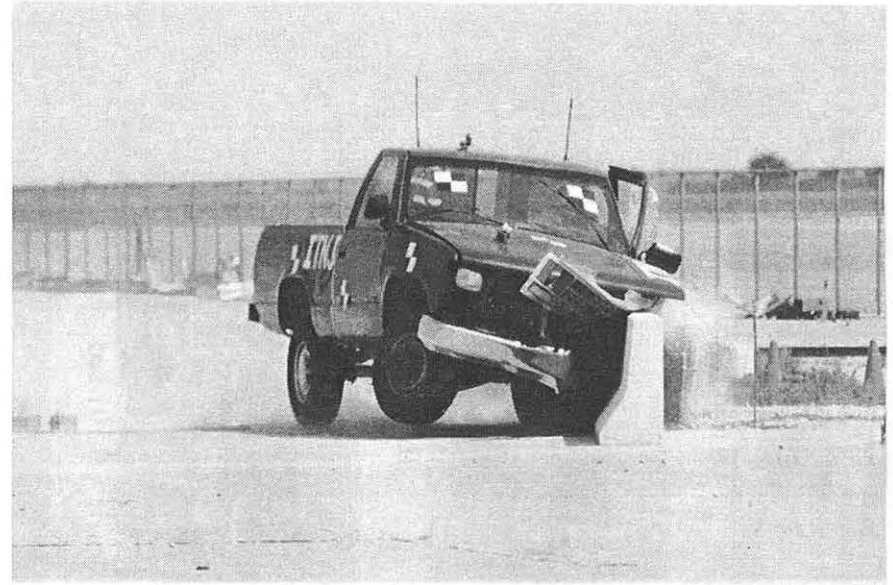


Figure 53. Documentary Photographs, Test ITNJ-3 (Design No. 3)

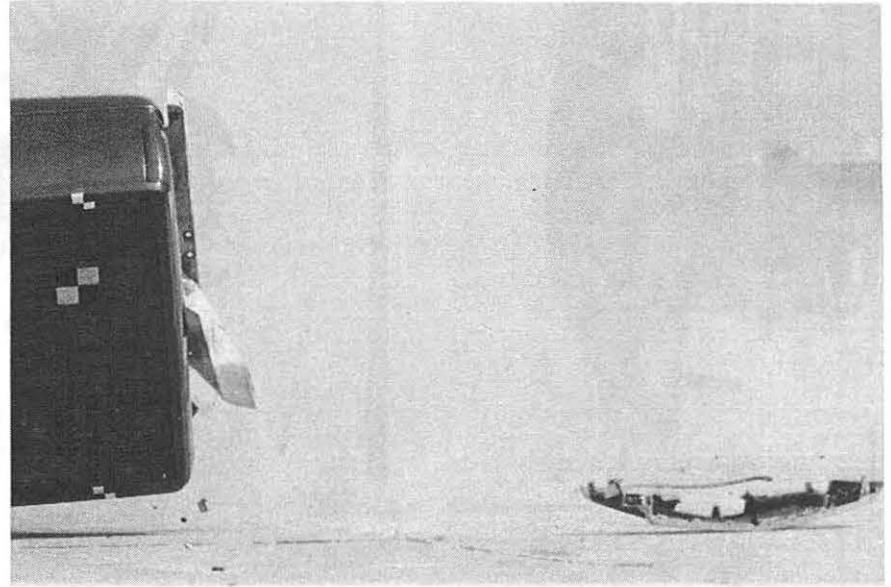
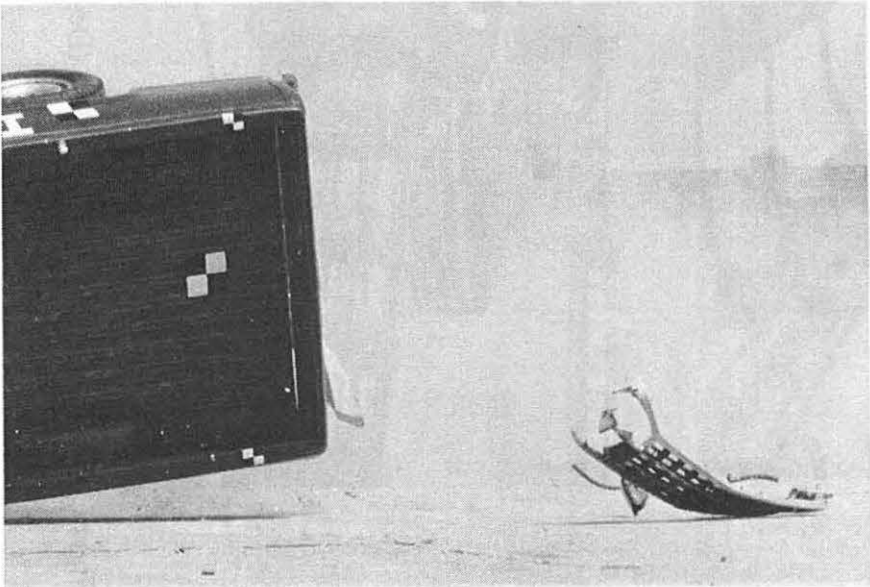
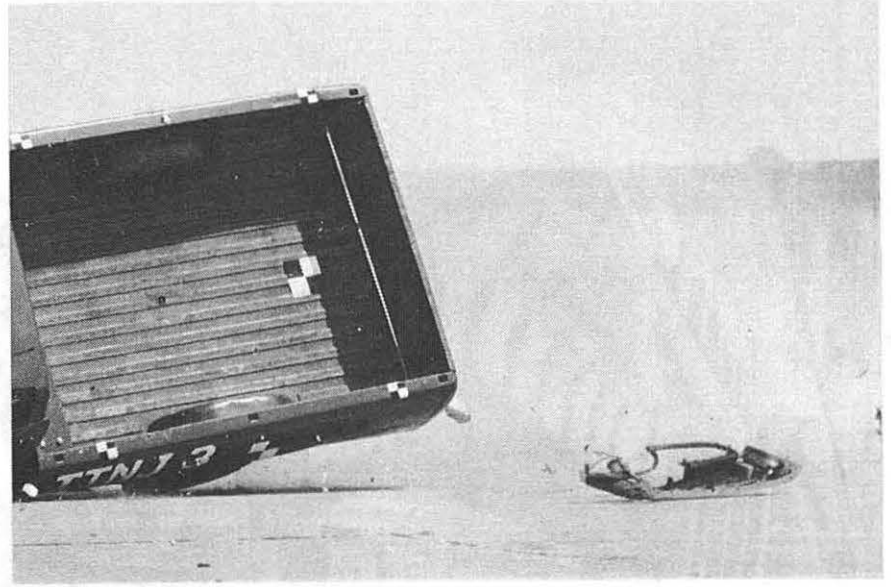
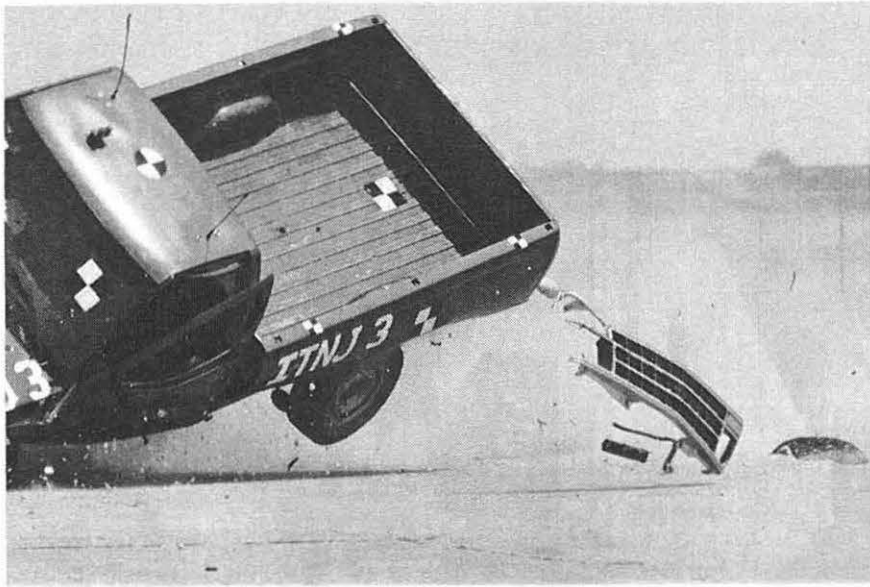


Figure 54. Documentary Photographs, Test ITNJ-3 (Design No. 3)



Figure 55. Impact Location, Test ITNJ-3 (Design No. 3)

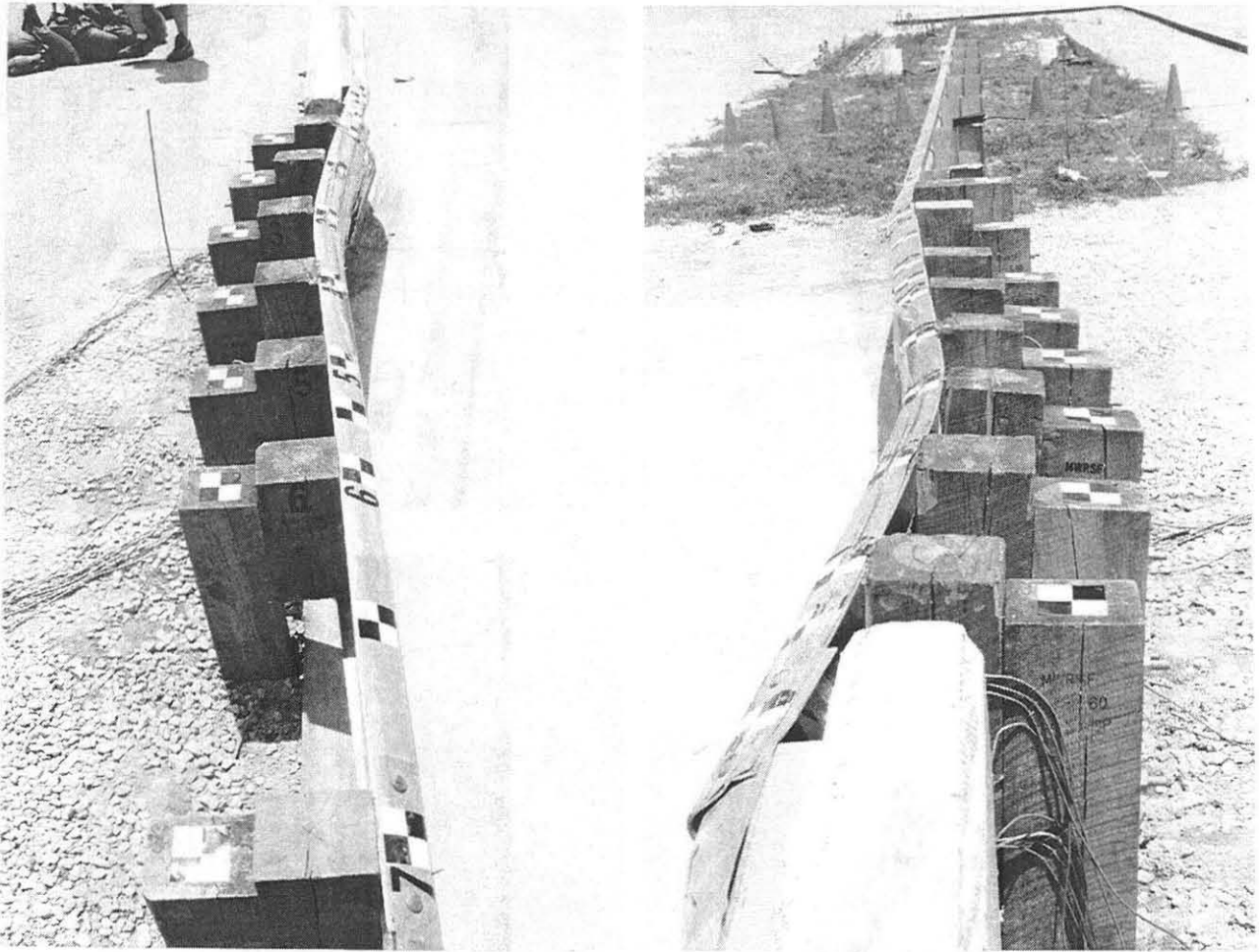


Figure 56. Barrier Damage, Test ITNJ-3 (Design No. 3)

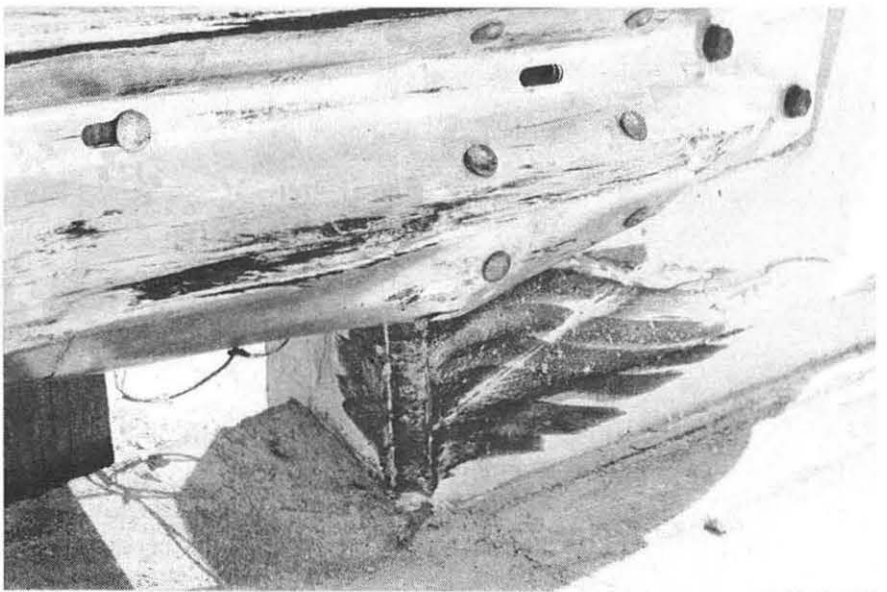
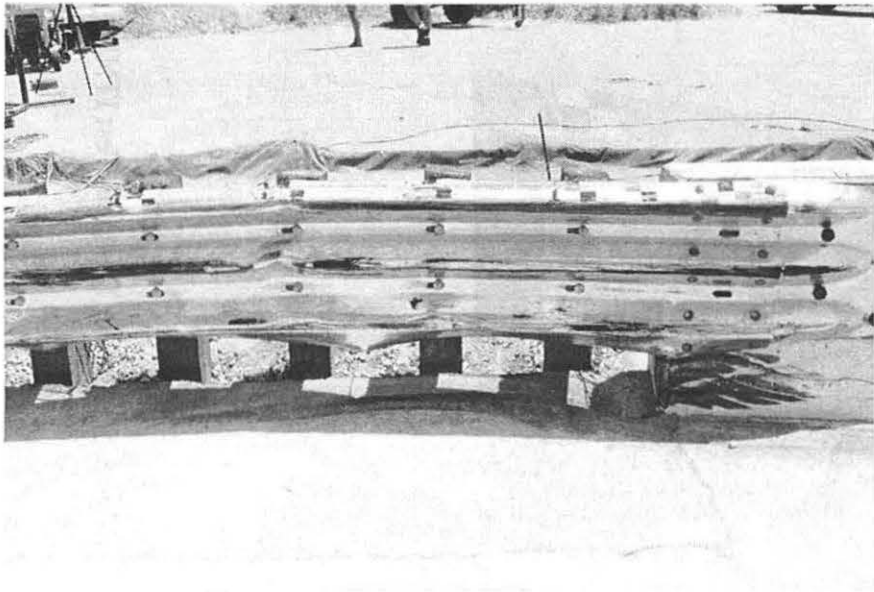
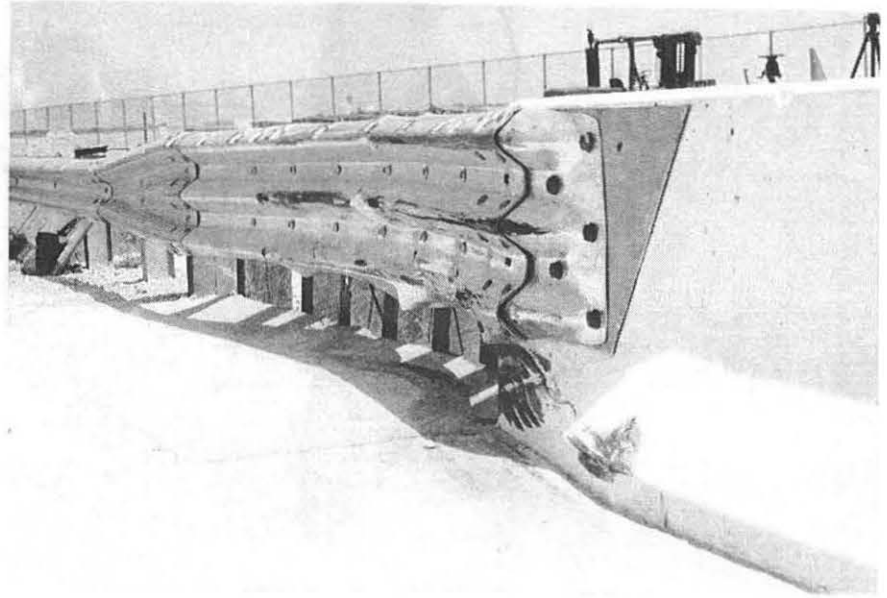
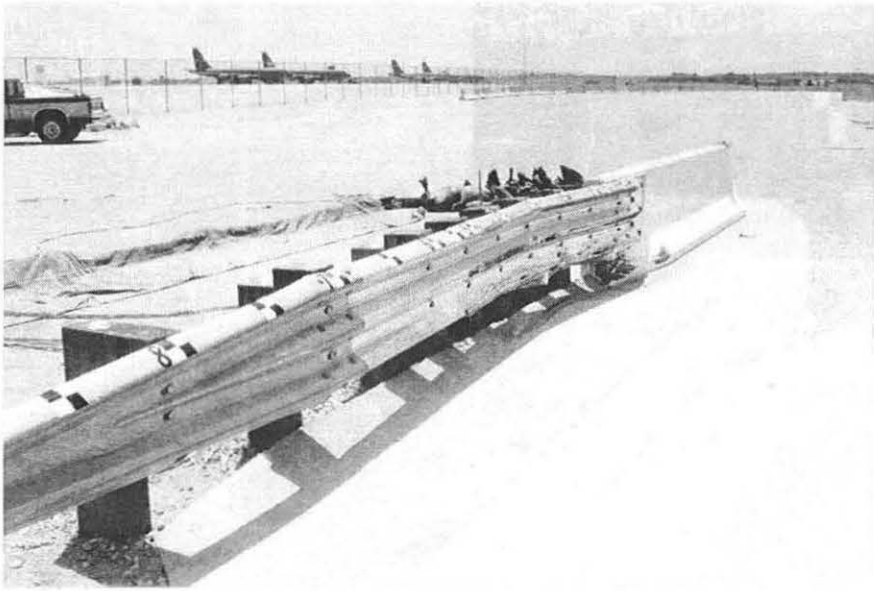


Figure 57. Barrier Damage, Test ITNJ-3 (Design No. 3)

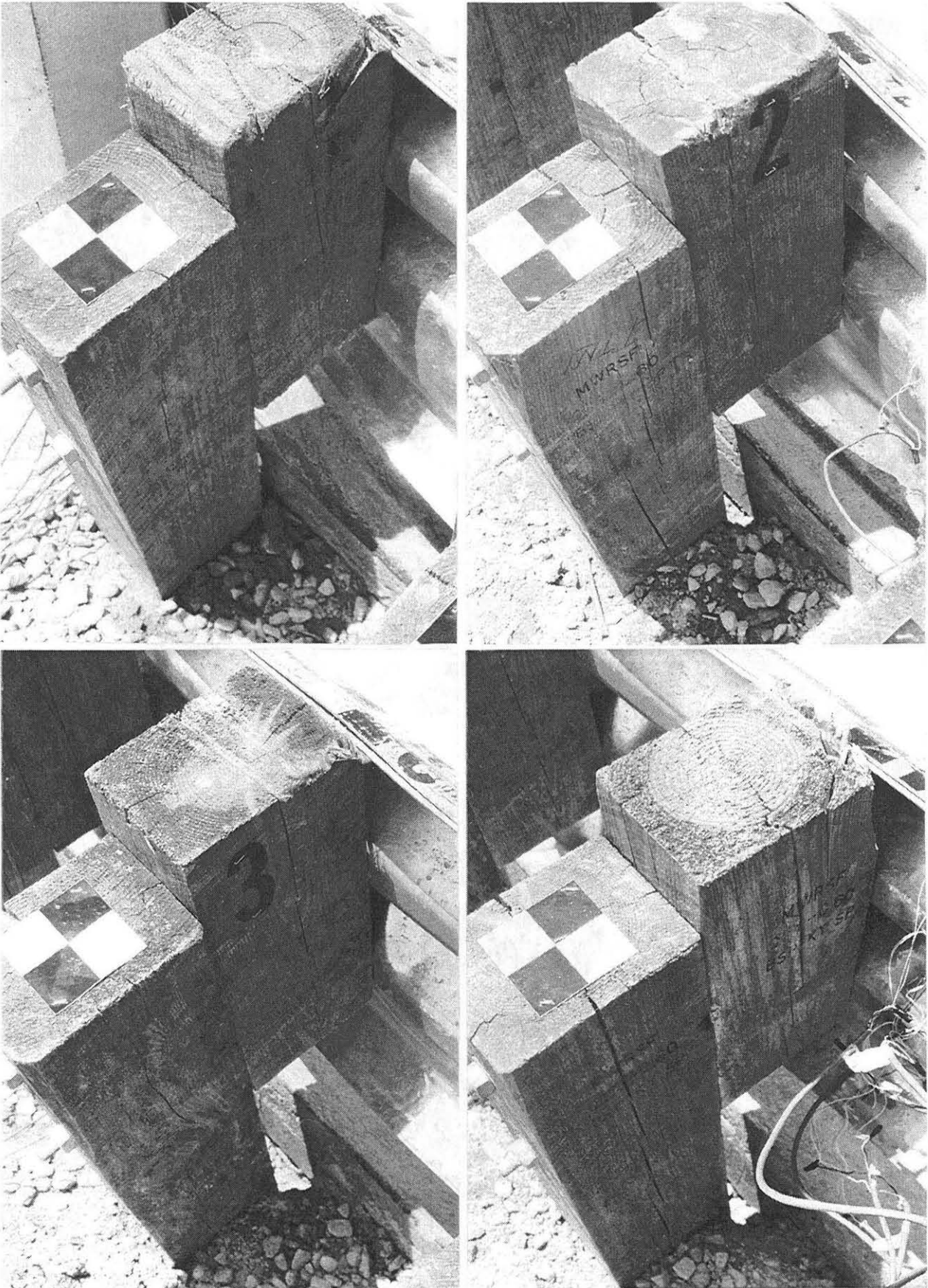


Figure 58. Final Post Positions, Test ITNJ-3 (Design No. 3)

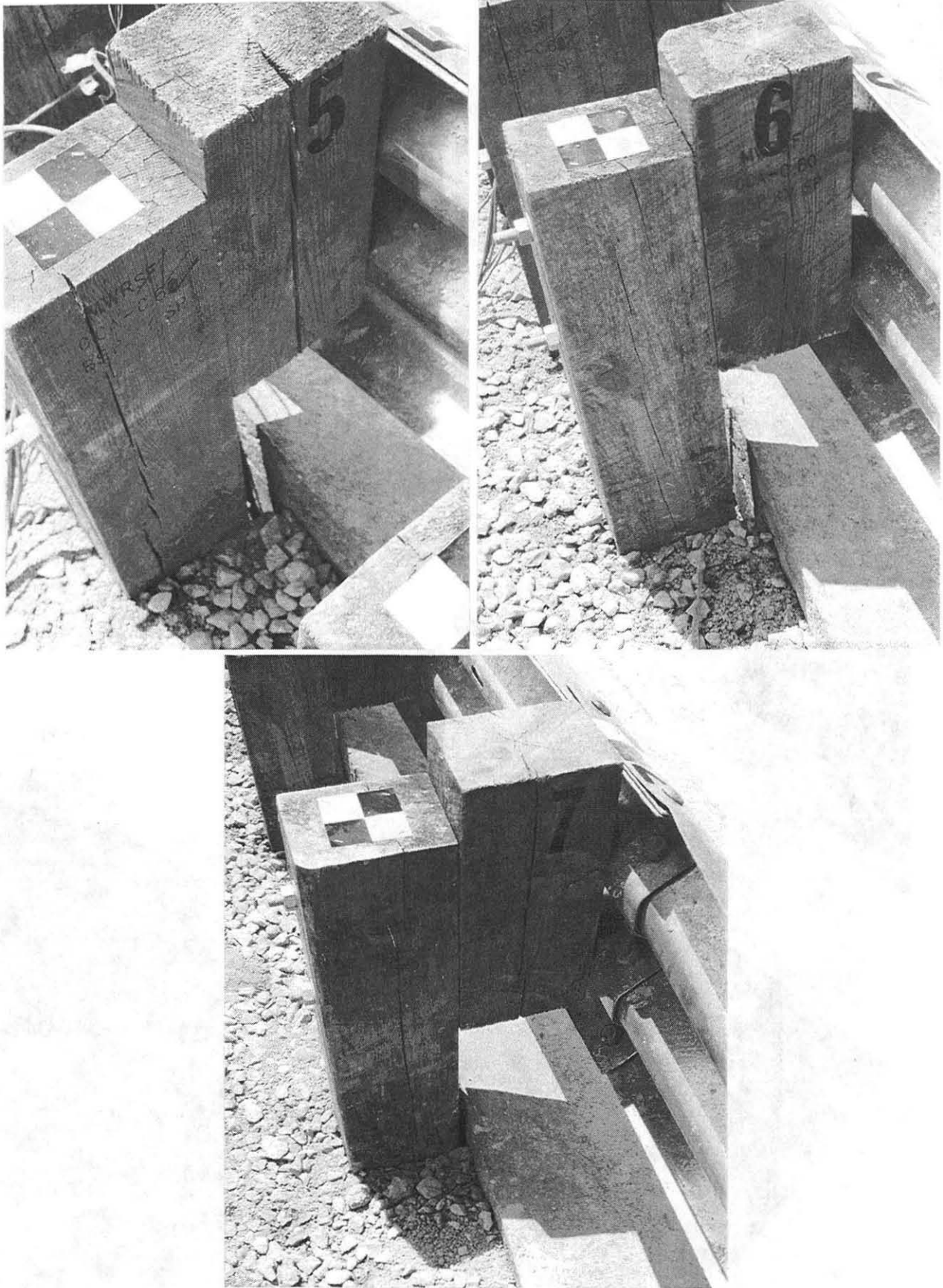


Figure 59. Final Post Positions, Test ITNJ-3 (Design No. 3)

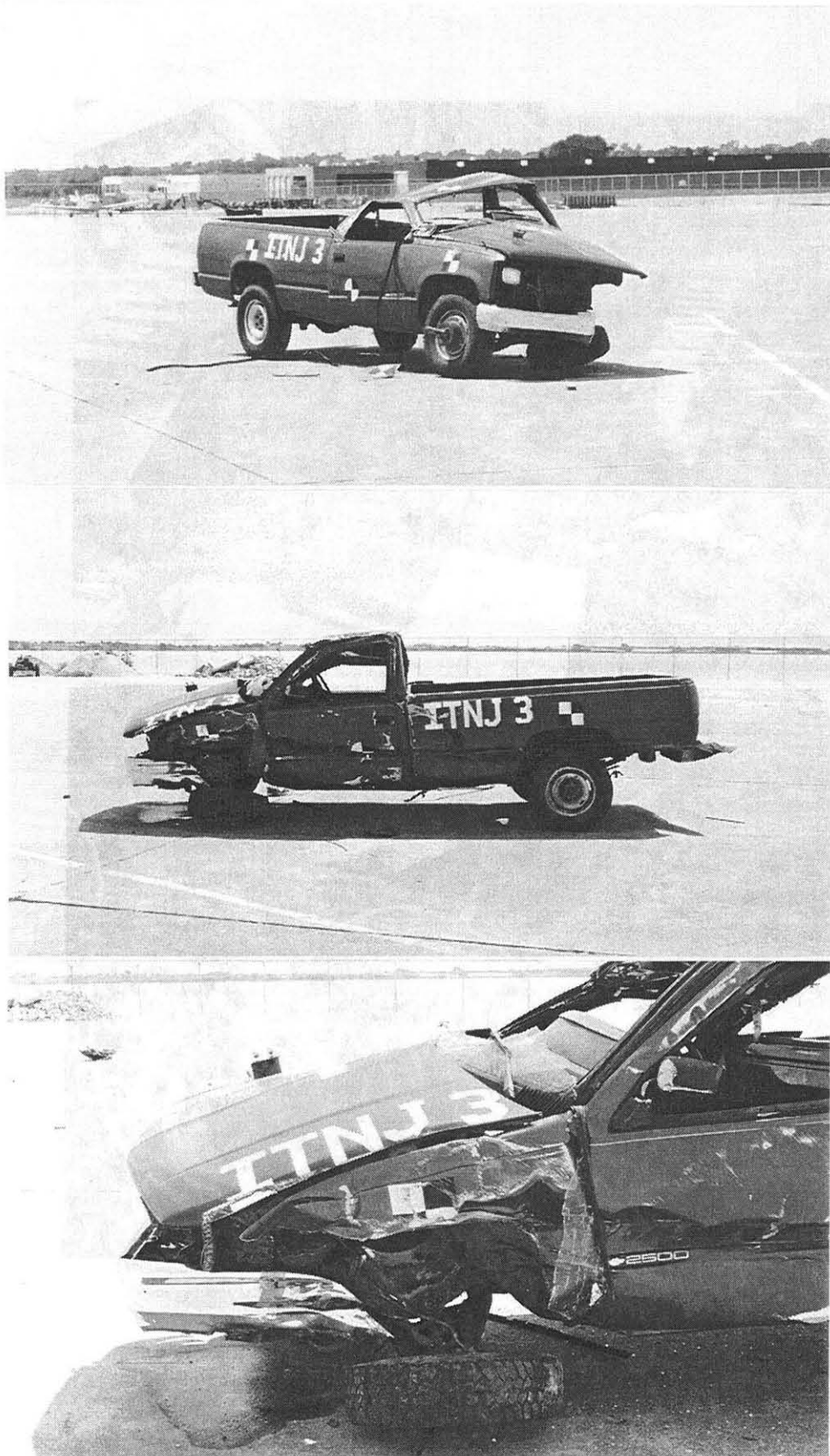


Figure 60. Vehicle Damage, Test ITNJ-3 (Design No. 3)

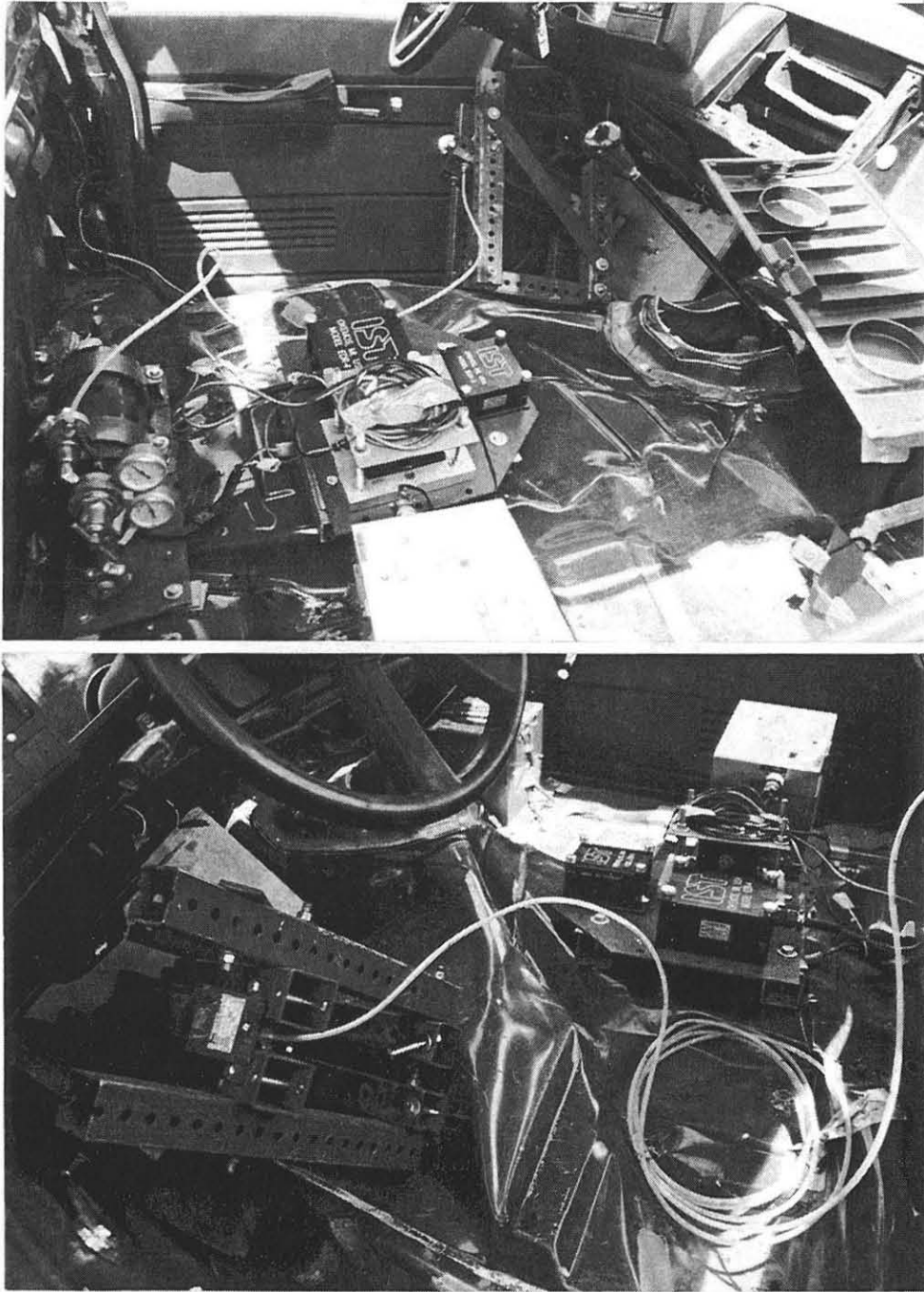


Figure 61. Occupant Compartment Deformation, Test ITNJ-3 (Design No. 3)

Table 4. Strain Gauge Results, Test ITNJ-3 (Design No. 3)

Hardware Type	Strain Gauge No.	Strain Gauge Location	Maximum μ Strain ¹ (in./in.)	Maximum Stress ² (ksi)	Comments
Thrie Beam	1	Note ³	437	13.10	Neutral axis above top peak on back of rail
	2	Note ³	769	23.08	Neutral axis below top peak on back of rail
	3	Note ³	2701	NA	Top valley on back of rail
	4	Note ³	478	14.34	Neutral axis above middle peak on back of rail
	5	Note ³	1487	44.62	Neutral axis below middle peak on back of rail
	6	Note ³	1757	NA	Bottom valley on back of rail
	7	Note ³	1901	NA	Neutral axis above bottom peak on back of rail
	8	Note ³	2318	NA	Neutral axis below bottom peak on back of rail
	9	Midspan 2/3	366	10.99	Neutral axis above middle peak on back of rail
	10	Midspan 2/3	1963	NA	Neutral axis below middle peak on back of rail
	11	Note ⁴	1651	49.53	Neutral axis above top peak on back of rail
	12	Note ⁴	393	11.79	Neutral axis below top peak on back of rail
	13	Note ⁴	2452	NA	Top valley on back of rail
	14	Note ⁴	497	14.92	Neutral axis above middle peak on back of rail
	15	Note ⁴	NA	NA	Neutral axis below middle peak on back of rail
	16	Note ⁴	1662	49.87	Bottom valley on back of rail
	17	Note ⁴	1135	34.06	Neutral axis above bottom peak on back of rail
	18	Note ⁴	NA	NA	Neutral axis below bottom peak on back of rail

¹ - All strain values are shown as the absolute value only.

² - All elastic stress values are shown as the absolute value only and calculated by multiplying the strain by the modulus of elasticity equal to 30,000 ksi. Minimum yield stress for the thrie beam is 50 ksi.

³ - Strain gauge location is 159 mm upstream of the concrete end section.

⁴ - Strain gauge location is 152 mm upstream of post no. 4.

NA - Not available.

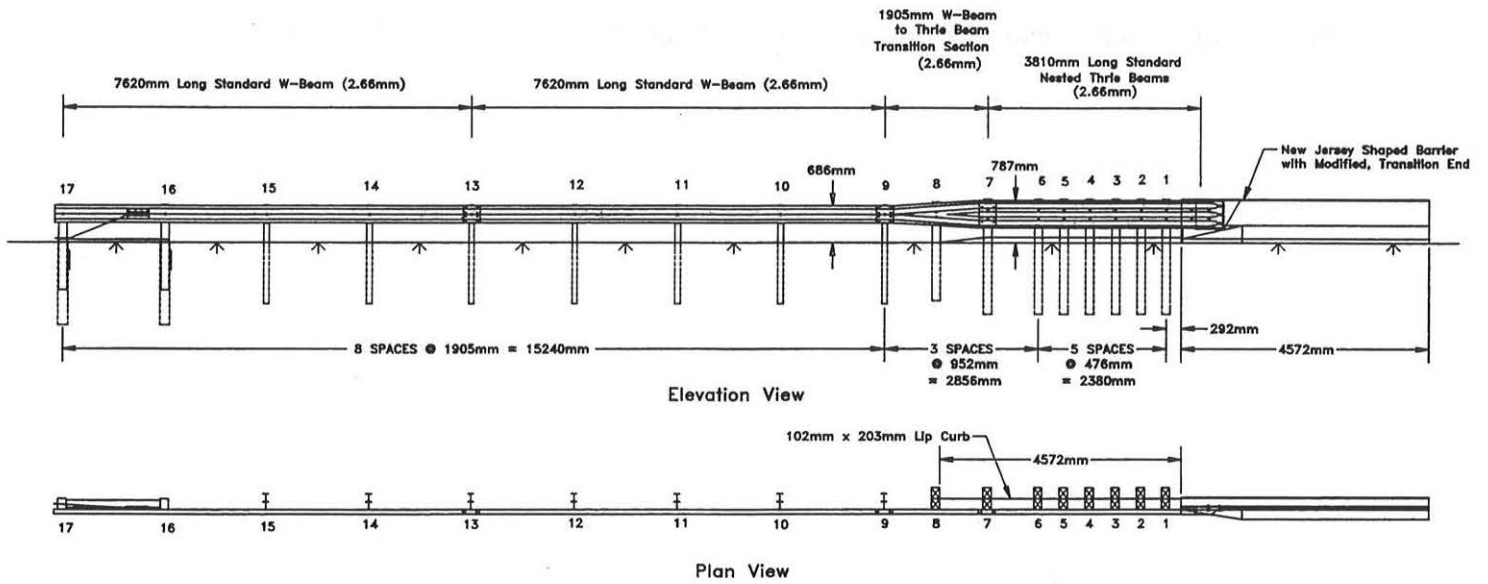
14 DISCUSSION AND MODIFICATIONS (DESIGN NO. 4)

Following the unsuccessful crash test of Design No. 3, it was necessary to determine the cause of the poor barrier performance and subsequent vehicle rollover so that design modifications could be made to the system. A careful examination of the damaged barrier system and an analysis of the test results revealed that the dynamic and permanent set barrier deflections were greater than those predicted. It is believed that these excessive barrier deflections occurred due to post-soil forces lower than expected.

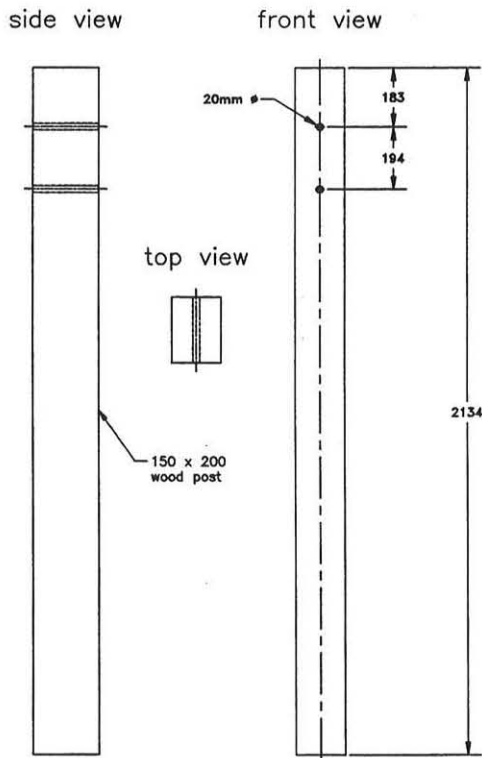
As a result of the extensive vehicle penetration into the barrier system, the pickup truck was redirected out of the barrier system at a higher than normal exit angle. During, vehicle redirection, the left-corner of the rear bumper mounted the top of the thrie beam, contacting several spacer blocks and the concrete end section. These two conditions led to significant roll, pitch, and yaw angular motions, resulting in vehicle rollover. Once again, the increased vehicle penetration and minor pocketing led to higher than expected impact forces being applied to the concrete end section, resulting in cracking of the safety shape barrier.

After this investigation, it was believed that the safety performance of the approach guardrail transition (Design No. 3) could be significantly improved with a reduction in dynamic and permanent set barrier deflections. One major modification was implemented for stiffening the approach guardrail transition. The embedment depth of post nos. 1 through 7 were increased by 229 mm, resulting in a total embedment depth of 1,321 mm. In addition, the top height of the wood posts were placed flush with the wood spacer blocks, thus requiring the use of 2,134-mm long posts. Also, the well-graded aggregate material used in Design No. 3, with a reduced amount of material in the middle sieve sizes, was replaced with the well-graded crushed limestone material used in Design No.

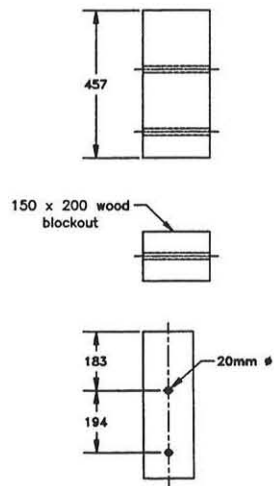
2. These modifications, incorporated in Design No. 4, are shown in Figures 62 and 63.



Thrie Beam Posts



Thrie Beam Spacers



Thrie Beam Support Details

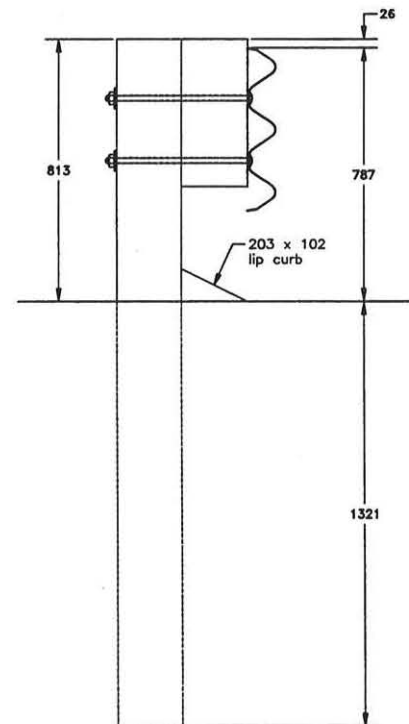


Figure 62. Barrier and Post Modifications, Design No. 4

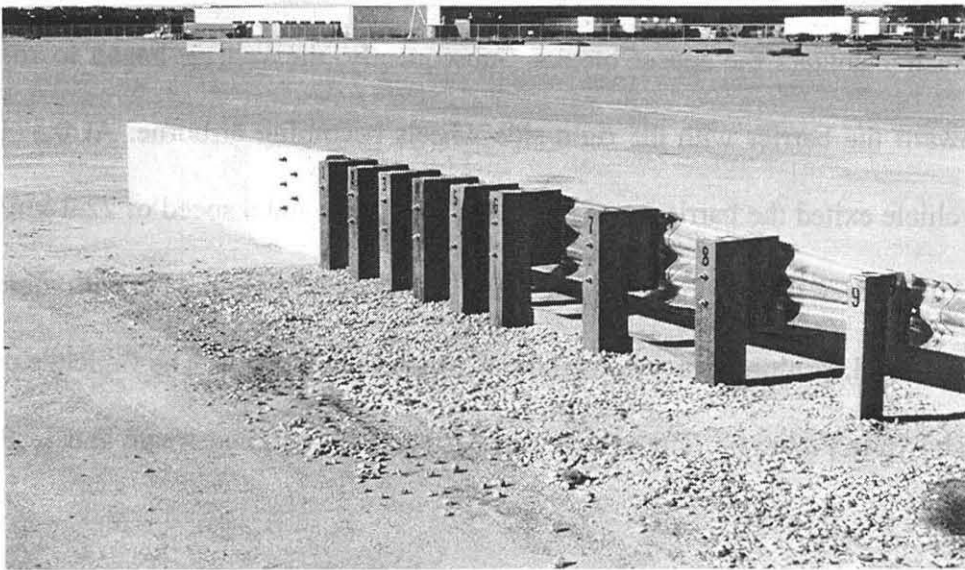
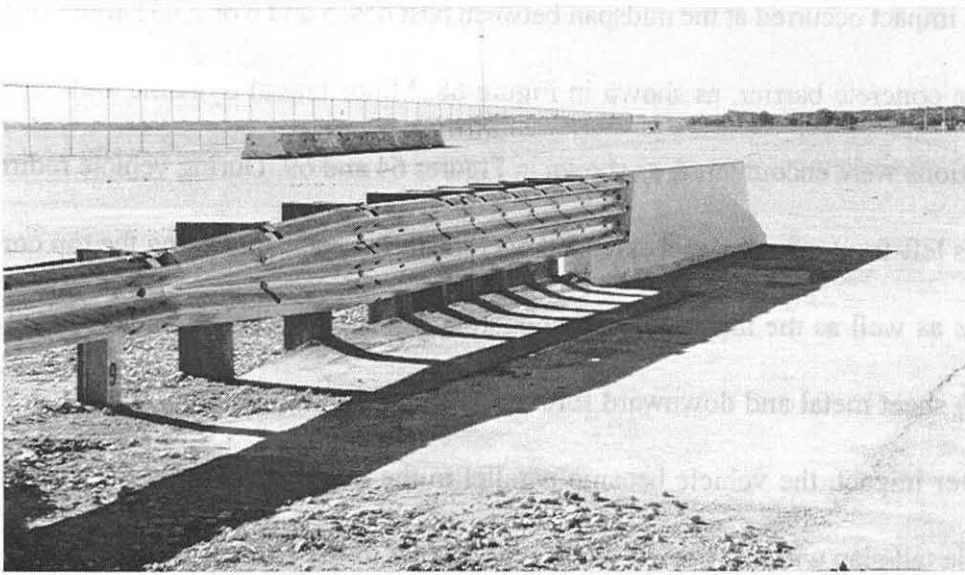
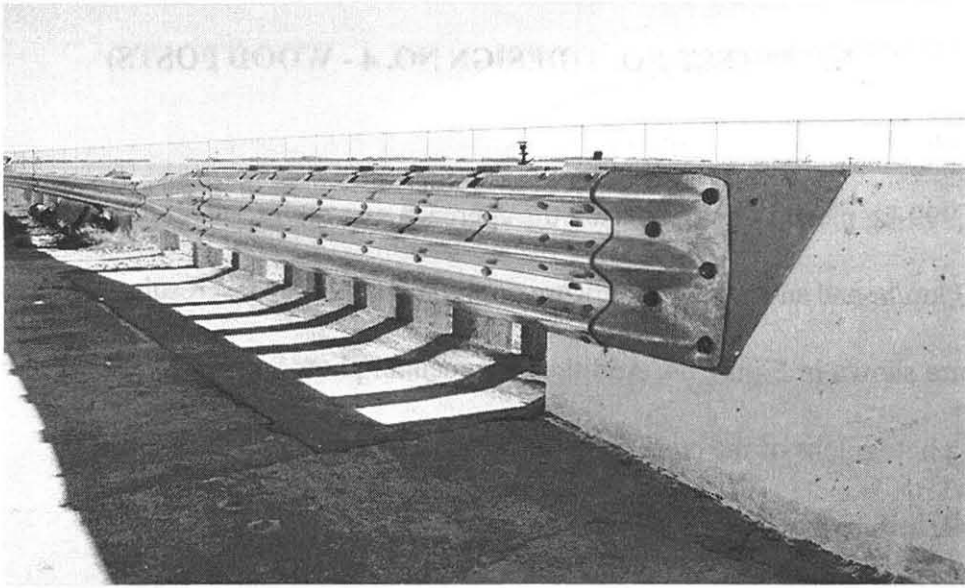


Figure 63. Approach Guardrail Transition, Design No. 4

15 CRASH TEST NO. 4 (DESIGN NO. 4 - WOOD POSTS)

15.1 Test ITNJ-4

The 1,999-kg pickup truck impacted the approach guardrail transition (Design No. 4) at a speed of 102.3 km/hr and an angle of 24.6 degrees. A summary of the test results and the sequential photographs are shown in Figure 64. Additional sequential photographs are shown in Figure 65. Documentary photographs of the crash test are shown in Figures 66 and 67.

15.2 Test Description

Initial impact occurred at the midspan between post nos. 5 and 6 or 2,435-mm upstream from the end of the concrete barrier, as shown in Figure 68. Minor lateral dynamic and permanent set barrier deflections were encountered, as shown in Figures 64 and 69. During vehicle redirection, the pickup truck's left-front quarter panel extended over the thrie beam, contacting the top corner of the spacer blocks as well as the top edge of the concrete end section. This contact caused moderate tearing of the sheet metal and downward forces applied to the left-front corner of the vehicle. At 0.190 sec after impact, the vehicle became parallel to the barrier with a velocity of 72.8 km/hr. During vehicle tail-slap with the barrier, the left-rear corner of the bumper did not mount the top of the thrie beam nor contact the spacer blocks. Subsequently, the vehicle began to roll counter-clockwise toward the barrier with the right-side wheels becoming airborne. At 0.371 sec after impact, the vehicle exited the barrier at an angle of 7.2 degrees and a speed of 72.3 km/hr. As the vehicle exited the barrier, the left-front wheel assembly contacted the ground but with minor counter-clockwise vehicle roll, resulting in a smooth and stable vehicle redirection. The vehicle's post-impact trajectory is shown in Figure 64. The vehicle came to rest 68.4 m downstream and 12.9 m behind the barrier.

15.3 Barrier Damage

Damage to the barrier was moderate, as shown in Figures 69 and 70. Barrier damage consisted mostly of deformed thrie beam and tire marks on the lower upstream face of the concrete end section. No cracking was observed in the concrete end section. The permanent set of the guardrail and posts is shown in Figures 69 and 70. The maximum lateral permanent set deflection was approximately 32 mm at post no. 4 through the midspan between post nos. 2 and 3, as measured in the field. The maximum lateral dynamic deflection was 99 mm at post no. 3, as determined from the high-speed film analysis. It is noted that some dynamic deflection measurements were not available for viewing from the overhead camera due to the vehicle extending over the barrier.

15.4 Vehicle Damage

Vehicle damage was moderate, as shown in Figure 71. The left-front quarter panel was crushed inward, and the left-side of the front bumper was also bent back toward the engine compartment. The left-front wheel assembly was deformed and pushed backward into the firewall. Longitudinal deformations, due to vehicle-rail interlock, were observed along the entire left-side of the vehicle. Maximum occupant compartment deformations to the floorboard and/or firewall in the lateral, longitudinal, and vertical directions were 114 mm, 89 mm, and 133 mm, respectively, as shown in Figure 72.

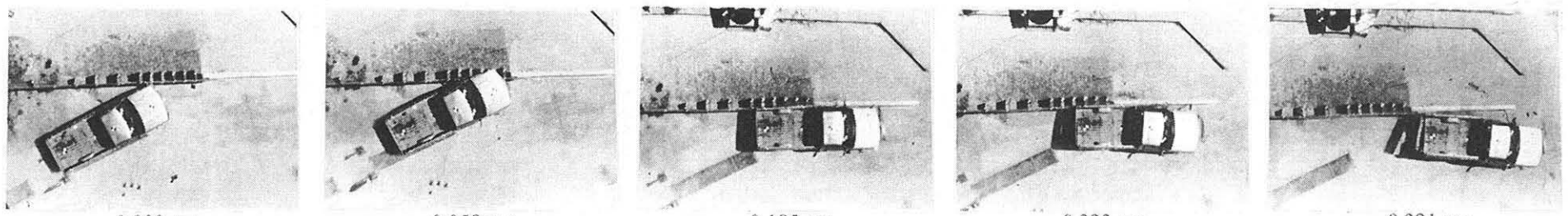
15.5 Occupant Risk Values

The normalized longitudinal and lateral occupant impact velocities were determined to be 7.74 m/sec and 6.59 m/sec, respectively. The maximum 0.010-sec average occupant ridedown decelerations in the longitudinal and lateral directions were 5.79 g's and 9.22 g's, respectively. It is noted that the occupant impact velocities (OIV) and occupant ridedown decelerations (ORD) were

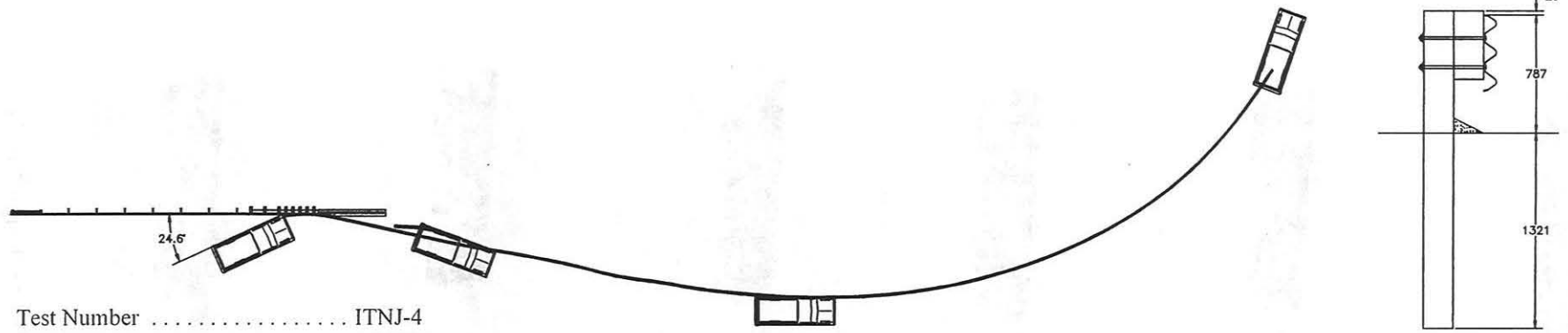
within the suggested limits provided in NCHRP Report 350. The results of the occupant risk, determined from accelerometer data, are summarized in Figure 64. Results are shown graphically in Appendix H.

15.6 Discussion

The analysis of the test results for test ITNJ-4 showed that the barrier adequately contained and redirected the vehicle with controlled lateral displacement of the barrier. Minor deformations to the occupant compartment were evident but not considered excessive enough to cause serious injuries to the occupants. The vehicle remained upright both during and after the collision. Minor vehicle roll, pitch, and yaw angular displacements were noted, but they were deemed acceptable because they did not adversely influence occupant safety criteria or cause rollover. After collision, the vehicle's trajectory intruded slightly into adjacent traffic lanes but was determined to be acceptable. In addition, the vehicle's exit angle was less than 60 percent of the impact angle. Therefore, test ITNJ-4 conducted on Design No. 4 was determined to be acceptable according to the NCHRP Report 350 criteria.



0.000 sec 0.058 sec 0.185 sec 0.223 sec 0.321 sec



105

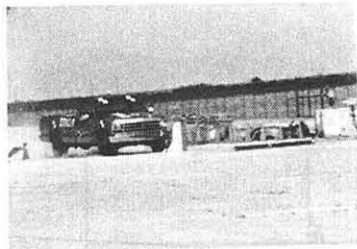
- Test Number ITNJ-4
- Date 9/10/97
- Appurtenance Approach Guardrail Transition to a NJ Safety Shape End Section w/ Curb
- Total Length 25.34 m
- Steel Thrie Beam (Nested)
 - Thickness 2.66 mm
 - Top Mounting Height 787 mm
- Wood Posts
 - Post Nos. 1 - 7 152 mm x 203 mm by 2134-mm long
 - Post Nos. 8 152 mm x 203 mm by 1829-mm long
- Wood Spacer Blocks
 - Post Nos. 1 - 8 152 mm x 203 mm by 457-mm long
- Steel Posts
 - Post Nos. 9 - 15 W150x13.5 by 1829-mm long
- Steel Spacer Blocks
 - Post Nos. 9 - 15 W150x13.5 by 337-mm long
- Soil Type Grading B - AASHTO M 147-65 (1990)
- Vehicle Model 1988 Chevrolet 2500 2WD
 - Curb 2,009 kg
 - Test Inertial 1,999 kg
 - Gross Static 1,999 kg
- Vehicle Speed
 - Impact 102.3 km/hr
 - Exit 72.3 km/hr

- Vehicle Angle
 - Impact 24.6 deg
 - Exit 7.2 deg
- Vehicle Snagging Contact on top of spacer blocks and concrete end section
- Vehicle Pocketing None
- Vehicle Stability Satisfactory
- Occupant Ridedown Deceleration (10 msec avg.)
 - Longitudinal 5.79/-6.05 < 20 G's
 - Lateral (not required) 9.22
- Occupant Impact Velocity (Normalized)
 - Longitudinal 7.74 < 12 m/s
 - Lateral (not required) 6.59
- Vehicle Damage Moderate
 - TAD¹⁸ 11-LFQ-5
 - SAE¹⁹ 11-LDEW3
- Vehicle Stopping Distance 68.4 m downstream
12.9 m behind
- Barrier Damage Moderate
- Maximum Deflections
 - Permanent Set 32 mm
 - Dynamic 99 mm (visible)

Figure 64. Summary of Test Results and Sequential Photographs, Test ITNJ-4 (Design No. 4)



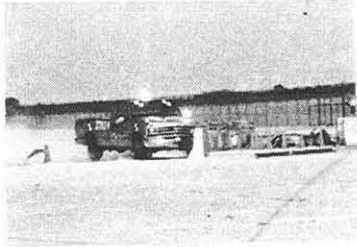
0.000 sec



0.000 sec



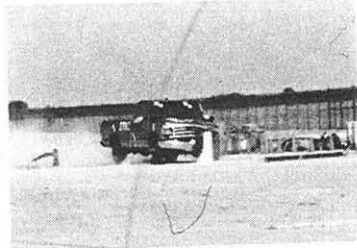
0.038 sec



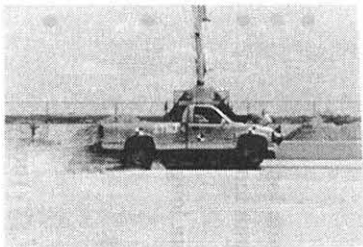
0.036 sec



0.076 sec



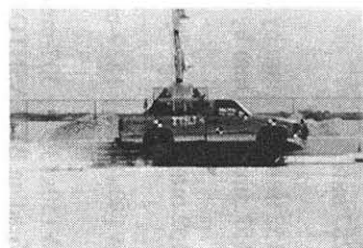
0.080 sec



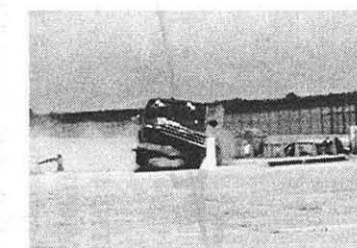
0.132 sec



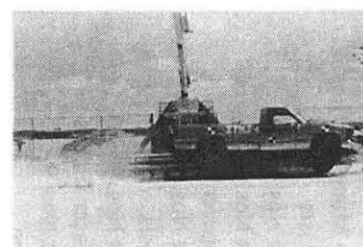
0.118 sec



0.194 sec



0.172 sec



0.260 sec



0.281 sec

Figure 65. Additional Sequential Photographs, Test ITNJ-4 (Design No. 4)



Figure 66. Documentary Photographs, Test ITNJ-4 (Design No. 4)

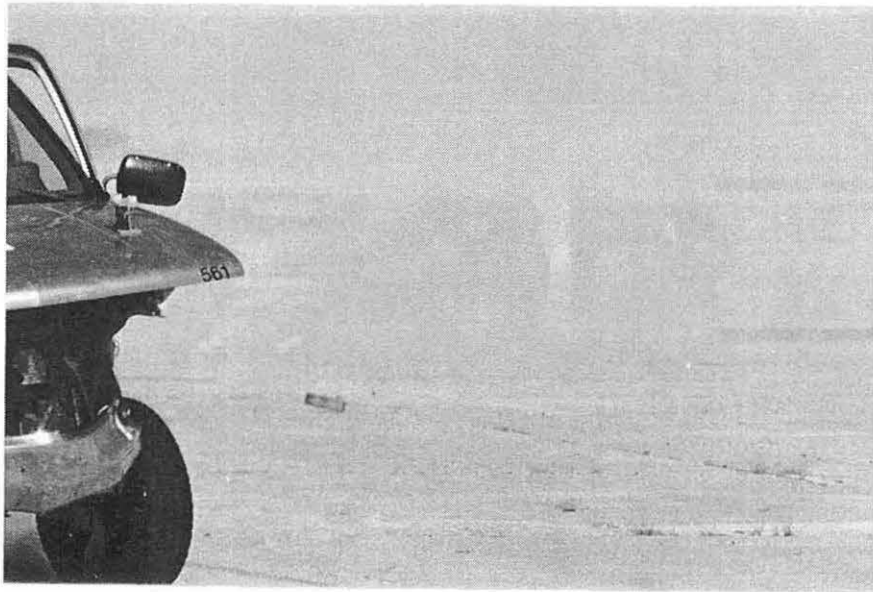
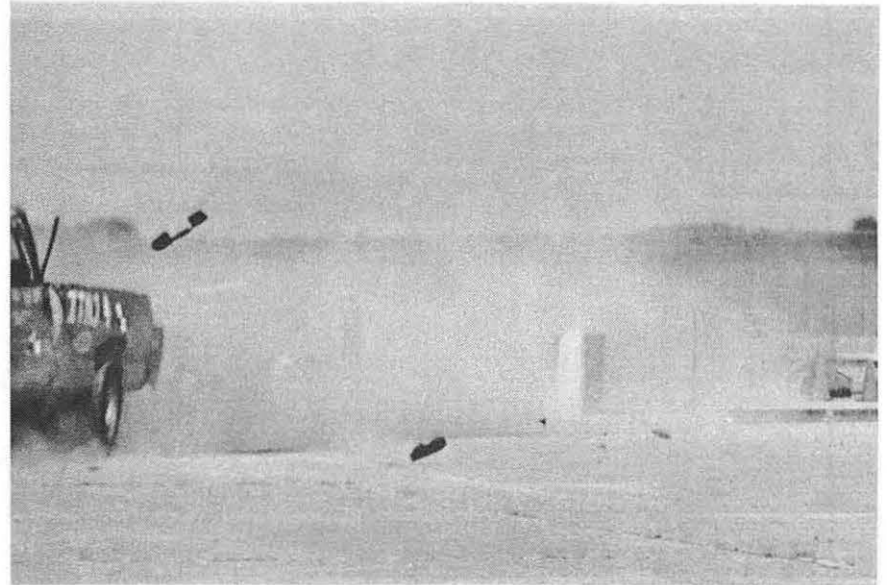


Figure 67. Documentary Photographs, Test ITNJ-4 (Design No. 4)

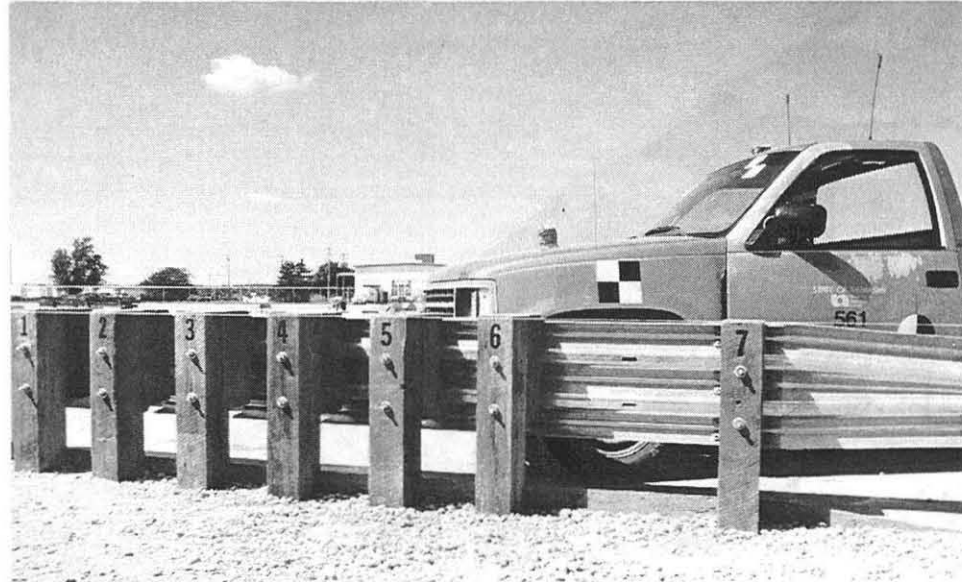
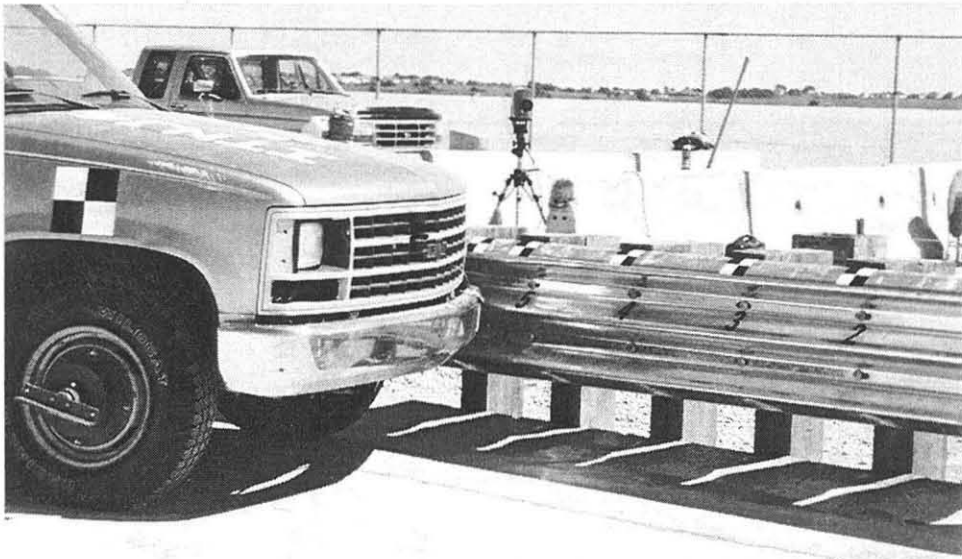


Figure 68. Impact Location, Test ITNJ-4 (Design No. 4)

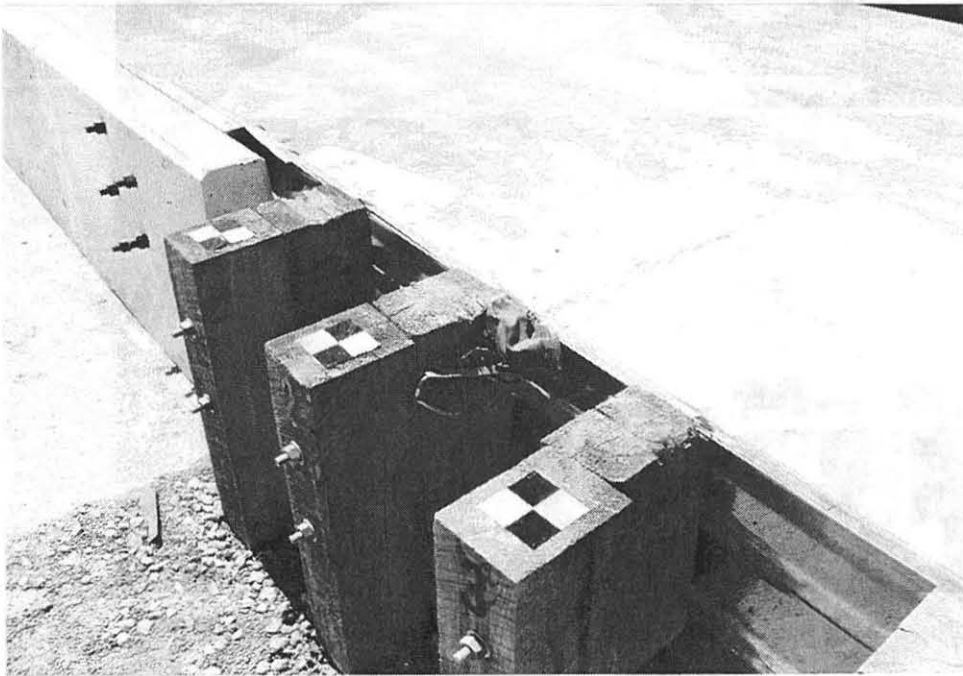
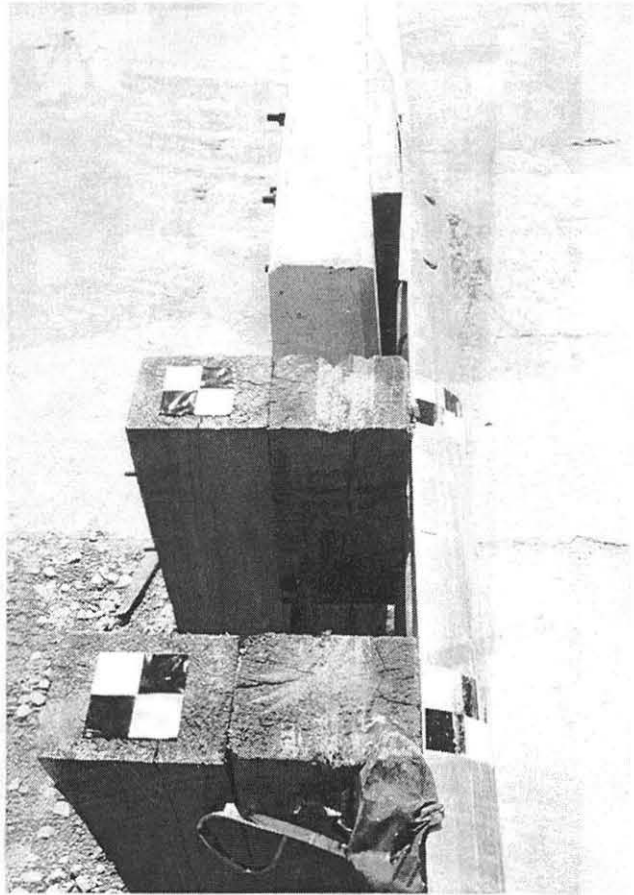
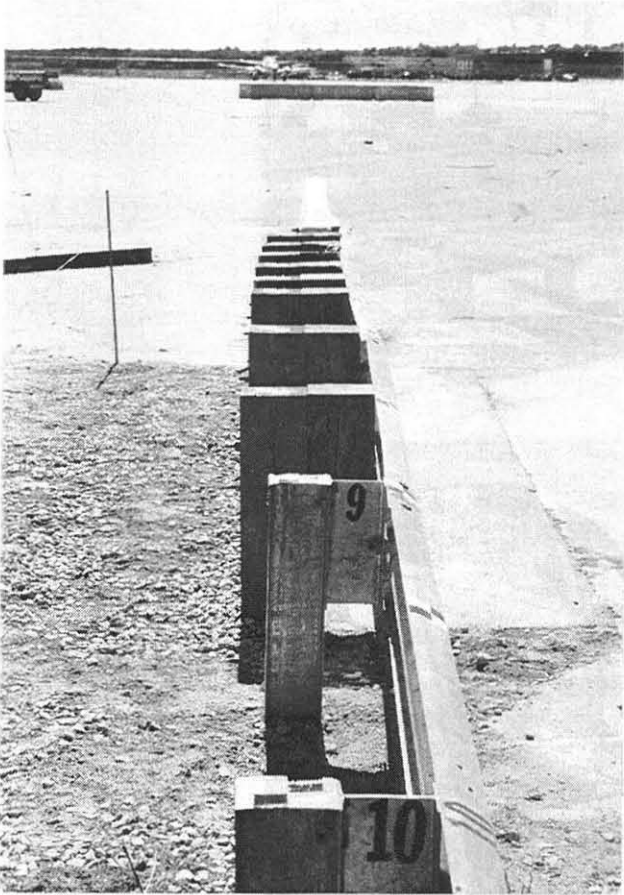


Figure 69. Barrier Damage, Test ITNJ-4 (Design No. 4)

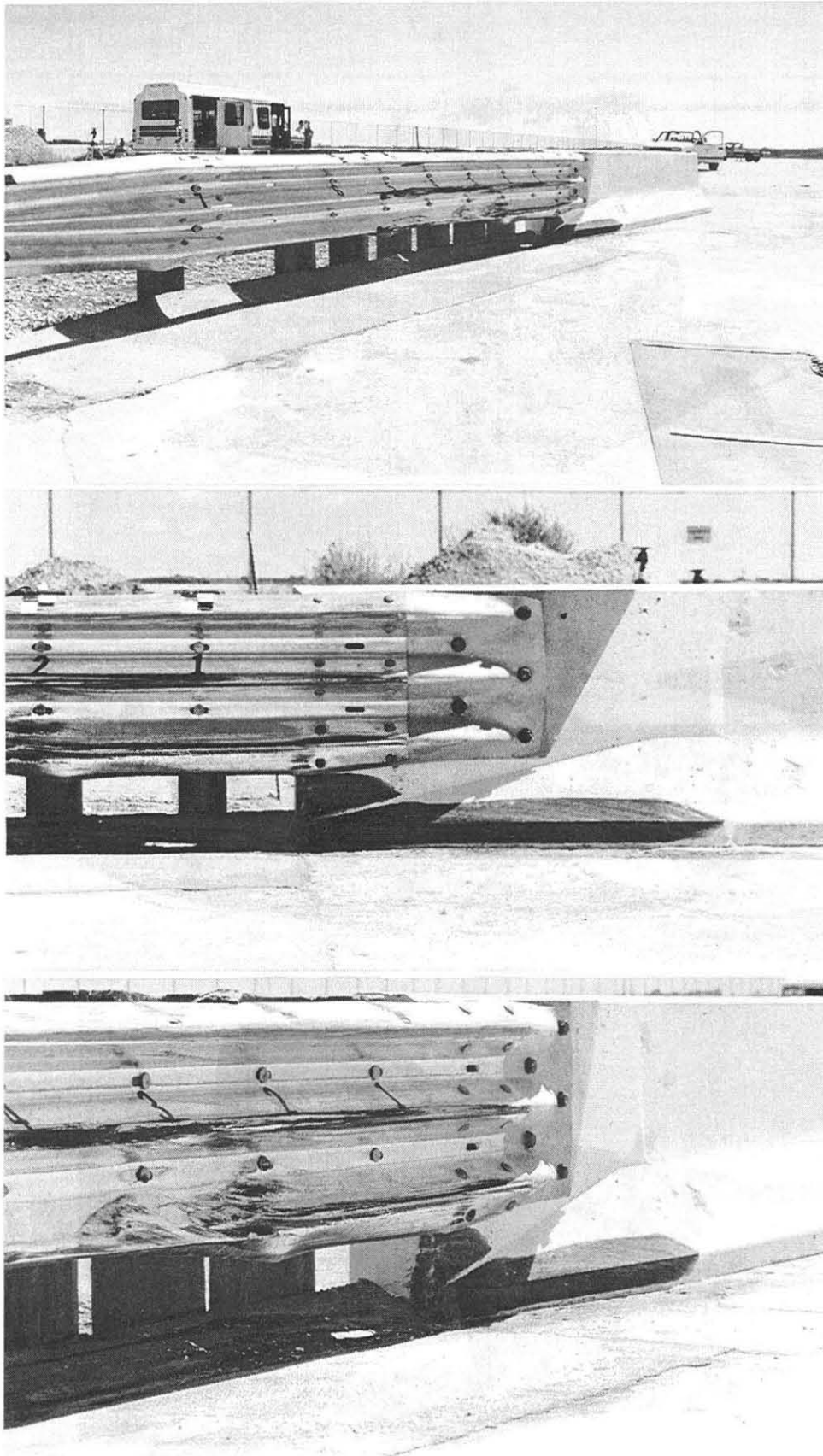


Figure 70. Barrier Damage, Test ITNJ-4 (Design No. 4)



Figure 71. Vehicle Damage, Test ITNJ-4 (Design No. 4)

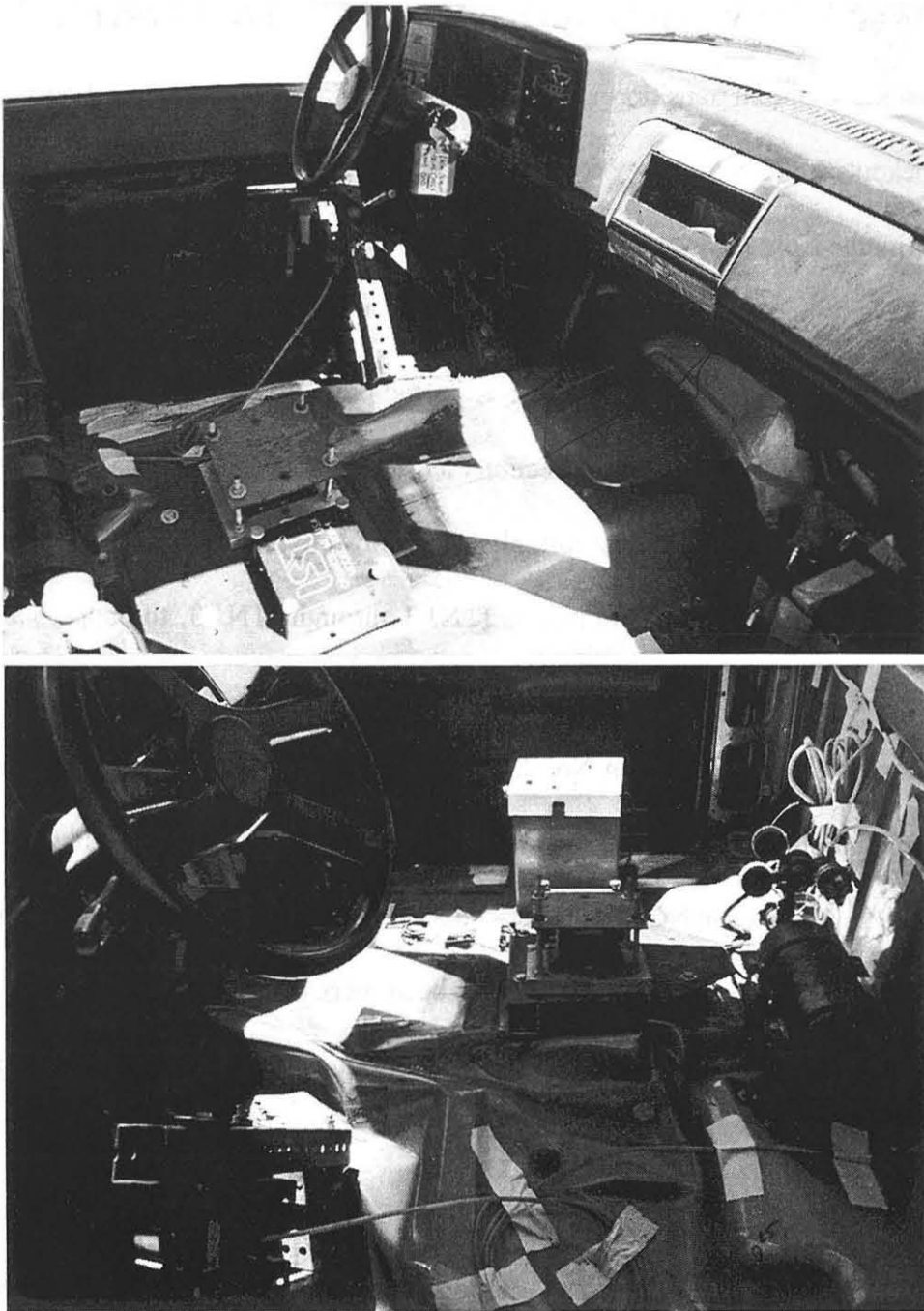


Figure 72. Occupant Compartment Deformation, Test ITNJ-4 (Design No. 4)

16 SUMMARY AND CONCLUSIONS - WOOD POST SYSTEM

An approach guardrail transition, consisting of three-beam guardrail, wood posts, structural tube spacer blockouts, and a New Jersey connector plate, was developed and full-scale vehicle crash tested for use with the New Jersey concrete safety shape barrier. Two full-scale vehicle crash tests were performed according to TL-3 of NCHRP Report 350. The first crash test, Test ITNJ-3 (Design No. 3), failed due to vehicle rollover. Lower than expected post-soil forces occurred, thus resulting in excessive barrier deflections. These deflections led to a higher than normal exit angle which occurred simultaneously with significant roll, pitch, and yaw angular motions.

Based on knowledge gained from tests ITNJ-1 through ITNJ-3, the approach guardrail transition system was redesigned. The primary changes were to use longer posts and the same crushed limestone soil used in Design No. 2. A second test, Test ITNJ-4 (Design No. 4), was performed on the modified system and was determined to be acceptable according to the safety performance criteria presented in NCHRP Report 350. Thus, an approach guardrail transition for use with the New Jersey concrete safety shape barrier has been successfully developed and meets current safety standards. A summary of the safety performance evaluation for the two tests is provided in Table 5.

It is believed that only minor modifications to the new design will be required to accommodate the F-shape concrete barrier. Additionally, it is believed that no further testing will be required since the F-shape is considered to behave slightly better than the New Jersey shape in crash testing (11-12). Finally, it is believed that this approach guardrail transition system would perform in an acceptable manner when attached to a vertical concrete end section that includes a similar chamfer configuration.

Table 5. Summary of Safety Performance Evaluation Results - Wood Post System

Evaluation Factors	Evaluation Criteria	Test ITNJ-3 (Design No. 3)	Test ITNJ-4 (Design No. 4)
Structural Adequacy	A. Test article should contain and redirect the vehicle; the vehicle should not penetrate, underide, or override the installation although controlled lateral deflection of the test article is acceptable.	U	S
Occupant Risk	D. Detached elements, fragments or other debris from the test article should not penetrate or show potential for penetrating the occupant compartment, or present an undue hazard to other traffic, pedestrians, or personnel in a work zone. Deformations of, or intrusions into, the occupant compartment that could cause serious injuries should not be permitted.	S	S
	F. The vehicle should remain upright during and after collision although moderate roll, pitching and yawing are acceptable.	U	S
Vehicle Trajectory	K. After collision it is preferable that the vehicle's trajectory not intrude into adjacent traffic lanes.	U	M
	L. The occupant impact velocity in the longitudinal direction should not exceed 12 m/sec and the occupant ridedown acceleration in the longitudinal direction should not exceed 20 G's.	S	S
	M. The exit angle from the test article preferably should be less than 60 percent of test impact angle, measured at time of vehicle loss of contact with test devise.	U	S

S - (Satisfactory)
M - (Marginal)
U - (Unsatisfactory)

17 REFERENCES

1. Ross, H.E., Sicking, D.L., Zimmer, R.A. and Michie, J.D., *Recommended Procedures for the Safety Performance Evaluation of Highway Features*, National Cooperative Research Program (NCHRP) Report No. 350, Transportation Research Board, Washington, D.C., 1993.
2. Faller, R.K., Soyland, K., and Sicking, D.L., *Approach Guardrail Transition for Single-Slope Concrete Barriers*, Transportation Research Record No. 1528, Transportation Research Board, National Research Council, Washington, D.C., 1996.
3. Soyland, K., Faller, R.K., Sicking, D.L., and Holloway, J.C., *Development and Testing of an Approach Guardrail Transition to a Single Slope Concrete Median Barrier*, Final Report to the Missouri Highway and Transportation Department, Project SPR-3(017), Transportation Report No. TRP-03-47-95, Midwest Roadside Safety Facility, University of Nebraska-Lincoln, November 1995.
4. Strybos, J.W., Mayer, J.B., and Bronstad, M.E., *Crash Test Evaluation of a Thrie Beam on Wood Post Transition*, Test Report No. FHWA-RD-95-XXX, Performed for the Federal Highway Administration, Eastern Federal Lands Highway Division, Performed by the Southwest Research Institute, San Antonio, Texas, April 1996.
5. Michie, J.D., *Recommended Procedures for the Safety Performance Evaluation of Highway Appurtenances*, National Cooperative Highway Research Program (NCHRP) Report No. 230, Transportation Research Board, Washington, D.C., March 1981.
6. Faller, R.K., Sicking, D.L., Rosson, B.T., Pfeifer, B.G., and Holloway, J.C., *Dynamic Evaluation of Missouri's Modified Bridge Anchor Section*, Final Report to the Missouri Highway and Transportation Department, Project RES1 (0099) P473, Report No. TRP-03-38-93, Midwest Roadside Safety Facility, University of Nebraska-Lincoln, February 1994.
7. Bligh, R.P., Ross, H.E., Jr., and Alberson, D.C., *Short-Radius Thrie Beam Treatment for Intersecting Streets and Curves*, Report No. FHWA/TX-95/1442-1F, Submitted to the Texas Department of Transportation, Performed by Texas Transportation Institute, November 1994.
8. Buth, C.E., Campise, W.L., Griffin, III, L.I., Love, M.L., and Sicking, D.L., *Performance Limits of Longitudinal Barrier Systems - Volume I - Summary Report*, Report No. FHWA/RD-86/153, Submitted to the Office of Safety and Traffic Operations, Federal Highway Administration, Performed by Texas Transportation Institute, May 1986.
9. Ivey, D.L., Robertson, R., and Buth, C.E., *Test and Evaluation of W-Beam and Thrie-Beam Guardrails*, Report No. FHWA/RD-82/071, Submitted to the Office of Research, Federal Highway Administration, Performed by Texas Transportation Institute, March 1986.

10. Ross, H.E., Jr., Perera, H.S., Sicking, D.L., and Bligh, R.P., *Roadside Safety Design for Small Vehicles*, National Cooperative Highway Research Program (NCHRP) Report No. 318, Transportation Research Board, Washington, D.C., May 1989.
11. Mak, K.K., and Sicking, D.L., *Rollover Caused by Concrete Safety Shape Barrier - Volume I: Technical Report and Volume II: Appendices*, Report Nos. FHWA-RD-88-219/220, Performed for the Office of Safety and Traffic Operations R&D, Federal Highway Administration, Performed by the Texas Transportation Institute, Texas A&M University, January 1989.
12. Buth, C.E., Hirsch, T.J., and McDevitt, C.F., *Performance Level 2 Bridge Railings*, Transportation Research Record No. 1258, Transportation Research Board, National Research Council, Washington D.C., 1990.
13. Hirsch, T.J., *Analytical Evaluation of Texas Bridge Rails to Contain Buses and Trucks*, Report No. FHWA/TX78-230-2, Submitted to Texas State Department of Transportation, Performed by Texas Transportation Institute, Texas A&M University, August 1978.
14. *AASHTO LRFD Bridge Design Specifications*, Customary U.S. Units - First Edition, American Association of State Highway and Transportation Officials (AASHTO), 1994.
15. Hinch, J., Yang, T-L, and Owings, R., *Guidance Systems for Vehicle Testing*, ENSCO, Inc., Springfield, VA 1986.
16. *Center of Gravity Test Code - SAE J874 March 1981*, SAE Handbook Vol. 4, Society of Automotive Engineers, Inc., Warrendale, Pennsylvania, 1986.
17. Powell, G.H., *BARRIER VII: A Computer Program For Evaluation of Automobile Barrier Systems*, Prepared for: Federal Highway Administration, Report No. FHWA RD-73-51, April 1973.
18. *Vehicle Damage Scale for Traffic Investigators*, Second Edition, Technical Bulletin No. 1, Traffic Accident Data (TAD) Project, National Safety Council, Chicago, Illinois, 1971.
19. *Collision Deformation Classification - Recommended Practice J224 March 1980*, Handbook Volume 4, Society of Automotive Engineers (SAE), Warrendale, Pennsylvania, 1985.

18 APPENDICES

1	Appendix A: [Faint text]
2	Appendix B: [Faint text]
3	Appendix C: [Faint text]
4	Appendix D: [Faint text]
5	Appendix E: [Faint text]
6	Appendix F: [Faint text]
7	Appendix G: [Faint text]
8	Appendix H: [Faint text]
9	Appendix I: [Faint text]
10	Appendix J: [Faint text]
11	Appendix K: [Faint text]
12	Appendix L: [Faint text]
13	Appendix M: [Faint text]
14	Appendix N: [Faint text]
15	Appendix O: [Faint text]
16	Appendix P: [Faint text]
17	Appendix Q: [Faint text]
18	Appendix R: [Faint text]
19	Appendix S: [Faint text]
20	Appendix T: [Faint text]
21	Appendix U: [Faint text]
22	Appendix V: [Faint text]
23	Appendix W: [Faint text]
24	Appendix X: [Faint text]
25	Appendix Y: [Faint text]
26	Appendix Z: [Faint text]

State	Safety Shape Bridge Rail Type	Concrete End Description	Drawing No.	Transition Segment Details						
				Guardrail			Posts			
				Thrie Beam	W-Beam to Thrie Beam	W-Beam	No.	Material Type	Sizes	Spacing
Iowa	NJ	Vertical Wall w/ Sloped Top and Flared End	RE-68	Nested 12-Gauge (12'-6")	12-Gauge (6'-3")		6	Wood	3 @ 10x10x72 3 @ 8x8x72	6 @ 3'-1½"
	F	Vertical Wall w/ Sloped Top and Flared End	RE-68	Nested 12-Gauge (3810 mm)	12-Gauge (1905 mm)		6	Wood	3 @ 250x250x1830 3 @ 200x200x1830	6 @ 952.5 mm
Kansas	TBD									
Minnesota	NJ	NJ Buttress w/ Long Flared Base and Long Tapered Curb	5-297.605			Nested 12-Gauge (12'-6") 12-Gauge (12'-6")	9	Wood	9 @ 6x8x84	4 @ 1'-6¾" ^A 4 @ 3'-1½" 1 @ 6'-3"
	NJ	NJ Buttress w/ Flared Base and Curb	5-297.606			Nested 12-Gauge C6x8.2 Rub Rail (12'-6") 12-Gauge C6x8.2 Rub Rail (12'-6")	11	Wood	11 @ 6x8x84	5 @ 1'-6¾" ^H 6 @ 3'-1½"
Missouri	NJ	Vertical Wall w/ Flared Base	606.22M	Nested 12-Gauge (12'-6")	12-Gauge (6'-3")		7	Steel	7 @ W6x9x72	2 @ 1'-6¾" ^A 5 @ 3'-1½"
Nebraska	NJ	Straight Vertical Buttress w/ Flared End	7040E(W)	Nested 12-Gauge (12'-6")	12-Gauge (6'-3")	12-Gauge (6'-3")	6	Wood	2 @ 10x10x72 4 @ 8x8x72	1 @ 6'-3" 4 @ 3'-1½" 1 @ 6'-3"
	NJ	Straight Vertical Buttress w/ Flared End	7040M(W)	Nested 12-Gauge (3810 mm)	12-Gauge (1905 mm)	12-Gauge (1905 mm)	6	Wood	2 @ 250x250x1830 4 @ 200x200x1830	1 @ 1905 mm 4 @ 952.5 mm 1 @ 1905 mm
	NJ	Straight Vertical Buttress w/ Flared End	7040E(S)	Nested 12-Gauge (12'-6") Single 12-Gauge (6'-3")	12-Gauge (6'-3")		9	Steel	8 @ W6x9x78 1 @ W6x9x72	1 @ 3'-0¾" ^B 2 @ 1'-6¾" 4 @ 3'-1½" 1 @ 6'-3"
	NJ	Straight Vertical Buttress w/ Flared End	7040M(S)	Nested 12-Gauge (3810 mm) Single 12-Gauge (1905 mm)	12-Gauge (1905 mm)		9	Steel	8 @ W150x13.5x1980 1 @ W150x13.5x1830	1 @ 924 mm ^C 2 @ 476 mm 4 @ 952.5 mm 1 @ 1905 mm
	NJ	Straight Vertical Buttress w/ Flared End	7041E(W)	Nested 12-Gauge (12'-6") Single 12-Gauge (12'-6")			6	Wood	2 @ 10x10x72 4 @ 8x8x72	1 @ 6'-3" 4 @ 3'-1½" 1 @ 6'-3"

	NJ	Straight Vertical Buttress w/ Flared End	7041M(W)	Nested 12-Gauge (3810 mm) Single 12-Gauge (3810 mm)			6	Wood	2 @ 250x250x1830 4 @ 200x200x1830	1 @ 1905 mm 4 @ 952.5 mm 1 @ 1905 mm
	NJ	Straight Vertical Buttress w/ Flared End	7041E(S)	Nested 12-Gauge (12'-6") Single 12-Gauge (12'-6")			9	Steel	8 @ W6x9x78 1 @ W6x9x72	1 @ 3'-0 ³ / ₈ " ^B 2 @ 1'-6 ³ / ₄ " 4 @ 3'-1 ¹ / ₂ " 1 @ 6'-3"
	NJ	Straight Vertical Buttress w/ Flared End	7041M(S)	Nested 12-Gauge (3810 mm) Single 12-Gauge (3810 mm)			9	Steel	8 @ W150x13.5x1980 1 @ W150x13.5x1830	1 @ 924 mm ^C 2 @ 476 mm 4 @ 952.5 mm 1 @ 1905 mm
South Dakota	NJ	Vertical Wall w/ Flared End and Sloped Base	630.29	Nested 12-Gauge (12'-6")	12-Gauge (6'-3")	12-Gauge (12'-6")	8	Wood	3 @ 10x10x72 4 @ 8x8x72 1 @ 6x8x72	6 @ 3'-1 ¹ / ₂ " ^D 2 @ 6'-3"
	NA	Concrete Bridge Railing	630.32	Nested 10-Gauge (12'-6")	12-Gauge (6'-3")	10-Gauge (12'-6")	10	Wood	10 @ 6x8x72	4 @ 1'-6 ³ / ₄ " ^E 4 @ 3'-1 ¹ / ₂ " 2 @ 6'-3"
Wisconsin	NJ	Vertical Wall	S.D.D.14 B 20-3a	Nested 12-Gauge (12'-6") Single 12-Gauge (12'-6")			9	Wood	9 @ 6x8x84	4 @ 1'-6 ³ / ₄ " ^A 4 @ 3'-1 ¹ / ₂ " 1 @ 6'-3"
MwRSF	NJ	Concrete Bridge Railing	New Design	Nested 12-Gauge (3810 mm)	12-Gauge (1905 mm)		9	Steel	7 @ W150x13.5x1981 2 @ W150x13.5x1829	6 @ 476 mm ^A 3 @ 952 mm
MwRSF	NJ	Concrete Bridge Railing	New Design	Nested 12-Gauge (3810 mm)	12-Gauge (1905 mm)		9	Wood	7 @ 152x203x2134 2 @ 152x203x1829	6 @ 476 mm ^A 3 @ 952 mm

^A - First spacing of 1'-6³/₄" actually has a clear span on 11¹/₂" from concrete end to the center of first post.

^B - First spacing of 3'-0³/₈" consists of two spacings of unknown dimensions.

^C - First spacing of 924 mm consists of two spacings of unknown dimensions.

^D - First spacing of 3'-1¹/₂" actually has a clear span on 1'-0¹/₄" from concrete end to the center of first post.

^E - First spacing of 1'-6³/₄" actually has a variable clear span distance from concrete end to the center of first post.

^F - First spacing of 1'-6³/₄" actually has a clear span on 7³/₄" from concrete end to the center of first post.

APPENDIX B

TYPICAL BARRIER VII INPUT FILE

Note that the example BARRIER VII input data file included in Appendix B corresponds with the critical impact point for test ITNJ-1.

6	1.45	1.50	15.00	1.0				
1	100.75	15.875	1	12.0	1	0	0	0
2	100.75	27.875	1	12.0	1	0	0	0
3	100.75	39.875	2	12.0	1	0	0	0
4	88.75	39.875	2	12.0	1	0	0	0
5	76.75	39.875	2	12.0	1	0	0	0
6	64.75	39.875	2	12.0	1	0	0	0
7	52.75	39.875	2	12.0	1	0	0	0
8	40.75	39.875	2	12.0	1	0	0	0
9	28.75	39.875	2	12.0	1	0	0	0
10	16.75	39.875	2	12.0	1	0	0	0
11	-13.25	39.875	3	12.0	1	0	0	0
12	-33.25	39.875	3	12.0	1	0	0	0
13	-53.25	39.875	3	12.0	1	0	0	0
14	-73.25	39.875	3	12.0	1	0	0	0
15	-93.25	39.875	3	12.0	1	0	0	0
16	-113.25	39.875	4	12.0	1	0	0	0
17	-113.25	-39.875	4	12.0	0	0	0	0
18	100.75	-39.875	1	12.0	0	0	0	0
19	69.25	37.75	5	1.0	1	0	0	0
20	-62.75	37.75	6	1.0	1	0	0	0
1	69.25	32.75	0.0	608.				
2	69.25	-32.75	0.0	608.				
3	-62.75	32.75	0.0	492.				
4	-62.75	-32.75	0.0	492.				
1	0.0	0.0						
3	721.875	0.0	25.0	62.14		0.0	0.0	1.0

APPENDIX C

ACCELEROMETER DATA ANALYSIS

Figure C-1. Graph of Longitudinal Deceleration, Test ITNJ-1

Figure C-2. Graph of Longitudinal Occupant Impact Velocity, Test ITNJ-1

Figure C-3. Graph of Longitudinal Occupant Displacement, Test ITNJ-1

Figure C-4. Graph of Lateral Deceleration, Test ITNJ-1

Figure C-5. Graph of Lateral Occupant Impact Velocity, Test ITNJ-1

Figure C-6. Graph of Lateral Occupant Displacement, Test ITNJ-1

W6: Longitudinal Deceleration - Test ITNJ-1

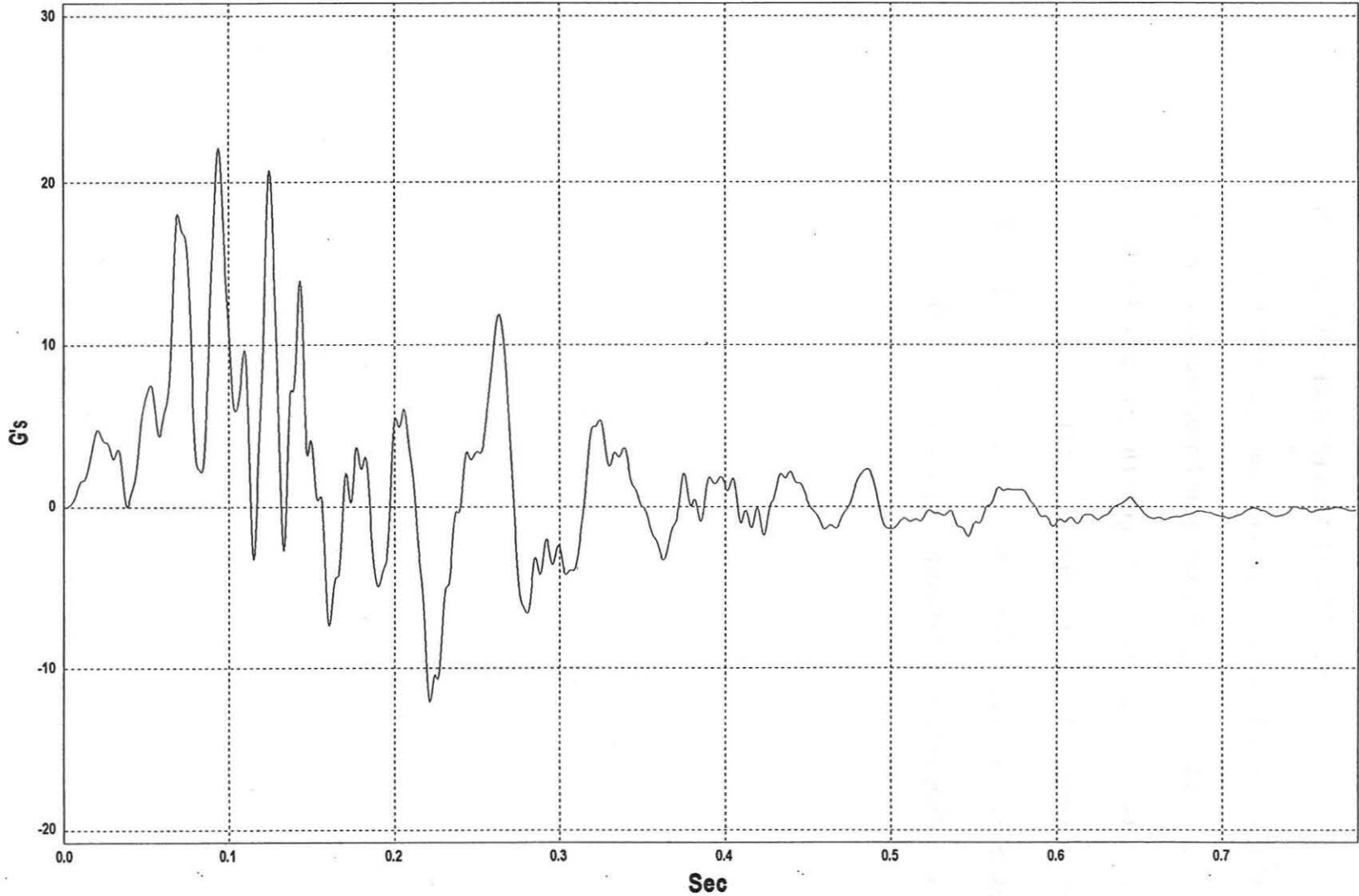


Figure C-1. Graph of Longitudinal Deceleration, Test ITNJ-1

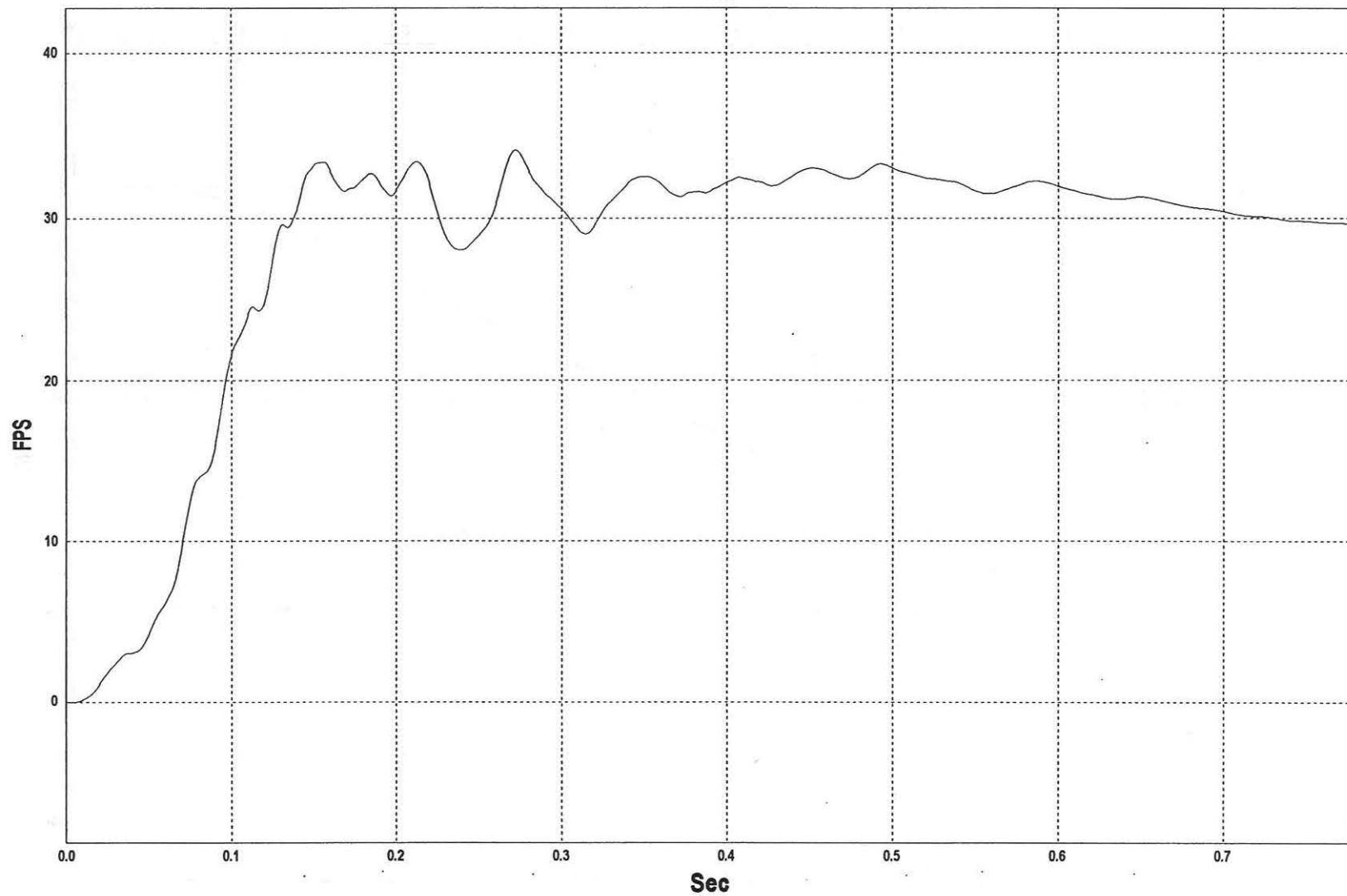
W7: Longitudinal Occupant Impact Velocity - Test ITNJ-1

Figure C-2. Graph of Longitudinal Occupant Impact Velocity, Test ITNJ-1

W12: Longitudinal Occupant Displacement - Test ITNJ-1

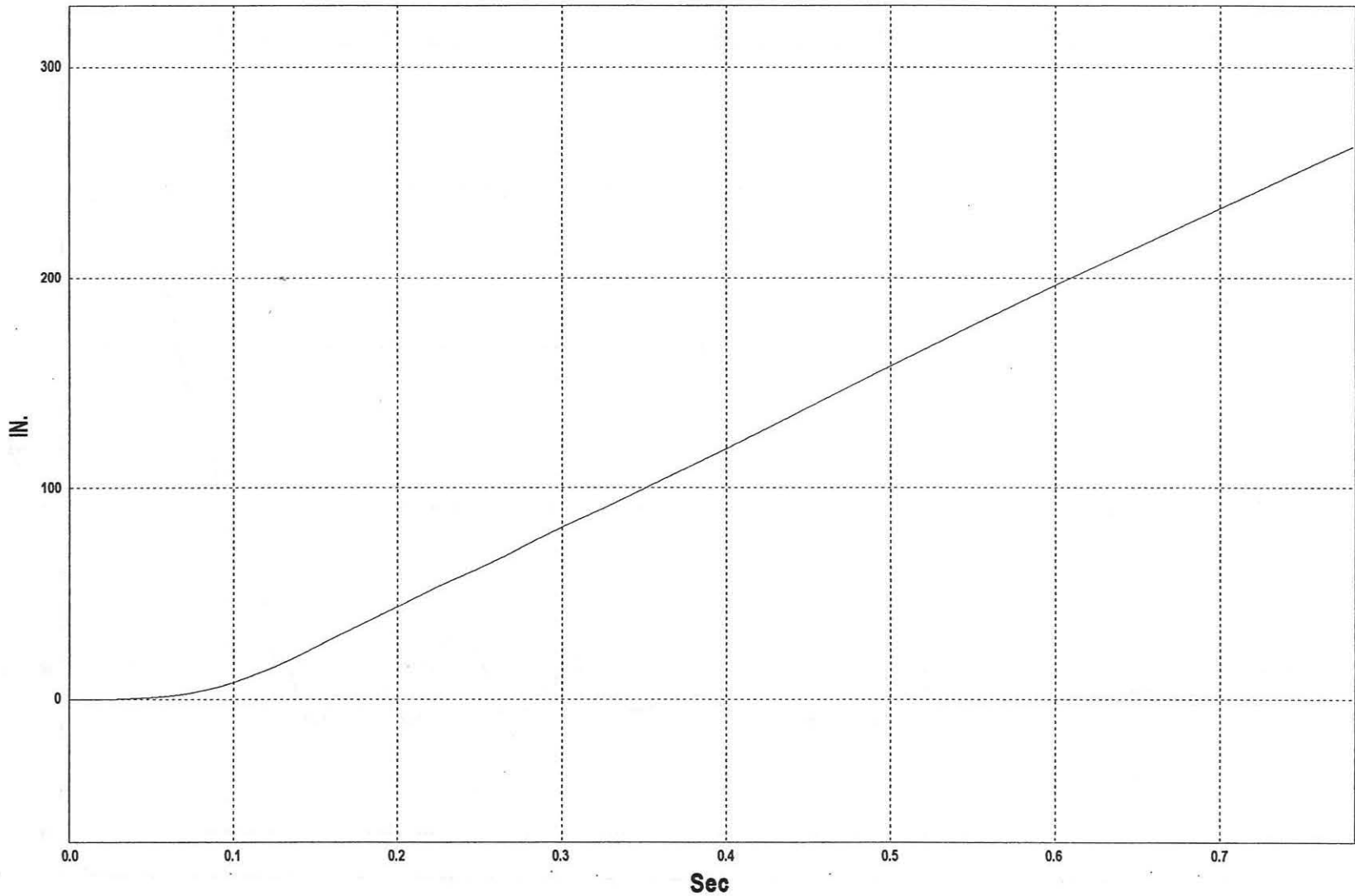


Figure C-3. Graph of Longitudinal Occupant Displacement, Test ITNJ-1

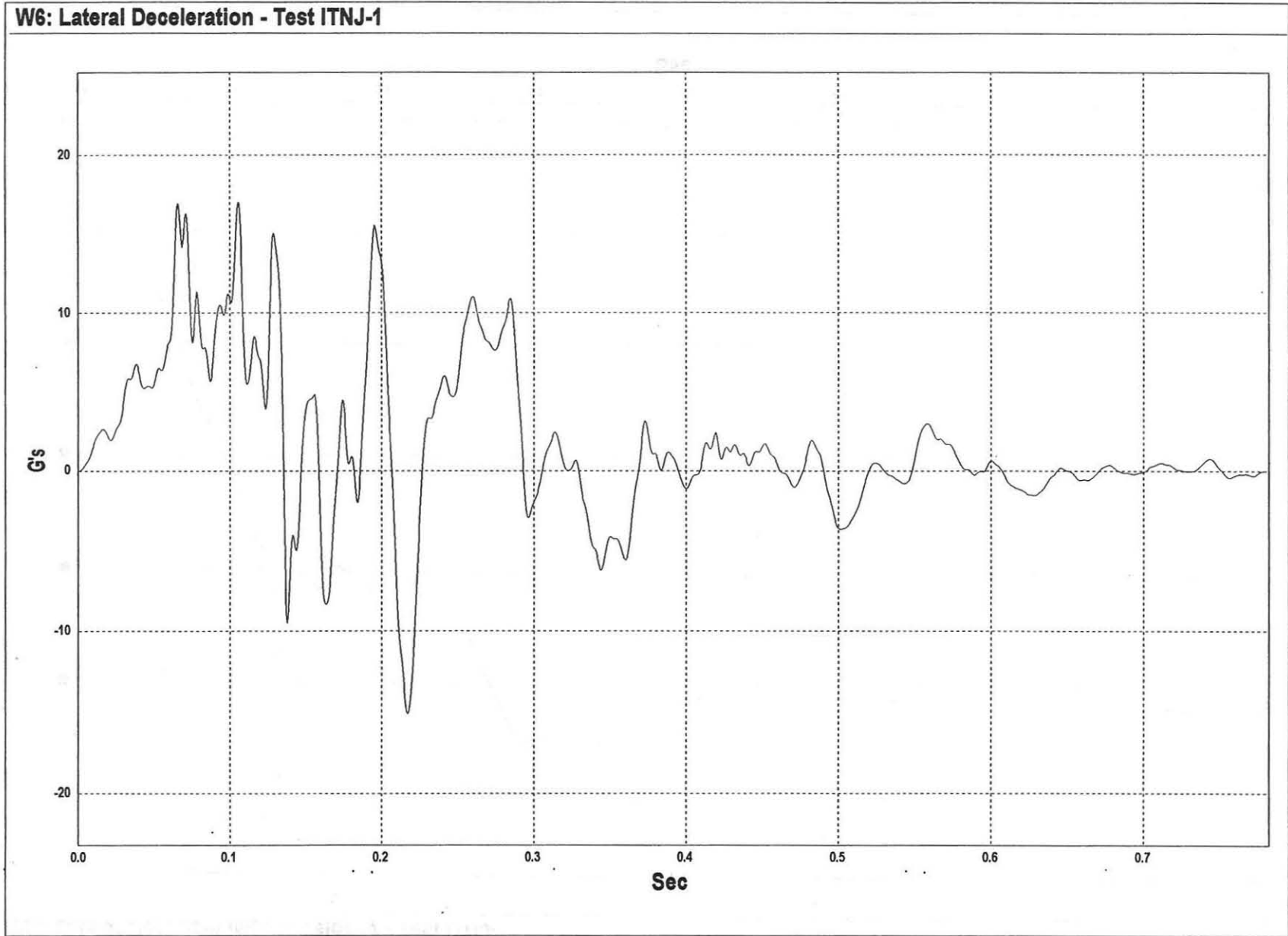


Figure C-4. Graph of Lateral Deceleration, Test ITNJ-1

W7: Lateral Occupant Impact Velocity - Test ITNJ-1

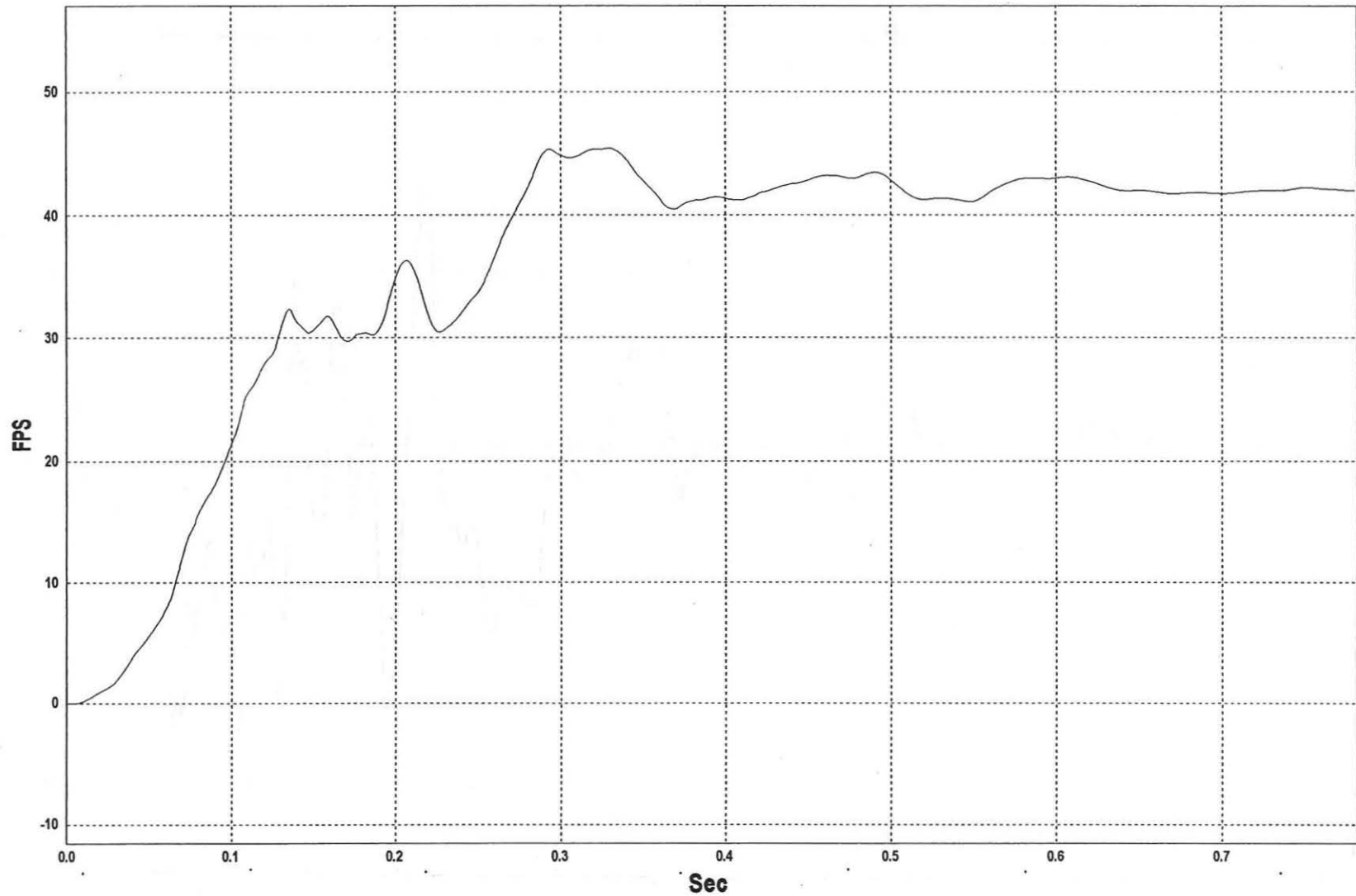


Figure C-5. Graph of Lateral Occupant Impact Velocity, Test ITNJ-1

W8: Lateral Occupant Displacement - Test ITNJ-1

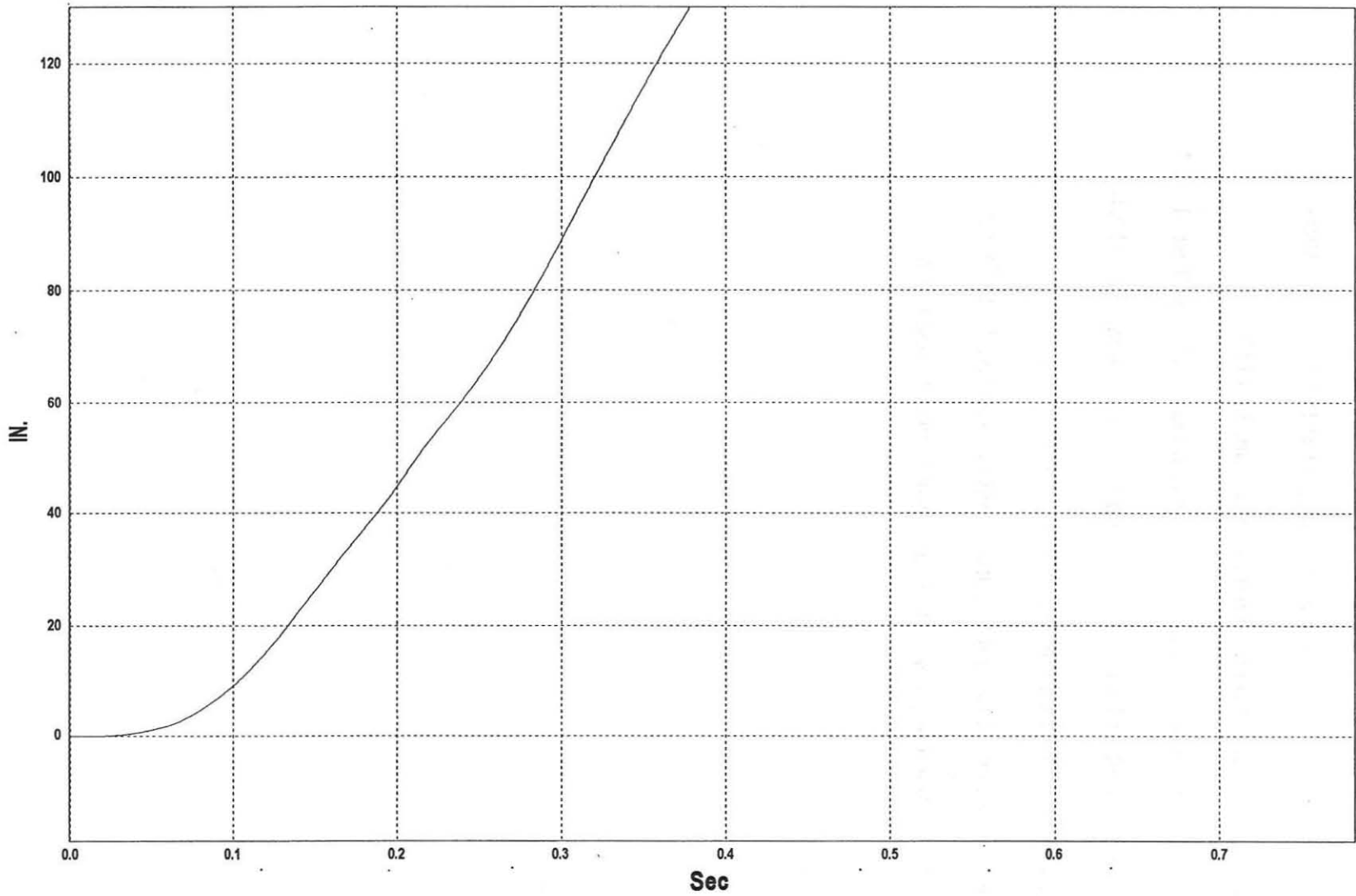


Figure C-6. Graph of Lateral Occupant Displacement, Test ITNJ-1

APPENDIX D

ACCELEROMETER DATA ANALYSIS

Figure D-1. Graph of Longitudinal Deceleration, Test ITNJ-2

Figure D-2. Graph of Longitudinal Occupant Impact Velocity, Test ITNJ-2

Figure D-3. Graph of Longitudinal Occupant Displacement, Test ITNJ-2

Figure D-4. Graph of Lateral Deceleration, Test ITNJ-2

Figure D-5. Graph of Lateral Occupant Impact Velocity, Test ITNJ-2

Figure D-6. Graph of Lateral Occupant Displacement, Test ITNJ-2

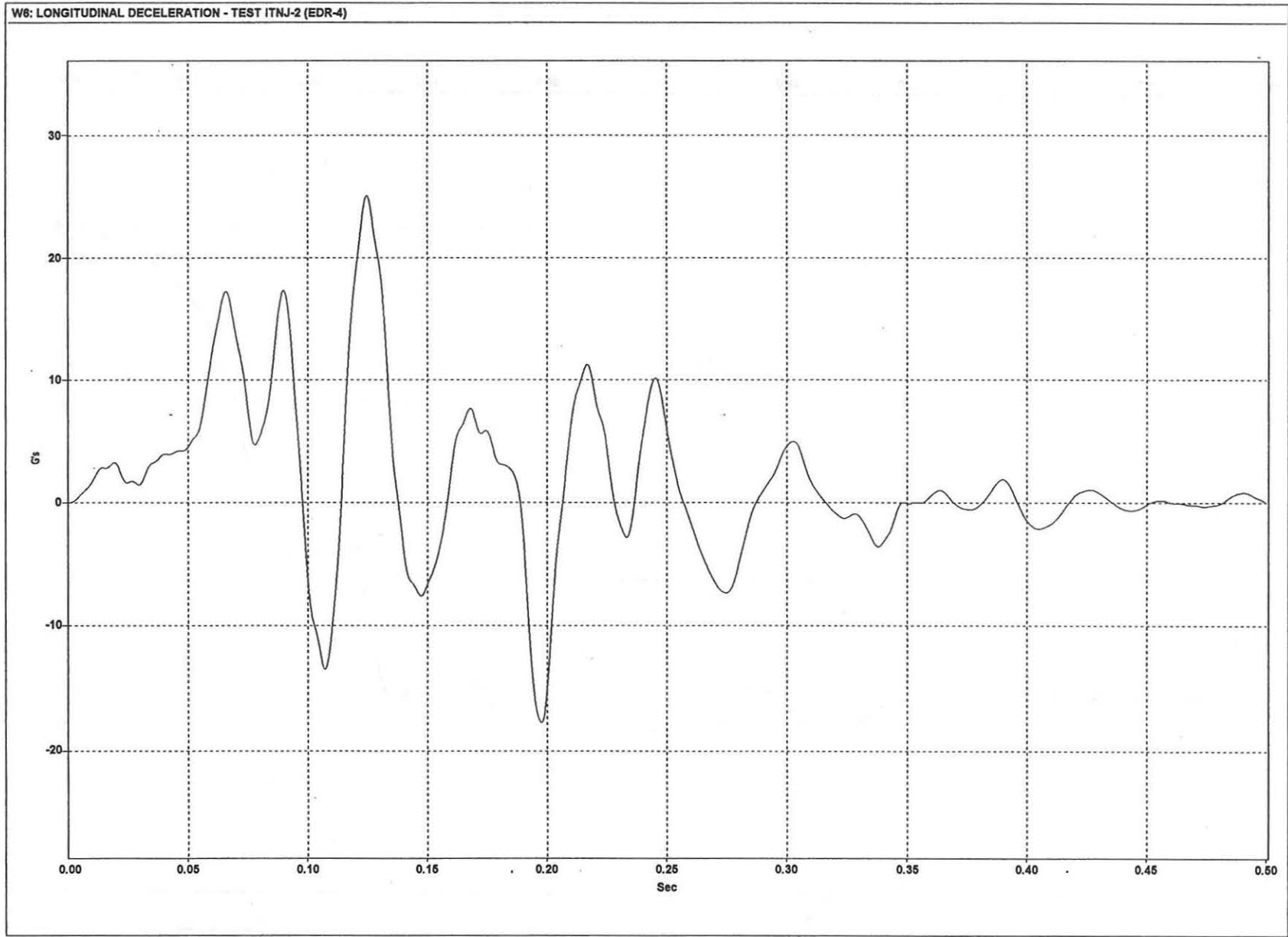


Figure D-1. Graph of Longitudinal Deceleration, Test ITNJ-2

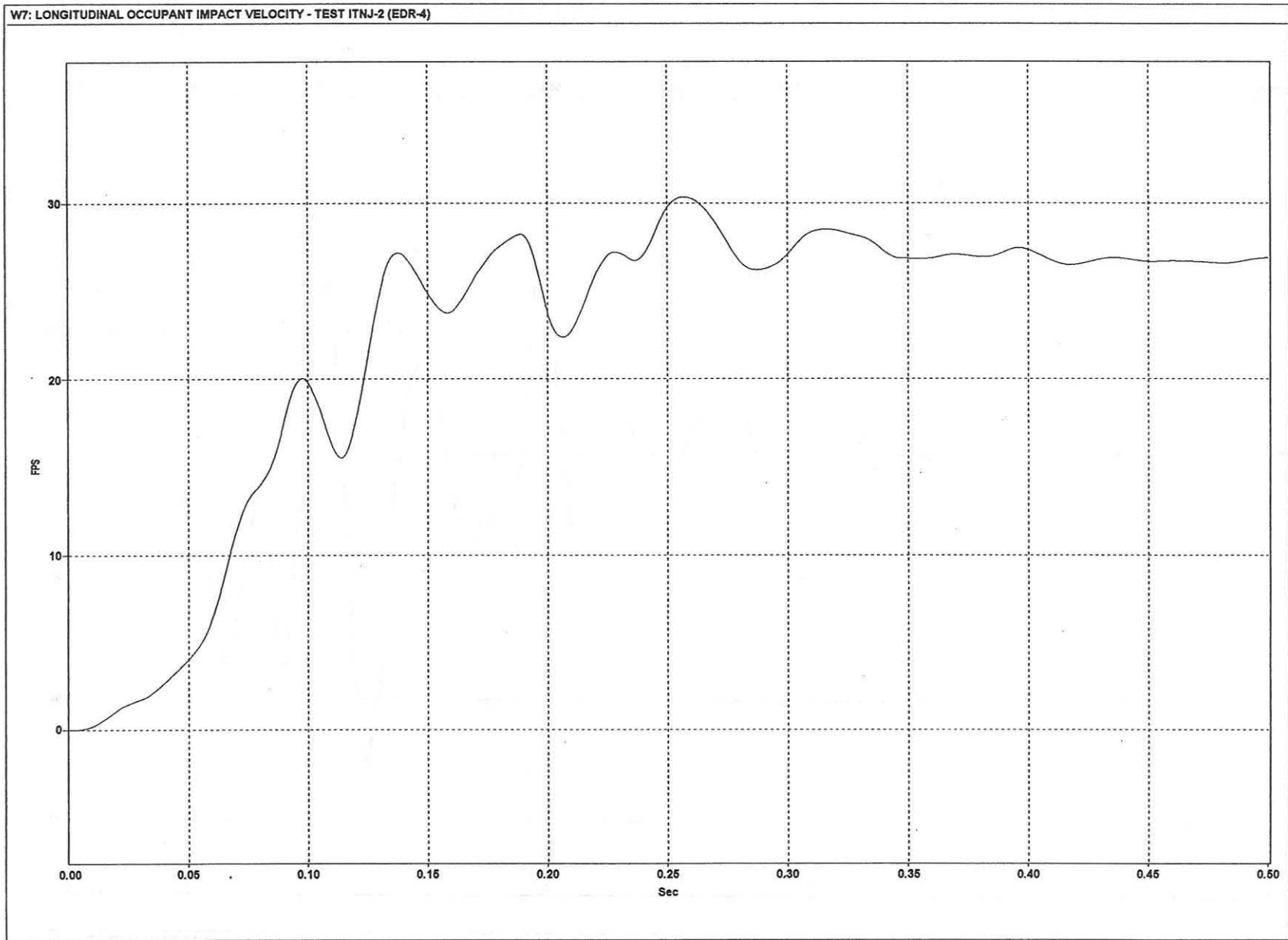


Figure D-2. Graph of Longitudinal Occupant Impact Velocity, Test ITNJ-2

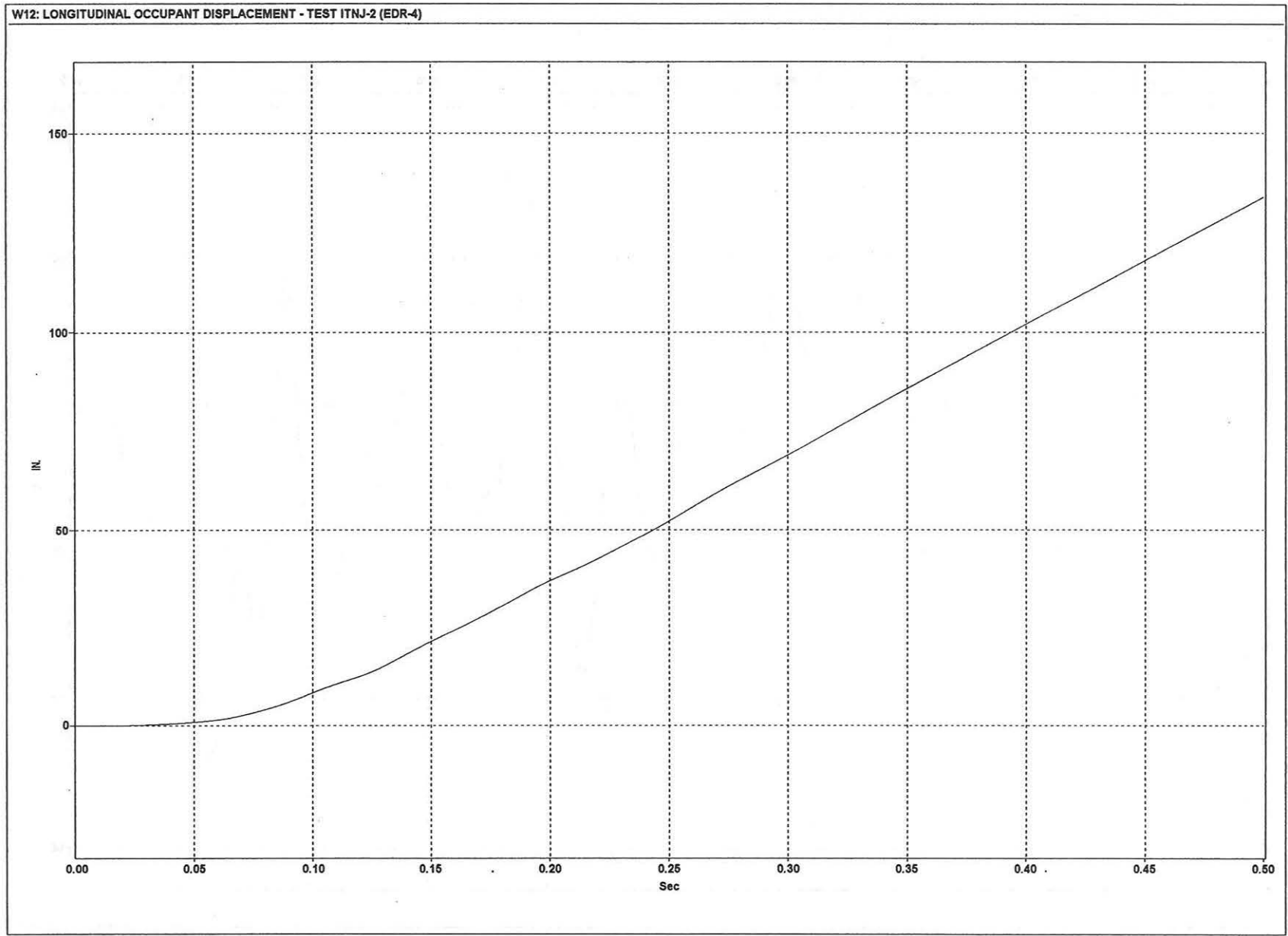


Figure D-3. Graph of Longitudinal Occupant Displacement, Test ITNJ-2

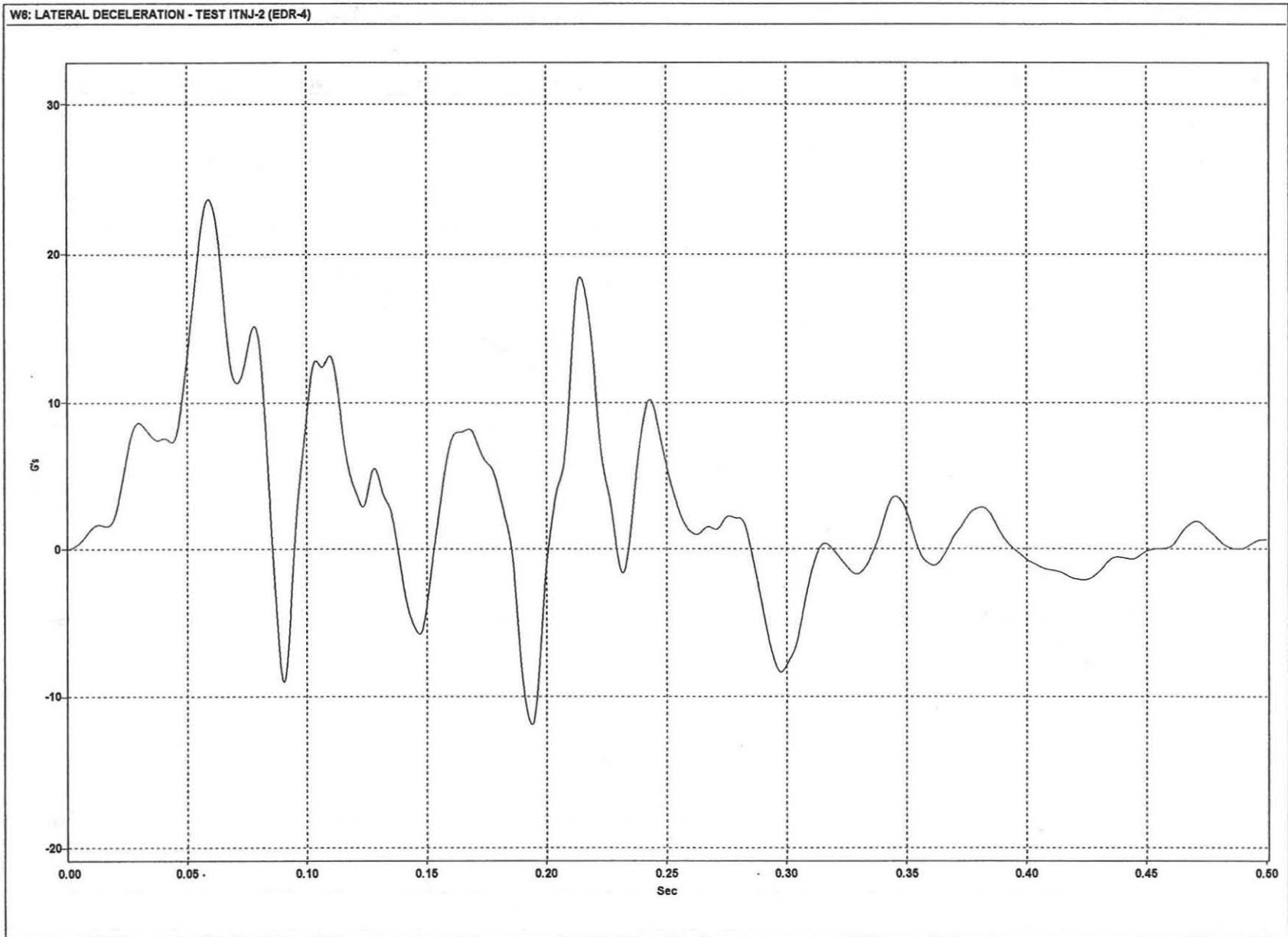


Figure D-4. Graph of Lateral Deceleration, Test ITNJ-2

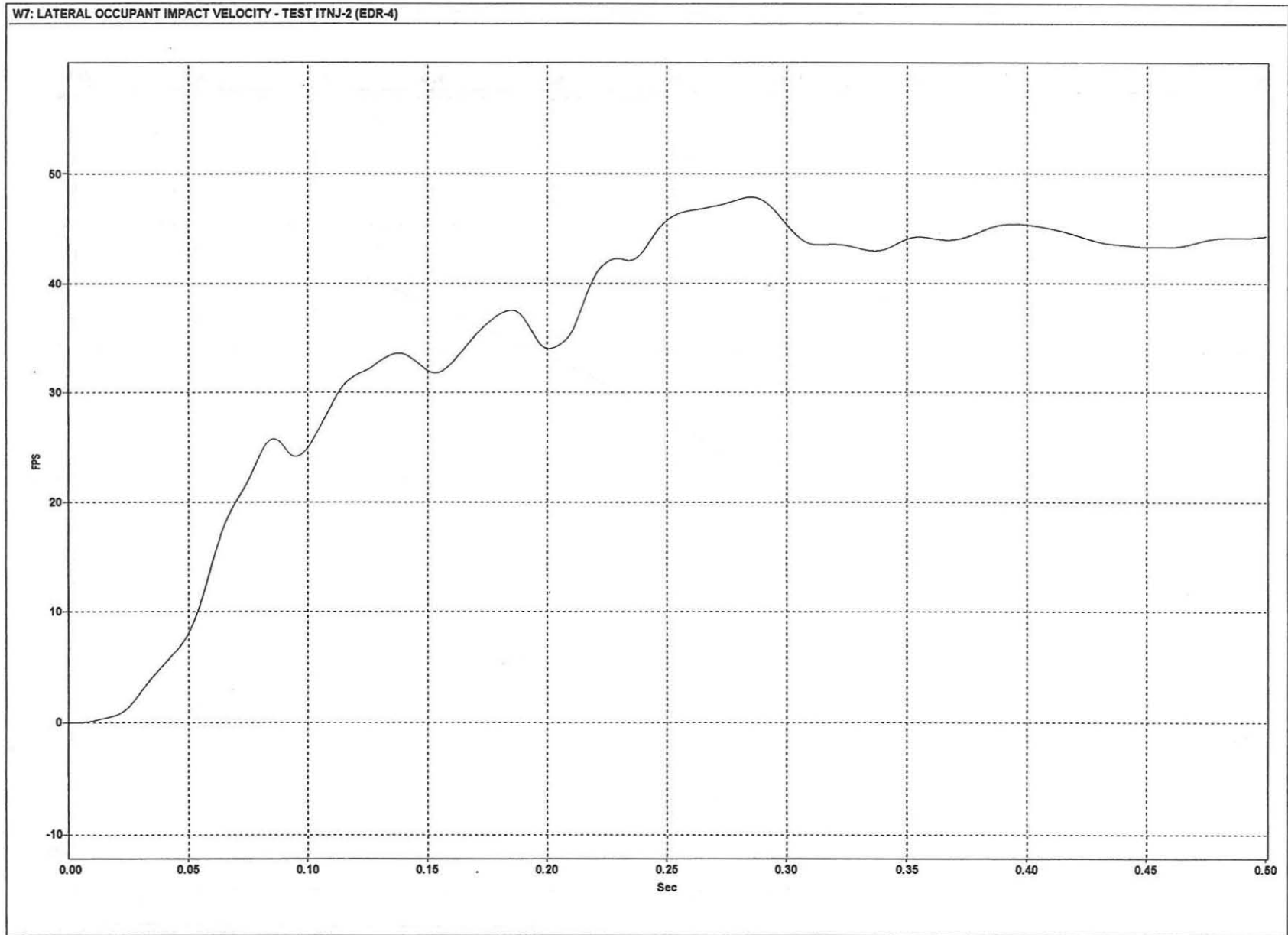


Figure D-5. Graph of Lateral Occupant Impact Velocity, Test ITNJ-2

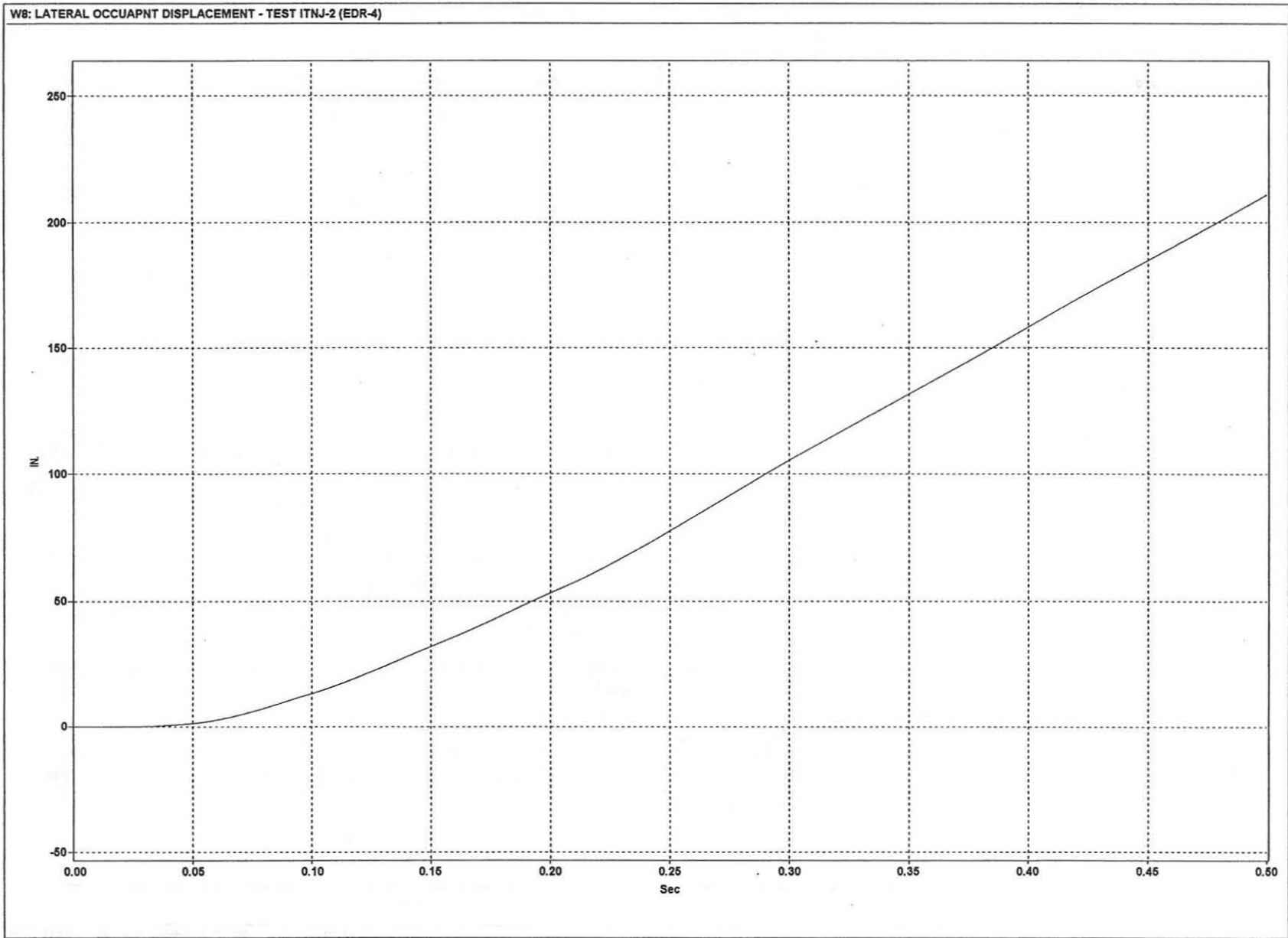


Figure D-6. Graph of Lateral Occupant Displacement, Test ITNJ-2

APPENDIX E

RATE TRANSDUCER DATA ANALYSIS

Figure E-1. Graph of Roll, Pitch, and Yaw Angular Displacements, Test ITNJ-2



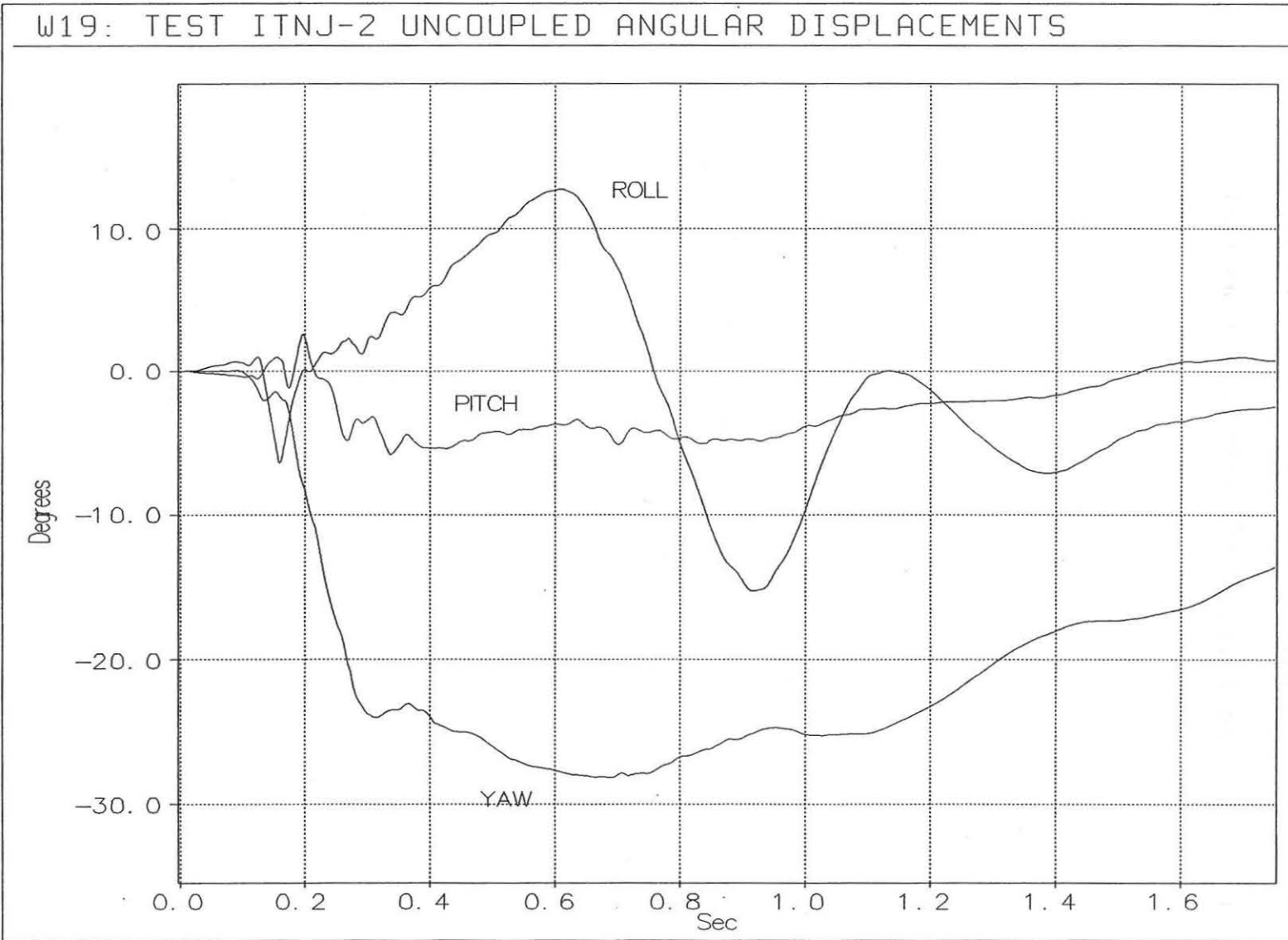


Figure E-1. Graph of Roll, Pitch, and Yaw Angular Displacements, Test ITNJ-2

APPENDIX F

ACCELEROMETER DATA ANALYSIS

Figure F-1. Graph of Longitudinal Deceleration, Test ITNJ-3

Figure F-2. Graph of Longitudinal Occupant Impact Velocity, Test ITNJ-3

Figure F-3. Graph of Longitudinal Occupant Displacement, Test ITNJ-3

Figure F-4. Graph of Lateral Deceleration, Test ITNJ-3

Figure F-5. Graph of Lateral Occupant Impact Velocity, Test ITNJ-3

Figure F-6. Graph of Lateral Occupant Displacement, Test ITNJ-3

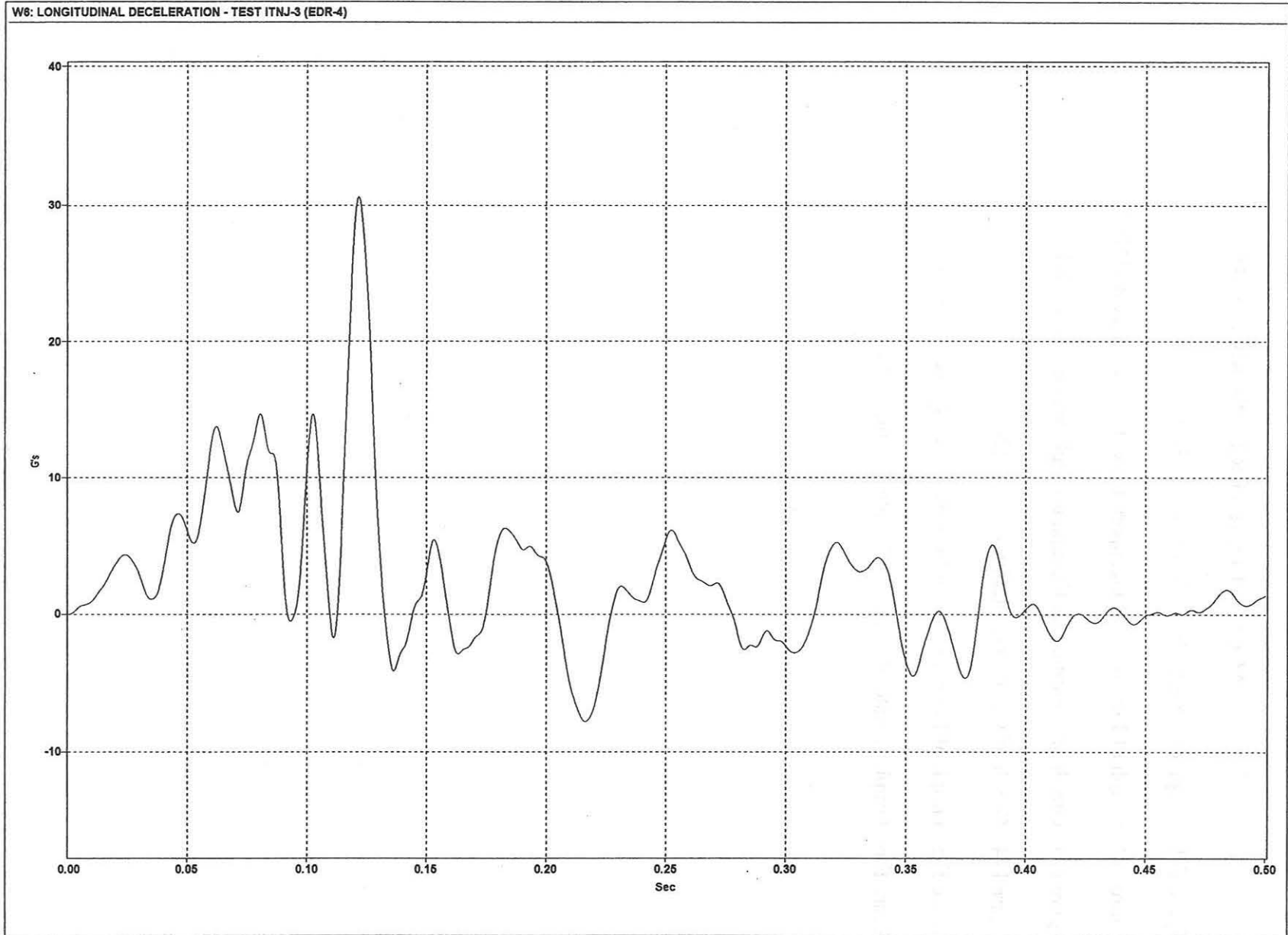


Figure F-1. Graph of Longitudinal Deceleration, Test ITNJ-3

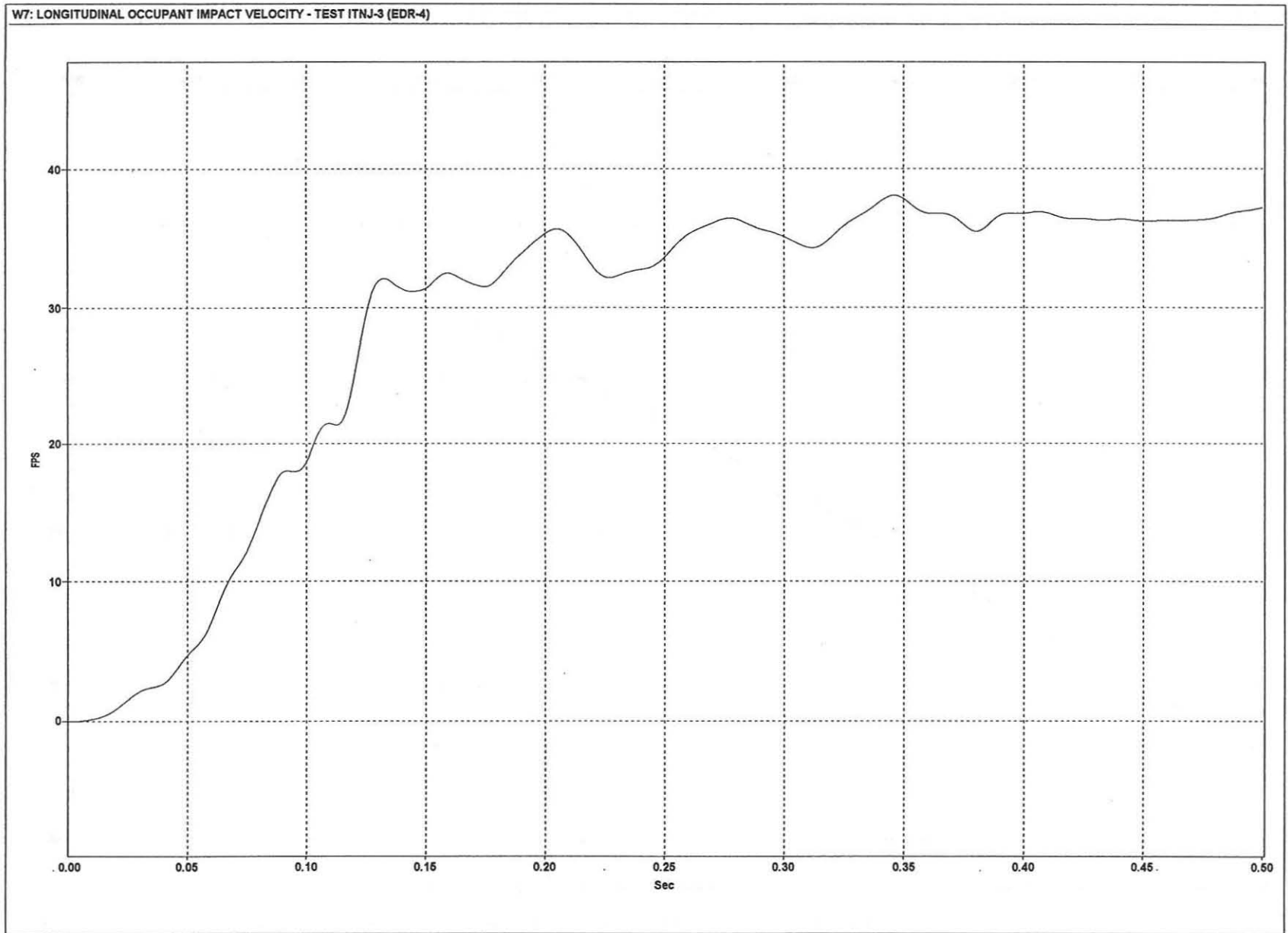


Figure F-2. Graph of Longitudinal Occupant Impact Velocity, Test ITNJ-3

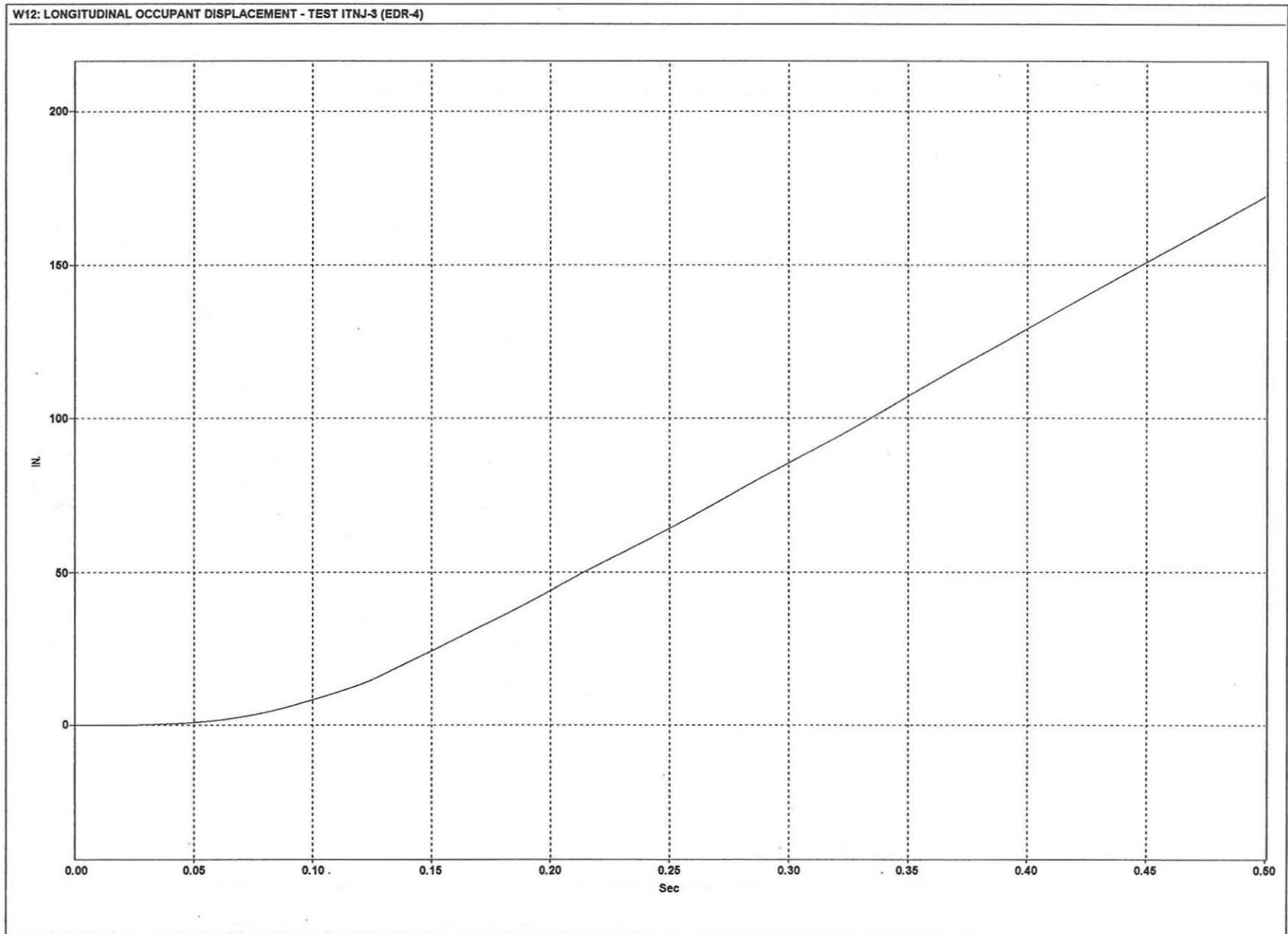


Figure F-3. Graph of Longitudinal Occupant Displacement, Test ITNJ-3

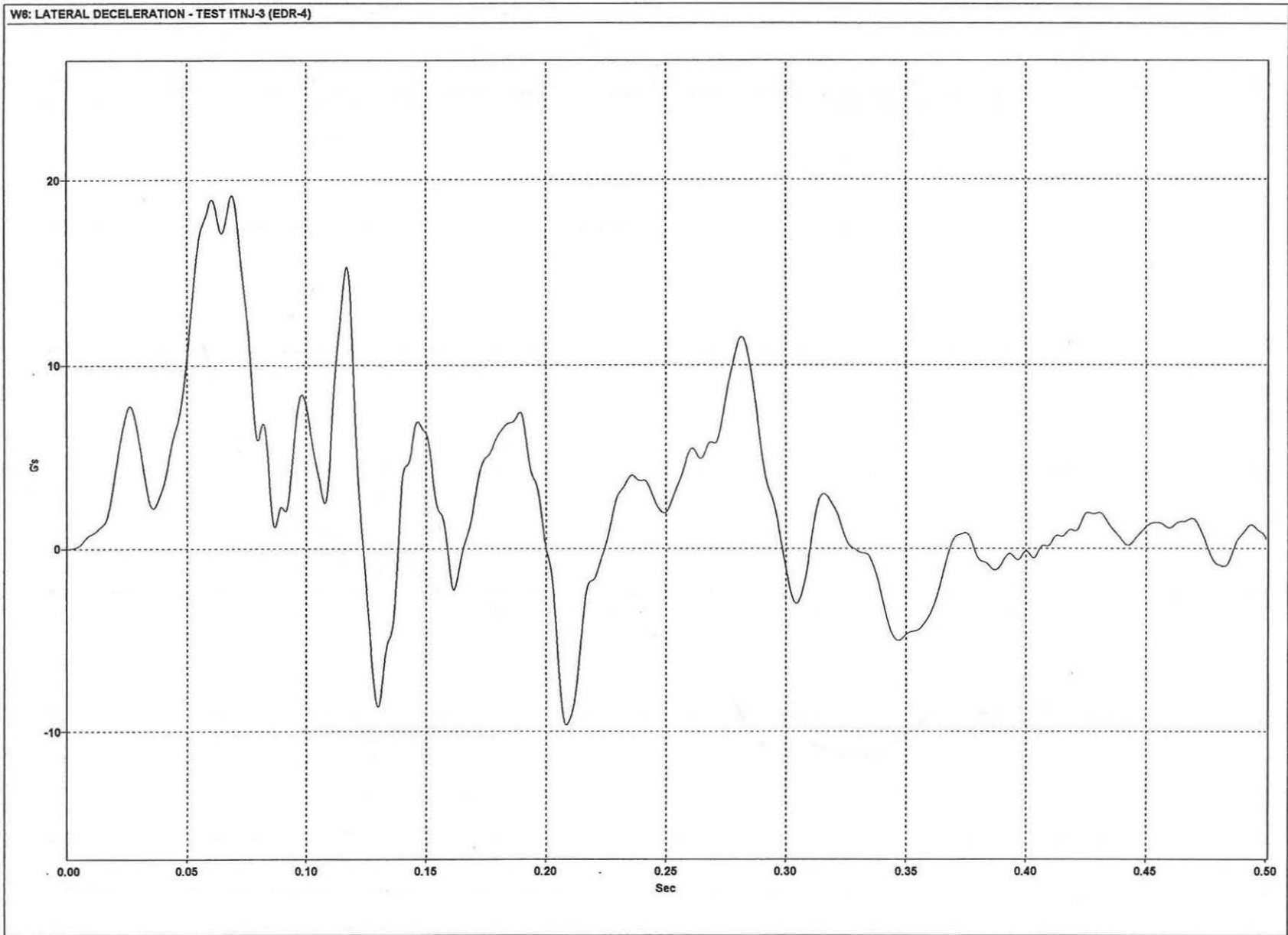


Figure F-4. Graph of Lateral Deceleration, Test ITNJ-3

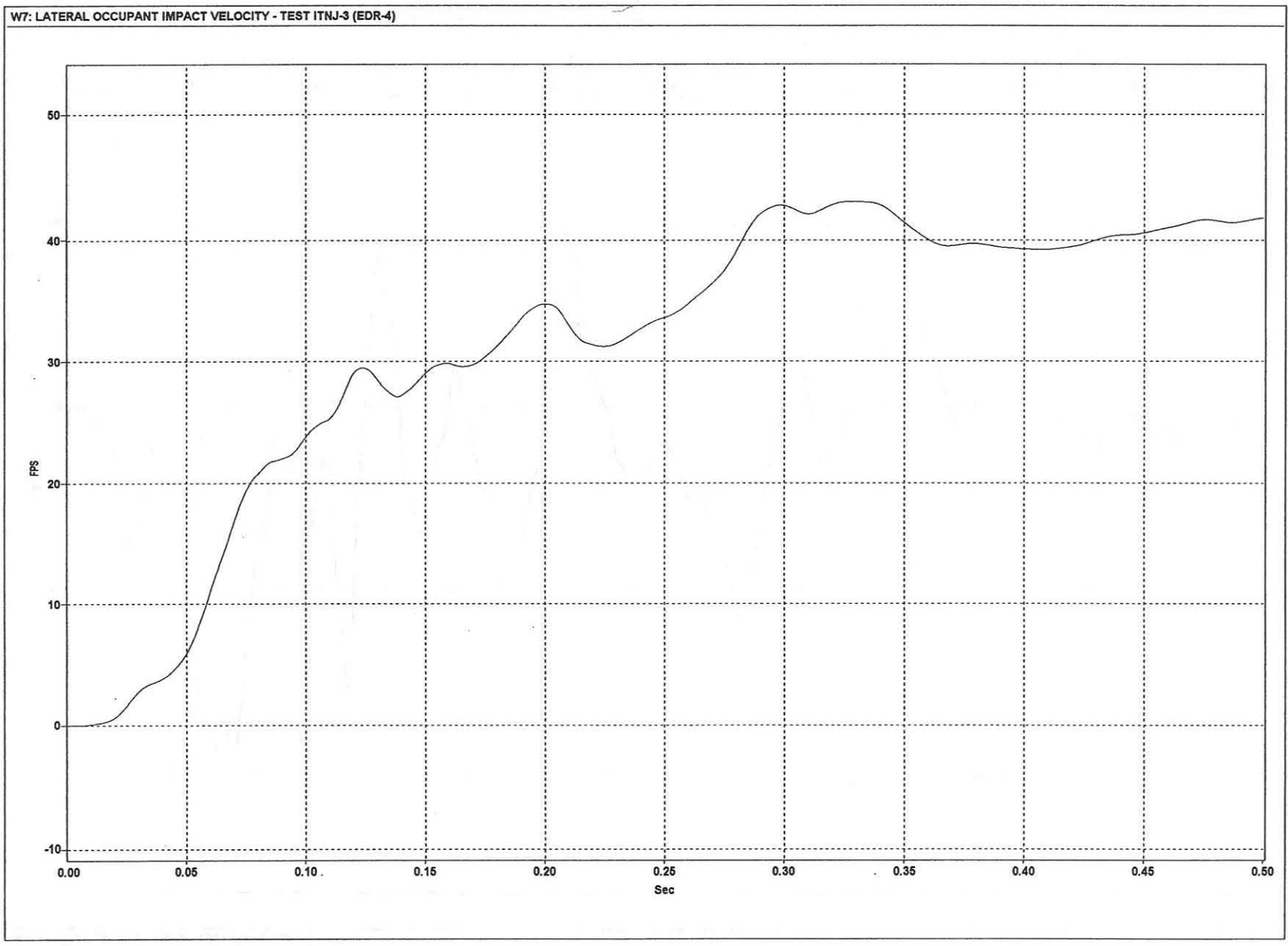


Figure F-5. Graph of Lateral Occupant Impact Velocity, Test ITNJ-3

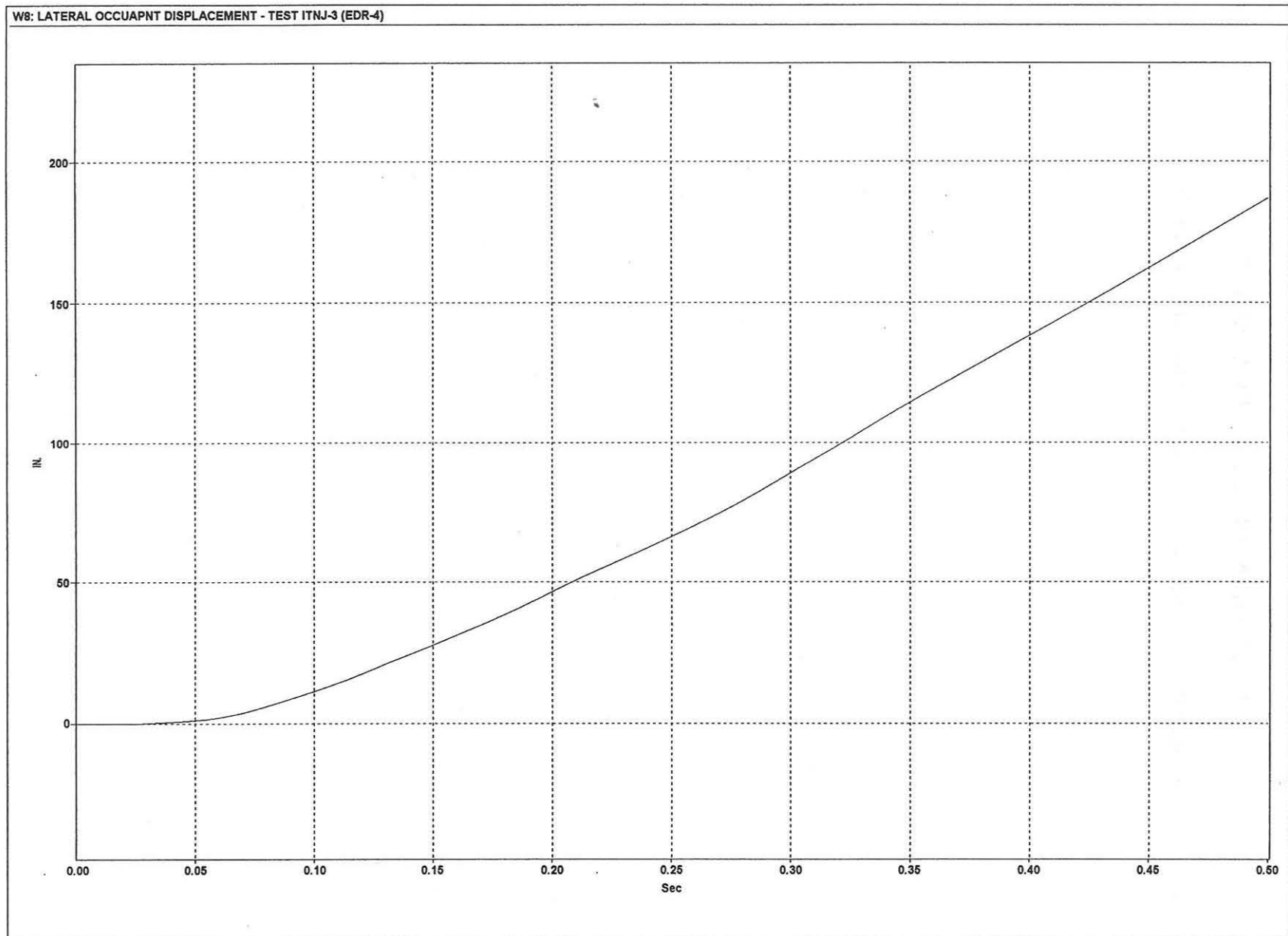


Figure F-6. Graph of Lateral Occupant Displacement, Test ITNJ-3

APPENDIX G

RATE TRANSDUCER DATA ANALYSIS

Figure G-1. Graph of Roll, Pitch, and Yaw Angular Displacements, Test ITNJ-3

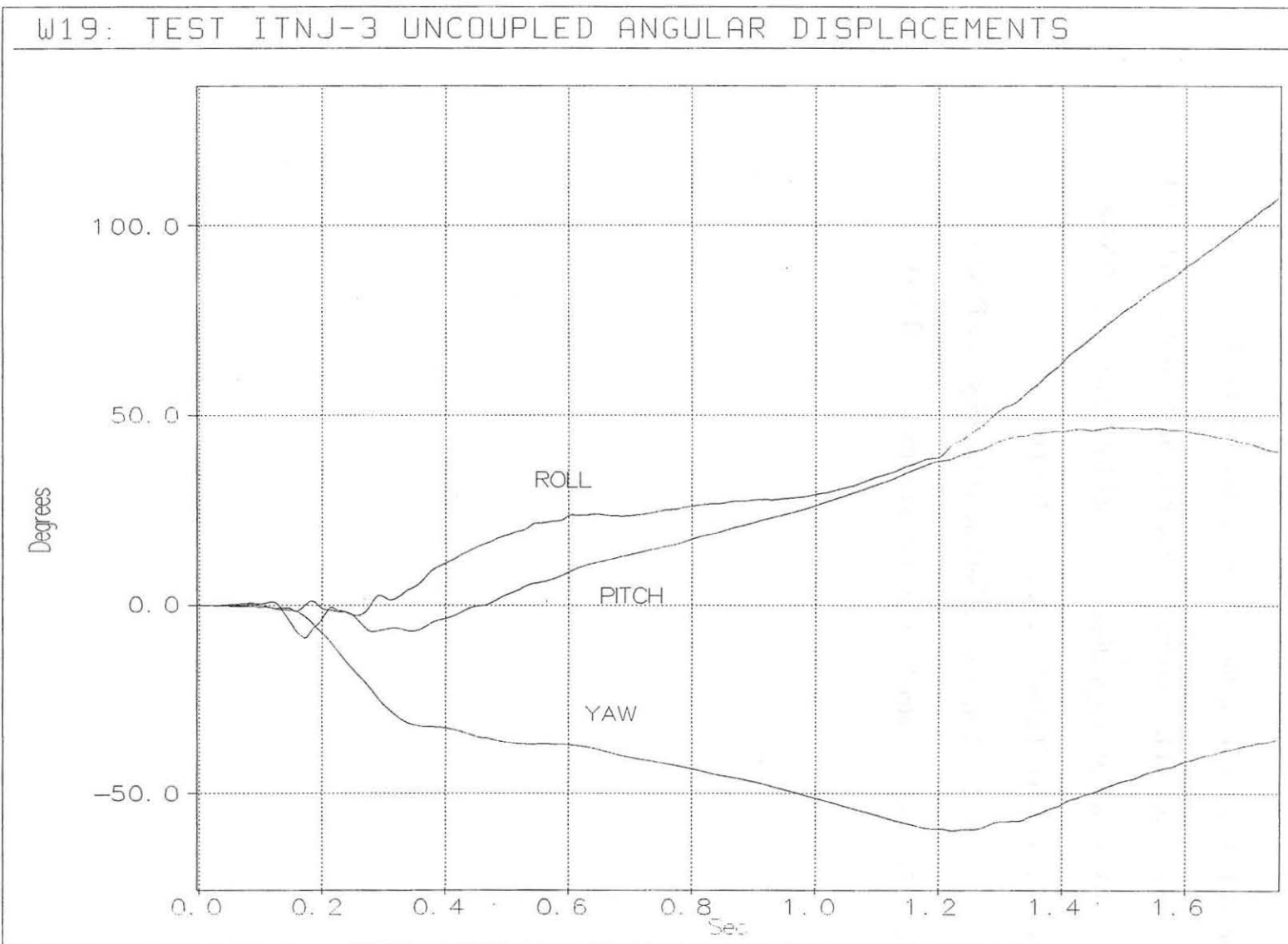


Figure G-1. Graph of Roll, Pitch, and Yaw Angular Displacements, Test ITNJ-3

APPENDIX H

ACCELEROMETER DATA ANALYSIS

Figure H-1. Graph of Longitudinal Deceleration, Test ITNJ-4

Figure H-2. Graph of Longitudinal Occupant Impact Velocity, Test ITNJ-4

Figure H-3. Graph of Longitudinal Occupant Displacement, Test ITNJ-4

Figure H-4. Graph of Lateral Deceleration, Test ITNJ-4

Figure H-5. Graph of Lateral Occupant Impact Velocity, Test ITNJ-4

Figure H-6. Graph of Lateral Occupant Displacement, Test ITNJ-4

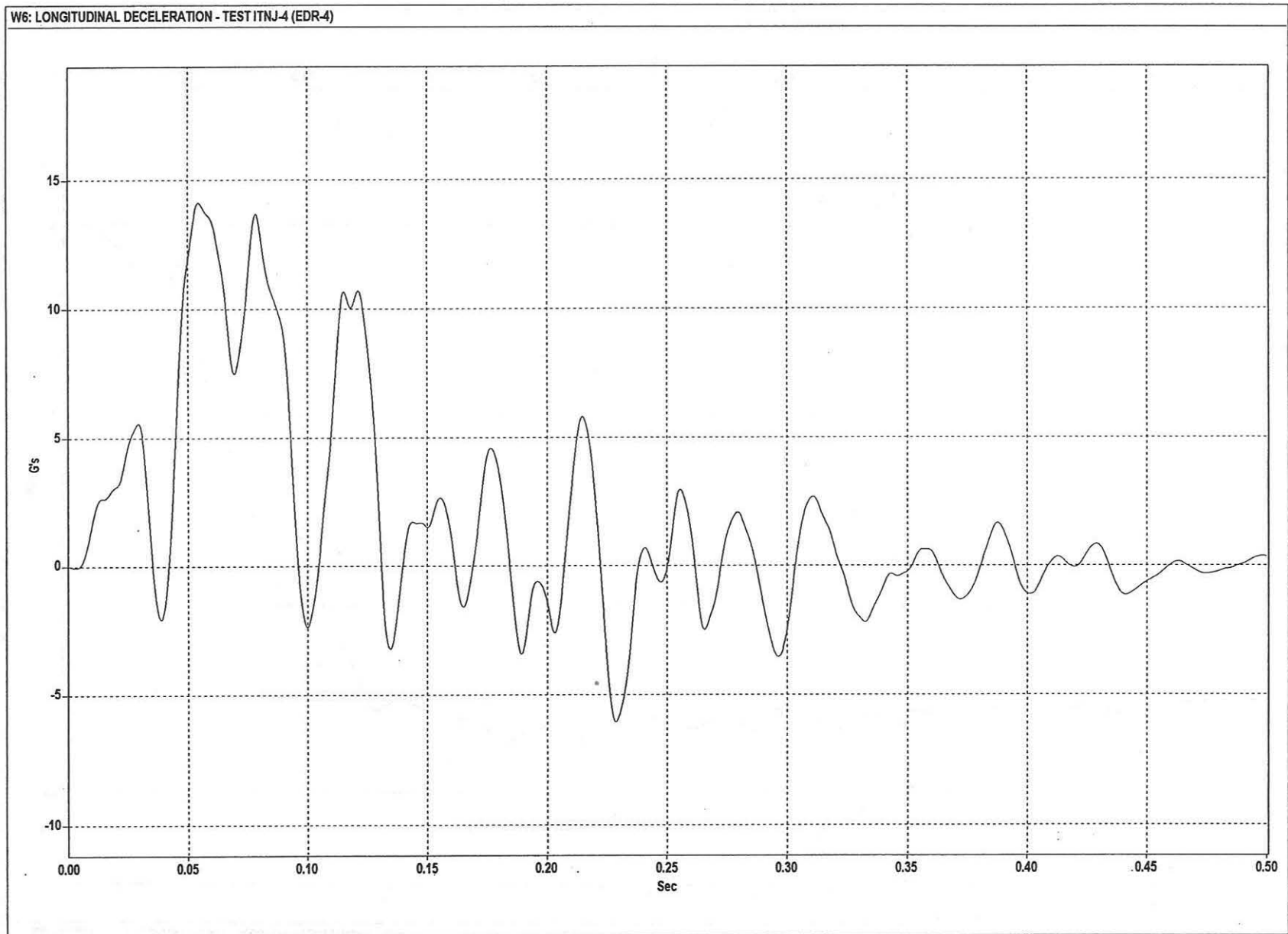


Figure H-1. Graph of Longitudinal Deceleration, Test ITNJ-4

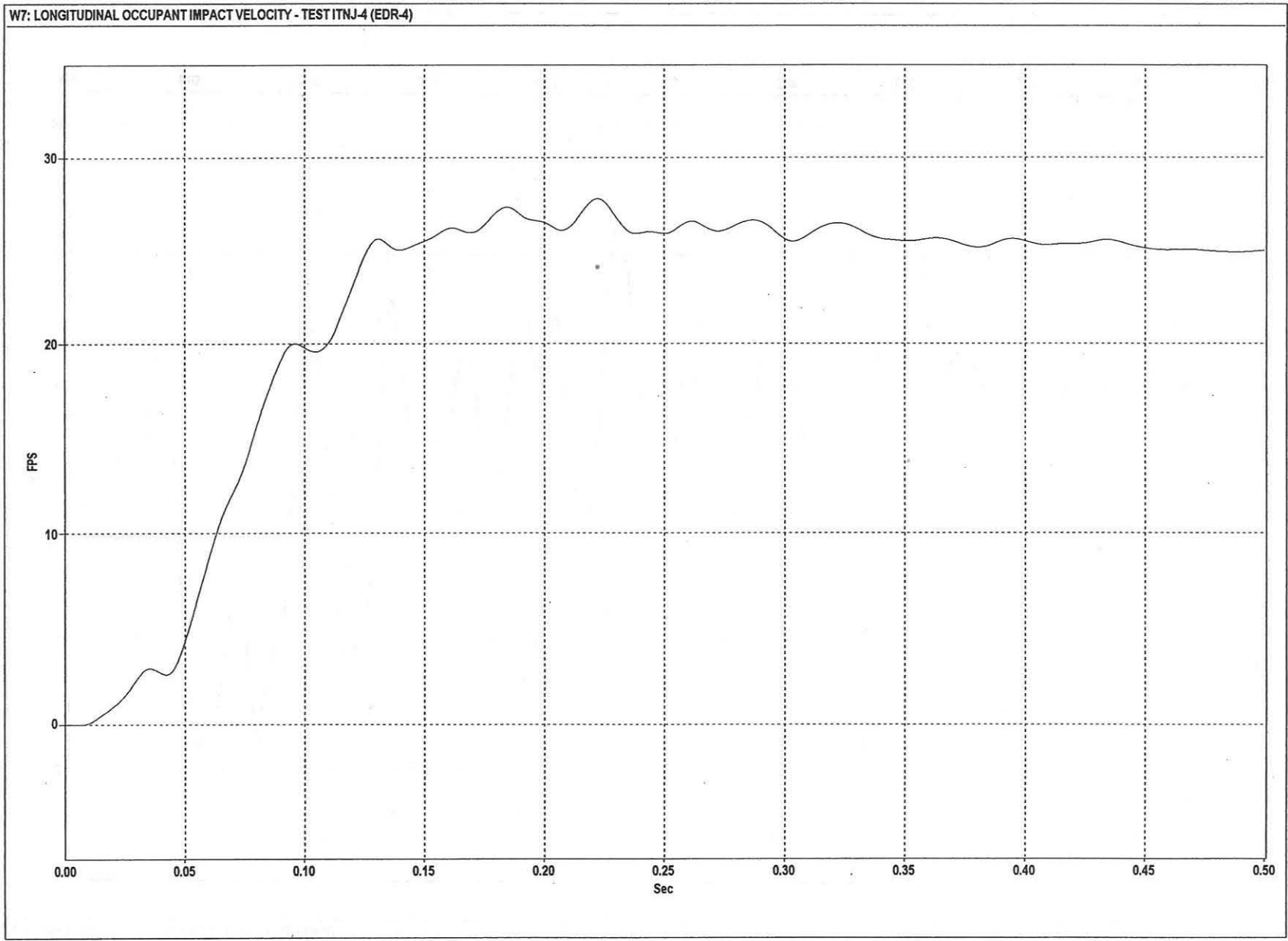


Figure H-2. Graph of Longitudinal Occupant Impact Velocity, Test ITNJ-4

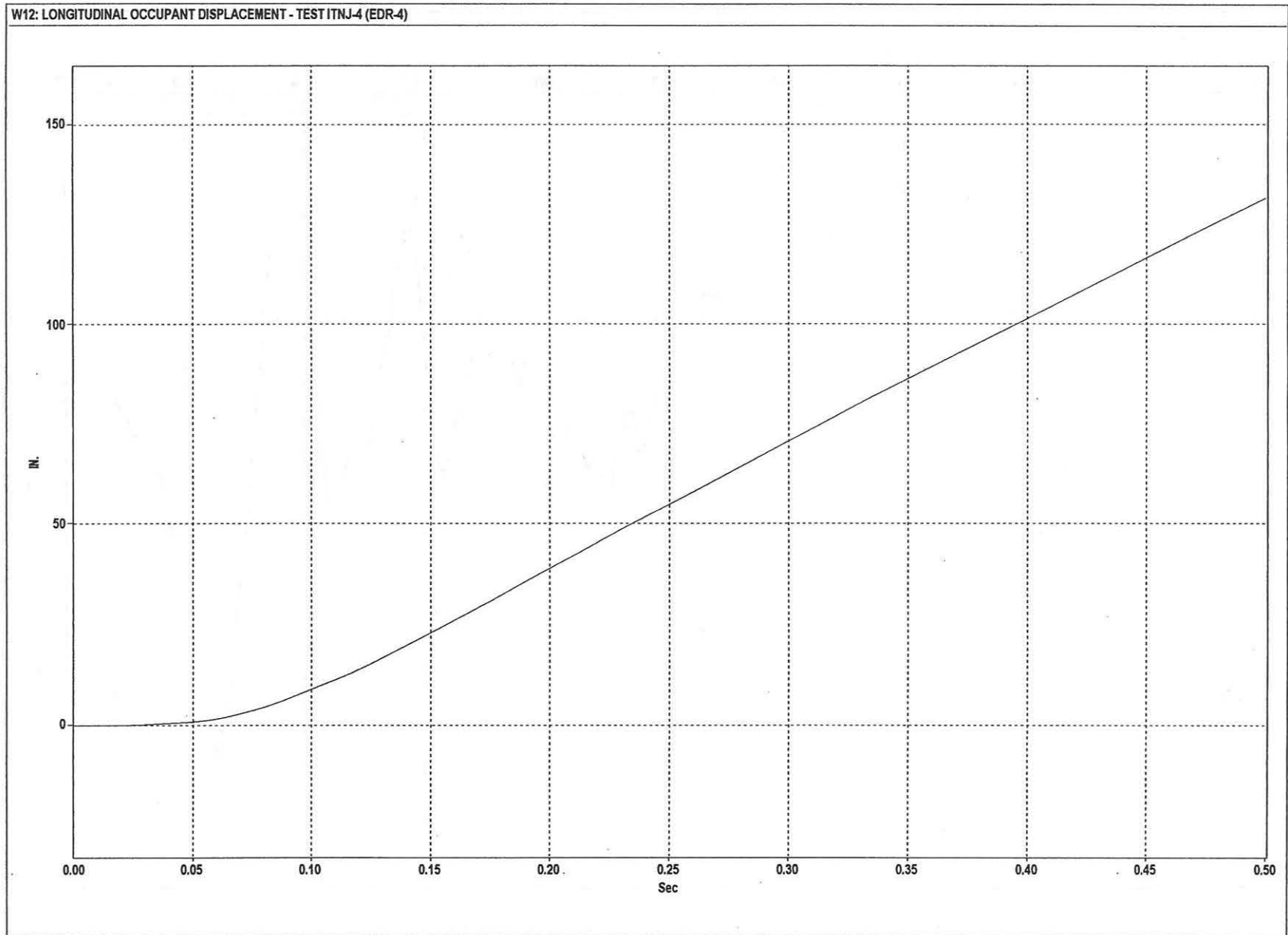


Figure H-3. Graph of Longitudinal Occupant Displacement, Test ITNJ-4

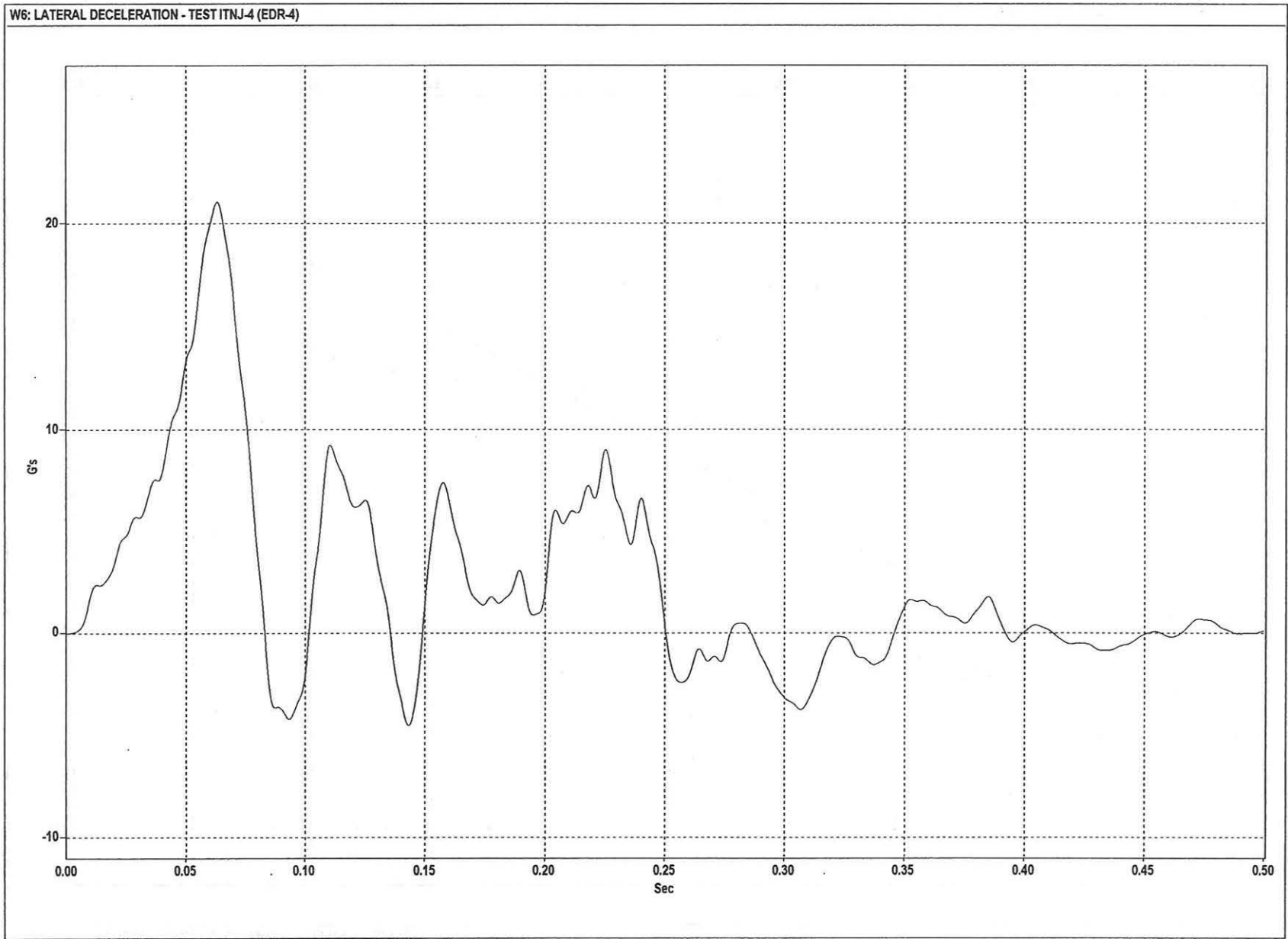


Figure H-4. Graph of Lateral Deceleration, Test ITNJ-4

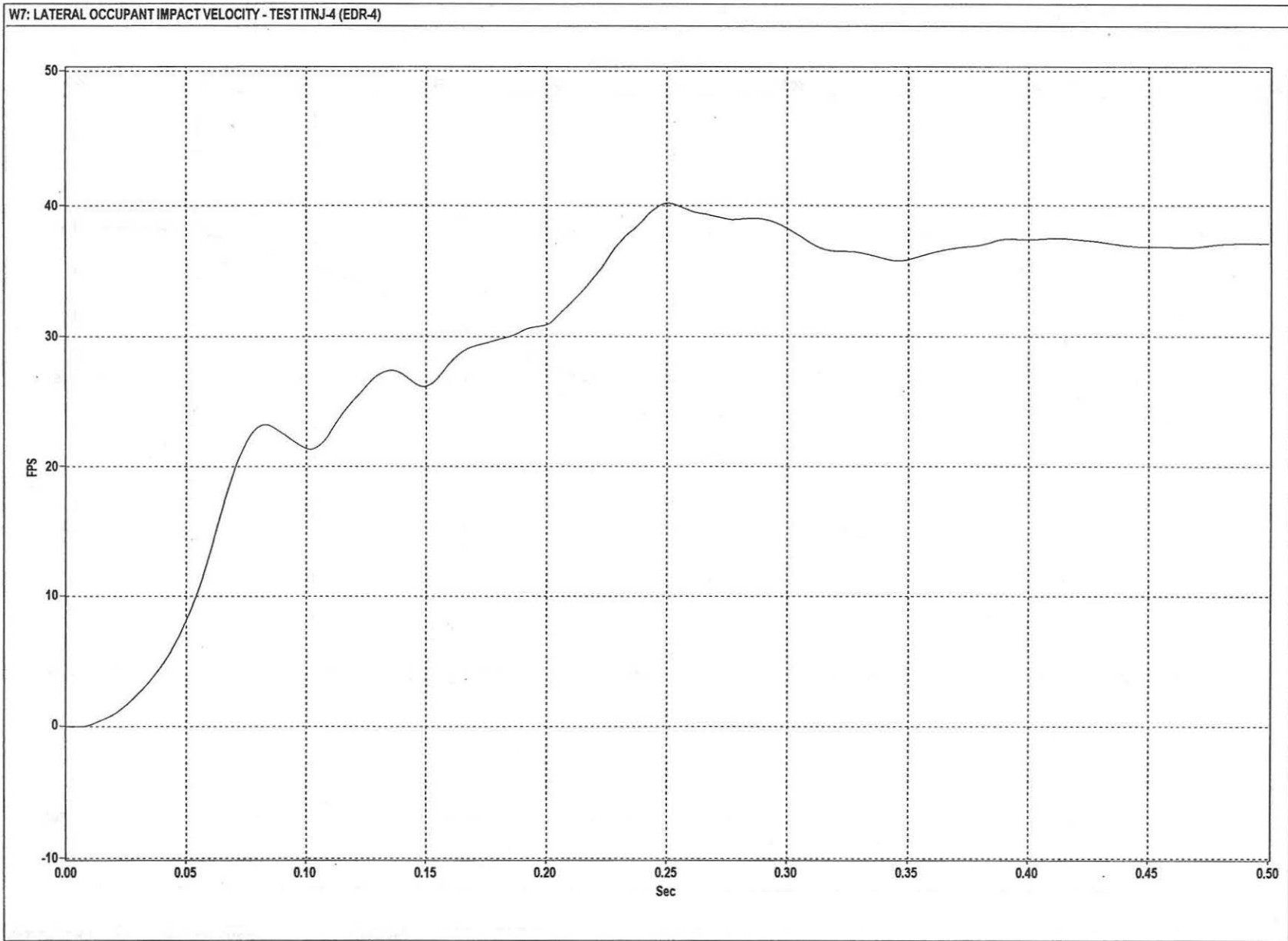


Figure H-5. Graph of Lateral Occupant Impact Velocity, Test ITNJ-4

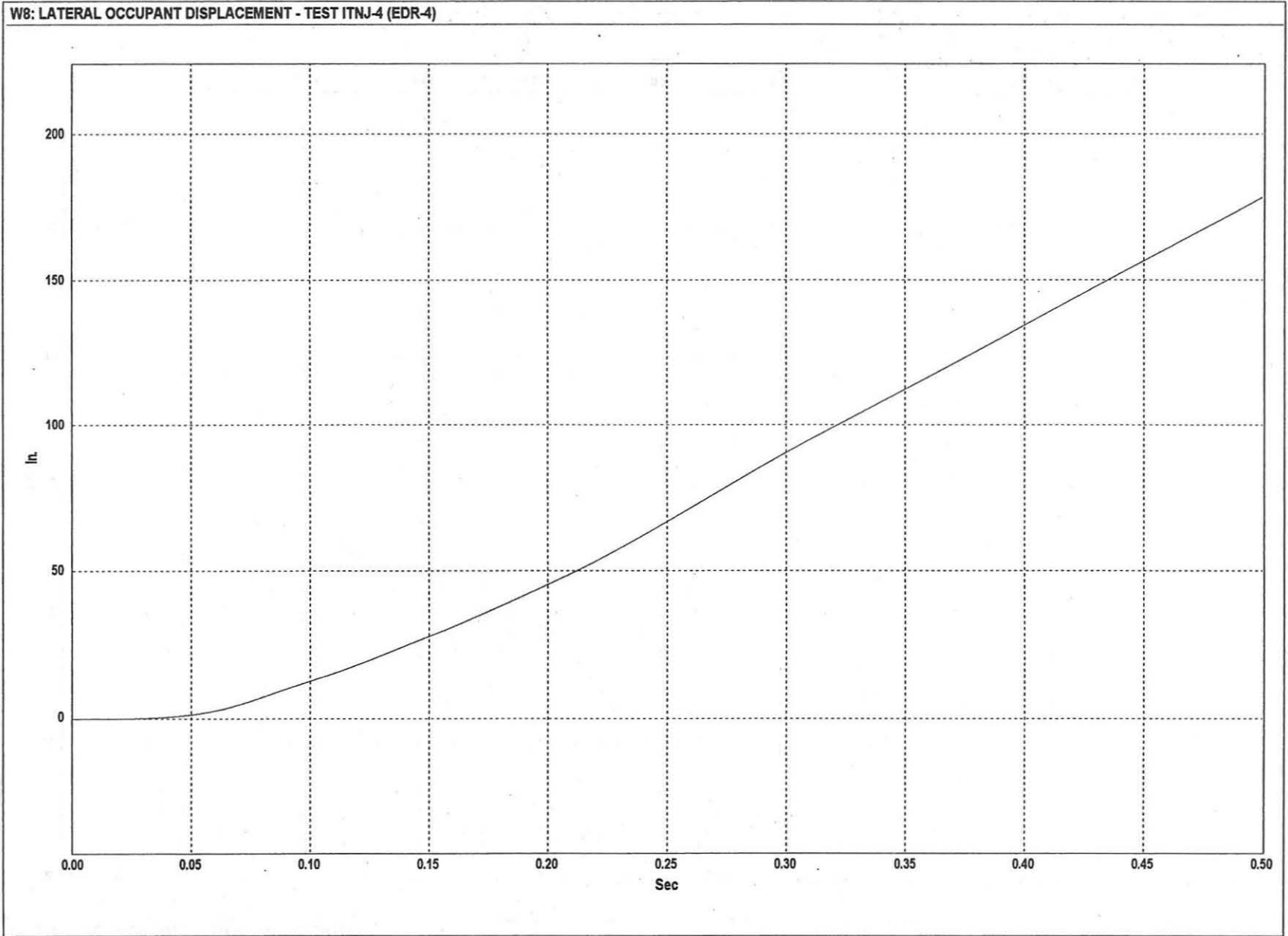


Figure H-6. Graph of Lateral Occupant Displacement, Test ITNJ-4